INCORPORATING TACIT KNOWLEDGE OF SOIL-LANDSCAPE RELATIONSHIPS FOR DIGITAL SOIL AND LANDSCAPE MAPPING APPLICATIONS

By

Bradley Allen Miller

A DISSERTATION

Submitted to
Michigan State University
in partial fulfillment of the requirements
for the degree of

Geography – Doctor of Philosophy

2013

ABSTRACT

INCORPORATING TACIT KNOWLEDGE OF SOIL-LANDSCAPE RELATIONSHIPS
FOR DIGITAL SOIL AND LANDSCAPE MAPPING APPLICATIONS

By

Bradley Allen Miller

The purpose of this dissertation is to develop and test a quantitative model for classifying hillslope position, using digital terrain analyses. The model is calibrated by, and validated against observations of soil scientists, while working in the field. Classifying the landscape into the five standard hillslope elements, or positions, in a manner that is transferable between landscapes, can greatly help soil sampling and mapping endeavors.

This dissertation begins by reviewing the role of environmental predictors in the conceptual models of soil geographers, at different scales, via a historical overview of soil maps. I conclude that the sum experience of soil science has recognized a hierarchy of scale in three of Dokuchaev's five factors of soil formation, proceeding in decreasing phenomenon scale: 1) climate, 2) parent material, and 3) relief. That relief is at the smallest phenomenon scale suggests that delineations on modern, county-level soil maps can perhaps be best disaggregated by increasing the resolution and applicability of topographic base maps used to construct those maps.

Today, LiDAR technology provides high resolution, elevation data, but requires contextual information if it is to be used for mapping landscape elements and soil cover patterns. Soil geomorphic research has long recognized the relationship between soil development and the contextual metric of hillslope position. However, the definitions for

hillslope positions are based on conceptual models that synthesize multiple terrain parameters, which are not always easily observed in elevation data alone. This dissertation develops and utilizes methods for calibrating analysis scales, classification breaks, and model structures to soil scientists' field observations, as a means of capturing their expert knowledge of hillslope position.

The result is a quantitative definition of hillslope position, which can be applied in digital terrain analysis. The optimal analysis scales observed for slope gradient, profile curvature, and relative elevation were 9 m, 63 m, and 135 m, respectively. The best performing model differentiates areas on the landscape using a decision tree hierarchy that divides the landscape first by slope gradient (breaks at 1.4 and 2.9°), then by profile curvature and relative elevation. The final model was also tested for sensitivity to quality of the digital elevation data used to calculate the various slope parameters. Because of the importance of analysis scale, grid resolution was equally important for obtaining accurate results as uncertainty in the elevation attribute.

By using the analysis scales, classification breaks, and model structure identified in this dissertation, hillslope position was determined consistently across a variety of Midwestern U.S. landscapes. The resulting hillslope position base map provides quantitative criteria for common soil map unit boundaries, study of geomorphic landscape patterns, and sampling strategies. This classification of hillslope position not only has the potential to increase soil map resolution by disaggregation of current delineations, but also offers consistency. Consistency increases the reliability of soil maps and allows for comparisons between landscapes.

Copyright by
BRADLEY ALLEN MILLER
2013

For Brigi and Nia

ACKNOWLEDGMENTS

Many outstanding people have contributed to my development and provided the encouragement that made it possible for me to reach this point. I am indebted to each of them. I wish to express my gratitude to everyone who has supported me in my endeavors leading to this dissertation.

In particular, I wish to thank my committee members, Dr. Randall Schaetzl, Dr. Ashton Shortridge, Dr. David Lusch, and Dr. Sasha Kravchenko for their patience and guidance. I greatly appreciate their advice and constructive comments on previous versions of this dissertation. My special thanks to Dr. Schaetzl for being my adviser and providing employment through the process of my Ph.D. program. I am also thankful for the support of the MSU Geography Department and its graduate student community.

Funding from the Soil Classifier Association of Michigan, the MSU Graduate College, and the American Association of Geographers facilitated my research and attendance of professional conferences; my thanks to them and their donors for their support. Also, thank you to Matt Bromley and Ryan Dermody of the U.S. Natural Resource Conservation Service for their assistance in providing data for this project.

I would also like to explicitly express my deepest gratitude to my mentors at Iowa State University, Dr. William Crumpton and Dr. Lee Burras. The analytical and critical thinking skills that they taught me have been invaluable to my continued success.

TABLE OF CONTENTS

LIST OF TABLES . . . . . **x**

LIST OF FIGURES . . . . . **xiii**

KEY TO ABBREVIATIONS . . . . . **xxi**

CHAPTER 1.
INTRODUCTION **1**

CHAPTER 2.
SCALE IN THE CONTEXT OF PROGRESS IN SOIL GEOGRAPHY **4**
Abstract 4
1. Introduction 5
1.2. Background on Scale in Soil Geography 8
2. Early Soil Geography (pre-19th Century) 10
2.1. The Importance of Base Maps 11
2.2. Classification 12
2.3. Understanding of Soil 16
3. Emergence of Soil Maps 17
3.1. Early Maps with Soil Attributes 17
3.2. Base Maps 19
3.2.1. Determining Location Accurately 19
3.2.2. Surveying 20
3.2.3. Thematic Maps 23
4. Small Cartographic Scale Maps (< 1:1 million) 27
4.1. Base Maps 27
4.2. Purpose and Strategies of Soil Mapping 27
5. Medium Cartographic Scale Maps (1:1 million to 1:25,000) 35
5.1 Base Maps 35
5.2. Purpose and Strategies for Soil Mapping 35
5.3. Overlap in Phenomena Scales 42
6. Large Cartographic Scale Maps (1:25,000 and larger) 43
6.1. Base Maps 43
6.2. Purpose and Strategies 45
6.3. Local Modification of Larger Scale Phenomenon 50
6.4. Untapped Potential 50
7. Joining Scales 53
8. Conclusions 62
REFERENCES 65

CHAPTER 3.
SEMANTIC CALIBRATION OF DIGITAL TERRAIN ANALYSIS SCALE 77
Abstract. 77
1. Introduction 78
2. Methods 81
2.1. Relating Field Assessment of Hillslope Position to Digital Terrain Analysis 81
2.2. Semantic Calibration of Analysis Scale 84
2.3. Study Area 88
3. Consideration of the Modifiable Area Unit Problem 94
4. Results 98
4.1. Analysis Scale Calibration of all Observation Points 98
4.2. Analysis Scale Calibration by Terrain Sub-regions 102
5. Discussion 111
6. Conclusions 114
APPENDIX 117
REFERENCES 135

CHAPTER 4.
DIGITAL CLASSIFICATION OF HILLSLOPE POSITION: DEVELOPING A BETTER BASE MAP FOR IMPROVING AND DISAGGREGATING EXISTING SOIL MAPS 140
Abstract 140
1. Introduction 141
1.1 Utility of Hillslope Position 141
1.2 Application to Digital Soil Mapping 145
2. Methods 147
2.1. General Setup 147
2.2 Decision Tree Models 151
2.2.1. Calibration of Classification Breaks 153
2.3. Linear Discriminant Analysis 155
2.4. Validation and Transferability 155
3. Results and Discussion 158
3.1. Calibration 158
3.2. Ottawa County Validation 160
3.2.1. Decision Tree Models 160
3.2.2. Linear Discriminant Analysis Model 165
3.3 Validation in Different Landscapes (Transferability) 166
3.4. Map Comparisons 173
3.4.1. Opportunity for Disaggregation of Existing Soil Map Units 184
3.5. A Quantified Definition for Hillslope Position 192
3.5.1. Applicability beyond Discrete Boundaries 193
4. Conclusions 194
APPENDIX 196
REFERENCES 204

CHAPTER 5.
THE IMPACT OF PARAMETER ACCURACY VERSUS RESOLUTION ON A SIMPLE HILLSLOPE POSITION CLASSIFICATION MODEL 210
Abstract 210
1. Introduction 211
2. Methods 213
2.1. Comparison of Different Elevation Data Sources 213
2.2. Isolating Effect of Grid Resolution 217
3. Results and Discussion 217
3.1 Sensitivity to LiDAR, NED, and SRTM as Data Sources 217
3.1.1. Analysis of LiDAR, NED, and SRTM Agreement by Test Zones 219
3.2. Sensitivity to Grid Resolution Alone 224
3.2.1. Analysis of Sensitivity to Grid Resolution by Test Zones 227
3.3. Comparison of Classification Agreements between Differing Data Sources and Grid Resolution 229
4. Conclusions 231
REFERENCES 233

CHAPTER 6.
CONCLUSIONS **237**

LIST OF TABLES

Table 2.1. Relationship between the top levels of zonal classification and the current version of Soil Taxonomy. 62

Table 3.1. Experimental matrix for varying combinations of DEM cell size and neighborhood size for varying analysis scale. 86

Table 3.2. Definition table for relating qualitative hillslope position descriptions to the DTA of profile curvature and relative elevation. Attributes highlighted in gray were used for the semantic calibration. 87

Table 3.3. Descriptive statistics of elevation and slope gradient for the three landscape sub-regions. 94

Table 3.4. Percent agreement results for profile curvature of all observation points. Concave and convex agree are the count of points where the digital and field assessments of slope profile shape were in agreement. Percent is the proportion of agreement out of the total number of points. 99

Table 3.5. Percent agreement results for relative elevation of all observation points. Low and high agree are the count of points where the digital and field assessments of relative elevation were in agreement. Percent is the proportion of agreement out of the total number of points. 101

Table 3.6. Mean absolute difference results for slope gradient of all observation points. 102

Table 3.7a. Percent agreement results for profile curvature of observation points in the dune landscape. Concave and convex agree are the count of points where the digital and field assessments of slope profile shape were in agreement. Percent is the proportion of agreement out of the total number of points. . . . 104

Table 3.7b. Percent agreement results for profile curvature of observation points in the hummocky landscape. Concave and convex agree are the count of points where the digital and field assessments of slope profile shape were in agreement. Percent is the proportion of agreement out of the total number of points. 105

Table 3.7c. Percent agreement results for profile curvature of observation points in the glacial lake plain landscape. Concave and convex agree are the count of points where the digital and field assessments of slope profile shape were in agreement. Percent is the proportion of agreement out of the total number of points. 106

Table 3.8a. Percent agreement results for relative elevation of observation points in the dune landscape. Low and high agree are the count of points where the digital and field assessments of relative elevation were in agreement. Percent is the proportion of agreement out of the total number of points. 107

Table 3.8b. Percent agreement results for relative elevation of observation points in the hummocky landscape. Low and high agree are the count of points where the digital and field assessments of relative elevation were in agreement. Percent is the proportion of agreement out of the total number of points. 108

Table 3.8c. Percent agreement results for relative elevation of observation points in the glacial lake plain landscape. Low and high agree are the count of points where the digital and field assessments of relative elevation were in agreement. Percent is the proportion of agreement out of the total number of points. 109

Table 3.9a. Mean absolute difference results for slope gradient of observation points in the dune landscape. 110

Table 3.9b. Mean absolute difference results for slope gradient of observation points in the hummocky hills landscape. 110

Table 3.9c. Mean absolute difference results for slope gradient of observation points in the glacial lake plain landscape. 111

Table 4.1. Definitional categories of terrain parameters by hillslope position. 153

Table 4.2. Statistics of calibration points categorized into the assessment groups of each model parameter. 159

Table 4.3. Classification breaks calibrated from the assessment group statistics of each model parameter. 159

Table 4.4. Percent agreement between soil scientists' field assessments and each hillslope position models' prediction by classification break method for Ottawa County, Michigan. 160

Table 4.5. Confusion matrixes for classification breaks based on the mid-point between assessment groups' means for a) PrcP decision tree (Kappa = 0.44), b) SlgP decision tree (Kappa = 0.49), and c) ReeP decision tree (Kappa = 0.27). 161

Table 4.6. Confusion matrixes for classification breaks based on the mid-point between assessment groups' medians for a) PrcP decision tree (Kappa = 0.35), b) SlgP decision tree (Kappa = 0.46), and c) ReeP decision tree (Kappa = 0.36). 162

Table 4.7. Confusion matrixes for classification breaks based on the confidence index to differentiate parameters for a) PrcP decision tree (Kappa = 0.45), b) SlgP decision tree (Kappa = 0.49), and c) ReeP decision tree (Kappa = 0.28). 163

Table 4.8. Confusion matrix for the LDA classification (Kappa = 0.26). 166

Table 4.9. Percent agreement between soil scientists' field assessments and each hillslope position models' prediction by classification break method for a) Dickinson County and b) Cedar County, Iowa. 167

Table 4.10. Confusion matrix for SlgP-med model prediction of field assessments of hillslope position in a) Dickinson County (Kappa = 0.35) and b) Cedar County, Iowa (Kappa = 0.37). 167

Table 4.11. Zonal statistics of the SlgP-med hillslope position model by SSURGO map units in Ottawa County, Michigan. 197

Table 4.12. Zonal statistics of the SlgP-med hillslope position model by SSURGO map units in Dickinson County, Iowa. 200

Table 4.13. Zonal statistics of the SlgP-med hillslope position model by SSURGO map units in Cedar County, Iowa. 202

Table 5.1. a) LiDAR-based, 3 m resolution, HP classification of all test points for context in evaluating confusion matrices comparing LiDAR-based classification of hillslope position with b) NED-based classification of hillslope position (Kappa = 0.36) and b) SRTM-based classification of hillslope position (Kappa = 0.14). . 219

Table 5.2. a) LiDAR-based, 3 m resolution, HP classification of all test points for context in evaluating confusion matrices comparing 3 m resolution classification with b) 9 m resolution classification (Kappa = 0.67) and c) 27 m resolution classification (Kappa = 0.47). 226

Table 5.3. Rates of disagreement and estimated causes of disagreement for a) Ottawa County, Michigan, b) Cedar County, Iowa, and c) Dickinson County, Iowa. 230

LIST OF FIGURES

Figure 2.1. Timeline of important developments in the scientific sphere of soil geography. Soil maps (white) are a product of both the scientific understanding of soil (light gray) and the geographic technologies available at the time (dark gray). Although soil geography has been valued since early civilizations, actual soil maps could not be produced until the needed geographic technology was available. 7

Figure 2.2. Reconstruction of Eratosthenes's map of the known world, ca. 194 BCE (Bunbury, 1883). This map pre-dates the use of cartographic scale. Outline of continents demonstrates the spatial distortion inherent to maps of the time. Labels are inconsequential. 13

Figure 2.3. Figure 2.3. Ptolemy's world map with latitudinal climate zones, reproduced by J. Pentius de Leucho (Leucho, 1511). The climate zones are labeled on the western side of the map. "Clima I" is comprised of the two latitude zones north and two zones south of the equator. Each subsequent latitude zone shown, proceeding north, is label sequentially with a different "Clima" number. All other labels are inconsequential. This map pre-dates the use of cartographic scale. 15

Figure 2.4. Section of the first systematically surveyed, topographic map of France, published between 1756 and 1815. Although this map was a milestone for accurate positioning of features, note the lack of elevation information. Cartographic scale was 1:86,400. (National Library of France, 2013) 22

Figure 2.5. The first geological map of Britain, produced by water coloring a pre-existing topographic map. Published by William Smith in 1815 (Library Foundation, Buffalo and Erie County Public Library, 2013). The title claims that by mapping the geologic strata, the varieties of soil are also shown (a). The cartographic scale of the original map (b) was approximately 1:316,000. For interpretation of the references to color in this and all other figures, the reader is referred to the electronic version of this dissertation. 25

Figure 2.6. Isotherm map of the world, based on the work of Humboldt. Lines dividing colors have similar temperatures and are breaks between climate zones. Labels are inconsequential. Cartographic scale not provided. (Woodbridge, 1823) 29

Figure 2.7. Isohumus belts identified by Dokuchaev based on quantitative point observations. Darker shading indicates higher content of soil humus. Labels are inconsequential. Cartographic scale was 1:4.2 million. (Dokuchaev, 1967) 30

Figure 2.8. Soil map of Africa based on zonal classification system. Note the pattern similarity between the soil map and the inset rainfall map. Labels are inconsequential. Cartographic scale was 1:10 million. (Shantz and Marbut, 1923). 33

Figure 2.9. General soil map of Wisconsin produced in the agrogeology style by Chamberlain. Shades of brown indicate different soil textures, the pattern of which can be compared to modern soil region maps (Figure 2.11). Map text is inconsequential. Cartographic scale not provided. (Chamberlain, 1882) 37

Figure 2.10. Soil map of Tama County, Iowa produced at a cartographic scale of 1:63,360 (Ely et al., 1904). Only five map units are delineated, which primarily differ in parent material. Variation of soils due to climate or relief is not included. Map text is inconsequential. 39

Figure 2.11. Soil regions of Wisconsin map published by the Wisconsin Geological and Natural History Survey. Cartographic scale was 1:710,000 (Madison and Gundlach, 1993). The spatial patterns in this map are very similar to the patterns in the earlier, agrogeology style soil map of Wisconsin. The two maps primarily differ due to more accurate spatial information being available for the modern soil map. 40

Figure 2.12. Soil associations of Iowa map published by the Iowa Agriculture and Home Economics Station. Cartographic scale was 1:506,880 (National Cooperative Soil Survey, 1978). This state soil map has a level of detail similar to the contemporary soil map of Wisconsin (Figure 2.11). The legend of this map is too large to be included in this dissertation format. However, both the Iowa Soil Association Map and the Soil Regions of Wisconsin map primarily represent the spatial distribution of geologic/parent materials. 41

Figure 2.13. Section of Hamilton County, Iowa soil map, constructed at the commonly used cartographic scale of 1:15,840 (Dideriksen, 1986). Note that although topographic features are being delineated, topographic sequences are not distinguishable in the aerial photograph base map. Map unit labels are inconsequential. 49

Figure 2.14. Illustration demonstrating the difference in detail between delineating light-dark soil cover patterns (corresponding to erosion-deposition zones) and the five hillslope positions commonly used in toposequences research. 52

Figure 2.15. Schematic of Fippin's proposed soil classification system (Fippin, 1911). Note the hierarchy of climate at the highest level followed by characteristics of parent material. At the series and type level, multiple, specific soil properties are listed, several of which have direct connections to topography. 55

Figure 2.16. Sheet 7 of 12 from soil map of the United States based on generalized soil series in the agrogeology classification style. Cartographic scale was 1:2.5 million (Marbut et al., 1931). Note the 'Arrangement of Sections' diagram in the lower-right corner for comparison of spatial patterns with Figure 2.17. Names of soil series are inconsequential. 57

Figure 2.17. Soil map of the U.S. based on great soil groups in the zonal classification style. Cartographic scale was 1:8 million (Marbut, 1931). Although some nested relationships can be observed between Figure 2.16 and 2.17, Marbut did not believe those relationships were sufficient to join the classification systems of the respective maps. Names of the great soil groups are inconsequential. 58

Figure 2.18. a) World map of soil orders as classified by U.S. Soil Taxonomy at a cartographic scale of 1:130 million (USDA-NRCS, 2005). b) Köppen-Geiger climate zones presented for comparison with U.S. Soil Taxonomy soil orders (climate zone map courtesy of www.theodora.com/maps, used with permission). 61

Figure 3.1. In order to classify the functional zones of hillslope position (a), soil scientists in the field synthesize their assessment of b) slope gradient, c) profile curvature, and d) relative elevation to determine the hillslope position of a location. 83

Figure 3.2. In this research, relative elevation is calculated on a neighborhood by neighborhood basis for each cell. a) First, a reference elevation ceiling is calculated by summing the neighborhood minimum and maximum elevations. b) Then, the central cell elevation is subtracted from the elevation ceiling to create an inverse elevation grid. c) By subtracting the inverse from the original elevation grid, a relative elevation grid is created with the mid-point between the neighborhood minimum and maximum having a value of zero. Elevation values above the mid-point are increasingly positive. Below the elevation mid-point, values are negative and decrease with vertical distance. 85

Figure 3.3. Location of study area, Ottawa County, in the lower peninsula of Michigan, U.S. The map also includes locations of field observation transect points and the three study sub-regions delineated for comparing terrain types. 91

Figure 3.4. Example images from the a) dune landscape, b) hummocky landscape, and c) glacial lake plain landscape. Photos by the author. 92

Figure 3.5. Digital terrain analysis of slope gradient for three terrain types. a) Hummocky hills landscape with moderate relief. b) Glacial lake plain with consistently low relief, but some narrow, steep sided drainage ditches. c) Example area of the dunes landscape with high relief. 93

Figure 3.6. Scale effect of the modifiable area unit problem on slope gradient. Fewer extreme values increase the likelihood of agreement/correlation. Sequence of graphs illustrates reduction in extreme values with reduction of random sample size at a) 10,000 points, b) 1,000 points, c) 100 points, and d) 50 points. 95

Figure 3.7. Scale effect of the modifiable area unit problem on profile curvature. Fewer extreme values increase the likelihood of agreement/correlation. Sequence of graphs illustrates reduction in extreme values with reduction of random sample size at a) 10,000 points, b) 1,000 points, c) 100 points, and d) 50 points. 96

Figure 3.8. Scale effect of the modifiable area unit problem on relative elevation. Fewer extreme values increase the likelihood of agreement/correlation. Sequence of graphs illustrates reduction in extreme values with reduction of random sample size at a) 10,000 points, b) 1,000 points, c) 100 points, and d) 50 points. 97

Figure 3.9. Example area from LiDAR elevation grid. Note the striped elevation patterns that can be seen in some portions of the example area. 119

Figure 3.10. Same example area processed as a hillshade from the LiDAR elevation grid, with no vertical exaggeration. Note the additional striped patterns that were not as apparent in the display of elevation in Figure 3.9. 120

Figure 3.11. Same example area processed as a hillshade from the LiDAR elevation grid, with elevation exaggerated by a factor of 3. Note the increased prominence of striped patterns, as compared to the hillshade without vertical exaggeration (Figure 3.10). 121

Figure 3.12. Location of cross sections examined in LiDAR elevation grid from Ottawa County, Michigan, USA. The longitudinal orientation of the cross section symbols indicates each profile line's orientation. 123

Figure 3.13. Evaluation of site 1. The spatial frequency of the striped pattern does not appear to be regular, but a few peaks occur at an interval of 30 m. The relief between the peaks appears to be approximately 30 cm. 124

Figure 3.14. Evaluation of site 2. The spatial frequency of the striped pattern does not appear to be regular, but a few peaks occur at an interval of 10 m. The relief between the peaks appears to be approximately 5 cm. 125

Figure 3.15. Evaluation of site 3. The spatial frequency of the striped pattern does have some regularity, with peaks occurring at an interval of 10 m. The relief between the peaks appears to be approximately 10 cm. 126

Figure 3.16. Evaluation of site 4. The spatial frequency of the striped pattern does not appear to be regular, but a few peaks occur at an interval of 10 m. The relief between the peaks appears to be approximately 10 cm or less. 127

Figure 3.17. Evaluation of site 5. The spatial frequency of the striped pattern is not strongly expressed in the cross section, but a few peaks occur at an interval of 10 m. The relief between the peaks appears to be approximately 20 cm or less. 128

Figure 3.18. Evaluation of site 6. The spatial frequency of the striped pattern does have some regularity, with peaks occurring at an interval of 25 m. The relief between the peaks appears to be approximately 10 to 15 cm. 129

Figure 3.19. Evaluation of site 7. The spatial frequency of the striped pattern is not strongly expressed in the cross section, but a few peaks occur at an interval of 5 m. The relief between the peaks appears to be approximately 10 cm. . . . 130

Figure 3.20. Evaluation of site 8. The spatial frequency of the striped pattern does not appear to be regular, but a few peaks occur at an interval of 10 m. The relief between the peaks appears to be approximately 5 cm. 131

Figure 3.21. Image of area surrounding cross section site 6. The area demonstrates the striped patterns commonly observed on row crop fields. Satellite image courtesy of USGS. 133

Figure 3.22. LiDAR based hillshade with 3x vertical exaggeration of the same area shown in figure A.13. Note the matching orientations of the striped pattern in both the tone of the aerial image and the hillshading from the elevation grid. 134

Figure 4.1. Illustration of the mental construct that soil scientists use to assess hillslope position in the field. 144

Figure 4.2. Example of subjective shift in soil map detail between cultivated fields (left) and adjacent forest land (right) in the 1:15,840 Soil Survey map of Boone County, Iowa (Andrews and Dideriksen, 1981). 146

Figure 4.3. Distribution of calibration points in Ottawa County, Michigan. Each set of calibration points represent mapping transects, walked by NRCS field soil scientists, and each contains 8-10 observations. 150

Figure 4.4. Diagrams for the three classification tree hierarchies. Each tree will be referred to by the parameter emphasized in the top level of the hierarchy, specifically: a) the profile curvature priority decision tree (PrcP), b) the slope gradient priority decision tree (SlgP), and c) the relative elevation priority decision tree (ReeP). 152

Figure 4.5. Conceptual illustration of the confidence index (CI) used for determining fuzzy membership. The shape of the CI curve for the middle class is calculated by a normal probability density function (PDF) based on the calibration group's mean and standard deviation. CI values for the low and high classes are calculated in the same manner, except that values on the opposite side of the mean from other classes are calculated as one plus the inverse of the PDF result. 155

Figure 4.6. Dickinson County, Iowa (a) and Cedar County, Iowa (b) were used to test the transferability of the models calibrated and validated in Ottawa County, Michigan (c). 157

Figure 4.7. Example of disagreement between field observations and a digital hillslope position classification. Clearly, the soil scientist would have ignored the drainage ditch in deciding if the flat area containing the observation points was a toeslope or summit (a). However, the digital model considered the low elevation values within the drainage ditch for the adjacent area equivalent to the relative elevation analysis scale (b). Satellite image courtesy of USGS. 169

Figure 4.8. Digital hillslope position map of Ottawa County, Michigan with validation points showing agreement or disagreement with the predicted classification. 170

Figure 4.9. Digital hillslope position map of Dickinson County, Iowa with validation points showing agreement or disagreement with the predicted classification. 171

Figure 4.10. Digital hillslope position map of Cedar County, Iowa with validation points showing agreement or disagreement with the predicted classification. 172

Figure 4.11. Example of SlgP-med hillslope position classification compared with current SSURGO delineations in Dickinson County, Iowa (overlain on a hillshade of the LiDAR elevation grid). Note the many areas that transition directly from summit to toeslope. These areas are also sensitive to sharp rises in elevation. For example, the raised road running north-south in the center of the map causes the adjacent flat areas to be digitally classified as toeslopes. 175

Figure 4.12. a) Block diagram of the Tama-Downs-Muscatine soil association from the NRCS Soil Survey Staff (2009). b) Zonal statistics of the SlgP-med hillslope position model by the SSURGO map units in Cedar County, Iowa. 178

Figure 4.13. a) Block diagram of the Canisteo-Clarion-Nicollet soil association from the NRCS Soil Survey Staff (2000). b) Zonal statistics of the SlgP-med hillslope position model by SSURGO map units of this soil association in Dickinson County, Iowa. 180

Figure 4.14. a) Block diagram of the Nester-Kawkawlin-Manistee soil association from the NRCS Soil Survey Staff (1985). b) Zonal statistics of the SlgP-med hillslope position model by SSURGO map units of this soil association in Ottawa County, Michigan. The sandy Manistee soil series is not currently mapped in Ottawa County. For a soil association on sand parent materials, see Figure 4.16. 181

Figure 4.15. a) Block diagram of the Deer Park-Dawson-Au Gres soil association from the Soil Survey Staff (1992). b) Zonal statistics of the SlgP-med hillslope position model by SSURGO map units of this soil association in Ottawa County, Michigan. The organic Dawson and Kinross soils are not currently mapped in Ottawa County. Instead, organic soils are classified as Adrian, Houghton, Edwards, or Linwood soil series (Sandy or sandy-skeletal, mixed, euic, mesic Terric Haplosaprists; Euic, mesic Typic Haplosaprists; Marly, euic, mesic Limnic Haplosaprist; Loamy, mixed, euic, mesic Terric Haplosaprists; respectively). 182

Figure 4.16. Examples of disaggregation opportunities in Cedar County, shown in a) plan view, and b) perspective view (relief exaggerated 3x). Numbers indicate matching points of reference. 1) Depressions identified by the model, potentially Garwin soil series, within Muscatine soil series delineations. 2) The Fayette soil series is described as occurring on interfluves and side-slopes. However, summits on the interfluves match the geographic setting for the Downs soil series. 186

Figure 4.17. Two depression inclusions identified by Soil Survey Staff located within delineations of the convex Clarion map unit in Dickinson County. Note the proximity of the inclusion points to isolated areas of toeslopes. In a) plan view, and b) perspective view (relief exaggerated 3x). 188

Figure 4.18. Nester soil series in Ottawa County, which is illustrated in the Soil Survey block diagram as varying in topography (Figure 4.14). Digital classification of hillslope position efficiently differentiates slope elements within this Nester soil delineation. In a) plan view, and b) perspective view (relief exaggerated 3x). Star indicates a matching point of reference. 190

Figure 5.1. Areas used for this study were a) Dickinson County, Iowa, b) Cedar County, Iowa, and c) Ottawa County, Michigan. 214

Figure 5.2. Terrain characteristics of test zones compared to HP classification agreement: LiDAR-based classification agreement with a) NED-based classification versus mean slope gradient, b) SRTM-based classification versus mean slope gradient, c) NED-based classification versus profile curvature range, d) SRTM-based classification versus profile curvature range, e) NED-based classification versus relative elevation range, f) SRTM-based classification versus relative elevation range. 221

Figure 5.3. Diagram for the classification tree tested in this study, which was validated in Chapter 4. 223

Figure 5.4. Terrain characteristics of test zones compared to HP classification agreement: original 3 m resolution grid and the same grid aggregated to a) 9 m resolution versus mean slope gradient, b) 27 m resolution classification versus mean slope gradient, c) 9 m resolution versus profile curvature range, d) 27 m resolution versus profile curvature range, e) 9 m resolution classification versus relative elevation range, f) 27 m resolution classification versus relative elevation range. 228

KEY TO ABBREVIATIONS

° - degrees

> - greater than

< - less than

% - percent

bs - backslope

BCE - before the common era

ca. - circa

CE - common era

CI - confidence index

DC - drainage class

DEM - digital elevation model

DTA - digital terrain analysis

ED - excessively drained

e.g. - exempli gratia (for example)

fs - footslope

GIS - geographic information systems

GPS - global positioning system

GRASS - Geographic Resources Analysis Support System

HP - hillslope position

i.e. - id est (that is)

km - kilometers

LDA - linear discriminant analysis

m - meters

MAUP - modifiable area unit problem

MLRA - major land resource area

MWD - moderately well drained

NED - national elevation dataset

OSSD - official soil series description

p. - page

PD - poorly drained

PDF - probability density function

PrcP - profile curvature priority

ReeP - relative elevation priority

RMSE - root mean square error

s.d. - standard deviation

sh - shoulder

SlgP - slope gradient priority

SRTM - Shuttle Radar Topography Mission

SSURGO - Soil Survey Geographic database

su - summit

SPD - somewhat poorly drained

ts - toeslope

U.S. - United States

USDA-NRCS - United States Department of Agriculture, Natural Resources Conservation Service

USGS - United States Geological Survey

U.S.S.R. - Union of Soviet Socialist Republics

VPD - very poorly drained

WD - well drained

CHAPTER 1. INTRODUCTION

The soil-landscape paradigm has been the dominant strategy for mapping soils for more than a century. This paradigm is based on the use of environmental correlations and spatial associations to predict the arrangement of soils from readily observable landscape features and climate data. Using this strategy, the U.S. Soil Survey has mapped practically the entire U.S., and with increasing resolution and accuracy as better base maps have become available. As soil surveyors have increased the resolution and corresponding analysis scale of soil maps, they have shifted to the environmental parameter best suited to predict soil variability at that scale. However, at the smallest analysis scales, the resolution of soil maps has been constrained by resolution of base maps of topography and land cover, and the technology to analyze these data.

The introduction of aerial photography in the 1930s improved the quality of base maps available to soil mappers and geographers to the point that they are now able to delineate individual landforms. As a result, soil map detail and quality markedly improved, illustrating that, for large cartographic scale soil maps, detailed base maps of topography and land cover are a key component of the mapping effort. However, aerial photographs are often not sufficient for differentiating the detailed hillslope positions that are necessary for accurate, high quality soil mapping efforts. Also, the manual process of interpreting aerial photography is time consuming, subjective, and impractical for mapping endeavors of large extents with increased resolution. New technologies, such as LiDAR, provide higher resolution base maps that can be interpreted objectively, by an automated process, but they lack the contextual information traditionally interpreted by soil geographers.

In contrast to aerial photography, newly available digital elevation data has sufficient resolution to identify details of topography and, potentially, to isolate hillslope positions. However, because hillslope position has mainly been used as a conceptual model in the field, the process for classifying hillslope position is currently locked within the tacit knowledge of field mappers in general, and soil scientists in particular. In order to automate the hillslope position component of soil scientists' mental models, parameters in the soil scientists' logic must be quantified and incorporated into digital soil models. Capturing all aspects of soil scientists' determination of hillslope position is a focus of this dissertation.

Although digital soil models have the potential to address some of these needs and concerns, models calibrated in one landscape often have not performed as well in other landscapes. This lack of transferability has been a major obstacle to the widespread use of digital soil models. In contrast, the current, mental model approach can be quickly adapted to new landscapes. Mental models are generally based on the soil-landscape paradigm and are refined by experience. The transferability of mental models is likely explained, at least in part, by the use of contextual parameters that are largely implicit, held within the tacit knowledge of the field soil mapper. Hillslope position is a prime example of a contextually based parameter used to predict soil cover patterns; soil mappers use their notion of slope position, while in the field, as a criterion for differentiating soil bodies. Obtaining this knowledge (of hillslope position) from aerial photographs, is possible, and is commonly done by the mappers in the office, prior to entering the field. However, better base maps that can more accurately delineate hillslope position for the mapper, in a logical, accurate, objective and repeatable manner, would go a long way toward increasing the accuracy and consistency of soil maps.

In order to incorporate this popular parameter for soil scientists' mental models into digital approaches, both explicit and implicit definitions of hillslope position need to be identified. This dissertation attempts to capture the full suite of considerations made by soil scientists in assessing the basic terrain metric of hillslope position, to create a digital model that is as transferable as the mental models they utilize. Specifically, I attempt to capture this expert knowledge by calibrating the analysis scale, classification breaks, and parameter priority of the model, directly to soil scientists' field observations.

In summary, the purpose of this dissertation is to develop a quantitative model for hillslope position. This model can improve soil maps by leveraging the new high resolution elevation data (i.e. LiDAR) and digital terrain analysis to characterize topographic attributes related to soil development, using concepts proven over decades of soil science and soil mapping. The hillslope position classification model can therefore be used under the soil-landscape paradigm, as an automated way to conceptualize topography, thereby increasing the efficiency, consistency, and resolution of soil maps. In addition to identifying common map unit boundaries, this digital model for classifying hillslope positions is useful for studying landscape patterns and designing sampling strategies.

CHAPTER 2. SCALE IN THE CONTEXT OF PROGRESS IN SOIL GEOGRAPHY

Abstract

Over time, the cartographic scale of soil maps has changed, as the geographic technology and the reasons for making the maps have evolved. Coincidently, the environmental factors deemed most important for the prediction of soil patterns have also changed. Advancements in soil science provide some explanation for the shifts in these emphases, but favored predictive factors have also corresponded with the cartographic scale used in soil maps. Before the implementation of Geographic Information Systems, analysis scale (the level of generalization used to measure phenomena) was linked to cartographic scale. Natural phenomena simply operate at different scales, making them more identifiable at certain analysis scales. This paper examines the phenomena scales for the soil formation factors of climate, organisms, relief, and parent material as they affect the spatial variability of soil properties. To accomplish this, I review soil maps that have been created during the history of soil science to determine how distinct categories of cartographic scale have corresponded to the selection of particular environmental predictors. The soil formation factors that soil scientists' found to be the most useful at different cartographic scales provides an empirical indication of the phenomenon scale of those respective factors. I find that small cartographic scale maps have tended to emphasize climate-vegetation zones. Medium cartographic scale maps have put more emphasis on parent material. And finally, large cartographic scale maps have relied more on topography. Recognition of the hierarchy of phenomenon scales is helpful for combining soil formation factors into a holistic understanding of soil geography and pattern.

Keywords: soil, mapping, formation factors, scale, history

1. Introduction

The purpose of this paper is to examine the relationship between soil knowledge and the evolution of soil maps. Specifically, I investigate changes in soil knowledge coinciding with changes in map scale. In order to analyze this relationship, the nature of soil maps must first be examined.

Soil maps, like all maps, are products of the geographer's understanding of the phenomena, geographic technology, and purpose (Brown, 1979; Thrower, 2007). Reviews on the history of soil science have tended to focus on the evolving scientific understanding of soil phenomena. This focus has led to the assumption that soil knowledge and soil classification systems have co-evolved over time (Cline, 1949; Simonson, 1962). However, this assumption overlooks the interaction between soil classification systems and the maps for which they are designed. Shifts in dominant theories may be as much a product of changes in geographic technology (i.e. scale) as actual improvement in soil knowledge.

In order to separate the influences of soil knowledge and geographic technology on soil maps, this paper first demonstrates how the scales of soil maps are dependent upon the available geographic technology (Figure 2.1). Base maps are prerequisite for the production of thematic maps, such as soil maps. Therefore, soil maps have been constrained to the cartographic scales of the available base maps. It then follows that the development of geographic soil principles should be considered in the context of scale. This paper identifies the

scale dependency of soil science concepts that at times in history have been viewed as contradictory.

Soil science made a major advancement in 1883 when Dokuchaev integrated several theories of soil formation by describing soil as the product of the interactions between climate, parent material, organisms, relief, and time (Dokuchaev, 1967). The identification of these factors began a revolution in how soil is conceptualized, studied and mapped (Huggett, 1975; Bockheim et al., 2005). However, an interest in emphasizing one factor over the others has continued, as reflected in the design of early soil classification systems (e.g. Whitney, 1909; Marbut, 1928). These ostensible conflicts in soil science appear less contradictory in the context of scale. Soil knowledge is always advancing. However, soil knowledge has also been focused through the lens of the cartographic scale being used to view the soil landscape. Therefore, progress in soil geographic knowledge will be better understood in the context of scale.

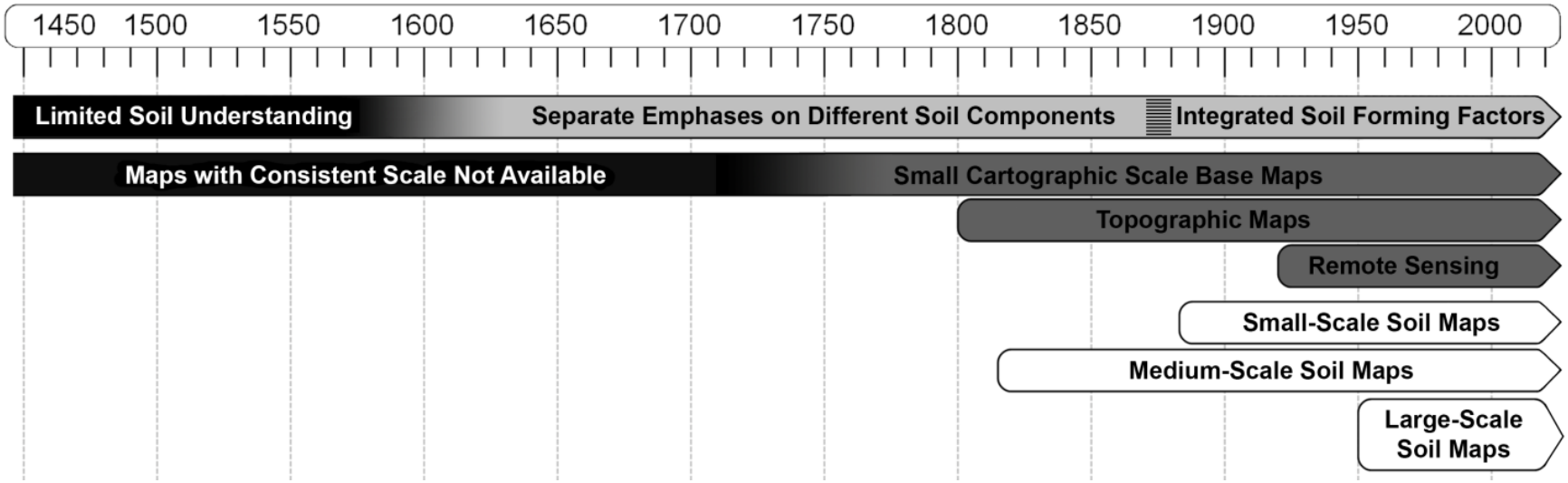


Figure 2.1. Timeline of important developments in the scientific sphere of soil geography. Soil maps (white) are a product of both the scientific understanding of soil (light gray) and the geographic technologies available at the time (dark gray). Although soil geography has been valued since early civilizations, actual soil maps could not be produced until the needed geographic technology was available.

1.2. Background on Scale in Soil Geography

There are multiple types of scale (Montello, 2001). Cartographic scale is the relationship between distance on the map and distance on the Earth. In contrast, analysis scale is the areal size of the map units, or level of generalization. Natural phenomena commonly display geographic structure, which makes a particular phenomenon more detectable at certain analysis scales. Therefore, adjusting analysis scale in order to detect phenomenon scale has been a tool in geography for identifying process scale. When the primary mode of analyzing spatial patterns was paper maps, cartographic and analysis scales were essentially linked. A small cartographic scale necessitated larger analysis scales. Use of broad extent maps, with small cartographic and large analysis scales, revealed only processes operating at large phenomenon scales and vice versa. Because phenomena governing soil development operate at different scales, when modelling soil, it is important to select the appropriate parameters for the scale of interest (Schoorl and Veldkamp, 2006). Because geographic information systems have decoupled cartographic scale from analysis scale, lessons learned in paper maps in terms of cartographic scale, should now be applied in terms of analysis scale.

Patterns observed at one analysis scale are often not observed at other analysis scales. This behavior is known as the scale effect component of the modifiable area unit problem (MAUP) (Armhein, 1995; Jelinski and Wu, 1996). Therefore, higher levels of generalization can in some cases provide more explanation of a spatial variable than levels of higher resolution (Moellering and Tobler, 1972). Once scientific understanding reached the point where soil mappers became aware of the major factors in soil formation, they were free to choose the

environmental predictors that best explain soil variability at the respective cartographic scale. Therefore, the emphasis on different environmental predictors at different cartographic scales reflects soil geographers' mental model of phenomenon scale for factors influencing the spatial distribution of soils. Although Marbut may not have recognized the scale effect of MAUP per se, he described his encounter with this problem in 1928, stating, "When we superpose over a soil map, maps of various kinds of climatic forces, and the various kinds of natural vegetation, we find certain definite relationships. When, however, we superpose a soil map of *mature* soils, a geological map, we find no relationship between the general broad, predominant characteristics of the soils and the characteristics of the geologic formations. In the same way when we superpose a topographic map over a map of mature soils we do not find a relationship. When, however, we superpose a topographic map or a geological map over a soil map on which all soils, both mature and immature, have been mapped, we find a clear relationship between both" (Marbut, 1951, p. 19). Marbut's observations illustrate how different analysis scales of soil will show greater correlation with different soil formation factors.

The current U.S. Soil Survey Manual recognizes different phenomena scales for soil formation factors by describing the distribution of soils as "the result of climate and living organisms acting on parent material, with topography or local relief exerting a modifying influence and with time required for soil-forming processes to act" (Soil Survey Staff, 1993, p. 8). However, the respective phenomenon scales for these soil formation factors has not been formally determined. In order to sort out the conditions driving the use of different cartographic scales at different times, in this paper I review the progress of soil maps in the

context of: 1) scientific understanding and 2) geographic technology (Figure 2.1). Then, by utilizing Keates' (1989) principle that the cartographic art of generalization reflects the knowledge of the map maker, I attempt to identify the phenomenon scale of the various soil forming factors as they have been utilized throughout history.

2. Early Soil Geography (pre-19th Century)

Ever since humans began sowing crops, and perhaps before, we have had a vested interest in the geography of soil. A mental map of where certain soil characteristics existed was likely used in deciding where to live and where to plant crops, as early as Neolithic times. Although the information about soils was probably gathered by trial and error, eventually some rational patterning emerged. Dating back to 3,000 – 2,000 BCE in central India, archeologists have found evidence of farming communities on the fertile black soils formed in the Deccan basalt, but not in the area north where these soils are absent (Shchetenko, 1968). In eastern Switzerland, land use patterns of settlements, fields, meadows, and pastures can be predicted by soil type, for farming systems dating back to 500 BCE (Widgren, 1979). Similarly, archeological sites in the U.S. have demonstrated a preference for drier soils for habitation (Almy, 1978).

The origin of many modern science concepts can be traced back to the Greeks of the Hellenistic Period. Although they did not utilize experimental methods to build certainty in predictions, they were particularly astute at observation. Beginning with Parmenides and Eudoxus (540-470 BCE), the Greeks recognized the connections among similar soils, vegetation, and climates in belts on the Earth (Isachenko, 1971; Krupenikov, 1993). The explorative spirit of

the Greeks between 800 and 300 BCE, somewhat necessitated by the decline of soil quality in Greece (Hillel, 1992), produced several geographical works describing lands of Europe, the Middle East, and North Africa. Included in those documentations are general descriptions of soils found in those travels.

2.1. The Importance of Base Maps

Many of the techniques for making the paper maps we know today began to appear after 600 BCE (Eratosthenes, 2010). However, the preferred method for describing soil geography remained as written narrative. There are two primary reasons for the lack of interest in producing a physical soil map: (1) understanding of soil was very basic and generalized, and (2) base maps of any kind at that time were extremely crude. The manual measurement of distance across land was relatively reliable. However, because a large amount of the geographic data was based on the narrative descriptions of explorers, assembling locations together on a two-dimensional format was not as reliable. For example, Herodotus (484-425 BCE) was highly critical of maps, because of their potential to be misleading. He believed that a map showing Persia as far away convinced the Spartans not to assist in the Ionian Revolt. Instead, he felt that his table of distances -rather than a map- provided more accurate information (Eratosthenes, 2010). The potential for maps to be misleading still exists today (Monmonier, 1996), but the primary issue with maps of any kind during this early time was accurately representing the position of all features consistently. Due to the difficulty in measuring position on the Earth, map scale was very inconsistent within early maps. Even though early maps essentially did not

have a cartographic scale, the relationship between extent and necessary generalization remains consistent with the modern use of map scale terms.

For the reasons described above, maps before 1500 CE were either small-scale, theoretical maps about the Earth or large-scale maps for civil purposes. The small-scale maps were popular with natural philosophers for the purpose of illustrating conceptualizations about the known world (e.g. Eratosthenes' map of the known world, Figure 2.2). Large-scale maps were generally produced for individual cities and for more practical purposes. For example, the Romans surveyed grid systems of "centuries" as a base map for city planning and levying of taxes (Dilke, 1987). Advances by Ptolemy (ca. 100-178 CE) in map projections and coordinate systems (including the prototype for latitude and longitude), greatly improved the utility of maps. However, it would take technological developments, namely the printing press, in the Early Modern period (ca. 1500-1800 CE) to popularize the use of maps per se (Brown, 1979).

2.2. Classification

Classifying the natural world was common practice in ancient Greece, especially after Aristotle's (384-322 BCE) Historia Animalium (Aristotle, 2002). It was a method for organizing complicated information and for debating philosophies. Aristotle's theory of definition set the stage for scientific exploration, by constructing classes by differentia and requiring an explanatory principle to set the definition (Bayer, 1998). Differentia of classes, therefore, require observable differences in characteristics. At different levels of detail, different contrasting properties are more or less important.

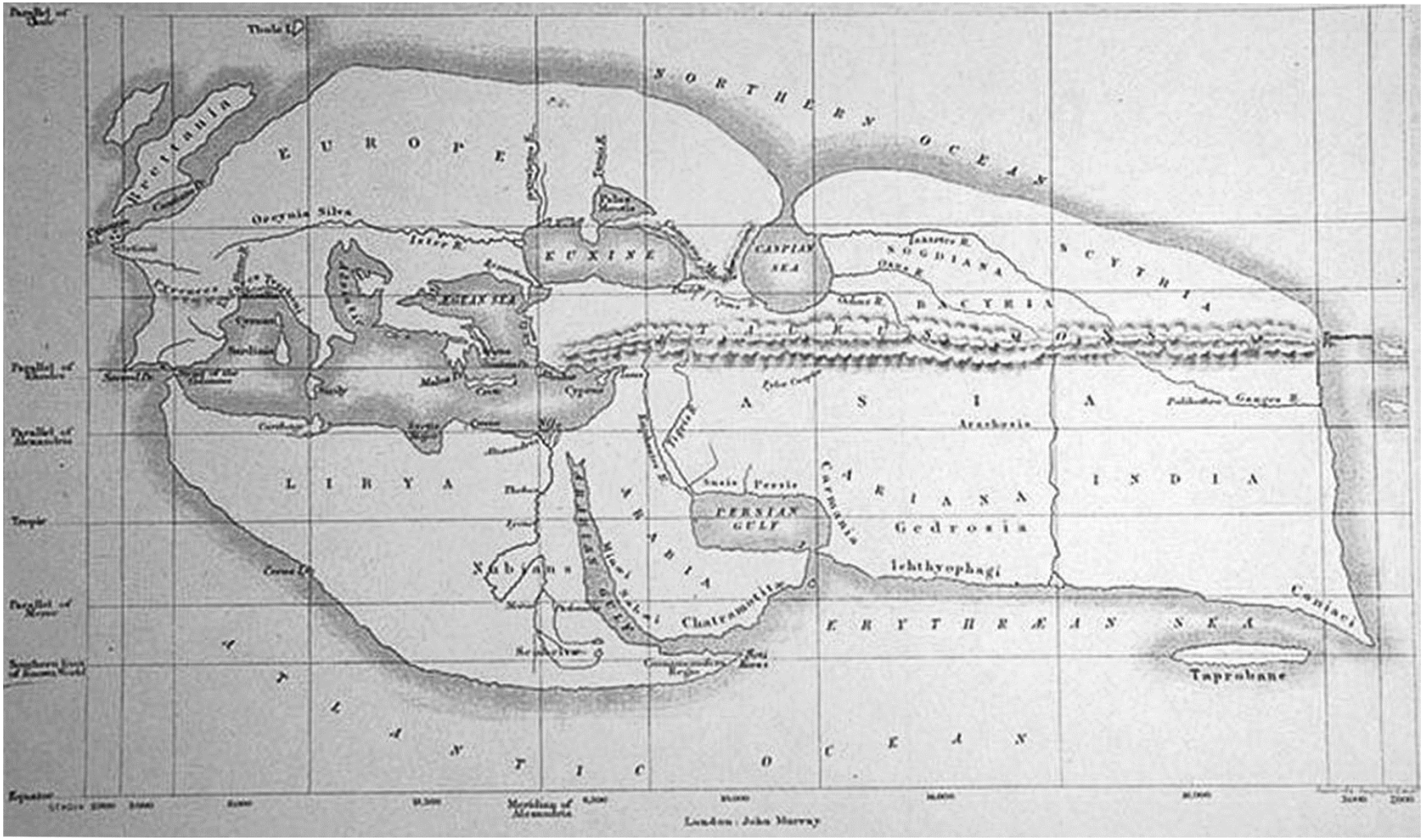


Figure 2.2. Reconstruction of Eratosthenes's map of the known world, ca. 194 BCE (Bunbury, 1883). This map pre-dates the use of cartographic scale. Outline of continents demonstrates the spatial distortion inherent to maps of the time. Labels are inconsequential.

An enduring example of an ancient Greek classification of the natural world is the classification of climates. There is evidence of Pythagoras (ca. 570-495 BCE) and his disciple Parmenides (ca. 540-480 BCE) conceptualizing the earth as a sphere with five climate zones. The central torrid zone was surrounded symmetrically by two temperate zones, which were followed by two frigid zones at the caps of the sphere (Harley and Woodward, 1987; Sanderson, 1999). Building on the work of earlier philosophers, Strabo (ca. 63 BCE – 24 CE) cited many examples of the correlation between climate and crops (Harley and Woodward, 1987). Ptolemy's summarization of the cumulative understanding of latitudinal climate zones are manifested in the reproductions of Ptolemy's world maps in the 16th century (Figure 2.3). Ptolemy extended the observation of climate-biological relationships by stating, "Reason herself asserts that all animals and all plants have a similarity under the same kind of climate" (p. 31, Ptolemy, 1932).

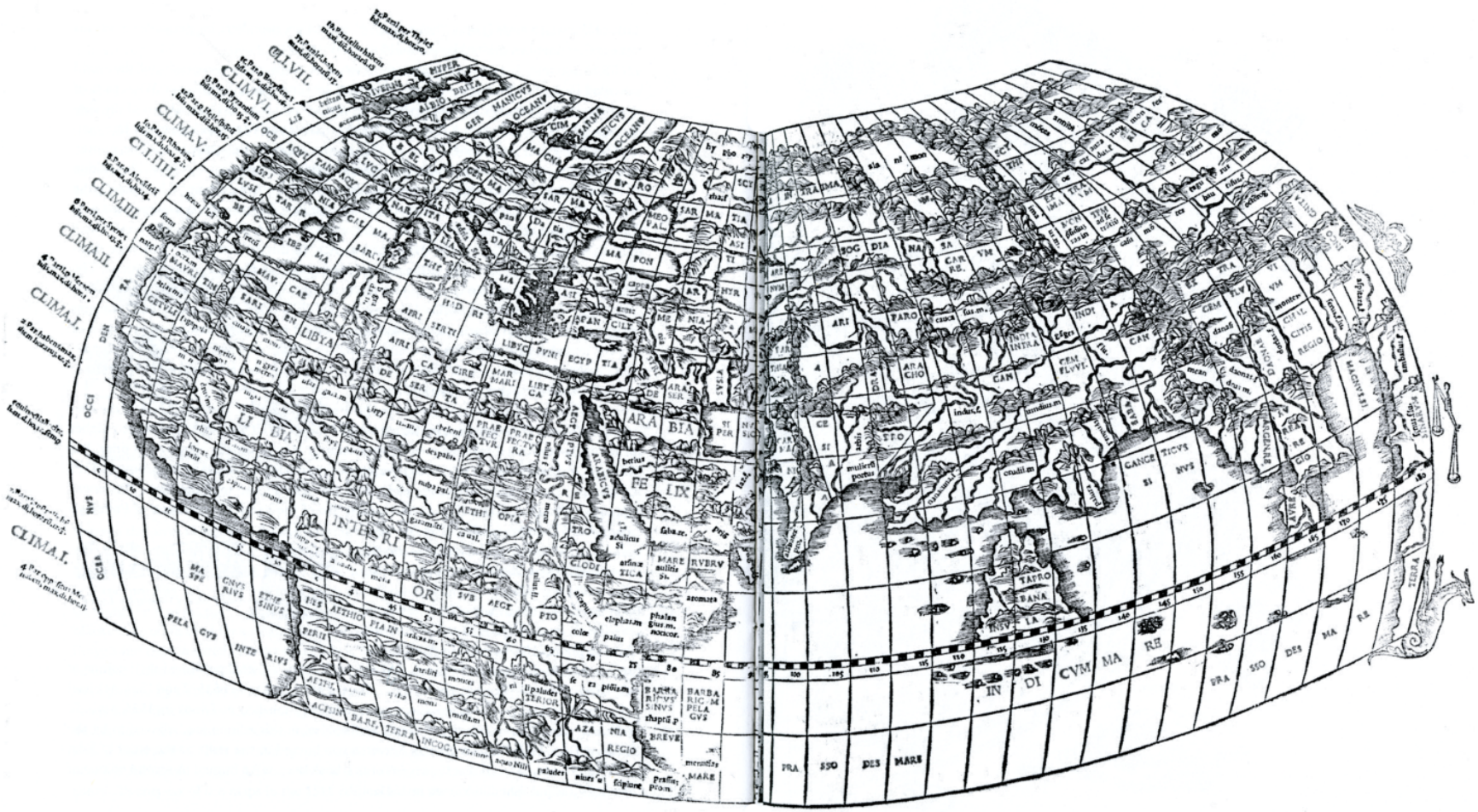


Figure 2.3. Ptolemy's world map with latitudinal climate zones, reproduced by J. Pentius de Leucho (Leucho, 1511). The climate zones are labeled on the western side of the map. "Clima I" is comprised of the two latitude zones north and two zones south of the equator. Each subsequent latitude zone shown, proceeding north, is label sequentially with a different "Clima" number. All other labels are inconsequential. This map pre-dates the use of cartographic scale.

2.3. Understanding of Soil

Limitations in the production, or even the conception of soil maps, were not only constrained by geographic technology, but also by the understanding of soil. Human understanding of soil has slowly improved since the time of the ancients, with only a few revolutionary shifts in perspective. Despite the disadvantage of not having a map, Herodotus (485-425 BCE) understood that the transport of silt from Ethiopia renewed the productivity of the Nile River floodplain (Strabo, 1917). He also described soils by texture and color. Egyptian soils were described as black, in contrast to the red soils of Libya. In Libya, Herodotus differentiated clayey from somewhat stony soils (Krupenikov, 1993). Heavily influenced by Herodotus, Theophrastus (371-287 BCE) also recognized the uniqueness of soil by location (Theophrastus, 1916). He distinguished soil characteristics of light through fatty, as well as limitations of saline soils. Theophrastus observed that different soils react differently to variations of weather and that different crops were better suited for different soils. Extending the soil geography of Theophrastus to predictive indicators, Marcus Cato (234-149 BCE) recalled a point made by Diophanes of Bithynia that, "you can judge whether land is fit for cultivation or not, either from the soil itself or from the vegetation growing on it" (p. 205, Cato, 1934). Strabo (ca. 64 BCE – 24 CE), summarized the work of Greek and Roman natural philosophers in his 17-volume *Geographica*. Included in the text are characterizations of the soils for each of the countries described and the additional description of volcanic soils (Krupenikov, 1993).

Strabo is the last known natural philosopher to give attention to soil geography before the Early Modern period. Even though the knowledge of natural philosophers was not widely

disseminated, academics at the time were nonetheless aware of the spatial variability of soil and its impacts on crops. For the next millennium and half, the primary theory on spatial soil variation remained an emphasis on soil texture with additional indicators from soil color and vegetation at both field and national scales.

3. Emergence of Soil Maps

3.1. Early Maps with Soil Attributes

The earliest known spatial representations, i.e., "mapping," of soil properties were tied to the assessment of land valuation at the scale of parcels or fields. In general, the valuation of land -from which the levying of taxes was based- was assessed by an index of soil productivity. Therefore this soil attribute was associated with documents of land ownership. Although not a soil map per se, the linking of soil data with the spatial information of property boundaries was an advancement toward the creation of a real soil map. Cadastral recordings of soil quality were fairly common in the feudal system of Western Europe for levying taxes. From the 6th to the 15th century, cadastrals in the Arabian Caliphates used soil productivity as a factor (with crop type) to levy taxes (Krupenikov, 1993). In China, the practice of classifying soils by productivity actually extends back to the second century BCE, when Count Hui ordered land to be divided by location and soil productivity (i.e. good, medium, poor) (Bichurin, 1841). Then between approximately 0 and 600 CE, 12 categories of soils were determined on the basis of suitability for growing different crops. From approximately 300 to 1951 CE, China compiled data

on land quality by crop fields, as well as with other physiographic properties, into special geographic descriptions called difanchzhi (Lee, 1921; Zaichikov, 1955).

Throughout this period, cadastral descriptions of soil geography increased in sophistication. By the 17th and 18th century, Swedish cadastral maps contained sufficient information for modern researchers to evaluate land-cover changes, after processing for geometric irregularities (Cousins, 2001). How cadastral maps were improved by reducing subjectivity is illustrated by the cadastral records maintained by Russia during this time, called Pistsovykh knigi. The Pistsovykh knigi surveys are believed to have been modeled after English cadastrals, but instead of being visually assessed, they had standards of assessment decreed from the central government in Moscow (Krupenikov, 1993). The Russian cadastral survey specified assessment every 80 sajenes (170.7 m) by 30 sajenes (64.0 m) for all land that was in estates or otherwise inhabited. Soils were classified as generous, medium, lean, or very lean. Subjectivity was reduced by a system of review and periodic checks against crop yields. After approximately 200 years of iteration, the resulting records were relatively refined works of soil geography (Sobolev, 1943). This cadastral survey is also remarkable for the government's willingness to fund the endeavor, which was expensive for the time (Merzon, 1956).

Although cadastral maps advanced the collection of soil geographic data, they lacked a fundamental theory of prediction and were generally constrained to units of land ownership. It is likely that land assessors had some type of mental model for interpreting the fields they viewed, but like the ancients, lacked a systematic approach to testing those relationships. Modern soil maps differ in that models of prediction are based on extensively tested

observations and a shared understanding of soil systems, not on the limited experience of individual mappers. Also, modern soil maps are no longer bound to property boundaries as base maps. The development of topographic maps would be a key advancement towards the goal of creating soil maps based on process related parameters.

3.2. Base Maps

3.2.1. Determining Location Accurately

Before thematic maps (e.g. geology and soil maps) would be considered viable endeavors, reliable base maps of the landscape needed to be made available. Among the key ingredients for producing a reliable base map was the accurate determination of position. The principles for determining position were mostly worked out by the ancients, but it would take inventions of the 17th century to produce instruments accurate enough to determine position within a few meters. The development of the needed technology was hastened by the Age of Exploration, which began in the 15th century (Brown, 1979). At that time, the calculation of latitude only needed the angular measurement of a celestial body at its maximum height in the sky and the assistance of mathematical tables based on previous observations. However, until devices measuring fractions of seconds were available, the measurement of the angle commonly had an error range of a couple of degrees (equivalent to approximately 100 km per degree, in the mid-latitudes). Important innovations for increasing both the accuracy and precision of measuring celestial angles were filar micrometers and the replacement of alidades with telescopes fitted with cross-hairs. After the invention of accurate devices for measuring

angles, the determination of longitude on land only required the establishment of a celestial clock (Brown, 1979). By 1676, sufficient data had been collected on the eclipses of Jupiter's satellites to be used as a consistent timepiece anywhere in the world.

3.2.2. Surveying

The production of base maps from the improved methods of location determination in the 17th century required the patronage of national governments. With an interest in improving infrastructure, which would in turn increase trade and tax revenue, in 1668 France became the first to sponsor a systematic survey of its lands (Brown, 1979). Without a good, natural map of the country, little information was known on where new canals, roads, and other infrastructure should be built. After establishing a series of points in a line using astronomic observations, detailed topographic surveying could be done, extending out from the established meridian line. Because of the time it took to produce such an accurate survey, the project focused on surveying France's border first. In 1739, seventy years after the meridian line was established, the first survey of France's border was completed. The topographic survey of France continued, requiring the investment of private investors and local governments through time of war. After four generations of the Cassini family had worked on this project, the first general topographic map of France was completed in 1815 (Cartography Associates, 2013) (Figure 2.4). After observing the experiences of France, other countries began initiating their own topographic surveys. By 1730, topographic surveys were underway in Bohemia, Moravia, Silesia, Lombardy, Transylvania, Austria, Hungary, and Germany (Brown, 1979). However, a systematic topographic survey of the U.S. did not start until much later (Wheeler,

1885). Because of the late start in producing accurate topographic surveys of the United States, when the United States Soil Survey would initiate relatively detailed soil mapping a decade later, it would have to do so without the benefit of a topographic base map for many areas (Lapham, 1949).

A dichotomy of small and large scale maps became more evident in the 19th century. By 1810, French geographic engineers were creating detailed contour maps with intervals as small as 2 meters (Robinson, 1971). At the same time, the popular curiosity about the world as a whole drove the creation of maps of large extents (Brown, 1979). The interest and use of small-scale maps in the 19th century is illustrated by the large quantity of atlases produced during this time. For example, Heinrich Berghaus produced the popular Physikalischer Atlas from 1837 to 1892, which contained small-scale maps of geology, hydrography, meteorology (climatology), magnetic fields, phytogeography, zoogeography, and ethnography (Brown, 1979).



Figure 2.4. Section of the first systematically surveyed, topographic map of France, published between 1756 and 1815. Although this map was a milestone for accurate positioning of features, note the lack of elevation information. Cartographic scale was 1:86,400. (National Library of France, 2013)

3.2.3. Thematic Maps

During the Age of Exploration (ca. 15th to 17th century), atlases grew from being a collection of base maps from around the world to also including thematic maps of those places. In 1890, Titov summarized the work of several mid to late 17th century Russian geographers, describing the regularities in the distribution of climate, vegetation, and soils (Krupenikov, 1993). Also in typical atlas style of the time, the French Constantin-François Volney (1757-1820), published *View of the Soils and Climatic Pictures of the United States of America* in 1804. This early physiographic description and map of North America compared Canada with Siberia and the prairies with the Russian steppes (Volney, 1804).

Because of the special equipment and time consuming work of determining accurate locations on the Earth's surface, from their inception, thematic maps (such as geology and soil maps) have generally relied on base maps. Before the 19th century, the hand coloring of illustrations and maps produced by a printing press were specialized professions. In fact, by the 1600s, coloring maps was a fashionable activity for the recreational studying of geography (Brown, 1979). With the new developments in positional accuracy, civil and natural maps became useful base maps on which to add thematic information. When agrogeologists met the newly available, accurate, topographic maps, a new synergy was found. William Smith's 1815 geology and soil map of England was built on printings of John Cary's 1812 topographic map (Figure 2.5). The geological attributes were added by hand, using water colors (University of New Hampshire, 2013). Stanisław Staszic's 1815 geology map of Eastern Europe used the same

approach, coloring topographic maps that were reproduced from earlier cartographers (Grigelis et al., 2011).

The reliance of thematic maps on base maps focused the production of thematic maps at the cartographic scale of the available base maps. The primary sponsors of base map production were national governments interested in outlining the borders of their realm first (Brown, 1979). Therefore, the first available, accurate, base maps were at the cartographic scale best suited for fitting the area of a country on the largest piece of paper available. In order to add detail to the maps, the cartographic scale needed to be increased, which required drawing the maps by adjoining sections of paper (e.g. Figure 2.5). These physical limitations essentially set the cartographic scale for maps in the 18th and 19th centuries. The spirit of the Age of Exploration had the desire to cover more area and include more information in the maps produced. The resulting cartographic scale of the maps was a compromise between that desire and the limitations of the cartographic medium.

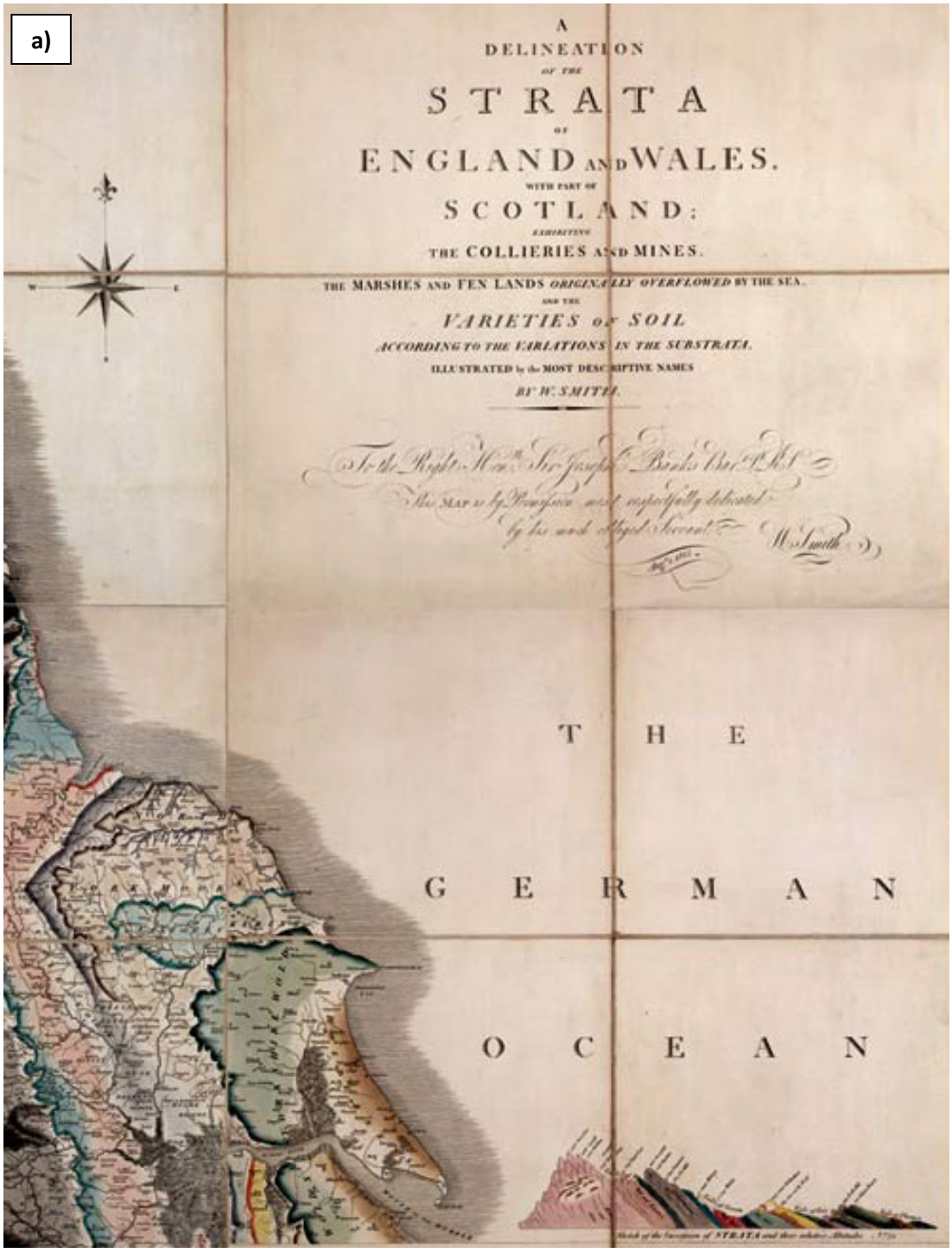


Figure 2.5. The first geological map of Britain, produced by water coloring a pre-existing topographic map. Published by William Smith in 1815 (Library Foundation, Buffalo and Erie County Public Library, 2013). The title claims that by mapping the geologic strata, the varieties of soil are also shown (a). The cartographic scale of the original map (b) was approximately 1:316,000. For interpretation of the references to color in this and all other figures, the reader is referred to the electronic version of this dissertation.

Figure 2.5 (cont'd)



4. Small Cartographic Scale Maps (< 1:1 million)

4.1. Base Maps

Early maps were so speculative that a basic outline of land masses was generally sufficient. However, during ancient times, even the configuration of the continents was highly theoretical. The scientific basis of continent outlines steadily improved during the Early Modern period (ca. 16th to 19th centuries). In 1554, Gerardus Mercator (1512-1594) improved Ptolemy's estimation of the Mediterranean Sea's length from 62° to 53° longitude, which was corrected to 41° longitude by Guillaume Delisle (1675-1726) in 1700 (Brown, 1979). The technology to geographically plot observations and examine generalized spatial patterns was available by the beginning of the 18th century. Although the same technology was needed to produce accurate large-scale maps, it would take much longer to map large areas of extent at that level of detail. For this reason, thematic maps used for scientific study tended to use small cartographic scales through the 19th century.

4.2. Purpose and Strategies of Soil Mapping

Alexander von Humboldt (1769-1859), considered to be one of the founders of geography (Hartshorne, 1958), popularized thematic maps of the world. He chose to use small cartographic scales and the corresponding generalization of details to identify the broad laws relating to the spatial distribution of climate (Robinson and Wallis, 1967). He first introduced isothermal lines when he read his essay on the distribution of heat over the globe before the

Académie Royale des Sciences in 1817. Humboldt based his isotherms on quantitative observations of temperature in the Americas and purposefully ignored small, local differences (Figure 2.6). He then examined the geographic trends of climate and vegetative forms to delineate climate-vegetation zones (Brown, 2006). Wladimir Köppen (1846-1940) later defined climate classifications by extending the work of Humboldt on climate-vegetation relationships (Köppen, 1884).

It is in this context that Vasily Dokuchaev (1846-1903) published his landmark work on the chernozem (Kovda and Dobrovolsky, 1974). Being a geologist by training, Dokuchaev had initially focused on geologic properties to explain the origin and distribution of the chernozem soil. When that approach proved unfruitful, he turned to humus data that had also been collected (Krupenikov, 1993). It is useful to note that the humus data collected was at sites deemed typical for the area. Selectively sampling 'typical' sites follows in the logic of Humboldt for ignoring local variation for the purpose of finding the processes operating across broad extents. Dokuchaev categorized his humus data points cartographically to derive "isohumus belts" (Figure 2.7). In this map, he observed a clear geographic pattern, with the highest humus content of the soils in a central southwest to northeast belt, with successive belts of less humus content to the north and south (Brown, 2006).

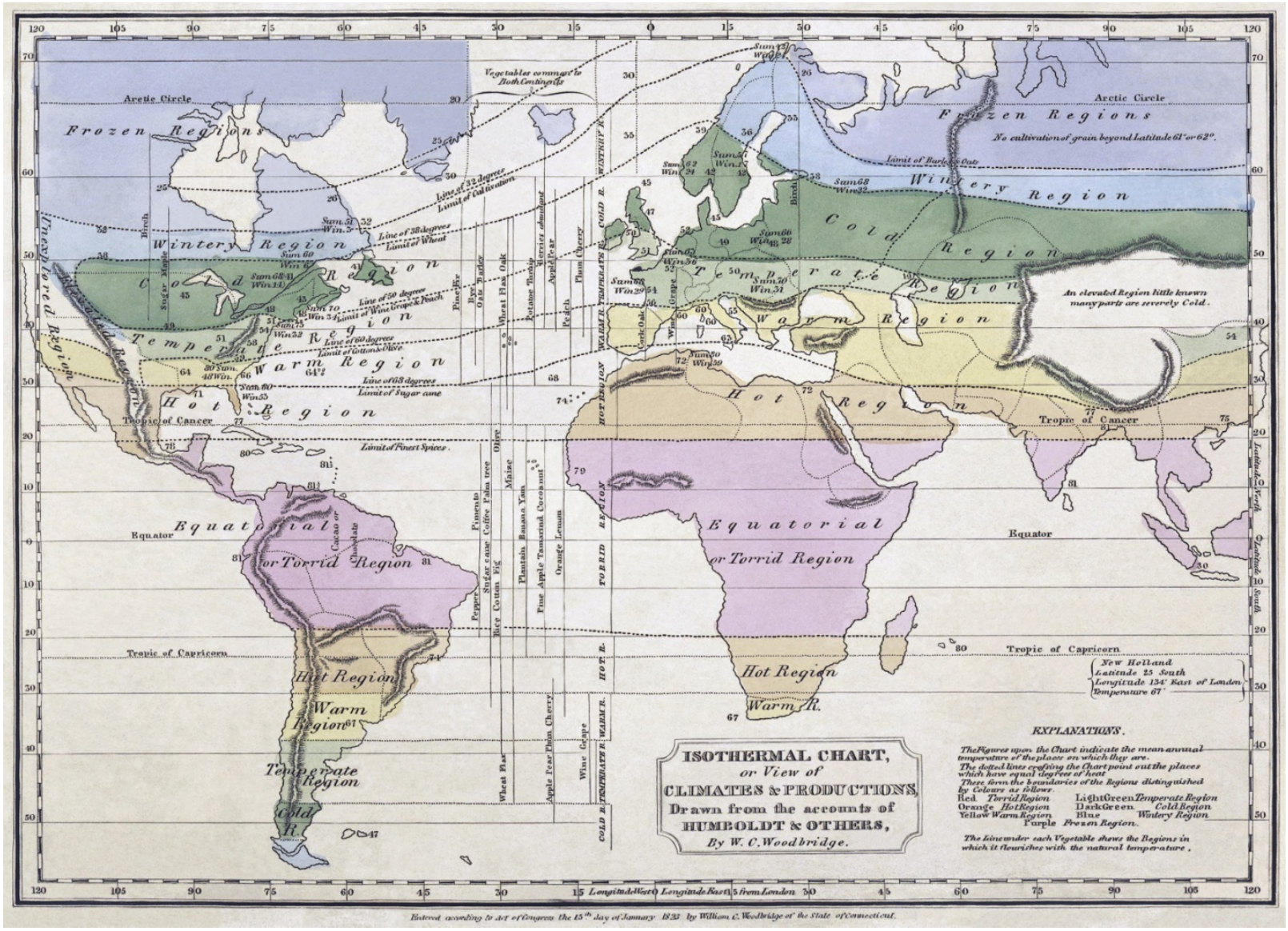


Figure 2.6. Isotherm map of the world, based on the work of Humboldt. Lines dividing colors have similar temperatures and are breaks between climate zones. Labels are inconsequential. Cartographic scale not provided. (Woodbridge, 1823)



Figure 2.7. Isohumus belts identified by Dokuchaev based on quantitative point observations. Darker shading indicates higher content of soil humus. Labels are inconsequential. Cartographic scale was 1:4.2 million. (Dokuchaev, 1967)

Dokuchaev later developed a soil classification system based on his experiences that zones of chernozem corresponded to belts of climate. Continuing from the observations of the ancients, describing climate and vegetation *zones* was still in vogue. With an interest in creating explanatory generalizations, classifying soils in a similar fashion as the Köppen-Geiger climate classification was a logical strategy. In that spirit, Dokuchaev divided soils by normal, transitional, and abnormal (Krupenikov, 1993). Then the classification system subdivided soils by "mode of origin," ranging from vegetative-normal to transported. Vegetative-normal was split according to climate zones and humus content. The first level of the classification system was a mechanism for dealing with scale. Normal soils were comprised of the predominant soil in a zone. Abnormal soils were the exceptions to the generalization.

Several versions of zonal soil classification systems have been used since Dokuchaev, each adapting to local conditions and experimenting with appropriate subdivisions (Krupenikov, 1993). However, all zonal classification systems focus on climate-vegetation relationships, and then use the classification of intrazonal and azonal soils to accommodate the exceptions to the broad soil regions (Baldwin et al., 1938; Duchaufour, 1982). Zonal classification systems identify the corresponding pattern of climate-vegetation zones as the optimal predictor for the general character of soils at large analysis scales. However, recognizing that local hydrologic and geologic phenomena can result in exceptions to the zonal generalization, intrazonal soils are the inclusions that generally cannot be drawn on a small cartographic scale map. Similarly, the exceptions of where the climate and vegetation processes have not had time to alter the parent material are also allowed as exceptions to the generalization, i.e., azonal soils.

Utilizing the concepts of zonal soil classification, geographers began regularly producing soil maps of countries and continents based on climate-vegetation zones. One of the early adopters was Curtis Fletcher Marbut (1863-1935), a student of the famous Harvard physical geographer William Morris Davis (1850-1934) (Davis, 1909; Holmes, 1955; Friend, 2000). While head of the U.S. Soil Survey, but before becoming chief of the Bureau of Soils (Helms, 2002), Marbut produced a generalized soil map of Africa (Figure 2.8), based on soil samples collected by botanist G.L. Shantz. The map used 16 classes of zonal soils at a 1:10 million scale (Shantz and Marbut, 1923). In 1928, Marbut presented a soil classification system to the U.S. Congress, which included zonal soils. Marbut focused his classification system on what he considered to be mature or normal soils. Classification of soils with imperfectly developed profiles or were deemed abnormal due to topography were weakly defined. In other words, undeveloped or abnormal soils were treated as the exceptions to the more important generalized trends of the normal soils. Even though Marbut used soil series as examples of different normal soils, the undefined immature and abnormal soils left the generalized classification system disconnected from the classification used for detailed soil maps (Baldwin et al., 1938).



Figure 2.8. Soil map of Africa based on zonal classification system. Note the pattern similarity between the soil map and the inset rainfall map. Labels are inconsequential. Cartographic scale was 1:10 million. (Shantz and Marbut, 1923).

The first two International Congresses of Soil Science (1927 and 1930) facilitated the widespread use of the bioclimatic-soil relationship for creating small cartographic scale soil maps. In the years following these meetings, many countries established soil surveying agencies and began mapping soils at small cartographic scales, in the Dokuchaevan zonal style. Among those, J. Prescott produced a map of Australia (1933). In 1936, the Russian V. Agafonoff published a soil map of France at a 1:2.5 million scale (Legros, 2006). At China's invitation, the American J. Thorp with a team of young Chinese pedologists mapped the soil zones of China at 1:7.5 million scale (Thorp, 1936; Gong et al., 2010). In 1937, a soil map of Europe was produced at a scale of 1:2.5 million (Stremme, 1997). The *Great Soviet World Atlas* is noteworthy from this time period because of the combination of maps presented (Gorkin and Schmidt, 1938). In addition to a 1:50 million soil map of the world, the atlas also included geologic, climate, and botanical maps at the same scale, for comparison. This atlas also contained a hierarchy of soil map scales. For the U.S.S.R., the increasing cartographic scales went from 1:15 million with 27 map units to 1:7.5 million with 31 map units.

The early 20th century explosion in the production of small cartographic scale soil maps was an extension of the Age of Exploration. Of course an underlying motivator was the discovery and planned exploitation of natural resources. However, this was also mixed with the Humboldtian tradition of scientific interest in identifying generalized laws that enhanced understanding of our world. Small cartographic scale maps using the zonal soil classifications satisfied the purpose for both of these motivations.

5. Medium Cartographic Scale Maps (1:1 million to 1:25,000)

5.1 Base Maps

Early soil mapping in the agrogeology tradition (emphasis on parent material) was generally interested in producing more detailed maps than the deductive approach of small-scale maps. Although interested in producing maps specific enough to provide guidance for crop selection (Whitney, 1900; Whitney, 1909), the coarse resolution of available base maps prevented early detailed soil maps from using large cartographic scales (Simonson, 1952). When the U.S. Soil Survey began in 1899, it had very little to work with in terms of base maps. The U.S. Geological Survey had produced topographic maps for only a small portion of the United States, generally focusing on areas of interest for mineral mining, irrigation, and land reclamation (Brown, 1979). The typical kit for U.S. soil surveyors included a six foot soil auger with extensions, a shovel, a compass, protractor and scale, and "a copy of the usually inadequate county or other available base map" (Lapham, 1949, p. 12). Soil boundaries were determined by frequent borings. When a topographic map wasn't available, soil boundaries would be sketched on a blank plat book. The plat books were generally based on the General Land Office surveys, which commonly had many errors (Lapham, 1949).

5.2. Purpose and Strategies for Soil Mapping

In contrast to making geographic generalizations across a large territory, at the turn of the 20th century, countries like the United States and Britain focused on mapping soils for smaller areas. Sir Edward Russell (1872-1965) and Sir A.D. Hall (1864-1942) acknowledged the

Russian climatic approach for describing soil variability at the continental scale by citing N. Tulaikoff's 1909 paper. However, they considered the climate of England to be relatively uniform and believed the long cropping history had obliterated native vegetation influences (Krupenikov, 1993). At the scale of the soil map they were creating, "it was a matter of experience that within the district there was a general correlation between soils and geological outcrop" (Hall and Russell, 1912, p. 186). Recognizing that generalizations were still needed, Hall and Russell avoided sampling exceptions to general trends such as steep slopes, hallows, and stream beds. Also, they noted that their map should be interpreted "in the light of local conditions, such as climate, water supply, and drainage" (Hall and Russell, 1912, p. 185).

In the U.S., the earliest effort recorded to map soil was in 1820, when the agricultural society of Albany County, New York, sponsored a geological survey (Coffey, 1911). The classification system in the resulting map divided the soil by transported (alluvion) and untransported (geest) soil. The untransported soil was then subdivided into five categories based on texture and relative landscape position. In 1882, T.C. Chamberlain produced the first map in the United States with 'soil' explicitly in the title. Chamberlain's *General Map of the Soils of Wisconsin* shows a strong influence from geology (Figure 2.9), with landscape cross-sections and eight soil classes, predominately based on texture (Tandarich, 2001; Hartemink et al., 2012). Although cartographic scales were not provided for these maps, they covered smaller extents than the small cartographic scale soil maps of the time.



Figure 2.9. General soil map of Wisconsin produced in the agrogeology style by Chamberlain. Shades of brown indicate different soil textures, the pattern of which can be compared to modern soil region maps (Figure 2.11). Map text is inconsequential. Cartographic scale not provided. (Chamberlain, 1882)

During M. Whitney's tenure as chief, the U.S. Bureau of Soils conducted extensive surveys at a cartographic scale of approximately 1:60,000 (Figure 2.10). These maps were in the agrogeology style of classifying soils by parent material, using data on soil physics and chemistry (Kellogg, 1974; Brevik, 2002). Whitney implemented a system of grouping soils of similar geologic material, but with different textures, into soil series. The series concept was modeled after geologists' use of the term for grouping a succession of beds in a sedimentary deposit with varying textures (Simonson, 1997). Today, the early concept of soil series is more analogous to soil associations in the U.S. Soil Survey. Statewide maps of soil associations, or more generalized soil regions, resemble updated versions of early agrogeology soil maps, and are popular educational tools for surface geology (Figure 2.11 and 2.12). The earlier soil map of Wisconsin (Figure 2.9) primarily differs from the modern soil regions map of Wisconsin due to more accurate spatial information. Both Wisconsin maps display similar patterns related to the spatial distribution of geologic/parent materials.

In the late 19th century, several countries began to increase the cartographic scale of their soil maps. Most of these efforts used medium cartographic scales and agrogeology style classifications (Krupenikov, 1993). For example, between 1870 and 1890, maps of parts of Prussia were produced at scales up to 1:25,000. In these Prussian soil maps, "diluvium" (moraine soils) were divided into 14 categories and alluvial soils into 32 geologic formations (e.g. valley alluvial sand). The map units indicated color, texture, structure, and physical condition.

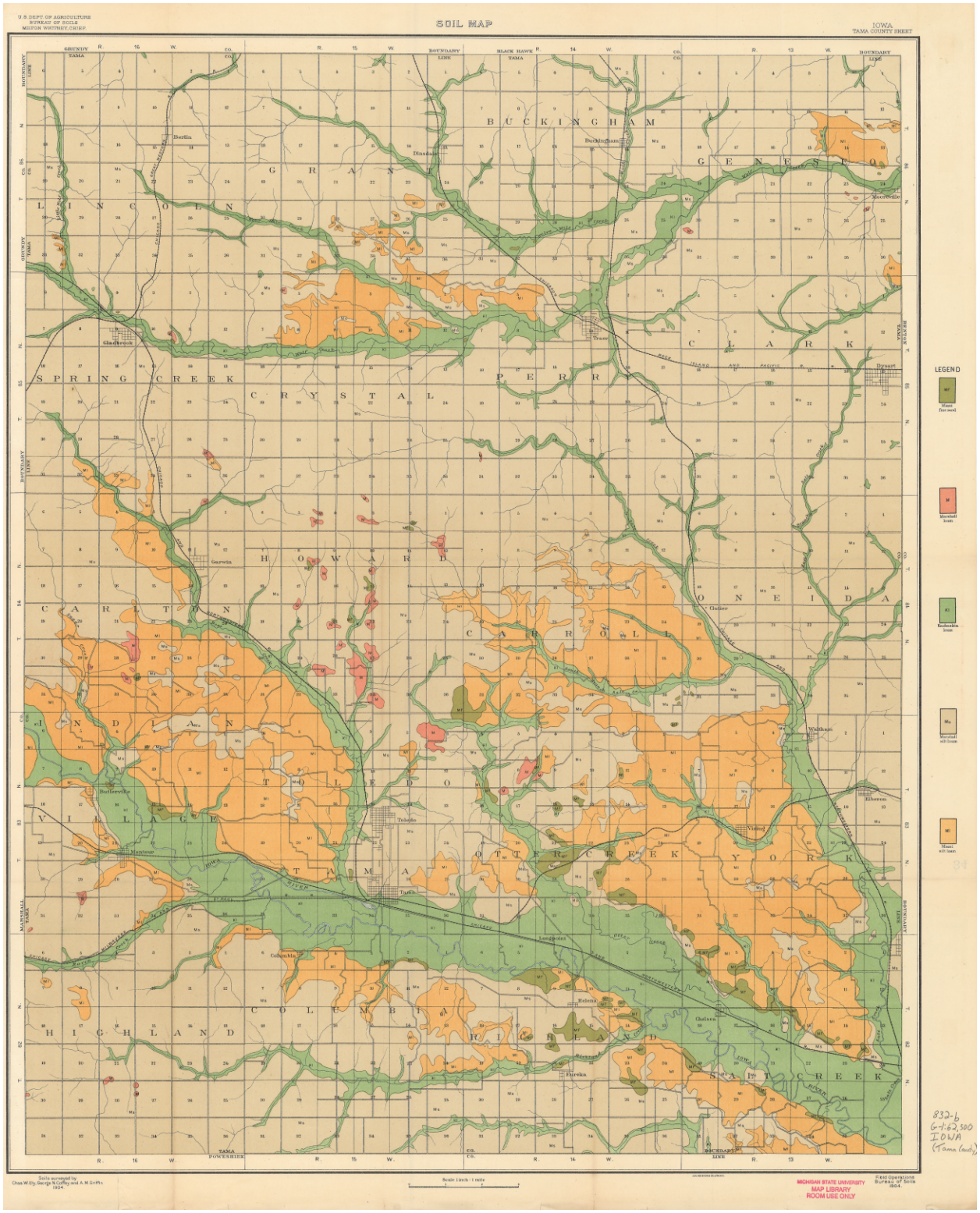


Figure 2.10. Soil map of Tama County, Iowa produced at a cartographic scale of 1:63,360 (Ely et al., 1904). Only five map units are delineated, which primarily differ in parent material. Variation of soils due to climate or relief is not included. Map text is inconsequential.

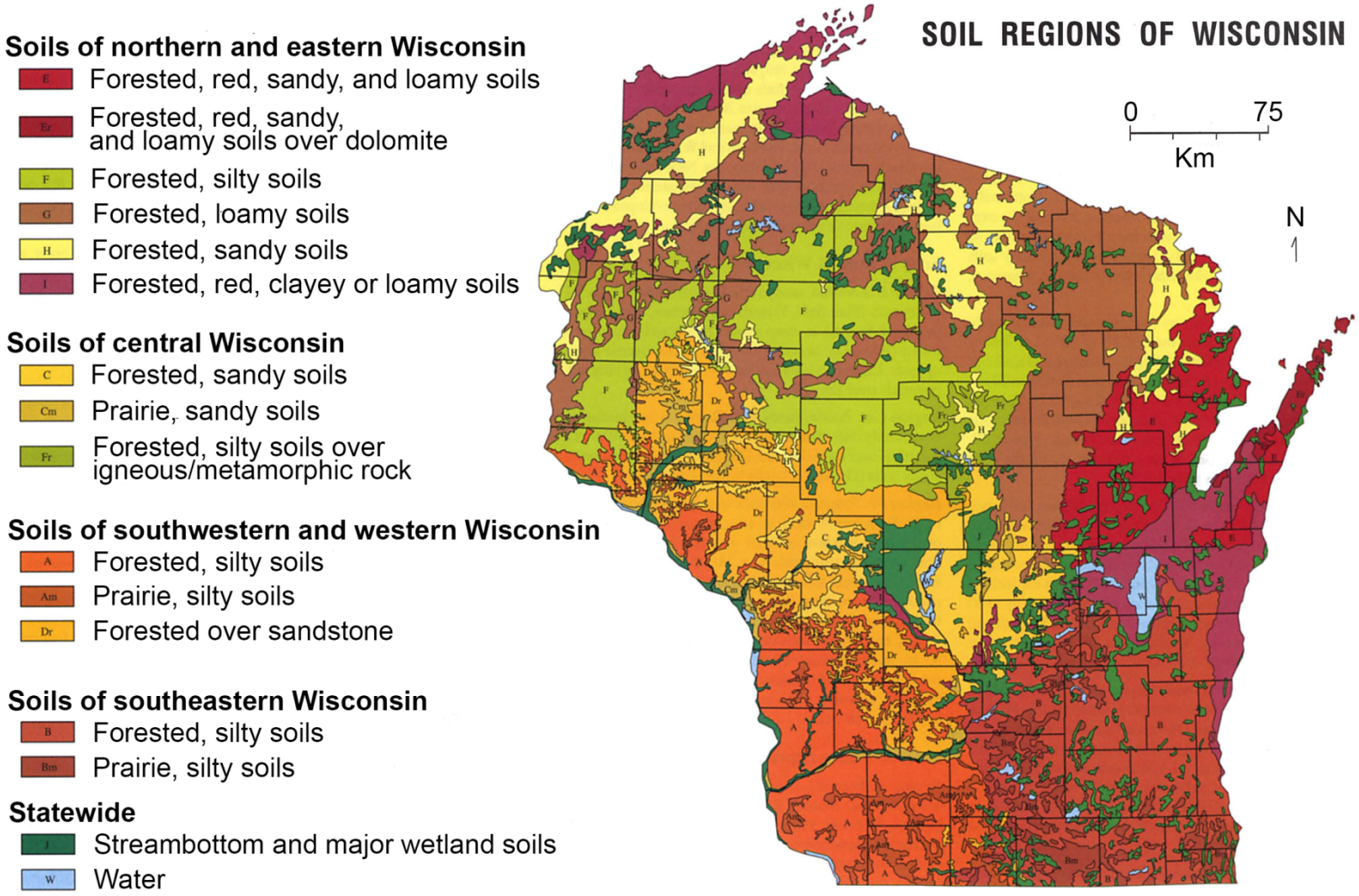


Figure 2.11. Soil regions of Wisconsin map published by the Wisconsin Geological and Natural History Survey. Cartographic scale was 1:710,000 (Madison and Gundlach, 1993). The spatial patterns in this map are very similar to the patterns in the earlier, agrogeology style soil map of Wisconsin. The two maps primarily differ due to more accurate spatial information being available for the modern soil map.

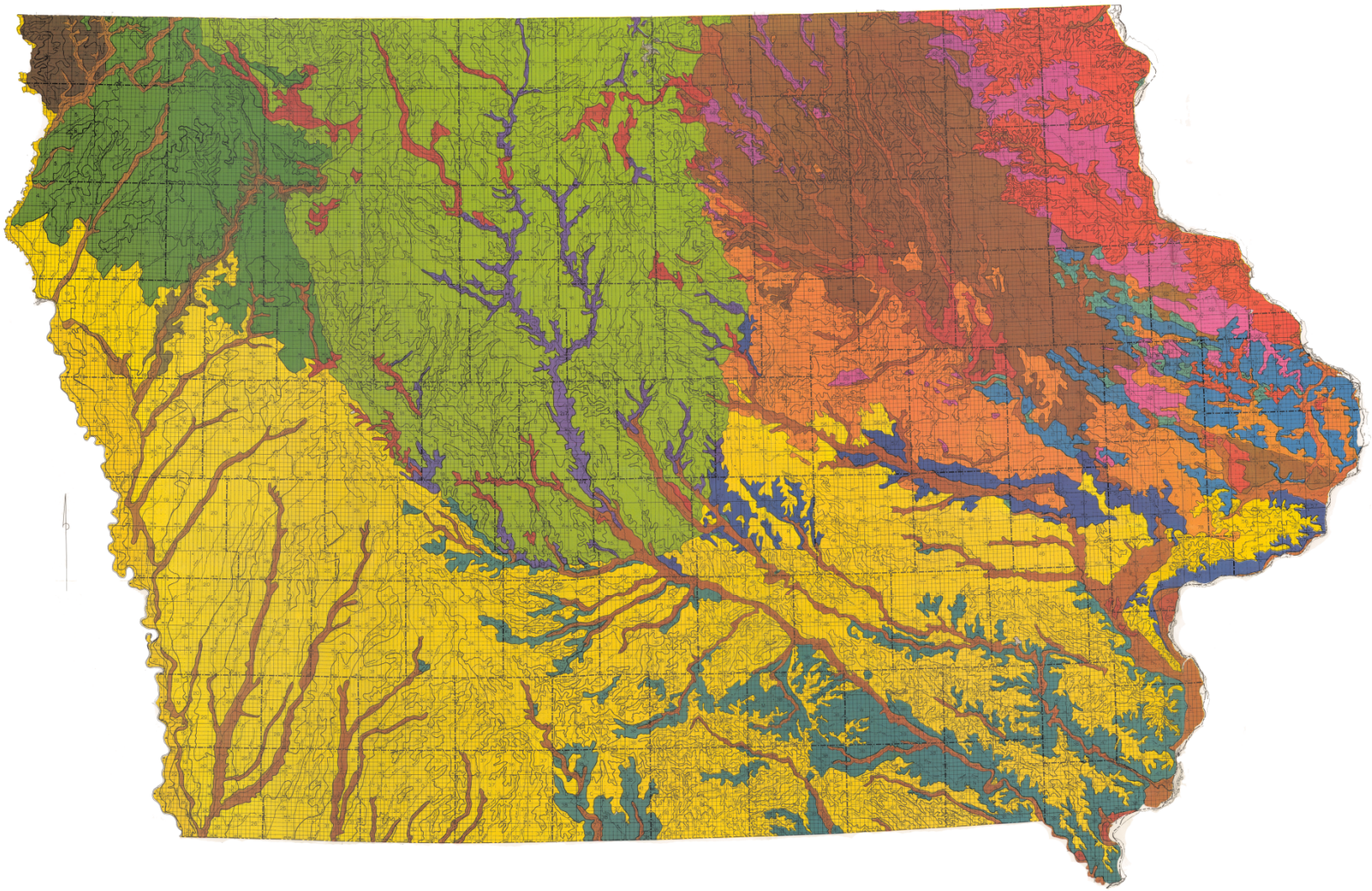


Figure 2.12. Soil associations of Iowa map published by the Iowa Agriculture and Home Economics Station. Cartographic scale was 1:506,880 (National Cooperative Soil Survey, 1978). This state soil map has a level of detail similar to the contemporary soil map of Wisconsin (Figure 2.11). The legend of this map is too large to be included in this dissertation format. However, both the Iowa Soil Association Map and the Soil Regions of Wisconsin map primarily represent the spatial distribution of geologic/parent materials.

Nonetheless, schools of soil science that had begun at smaller cartographic scales did not remain static. After the establishment of climate-vegetation based, small-scale soil maps, Russian soil scientists began to experiment with using other factors for differentiating soil groups for higher resolution soil maps. For example, L. Prasolov subdivided previous soil zones of European Russia into 35 regions based on the criteria of parent material and landscape relief (1922).

5.3. Overlap in Phenomena Scales

The choice of emphasizing parent material or climate-vegetation relationships has been a contentious debate over the history of soil science (Cline, 1977; Krupenikov, 1993). For the most part, the two perspectives correspond to respective cartographic scale, which was also a function of map purpose. However, the divide between maps emphasizing parent material and those emphasizing climate-vegetation relationships is blurry. Although soil maps at medium cartographic scales have mostly focused on parent material, vegetation influences are sometimes included. For example, in the recent 1:710,000 scale, *Soil Regions of Wisconsin* map, a few map units are subdivided between forest and prairie vegetation (Figure 2.11). This map is at the smaller end of the medium cartographic scale map spectrum, covering an area large enough for part of the geographic structure of the bioclimatic phenomenon to be observed.

6. Large Cartographic Scale Maps (1:25,000 and larger)

6.1. Base Maps

The ability to locate features accurately and with greater detail in soil surveys was markedly enhanced by the use of aerial photography. Many advances during World War I improved the utility of aerial photographs for map making (Smith, 1985). Soon thereafter, the U.S. Geological Survey began using aerial photography for making topographic maps (Davey, 1935). Aerial photography for soil survey work was proposed as early as 1923 (Cobb, 1923), but the Bureau of Chemistry and Soils showed little interest in taking on the expense. Thomas Bushnell (1899-1976) compared soil mapping with and without aerial photography, and made three main points on the advantages of using aerial photography: 1) improved consistency, 2) reduced cartographic demands for the determination of location, and 3) improved accuracy, in a manner that could be reviewed. Despite the clear advantages to using aerial photography, Bushnell understood why aerial photography for soil surveying would not be officially adopted for quite some time. The foremost of those reasons was the inertia in current procedures for soil mapping. Bushnell also noted that the contemporary American Association of Soil Surveyors was more about soil science than survey science. He was not critical of pedon-based research, but prophetically commented that the association would be more aptly named the Soil Science Society. Regarding the focus of the American Association of Soil Surveyors, Bushnell observed that "Soil Survey – apparently intended to imply a 50-50 balance between the Soil and the Survey – It is about like Mutt's rabbit hash – 50-50 mixture of rabbit and horse – 1 horse

and 1 rabbit. In our association the soil study has grown to the size of a ton horse and the survey has shrunken to the size of a small cottontail" (Bushnell, 1929, p. 23).

The use of aerial photography in soil survey operations in the United States was gradually adopted as commercial aerial photography (Bushnell, 1932) or state level aerial photographs became more widely available. Michigan was the first to report use of a mirror stereoscope in soil mapping, allowing for soil boundary determinations over areas that were thick in vegetation or otherwise difficult to traverse (Millar, 1932). In 1951, standards for interpreting aerial photographs were added to the U.S. Soil Survey Manual (Soil Survey Staff, 1951). By the end of the 20th century it would be common practice for the U.S. Soil Survey to use aerial photographs taken with a 153 millimeter lens, resulting in a 23 centimeter square image with a scale between 1:38,000 and 1:80,000 (Soil Survey Staff, 1993).

Aerial photography improved the U.S. Soil Survey products by facilitating greater detail and accuracy in the maps produced. However, some have criticized the U.S. Soil Survey for not increasing the efficiency of soil mapping by continuing to require extensive ground observations and field sampling of every delineation (e.g. Brown, 2006). On the other hand, Pomerening and Cline (1953) compared aerial photo interpretation with field mapping. They found that soil series were mapped correctly 84% of the time for field mapping, but only 66% of the time for aerial photo interpretation without field reconnaissance. A similar pattern continued for individual soil attributes such as drainage class, parent material, and land use capability.

Even though aerial photography had greatly increased the level of detail that could be practically included in a soil map, there were still limits. Richard Arnold (1929-) (2006)

summarized the practical limits of minimum delineation size on paper maps as being relative to the legibility of identifying symbols and colors, as well as levels of spatial accuracy. For example, errors of location and internal composition increase as delineation size decreases. Therefore, the decision of cartographic scale depends on the purpose, degree of boundary precision, and the maximum amount of acceptable error. In the U.S. Soil Survey program, those limits are expressed by definitions of map orders (Schoeneberger at al., 2012).

Today, geographic information systems have eliminated the issue of legibility limiting the minimum delineation size, but it has not eliminated issues of spatial accuracy. Remote sensing and geographic information systems, beginning in the latter half of the 20th century and continuing today, are revolutionizing how geographic information is displayed and improving the quality of base maps. These new opportunities challenge our understanding of the soil landscape and how to best represent that knowledge on new soil maps.

6.2. Purpose and Strategies

Almost immediately after Dokuchaev published his small cartographic scale map of chernozems, Russian soil scientists began producing larger scale maps in select locations, to improve land assessment and address local agricultural problems (Krupenikov, 1993). Nikolai Sibirtsev (1860-1900), a student of Dokuchaev, conducted detailed soil surveys and discovered the need to subdivide landscape components at finer scales. For these more detailed surveys, he began to use topographic features for drawing soil boundaries (Sibirtsev, 1966). Since that time, Russian scientists have continued to study the spatial patterns of soil with respect to elements of relief, culminating in the concept of elementary soil areals, forming a soil mantle

structure (Fridland, 1974). V.M. Fridland observed that the repeating, geographic structure of elementary soil areals is only seen by the creation of detailed, large cartographic scale maps.

Soil geographers in the U.S. had a similar experience to the Russians as they created maps with increasing detail. Even before aerial photography was widely available, U.S. soil surveyors worked to increase the level of detail in soil maps to provide support for land use and management. As early as 1902, U.S. soil scientists began observing topography related soil patterns within parent material based map units (Marean, 1902; Bushnell, 1943). Simonson (1952) illustrated the progress of increasing soil map detail, using Tama County, Iowa as an example. Between 1904 and 1938, the number of map units for the 1,800 km^2 county increased from five to fifty. In 1904, a soil surveyor could map 13 km^2/day. By the 1950s, a soil surveyor would only map between one to three km^2/day. With the more detailed soil maps, the rate of mapping depended on the complexity of the soil pattern and readily observable features in the aerial photograph (i.e. topography). The description of relief in the first U.S. Soil Survey Manual (Kellogg, 1937) illustrates the detail limitation for the cartographic scale of soil maps being produced at the time. Relief was categorized as normal, flat upland, hilly, and flat lowland. Because the U.S. Soil Survey was beginning to map delineations small enough to capture components of landforms, a very brief note is included on length of slopes and curvature modifying soils. As soon as the level of soil map detail began to increase in 1904, U.S. soil geographers began having problems with emphasizing parent material for explaining the spatial variability of soils (Simonson, 1991). Encountering these problems instigated a reevaluation of soil science concepts.

A landmark in recognizing topographic differentia in soil mapping was the establishment of the term “catena.” The term was introduced by Geoffrey Milne (1898-1942), who implemented the concept while assigned the task of constructing two soil maps of East Africa, each for separate purposes: 1) a detailed (large cartographic scale) map for agricultural management, and 2) a regional (small cartographic scale) map for inclusion in a world soil map. To aid in the production of the large cartographic scale map, Milne observed repeating patterns of soils on similar hillslope positions. Seeing the general benefits to utilizing topographic soil cover patterns, Milne defined the concept of a catena as “a unit of mapping convenience…, a grouping of soils which while they fall wide apart in a natural system of classification on account of fundamental and morphological differences, are yet linked in their occurrence by conditions of topography and are repeated in the same relationship to each other wherever the same conditions are met with” (Milne, 1935a, p. 197). Milne’s original proposal of a catena was for mapping soil complexes with repeating internal patterns. The limitation of mapping soil complexes, instead of individual soils within the pattern, was probably due to the limitation in base maps of sufficient quality. When Milne learned of soil geographers in the U.S. mapping the component soils of a repeating pattern based on the catena concept, he thought it an appropriate extension of his original proposal (Bushnell, 1943).

Early in the development of large-scale soil maps, soil scientists focused their attention on the study of pedogenic processes controlled by topography. The processes identified by Milne were erosion-deposition (Milne, 1936) and corresponding changes in parent material (Milne, 1935b). In Canada, John Ellis (1890-1973) then described the influence of topography on hydrologic flow pathways, resulting in differences in drainage and corresponding soil properties

(Ellis, 1938). These early studies on topographic relationships to pedogenesis and resulting soil properties have been expanded upon by many researchers (e.g. Ruhe and Walker, 1968; Walker and Ruhe, 1968; Kleiss, 1970; Furley, 1971; Malo et al., 1974; Hall, 1983; Gregorich and Anderson, 1985; Donald et al., 1993; Stolt et al., 1993).

Taking advantage of improving aerial photographs as base maps, some countries have been producing maps at larger cartographic scales. Utilizing topographic-soil relationships identifiable in aerial photographs, the U.S. Soil Survey has mapped the majority of its territory at cartographic scales between 1:12,000 to 1:24,000 (Figure 2.13) (Soil Survey Staff, 2013). Few countries have mapped soils at this level of detail, with field verification, for such large extents. With the exception of several countries in southeastern Europe, most European countries have only mapped select areas with particular land use management needs at large cartographic scales (Bullock et al., 2005). Countries that have mapped soil at scales greater than 1:65,000 have done so with soil series being the lowest order of classification. That concept of soil series, like the U.S. concept, has evolved from grouping soils with similar parent materials to subdividing by differences in profile characteristics caused by relief or other external features (Hollis and Avery, 1997).

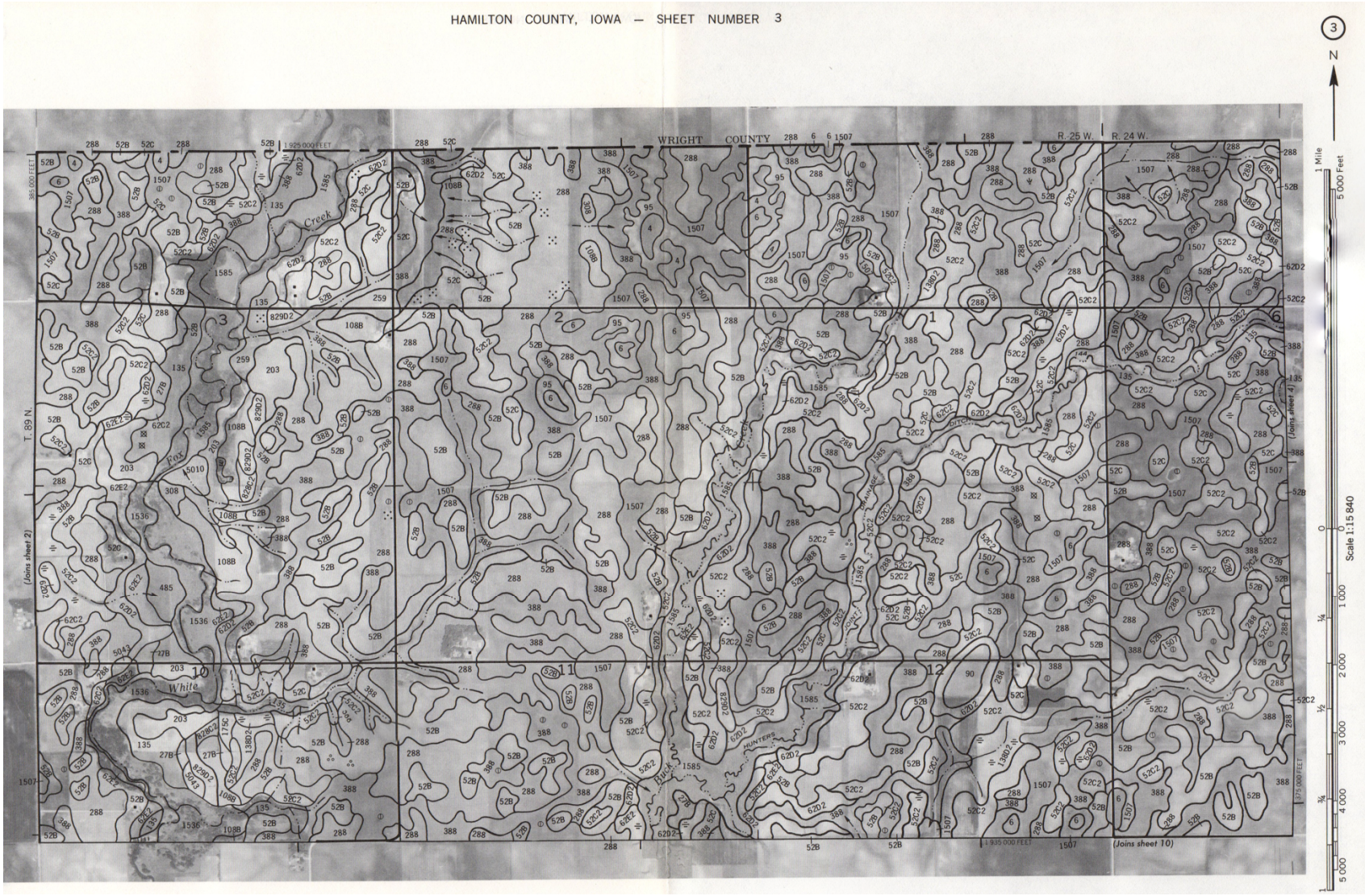


Figure 2.13. Section of Hamilton County, Iowa soil map, constructed at the commonly used cartographic scale of 1:15,840 (Dideriksen, 1986). Note that although topographic features are being delineated, topographic sequences are not distinguishable in the aerial photograph base map. Map unit labels are inconsequential.

6.3. Local Modification of Larger Scale Phenomenon

Larger scale phenomenon, such as climate-vegetation zones and physiographic regions, are obviously modified locally by topography. Topography modifies local climate and vegetation communities by directing hydrologic flow (Ellis, 1938) and controlling the amount of insolation received (Hunckler and Schaetzl, 1997; Beaudette and O'Green, 2009). Topography also modifies the spatial pattern of surface geology by exposing different stratigraphic units across hillslopes (Ruhe et al., 1967) and sorting of transported sediments (Milne, 1936; Schaetzl 2013). These local exceptions do not invalidate generalizations. The purpose of generalization is to provide the map user with the most important information that can be represented at the given cartographic scale (Keates, 1989). Generalization is also a tool in the deductive approach of science of utilizing broadly applicable theories to identify exceptions, which become new areas of inquiry. Considering levels of generalization, corresponding to phenomenon scale, add increasing spatial accuracy to our understanding of natural phenomena.

6.4. Untapped Potential

Under the theory that soil classification -and by association, soil maps- have evolved with improved understanding of soil, the identification of topographic-soil relationships was in itself an advancement of soil science. However, this advancement in understanding also coincided with increases in cartographic scale and the availability of better base maps. As illustrated by the examples in this paper, the level of detail in a soil map is often dependent upon the level of detail in the available base map. By 1952, the transition to aerial photographs as base maps allowed the progression of detailed soil maps in the U.S. from a cartographic scale

of 1:63,360 to 1:24,000 (Simonson, 1952). Today, many of the U.S. Soil Survey maps are available at a cartographic scale of 1:15,840, but the corresponding minimum delineation size of one hectare leaves many delineations as soil complexes (Soil Survey Division Staff, 1993).

Geomorphic studies of landscapes have demonstrated the predictable patterning of soil distributions that exists due to the interaction of topography and pedogenic processes (Milne, 1936; Ellis, 1938; Walker and Ruhe, 1968; Steinwand and Fenton, 1995). For this reason, dividing the landscape into toposequences or geomorphic components has become standard practice in soil science research (e.g. Young and Hammer, 2000; Zebarth et al., 2002; Martin and Timmer, 2006; Vanwalleghem et al., 2010). Although not perfectly suited for all landscapes, the most commonly used descriptors of topographic process zones are the five hillslope profile elements described in the *Handbook of Soil Science* (Wysocki et al., 2000).

The resources for delineating all five hillslope profile elements on large cartographic scale maps have not been available in the past. Instead, delineation of topographic soil cover patterns has often been limited to the light-dark patterns visible in aerial photographs (Figure 2.13), analogous to high ground – low ground landscape elements (Bushnell, 1943). The result has been the use of only two or three topographic units in differentiating soils in many areas, compared to the five units commonly used in studies of toposequences (Figure 2.14).

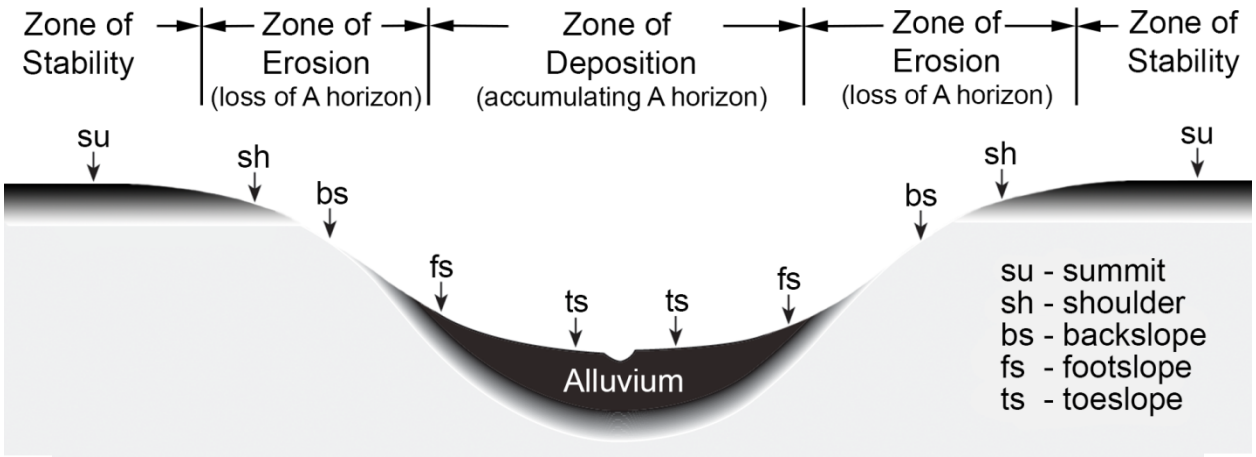


Figure 2.14. Illustration demonstrating the difference in detail between delineating light-dark soil cover patterns (corresponding to erosion-deposition zones) and the five hillslope positions commonly used in toposequences research.

Although remote sensing technology has continued to improve, the resources to manually enhance soil delineations are unlikely to be forthcoming. The recent advent of high resolution digital elevation data combined with digital terrain analysis provides an opportunity to complete the progression of applying observed process scales to improve soil maps. While some have advocated a purely continuous field approach to producing more detailed soil maps (Heuvelink and Webster, 2001; Grunwald, 2003), others view the continuous field and discrete classification approaches as complimentary (Biondi et al., 2004; Ibáñez et al., 2005; Ibáñez and Saldaña, 2008). Continuing the strategies used by past soil geographers, particularly the concept of soil as a natural body, to create detailed soil maps at the current level of understanding process scale offers an untapped potential for analyzing geographic patterns (e.g. Fridland, 1974; Fridland, 1976; Hole, 1978; Hole and Campbell, 1985).

Global positioning systems (GPS) and geographic information systems (GIS) free soil mapping from the past limitations of geographic technology. GPS removes the need of a base

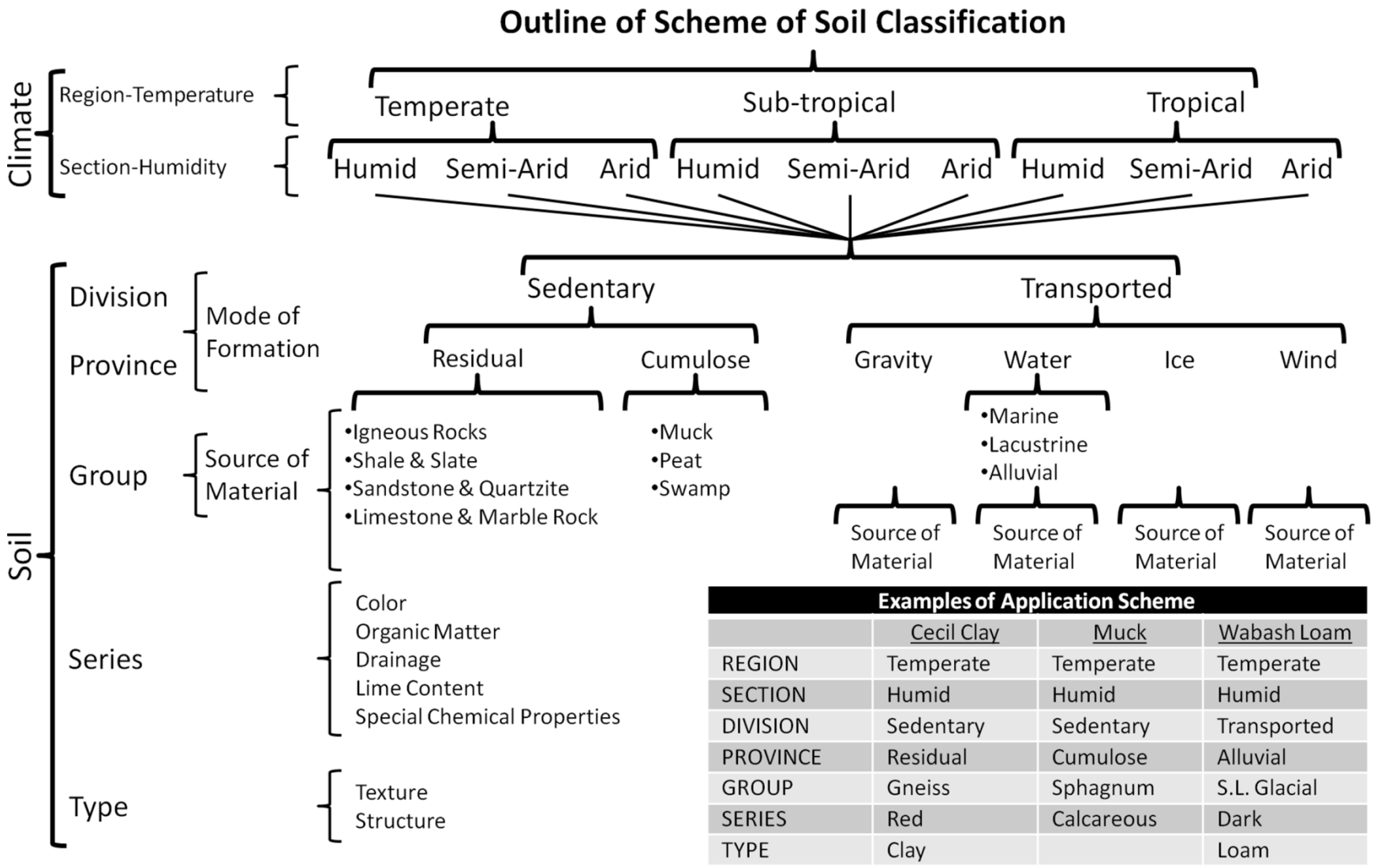
map to efficiently identify locations. GIS provides a medium without the cartographic scale constraints of paper maps. Therefore, the past limitations of geographic technology are no longer restricting the analysis scales of soil maps. These new technologies provide the opportunity to investigate smaller analysis scales as well as integrate the phenomena observed in different scales of paper maps.

7. Joining Scales

Prior to the acceptance of the multi-factor approach to soil science, numerous classification systems were proposed, each based on the favored theory of soil formation or the soil property believed to be the most critical for plant growth (Krupenikov, 1993). The emphasis of particular soil properties deemed important by the soil expert has remained a common theme for soil classification systems (Krasilnikov and Arnold, 2009). When Dokuchaev's zonal classification gained acceptance, most soil geographers were using agrogeology style classification systems as a guide for creating medium cartographic scale soil maps. The climate-vegetation emphasis of Dokuchaev's classification system was welcomed by agronomists at the time, who had observed the important role of humus for plant growth (Krupenikov, 1993). Conversely, many agrogeologists remained loyal to their observations of the mineral component, particularly mineral weathering, providing nutrients, and soil texture, affecting plant available water (Fallou, 1862; Whitney, 1892; Tisdale et al., 1993). This created a dichotomy of soil science perspectives, which has often been described as a transition in soil science understanding (e.g. Brevik and Hartemink, 2010). However, the divide was not only a

contrast in experts choosing different properties to emphasize, but also a duality between classification systems supported by small scale versus medium scale soil maps.

The problem of phenomena operating at different scales was a major reason for the difficulties in deriving a universal soil classification system in the first half of the 20th century (Helms, 2002). Soil classification systems designed for small cartographic scales seemed inadequate at large cartographic scales. Conversely, classification systems designed for larger cartographic scales contained too many divisions to be represented on a large extent map. Leading up to the development of the U.S. Soil Taxonomy, the debate over fundamental theories of soil science and how to create a unified soil classification system was a regular topic for soil scientists in the U.S. (Kellogg, 1974; Helms, 2002). With the goal of creating a classification system that distinguished unique soils that were uniform in agricultural value, Elmer O. Fippin (1879-1949) proposed a classification hierarchy that mirrors the phenomena scale hierarchy observed in soil maps (Fippin, 1911). In Fippin's proposed classification scheme, the emphasis was on the definition of series by properties, with further refinement of series to types by texture and structure. After these individuals with uniform properties of agricultural interest were identified, they were grouped by parent material and then by climate characteristics (Figure 2.15). Although not officially adopted in the U.S., this proposed classification scheme illustrates the early underpinning philosophy that would later shape the U.S. Soil Taxonomy (Soil Survey Staff, 1975).



Examples of Application Scheme			
	Cecil Clay	Muck	Wabash Loam
REGION	Temperate	Temperate	Temperate
SECTION	Humid	Humid	Humid
DIVISION	Sedentary	Sedentary	Transported
PROVINCE	Residual	Cumulose	Alluvial
GROUP	Gneiss	Sphagnum	S.L. Glacial
SERIES	Red	Calcareous	Dark
TYPE	Clay		Loam

Figure 2.15. Schematic of Fippin's proposed soil classification system (Fippin, 1911). Note the hierarchy of climate at the highest level followed by characteristics of parent material. At the series and type level, multiple, specific soil properties are listed, several of which have direct connections to topography.

When C.F. Marbut became chief of the U.S. Bureau of Chemistry and Soils in 1927 (Helms, 2002), he added zonal classification in parallel to the U.S. Soil Survey's pre-existing mode of mapping soils in the agrogeology style. Marbut then worked to bridge the zonal classification of small-scale maps with the agrogeology classification system of medium-scale soil maps, but was unable to reconcile the two. In one of his last publications, Marbut included two soil maps of the U.S.: 1) a 1:2.5 million scale map of generalized soil series in 12 sheets (Figure 2.16) and 2) a 1:8 million scale map based on great soil groups (Figure 2.17) (Marbut, 1935). Although there is some alignment in the boundaries between the two maps, Marbut did not believe these alignments were sufficient to unify the two soil classification systems.

Following Marbut as chief of the U.S. Bureau of Soils, Charles E. Kellogg (1902-1980) continued the effort for a unified soil taxonomy for the United States, which would also continue Marbut's emphasis on quantifiable facts. Quantified classification criteria would be useful not only for repeatable classifications, but also for improved use and suitability interpretations. The first of these classification schemes was a revised version of Marbut's zonal classification in the *1938 Yearbook of Agriculture: Soils and Men* (Baldwin et al., 1938). Although that classification scheme was revised again in 1949, there remained several anomalous soils that did not fit well with upper-level classification categories (Helms, 2002). In other words, it was unsatisfactory to have soils with unique properties -important to use and management- that could not be differentiated by relationships to climate-vegetation.

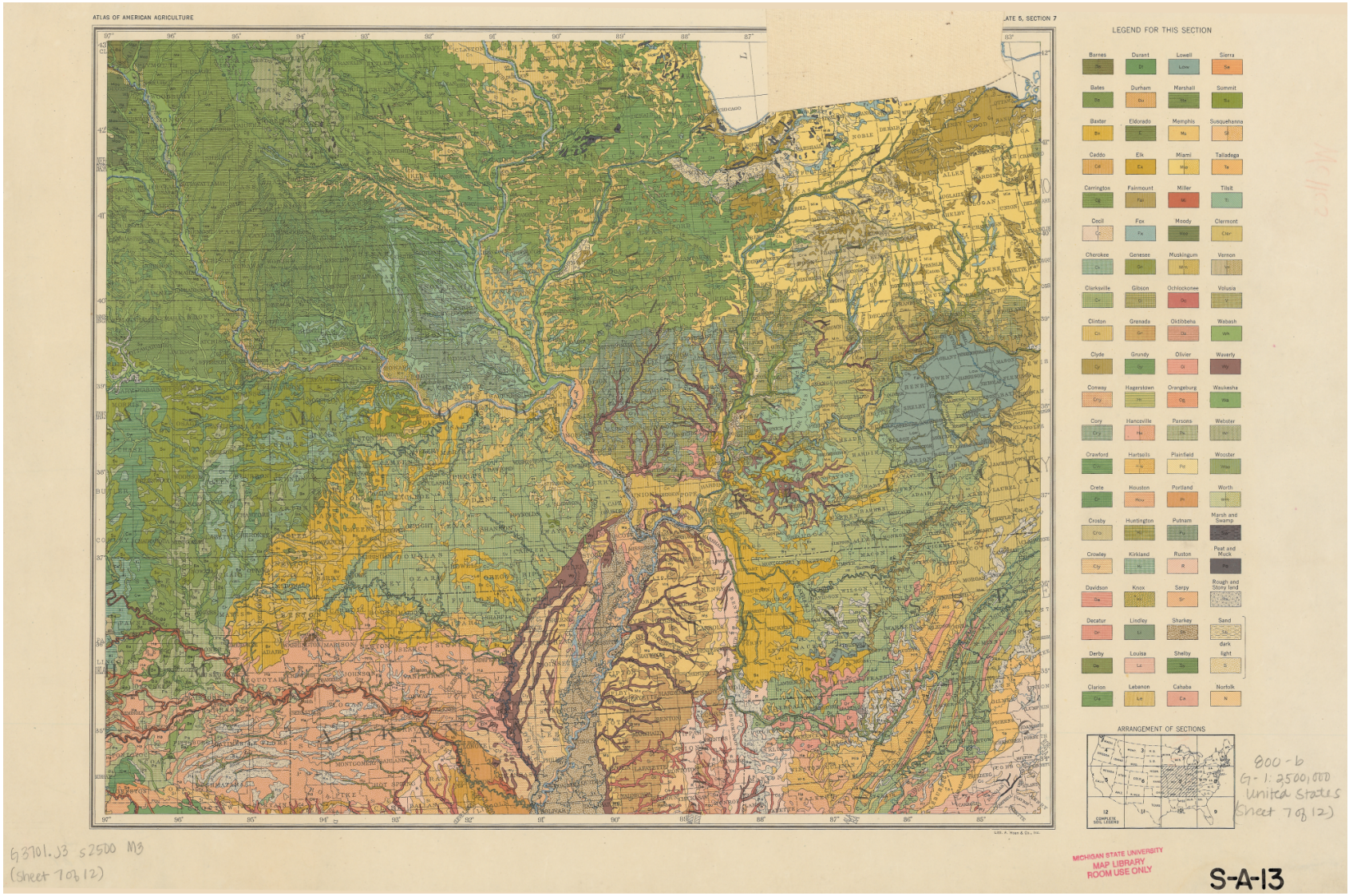


Figure 2.16. Sheet 7 of 12 from soil map of the United States based on generalized soil series in the agrogeology classification style. Cartographic scale was 1:2.5 million (Marbut et al., 1931). Note the 'Arrangement of Sections' diagram in the lower-right corner for comparison of spatial patterns with Figure 2.17. Names of soil series are inconsequential.

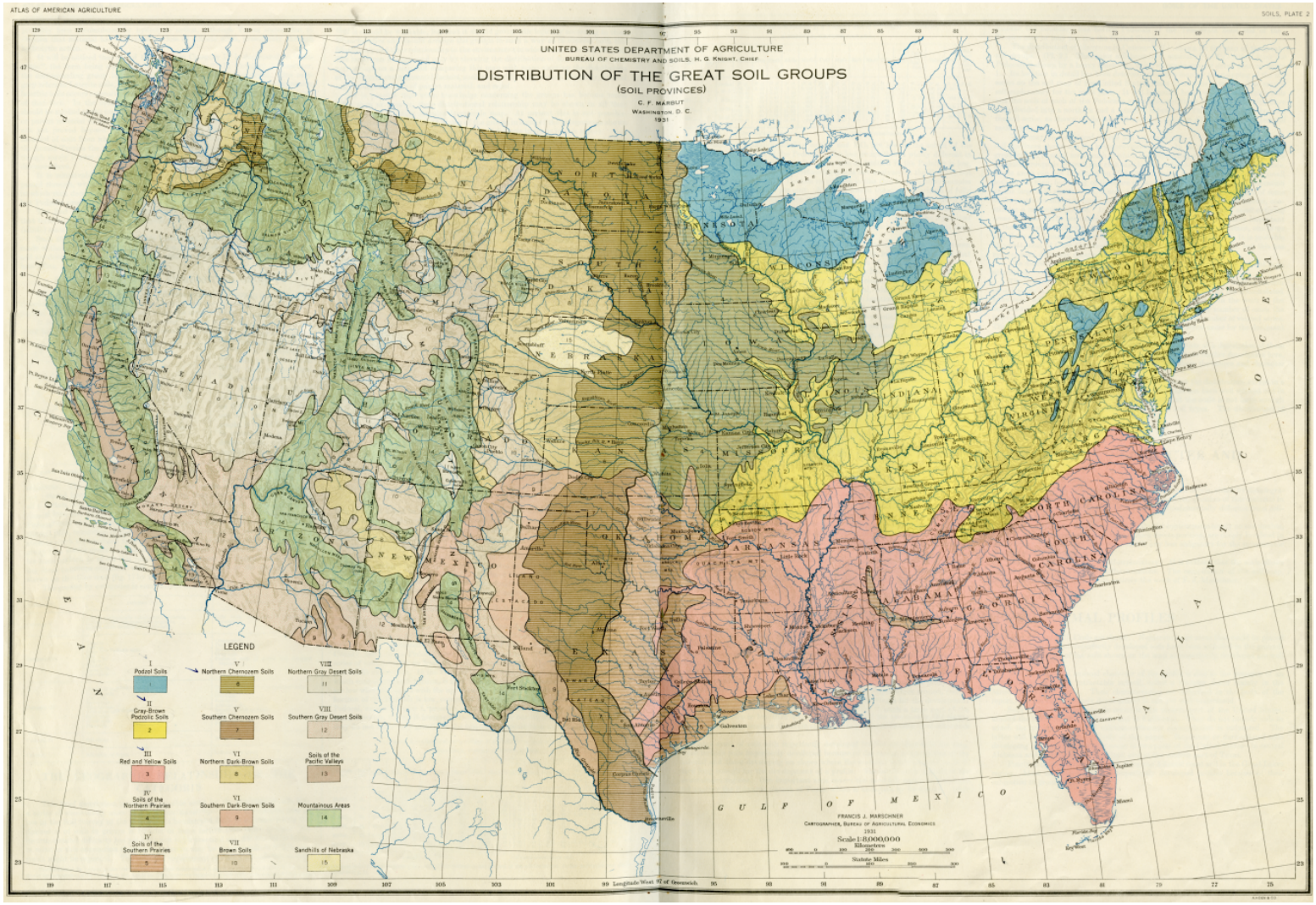


Figure 2.17. Soil map of the U.S. based on great soil groups in the zonal classification style. Cartographic scale was 1:8 million (Marbut, 1931). Although some nested relationships can be observed between Figure 2.16 and 2.17, Marbut did not believe those relationships were sufficient to join the classification systems of the respective maps. Names of the great soil groups are inconsequential.

In 1951, Kellogg assigned the task of a new classification system, built upward from the characteristics of individual soil series, to Guy D. Smith (1907-1981) (Helms, 2002). Smith used a community review process to develop quantitative definitions for grouping all soils in a hierarchal classification (Simonson, 1991). These efforts resulted in the seventh approximation of the U.S. Soil Taxonomy (Soil Survey Staff, 1960). Central to the differentia was the soil anatomy, which later became termed diagnostic horizons. These horizons are layers distinguishable from other layers by a set of properties, and formed by pedogenic processes (Soil Survey Staff, 1993). Although the U.S. Soil Taxonomy is often heralded for its use of quantified classification rules (Cline, 1977; Mermut and Eswaran, 2001), it also accomplished a great feat in joining classifications based on small and large scale phenomena.

Although the quantification applied in the U.S. Soil Taxonomy had several benefits for the utilization and management of soils, it was a step away from the traditional use of geographic attributes. “When soil series were redefined to be in compliance with the class limits imposed by the hierarchy of Soil Taxonomy, they no longer were landscape map units. They assumed the role of providing identity only to pedons” (Arnold, 2006, p. 56). However, that disconnect does not mean that the system was constructed without the lessons learned from soil geography. Because of the recognized importance of soil forming factors for producing the diagnostic horizons and in predictive landscape models for soil mapping, the Soil Taxonomy hierarchy does, in many ways, reflect soil formation factors (Ahrens et al., 2002). In Smith’s words, “Genesis does not appear in the definitions of the taxa but lies behind them” (Smith, 1983, p. 43). For example, several of the soil orders correspond with broad vegetation communities, and the suborders correspond with soil climate. Although no longer defined by

environmental correlation, the principles of scale that allowed zonal classification systems to be delineated on small-scale maps remained in Soil Taxonomy. For this reason, in theory, soil map units in large cartographic scale maps can be classified using the lowest order of the hierarchy, while higher orders can be represented on small cartographic scale maps (Figure 2.18).

Smith did not use spatial variability as a constraining rationale for organizing the U.S. Soil Taxonomy, which allows for some classification differentia to be raised in the hierarchy level due to properties considered to be of high importance. For example, in the controlling factors for the twelve Soil Taxonomy orders summarized by Brevik (2002), seven are based on bioclimatic-soil relationships and two are differentiated by the lack of time for bioclimatic processes to modify the parent material. The remaining three orders are based on hydrologic or geologic phenomena, which result in soil properties important to land management and still have large extents. Like zonal classification systems, Soil Taxonomy orders place greater emphasis on bioclimatic differentia, with a few additional categories to allow for exceptions (Table 2.1). Therefore, even though soil classifications systems have no obligation to be organized in a hierarchy of phenomena scales, as a matter of mapping practicality, the U.S. Soil Taxonomy still reflects soil geographers' experience of shifting dominant soil forming factors at different analysis scales. Although the main purpose of Soil Taxonomy was to be based on observable properties considered important to use and management, the multi-level taxonomic hierarchy of the system was organized to accommodate both small and large cartographic scale maps (Smith, 1986). Despite criticisms that Soil Taxonomy is disconnected from soil-forming processes (Bockheim and Gennadiyev, 2000), the mirroring of process scale in the classification hierarchy is one of the threads that link classification definitions back to processes.

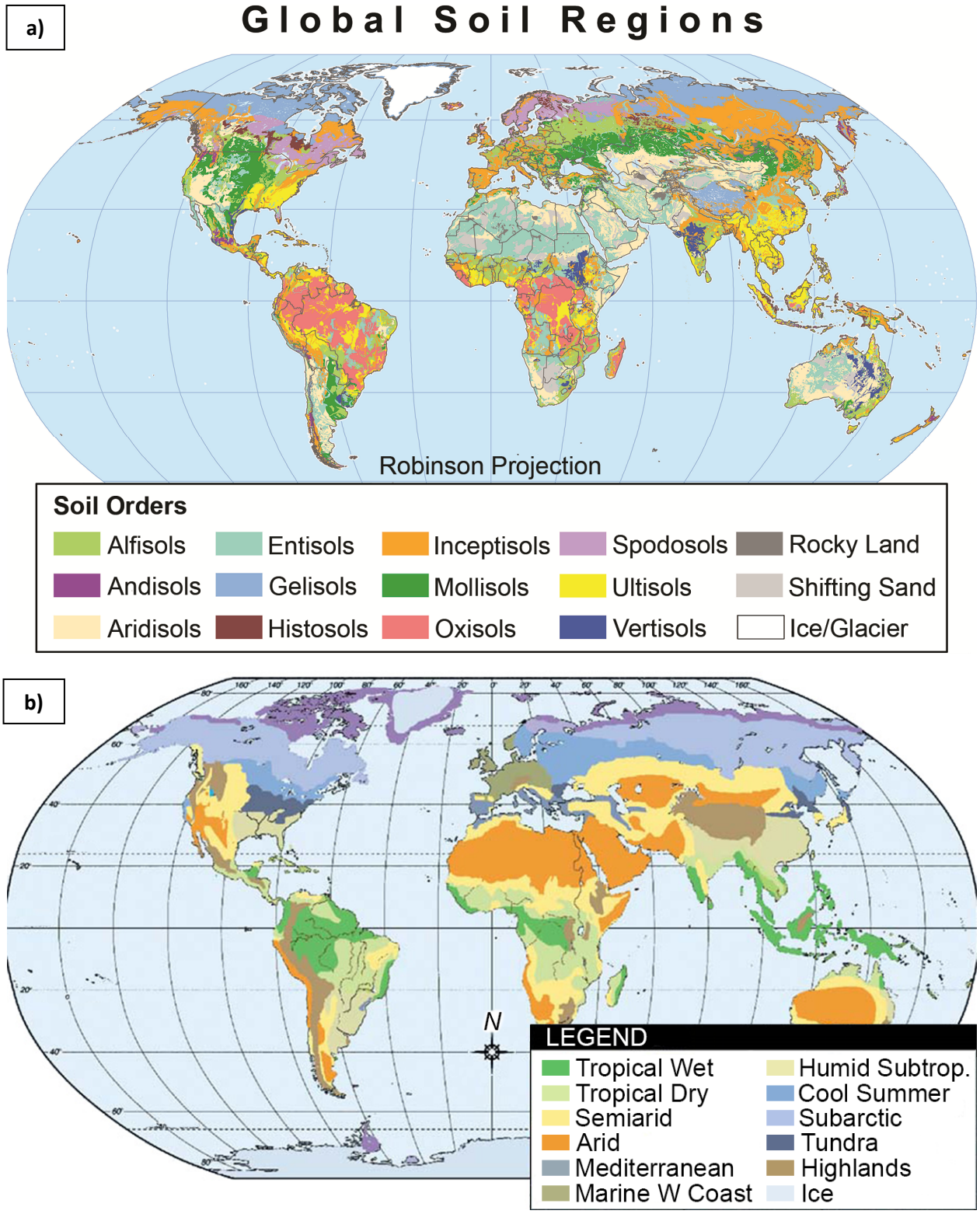


Figure 2.18. a) World map of soil orders as classified by U.S. Soil Taxonomy at a cartographic scale of 1:130 million (USDA-NRCS, 2005). b) Köppen-Geiger climate zones presented for comparison with U.S. Soil Taxonomy soil orders (climate zone map modified from www.theodora.com/maps, used with permission).

Table 2.1. Relationship between the top levels of zonal classification and the current version of Soil Taxonomy.

Zonal	**Intrazonal**	**Azonal**
Climate-Vegetation	*Exceptions based on geology or hydrology*	*Exceptions based on time*
Alfisols	Histosols	Entisols
Aridisols	Andisols	Inceptisols (some)
Gelisols	Vertisols	
Mollisols		
Oxisols		
Spodosols		
Ultisols		
Inceptisols (some)		

8. Conclusions

Soil maps have evolved through and alongside the advancement of soil knowledge and geographic technology. Soil maps at different cartographic scales - and by association, different analysis scales - have utilized the environmental predictor found best suited for explaining spatial variability at the respective scales. After such time as soil knowledge was able to recognize the influence of multiple environmental factors on resulting soil properties, ca. 1860-1880, soil scientists' selection of environmental predictors reflects the conceptual model adopted for the respective scale. Comparisons of soil maps of varying cartographic scales reveals three distinct groups: 1) small cartographic scale maps emphasizing bioclimatic relationships, 2) medium cartographic scale maps emphasizing parent material relationships, and 3) large cartographic scale maps emphasizing topographic relationships.

The correspondence between cartographic scale and soil scientists' selection of a respective environmental factor for predicting soil variability suggests that the process

phenomena embodied in Dokuchaev's factors of soil formation are certainly operative, but are perhaps best expressed at different scales. Over time, the experiences of soil scientists have been tuned to the environmental factor that best explains the spatial variability of the soil at the operative or explanative scale of the map they are producing. At times, this association has led to contentious debates over which factor provides the best prediction of geographic soil patterns. In some cases, not recognizing the scale effect of MAUP has led to outright rejection of valid, large scale phenomena when local exceptions are found (e.g. Beadle, 1951). However, debates over the most important soil forming factor may have been moot, because the optimal predictor of soil spatial variability is usually a function of analysis scale.

The potential for mapping soils at fine analysis scales (large cartographic scales) has not yet been fully utilized. Until recently, limitations in quality base maps (i.e. detailed representations of topography) have made extending modern soil geomorphology principles across large extents impractical. Technological advancements provide the opportunity to create better base maps, which in turn offer the ability to bring soil map detail to the level of process scales studied in soil geomorphic research.

The introduction of geographic information systems and digital mapping products to soil mapping has decoupled cartographic scale from analysis scale. To learn from the experience of past soil geographers, and to avoid repeating mistakes, it is important to apply lessons learned by cartographic scale with paper maps to analysis scales of digital maps. This paper demonstrated that past soil mapping approaches were based on conceptual models calibrated to the cartographic/analysis scale of the map. The conceptual models were tuned to the

phenomena governing the spatial distribution of soil, which differed by map scale. Like traditional soil modelers, it is important for digital soil modelers to select the appropriate environmental predictors for the analysis scale of interest. An approach to integrating phenomena scales to conceptualize soil geography is to subdivide coarse scale phenomena by finer scale phenomena, as is commonly done in modern soil classification systems. This framework of layering soil formation factors by a hierarchy of scale utilizes the experience of past soil geographers to form a holistic understanding of soil geography and pattern.

REFERENCES

REFERENCES

Agafonoff, V. 1936. Les Sols de France au Point de vue Pédologique (avec carte 1:2,500,000). Paris.

Ahrens, R.J., T.J. Rice, H. Eswaran. 2002. Soil classification: Past and present. National Cooperative Soil Survey Newsletter. 19:1-5.

Almy, M.M. 1978. The archeological potential of soil survey reports. The Florida Anthropologist. 31(3):75-91.

Aristotle. 2002. Historia Animalium. D.M. Balme (ed.). Cambridge University Press. Cambridge, United Kingdom.

Armhein, C.G. 1995. Searching for the elusive aggregation effect: Evidence from statistical simulations. Environment and Planning A. 27(1):105-119.

Arnold, R.W. 2006. Soil survey and soil classification. *In* S. Grunwald (ed.). Environmental Soil-Landscape Modeling: Geographic Information Technologies and Pedometrics. Taylor & Francis Group. Boca Raton.

Baldwin, M., C.E. Kellogg, and J. Thorp. 1938. Soil Classification. *In* Soils and Men: Yearbook of Agriculture. Washington, D.C.

Bayer, G. 1998. Classification and explanation in Aristotle's theory of definition. Journal of the History of Philosophy. 36(4):487-505.

Beadle, N.C.W. 1951. The misuse of climate as an indicator of vegetation and soils. Ecology. 32(3):343-345.

Beaudette, D.E. and A.T. O'Green. 2009. Quantifying the aspect affect: an application of solar radiation modeling for soil survey. Soil Science Society of America. 73(4):1345-1352.

Bichurin, N.Y. 1841. Land revenue in China. Moskvityanin. pt. 4, no. 12.

Biondi, E. E. Feoli, and V. Zucarello. 2004. Modelling environmental responses of plant associations: A review of some critical concepts in vegetation study. Critical Reviews in Plant Sciences. 23:149-156.

Bockheim, J.G. and A.N. Gennadiyev. 2000. The role of soil-forming processes in the definition of taxa in Soil Taxonomy and the World Soil Reference Base. Geoderma. 95:53-72.

Bockheim, J.G., A.N. Gennadiyev, R.D. Hammer, and J.P. Tandarich. 2005. Historical developments of key concepts in pedology. Geoderma. 124:23-36. doi: 10.1016/j.geoderma.2004.03.004

Brevik, E.C. 2002. Soil classification in geology textbooks. Journal of Geoscience Education. 50(5):539-543.

Brevik, E.C. and A.E. Hartemink. 2010. Early soil knowledge and the birth and development of soil science. Catena. 83:23-33. doi: 10.1016./j.catena.2010.06.011

Brown, D.J. 2006. A historical perspective on soil-landscape modeling. *In* S. Grunwald (ed.). Environmental Soil-Landscape Modeling: Geographic Information Technologies and Pedometrics. Taylor & Francis Group. Boca Raton.

Brown, L.A. 1979. The Story of Maps. Dover Publications, Inc. New York.

Bullock, P., R.J.A. Jones, B. Houšková, and L. Montanarella. 2005. Soil resources of Europe: An overview. *In* R.J.A. Jones, B. Houšková, P. Bullock, and L. Montanarella (eds.). Soil Resources of Europe. Second Edition. European Soil Bureau, Institute for Environment & Sustainability.

Bunbury, E.H. 1883. A History of Ancient Geography among the Greeks and Romans from the Earliest Ages till the Fall of the Roman Empire. John Murray. London.

Bushnell, T.M. 1929. Aerial photography and soil survey. American Association of Soil Surveyors Bulletin. 10:23-28.

Bushnell, T.M. 1932. A new technique in soil mapping. American Soil Survey Association Bulletin. 13:74-81.

Bushnell, T.M. 1943. Some aspects of the soil catena concept. Soil Science Society Proceedings. 7(C):466-476.

Cartography Associates. 2013. (Composite of) Carte de France. Levee par ordre du Roy. (1750-1815). Available online at: http://www.davidrumsey.com. Accessed [4/15/2012].

Cato, M.P. 1934. On Agriculture (W.D. Hooper, Trans.). Harvard University Press. Cambridge, Massachusetts.

Chamberlain, W.C. 1882. General Map of the Soils of Wisconsin. Geology of Wisconsin. Survey of 1873-1879 Atlas. Plate IIB. Available online at: http://digital.library.wisc.edu/1711.dl/EcoNatRes.GeoWIAtlas. Accessed [4/15/2012].

Cline, M.G. 1949. Basic principles of soil classification. Soil Science. 67(2):81-91.

Cline, M.G. 1977. Historical highlights in soil genesis, morphology, and classification. Soil Science Society of America Journal. 41(2):250-254.

Cobb, W.B. 1923. Possibilities of the airplane in soil survey work. American Association of Soil Survey Workers Bulletin. 4:77-80.

Coffey, G.N. 1911. The development of soil survey work in the United States with a brief reference to foreign countries. Proceedings of the American Society of Agronomy. 3:115-129.

Cousins, S.A.O. 2001. Analysis of land-cover transitions based on 17th and 18th century cadastral maps and aerial photographs. Landscape Ecology. 16:41-54.

Davey, H.C. 1935. Brief outline of aerial photographic work in the U.S. Geological Survey. Photogrammetric Engineering. 1:3.

Davis, W.M. 1909. Geographical Essays. Ginn and Company. Boston.

Dideriksen, R.O. 1986. Soil Survey of Hamilton County, Iowa. U.S. Department of Agriculture, Soil Conservation Service.

Dilke, O.A.W. 1987. Roman large-scale mapping in the early empire. *In* J.B. Harley and D. Woodward. The History of Cartography. University of Chicago Press. Chicago.

Dokuchaev, V.V. 1967. The Russian Chernozem (N. Kaner, Trans.). Israel Program for Scientific Translations. Jerusalem.

Donald, R.G., D.W. Anderson, J.W.B. Stewart. 1993. The distribution of selected soil properties in relation to landscape morphology in forested Gray Luvisol soils. Canadian Journal of Soil Science. 73:165-172.

Duchaufour, P. 1982. Pedology: Pedogenesis and Classification (T.R. Paton, Trans.). George Allen & Unwin. London.

Ellis, J.H. 1938. The soils of Manitoba. Manitoba Economic Survey Board. Winnipeg, Manitoba.

Ely, C.W., G.N. Coffey, and A.M. Griffin. 1904. Soil Map: Iowa, Tama County Sheet. U.S. Department of Agriculture, Bureau of Soils.

Eratosthenes. 2010. Geographika (D.W. Roller, Trans.). Princeton University Press. Princeton, New Jersey.

Fallou, F.A. 1862. Pedology, or, General and Specific Soil Science [Pédologie oder allgemeine und besondere Bodenkunde]. C.U. Werner. Dresden.

Friend, D.A. 2000. Revisiting William Morris Davis and Walther Penck to propose a general model of slope “evolution” in deserts. Professional Geographer. 52:164-178.

Fippin, E.O. 1911. The practical classification of soils. Agronomy Journal. 3(1):76-89.

Fridland, V.M. 1974. Structure of the soil mantle. Geoderma. 12:35-41.

Fridland, V.M. 1976. Pattern of Soil Cover. Israel Program for Scientific Translations. Jerusalem.

Furley, P.A. 1971. Relationships between slope form and soil properties developed over chalk parent materials. Institute of British Geographers Special Publication. 3:141-163.

Gong, Z., J.L. Darilek, Z. Wang, B. Huang, and G. Zhang. 2010. American soil scientists' contribution to Chinese Pedology in the 20th century. Soil Survey Horizons. 50:3-9.

Gorkin, A.F., and O.J. Schmidt. 1938. Great Soviet World Atlas (G.B. Cressey, A. Perejda and V. Washburne, Trans.). Edwards Brothers, Inc. Ann Arbor, Michigan.

Gregorich, E.G. and D.W. Anderson. 1985. Effects of cultivation and erosion on soils of four toposequences in the Canadian prairies. Geoderma. 36(3-4):343-354.

Grigelis, A., Z. Wójcik, W. Narębski, L.Z. Gelumbauskaitė, and J. Kozák. 2011. Stanisław Staszic: an early surveyor of the geology of Central and Eastern Europe. Annals of Science. 68(2):199-228. doi:10.1080.00033790.2010.511263.

Grunwald, S. 2003. Introduction. Pedometron. 13:4-6.

Hall, G.F. 1983. Pedology and geomorphology. *In* L.P. Wilding, N.E. Smeck, and G.F. Hall (eds.). Pedogenesis and Soil Taxonomy: I. Concepts and Interactions. Elsevier. Amsterdam.

Hall, A.D. and E.J. Russell. 1912. On the causes of the high nutritive value and fertility of the fatting pastures of Romney marsh and other marshes in the s.e. of England. The Journal of Agricultural Science. 4(4):339-370.

Harley, J.B. and D. Woodward. 1987. The History of Cartography. Volume 1. University of Chicago Press.

Hartemink, A.E., B. Lowery, and C. Wacker. 2012. Soil maps of Wisconsin. Geoderma. 189-190:451-461. doi:10.1016/j.geoderma.2012.05.025

Hartshorne, R. 1958. The concept of geography as a science of space, from Kant to Humboldt to Hettner. Annals of the Association of American Geographers. 48(2):97-108.

Helms, D. 2002. Early leaders of the soil survey. *In* D. Helms, A.B.W. Effland, and P.J. Durana (eds.). Profiles in the History of the U.S. Soil Survey. Iowa State Press. Ames, Iowa.

Heuvelink, G.B.M. and R. Webster. 2001. Modelling soil variation: Past, present, and future. Geoderma. 100:269-301.

Hillel, D. 1992. Out of the Earth: Civilization and the Life of the Soil. University of California Press. Berkeley, California.

Hole, F.D. 1978. An approach to landscape analysis with emphasis on soils. Geoderma. 21(1):1-23.

Hole, F.D. and J.B. Campbell. 1985. Soil Landscape Analysis. Rowman & Allanheld. Totowa, New Jersey.

Hollis, J.M. and B.W. Avery. 1997. History of soil survey and development of the soil series concept in the U.K. *In* D.H. Yaalon and S. Berkowicz (eds.). History of Soil Science: International Perspectives. Advances in Geoecology. vol. 29. Catena-Verlag. Reiskirchen, Germany.

Holmes, C.D. 1955. Geomorphic development in humid and arid regions: A synthesis. American Journal of Science. 253:377-390.

Huggett, R.J. 1975. Soil landscape systems: A model of soil genesis. Geoderma. 13:1-22.

Hunckler, R.V. and R.J. Schaetzl. 1997. Spodosol development as affected by geomorphic aspect, Baraga County, Michigan. Soil Science Society of America Journal. 61(4):1105-1115.

Ibáñez, J.J., M.R. Ramos, J.A. Zinck, and A. Brú. 2005. Classical pedology questioned and defended. Eurasian Soil Science. 38(1):S75-S80.

Ibáñez, J.J. and A. Saldaña. 2008. The continuum dilemma in pedometrics and pedology. *In* P. Krasilnikov, F. Carré, and L. Montanarella (eds.). Soil Geography and Geostatistics: Concepts and Applications. JRC Scientific and Technical Reports.

Isachenko, A.G. 1971. Razvitie geograficheskikh idei [Development of Geographical Ideas]. Mysl'. Moscow.

Jelinski, D.E. and J. Wu. 1996. The modifiable areal unit problem and implications for landscape ecology. Landscape Ecology. 11(3):129-140.

Keates, J.S. 1989. Cartographic Design and Production. Wiley. New York.

Kellogg, C.E. 1937. Soil Survey Manual. U.S. Department of Agriculture Miscellaneous Publication Number 274. U.S. Department of Agriculture. Washington, D.C.

Kellogg, C.E. 1974. Soil genesis, classification, and cartography: 1924-1974. Geoderma. 12:347-362.

Kleiss, H.J. 1970. Hillslope sedimentation and soil formation in northeastern Iowa. Soil Science Society of America Proceedings. 34:287-290.

Kovda, V.A. and G.V. Dobrovolsky. 1974. Soviet pedology to the 10th International Congress of Soil Science (the centenary of soil science in Russia). Geoderma. 12:1-16.

Köppen, W., 1884. Die Wärmezonen der Erde, nach der Dauer der heissen, gemässigten und kalten Zeit und nach der Wirkung der Wärme auf die organische Welt betrachtet (The thermal zones of the earth according to the duration of hot, moderate and cold periods and to the impact of heat on the organic world).Meteorol. Z. 1:215–226. Translated and edited by: Volken, E. and Bronnimann, S. 2011. Meteorol. Z. 220:2351–2360.

Krasilnikov, P. and R. Arnold. 2009. Soil classifications and their correlations. *In* P. Krasilnikov, J. Ibáñez Martí, R. Arnold, and S. Shoba (eds.). A Handbook of Soil Terminology, Correlation and Classification. Earthscan. London.

Krupenikov, I.A. 1993. History of Soil Science (A.K. Dhote, Trans.). A.A. Balkema Publishers. Brookfield, Vermont.

Lapham, M.H. 1949. Crisscross Trails: Narrative of a Soil Surveyor. W.E. Berg. Berkeley, California.

Lee, M.P. 1921. The economic history of china: with special reference to agriculture. *In* The faculty of Political Science of Columbia University (eds.). Studies in History Economics and Public Law. Vol. 39. Columbia University. New York.

Legros, J. 2006. Classification systems: French. *In* R. Lal (ed.). Encyclopedia of Soil Science. Taylor & Francis. doi: 10.1081/E-ESS-120042644.

Leucho, J.P. 1511. World map from Ptolemy, Geographia. James Ford Bell Library, University of Minnesota. Available online: https://www.lib.umn.edu/apps/bell/map/PTO/TOUR/1511alg.html. Accessed [4/15/2013].

Library Foundation, Buffalo and Erie County Public Library. 2013. A Delineation of the Strata of England and Wales with part of Scotland: Exhibiting the Collieries and Mines, the Marshes and Fen Lands Originally Overflowed by the Sea, and the Varieties of Soil According to Variations in the Substrata, Illustrated by the Most Descriptive Names. Available online at: http://en.wikipedia.org/wiki/File:Geological_map_Britain_William_Smith_1815.jpg. Accessed [4/15/2013].

Madison, F.W. and H.F. Gundlach. 1993. Soil Regions of Wisconsin. Wisconsin Geological and Natural History Survey. Madison, Wisconsin.

Malo, D.D., B.K. Worchester, D.K. Cassel, and K.D. Matzdorf. 1974. Soil-landscape relationships in a closed drainage system. Soil Science Society of America Proceedings. 38:813-818.

Marbut, C.F. 1928. A scheme for soil classification. Commission V, Proceedings and Papers, First International Congress of Soil Science. June 13-22, 1927, Washington D.C., p. 1-31.

Marbut, C.F. 1931. Distribution of the Great Soil Groups (Soil Provinces). U.S. Department of Agriculture, Bureau of Chemistry and Soils. Washington, D.C.

Marbut, C.F., and associates in the Soil Survey. 1931. Soil Map of the United States. U.S. Department of Agriculture. Washington, D.C.

Marbut, C.F. 1935. Soils of the United States. *In* Atlas of American Agriculture. Part III.

Marbut, C.F. 1951. Soils: Their Genesis and Classification. A memorial volume of lectures given in the Graduate School of the United States Department of Agriculture in 1928**.** Soil Science Society of America. Madison, WI.

Marean, H.W. 1902. Soil Survey, Posey County, Indiana. U.S. Department of Agriculture, Bureau of Soils. Washington, D.C.

Martin, W.K.E. and V.R. Timmer. 2006. Capturing spatial variability of soil and litter properties in a forest stand by landform segmentation procedures. Geoderma. 132(1-2):169-181.

Mermut, A.R. and H. Eswaran. 2001. Some major developments in soil science since the mid-1960s. Geoderma. 100:403-426.

Merzon, A.T. 1956. Cadastres and Inventories of the 15th-17th Centuries [Pistovye v perenisnye knigi XV-XVII vv]. Izd. Mosk. Gos. Arkhivn. In-ta, Moscow.

Millar, C.E. 1932. The use of aerial photographs in the Michigan land economic survey. Soil Science Society of America Journal. 13:82-85.

Milne, G. 1935a. Some suggested units of classification and mapping particularly for East African soils. Soil Research. 4(3).

Milne, G. 1935b. Composite units for the mapping of complex soil associations. Transactions of the 3rd International Congress of Soil Science. 1:345-347.

Milne, G. 1936. Normal erosion as a factor in soil profile development. Nature. 138:548-549.

Moellering, H. and W. Tobler. 1972. Geographical variances. Geographical Analysis. 4(1):34-50.

Monmonier, M.S. 1996. How to Lie with Maps. University of Chicago Press. Chicago.

Montello, D.R. 2001. Scale in geography. *In* N.J. Smelser and P.B. Baltes (eds.). International Encyclopedia of the Social & Behavioral Sciences. Pergamon Press. Oxford.

National Cooperative Soil Survey. 1978. Iowa Soil Association Map. Iowa Agriculture and Home Economics Experiment Station.

National Library of France. 2013. Carte de Cassini. Available online: http://commons.wikimedia.org/wiki/File:Cassini_map_of_France_68.png. Accessed [4/15/2013].

Pomerening, J.A. and M.G. Cline. 1953. The accuracy of soil maps prepared by various methods that use aerial photograph interpretation. Photogrammetric Engineering. 19(5):809-817.

Prasolov, L.I. 1922. Soil Regions of the European Part of Russia [Pochvennye oblasti Evropeiskoi Rossii]. Petrograd.

Prescott, J.A. 1933. The soil zones of Australia. Soil Resources. 3:133-145.

Ptolemy. 1932. Geography of Claudius Ptolemy (E.L. Stevenson, Trans.). The New York Public Library. New York.

Robinson, A. 1971. The genealogy of the isopleth. The Cartographic Journal. 8(1):49-53.

Robinson, A.H. and H.M. Wallis. 1967. Humboldt's map of isothermal lines: A milestone for thematic cartography. The Cartographic Journal. 4(2):119-123.

Ruhe, R.V., R.B. Daniels, and J.G. Cady. 1967. Landscape evolution and soil formation in southwestern Iowa. USDA-SCS Technical Bulletin. 1349.

Ruhe, R.V. and P.H. Walker. 1968. Hillslope models and soil formation. I. open systems. Transactions of the 9th International Congress of Soil Science. 4:551-560.

Sanderson, M. 1999. The classification of climates from Pythagoras to Koeppen. Bulletin of the American Meteorological Society. 80(4):669-673.

Schaetzl, R.J. 2013. Catenas and Soils. *In* J.F. Shroder (ed.). Treatise on Geomorphology, Vol. 4. Academic Press. San Diego, California. pp. 145-158.

Schoeneberger, P.J., D.A. Wysocki, E.C. Benham, and Soil Survey Staff. 2012. Field Book for Describing and Sampling Soils, Version 3.0. U.S. Department of Agriculture, Natural Resource Conservation Service. Lincoln, Nebraska.

Schoorl, J.M. and A. Veldkamp. 2006. Multiscale soil-landscape process modeling. *In* S. Grunwald (ed.). Environmental Soil-Landscape Modeling: Geographic Information Technologies and Pedometrics. Taylor & Francis Group. Boca Raton.

Shantz, H.L. and C.F. Marbut. 1923. The Vegetation and Soils of Africa. National Research Council and American Geographical Society. New York.

Shchetenko, A.Y. 1968. The Most Ancient Agrarian Cultures of the Deccan [Drevneishie zemledel'cheskie kul'tury Dekana]. Nauka. Leningrad.

Sibirtsev, N.M. 1966. Selected Works (N. Kaner, Trans.). Israel Program for Scientific Translations. Jerusalem.

Simonson, R.W. 1952. Lessons from the first half century of soil survey: II. mapping of soils. Soil Science. 74:323-330.

Simonson, R.W. 1962. Soil classification in the United States. Science. 137(3535):1027-1034.

Simonson, R.W. 1991. The U.S. soil survey – contributions to soil science and its application. Geoderma. 48:1-16.

Simonson, R.W. 1997. Evolution of soil series and type concepts in the United States. *In* D.H. Yaalon and S. Berkowicz (eds.). History of Soil Science: International Perspectives. Advances in Geoecology. vol. 29. Catena-Verlag. Reiskirchen, Germany.

Smith, C.B. 1985. Air Spy. American Society for Photogrammetry Foundation. Falls Church, Virginia.

Smith, G.D. 1983. Historical development of soil taxonomy-background. *In* L.P. Wilding, N.E. Smeck, and G.F. Hall (eds.). Pedogenesis and Soil Taxonomy: I. Concepts and Interactions. Elsevier. Amsterdam.

Smith, G.D. 1986. The Guy Smith Interviews: Rationale for Concepts in Soil Taxonomy. U.S. Department of Agriculture. SMSS Technical Monograph No. 11. Washington, D.C.

Smith, W. 1815. A Delineation of the Strata of England and Wales with part of Scotland: Exhibiting the Collieries and Mines, the Marshes and Fen Lands Originally Overflowed by the Sea, and the Varieties of Soil According to Variations in the Substrata, Illustrated by the Most Descriptive Names.

Sobolev, S.S. 1943. Developments in geography and mapping of soils in Russia: from medieval Russia to Dokuchaev [O razvitii geografii I kartografii pochv v Rossi: ot Drevnei Rusi do Dokuchaeva]. Pochvovedenie. 5-6.

Soil Survey Staff. 1951. Soil Survey Manual. U.S. Department of Agriculture Handbook No. 18. Washington, D.C.

Soil Survey Staff. 1960. Soil Classification, a Comprehensive System, 7th Approximation. U.S. Government Printing Office. Washington, D.C.

Soil Survey Staff. 1975. Soil Taxonomy: A Basic System of Soil Classification for Making and Interpreting Soil Surveys. Agricultural Handbook No. 436. U.S. Government Printing Office. Washington, D.C.

Soil Survey Staff. 1993. Soil Survey Manual. U.S. Department of Agriculture Handbook No. 18. Washington, D.C.

Soil Survey Staff. 2013. Soil Survey Manual. Soil Survey Geographic (SSURGO) Database. Available online: http://www.soils.usda.gov/survey/geography/ssurgo/. Accessed [5/9/2013].

Steinwand, A.L. and T.E. Fenton. 1995. Landscape evolution and shallow groundwater hydrology of a till landscape in central Iowa. Soil Science Society of America Journal. 59(5):1370-1377.

Stolt, M.H., J.C. Baker, and T.W. Simpson. 1993. Soil-landscape relationships in Virginia: II. reconstruction analysis and soil genesis. Soil Science Society of America Journal. 57:422-428.

Strabo. 1917. The Geography of Strabo (H.L. Jones and J.R.S. Sterrett, Trans.). G.P. Putnam's Sons. New York.

Stremme, H.E. 1997. Preparation of the collaborative soil maps of Europe, 1927 and 1937. *In* D.H. Yaalon and S. Berkowicz (eds.). History of Soil Science: International Perspectives. Advances in Geoecology. vol. 29. Catena-Verlag. Reiskirchen, Germany.

Tandarich, J.P. 2001. Wisconsin agricultural geologists: Ahead of their time. Geoscience Wisconsin. 18:21-26.

Theophrastus. 1916. Enquiry into Plants and Minor Odours and Weather Signs (A. Hort, Trans.). W. Heinemann. London.

Thorp, J.A. (ed.) 1936. Geography of the Soils in China. Special Soil Publ., Ser. B1:1–244.

Thrower, N.J.W. 2007. Maps and Civilization: Cartography in Culture and Society. Third edition. University of Chicago Press. Chicago.

Tisdale, S.L., W.L. Nelson, J.D. Beaton, J.L. Havlin. 1993. Soil Fertility and Fertilizers, 5th Edition. MacMillan Publishing Company. New York.

University of New Hampshire. 2013. William Smith's Geological Map of England and Wales and Part of Scotland, 1815-1817. Available online: http://www.unh.edu/esci/WilliamSmiths-StrataIdentified/i/explanatory.html. Accessed [4/15/2013].

USDA-NRCS. 2005. Global Soil Regions Map. U.S. Department of Agriculture, Natural Resource Conservation Service. Available online at: http://soils.usda.gov/use/worldsoils/mapindex/order.html. Accessed [4/15/2013].

Vanwalleghem, T., J. Poesen, A. McBratney, and J. Deckers. 2010. Spatial variability of soil horizon depth in natural loess-derived soils. Geoderma. 157:37-45.

Volney, C.F. 1804. View of the Climate and Soil of the United States of America (C.B. Brown, Trans.). J. Conrad & Co. Philadelphia, Pennsylvania.

Walker, P.H. and R.V. Ruhe. 1968. Hillslope models and soil formation. II. Closed systems. Transactions of the 9th International Congress of Soil Science. 58:561-568.

Wheeler, G.M. 1885. Facts Concerning the Origin, Organization, Administration, Functions, History, and Progress, of the Principal Government Land and Marine Surveys of the World, Being Extracts from the Report on the Third International Geographical Congress and Exhibition. Government Printing Office. Washington, D.C.

Whitney, M. 1892. Some Physical Properties of Soils in their Relation to Moisture and Crop Distribution. U.S. Department of Agriculture, Weather Bureau. Bulletin No. 4. Washington, D.C.

Whitney, M. 1900. Field Operations of the Division of Soils. U.S. Department of Agriculture, Bureau of Soils. Washington, D.C.

Whitney, M. 1909. Field Operations of the Bureau of Soils. U.S. Department of Agriculture, Bureau of Soils. Washington, D.C.

Widgren, M. 1979. A simulation model of farming systems and land use in Sweden during the early Iron Age (c. 500 B.C.-550 A.D.). Journal of Historical Geography. 5(1):21-32.

Woodbridge, W.C. 1823. Isotherm chart, or, view of climates & productions, Drawn from the accounts of Humboldt & Others. New York Public Library. Available online: http://digitalgallery.nypl.org/nypldigital/id?465012. Accessed [4/15/2013].

Wysocki, D.A., P.J. Schoeneberger, and H.E. LaGarry. 2000. Geomorphology of soil landscapes. *In* M.E. Sumner (ed.). Handbook of Soil Science. CRC Press. Boca Raton, Florida.

Young, F.J. and R.D. Hammer. 2000. Soil-landform relationships on a loess-mantled upland landscape in Missouri. Soil Science Society of America Journal. 64(4):1443-1454.

Zaichikov, V.T. 1955. Voyagers of Ancient China and Geographic Studies in the People's Republic of China [Puteshestvenniki drevnego Kitaya I geograpficheskie issledovaniya v Kitaiskoi Narodnoi Respublike]xd. Geografgiz. Moscow.

Zebarth, B.J., H. Rees, J. Walsh, L. Chow, and D.J. Pennock. 2002. Soil variation within a hummocky podzolic landscape under intensive potato production. Geoderma. 110(1):19-23.

CHAPTER 3. SEMANTIC CALIBRATION OF DIGITAL TERRAIN ANALYSIS SCALE

Abstract

Digital terrain analysis (DTA) provides efficient, repeatable, and quantified metrics of landscape characteristics that are important to the Earth sciences, particularly for detailed soil mapping applications. However, DTA has not been field tested to the extent that traditional field metrics of topography have been. Human assessment of topography synthesizes multiple parameters at multiple scales to characterize a landscape, based on field experience. In order to capture the analysis scale used by field scientists, I calibrated the DTA metrics of profile curvature, relative elevation, and slope gradient in the context of the commonly used field description of hillslope position. A peak in agreement between field assessment and digital terrain analysis was found at field equivalent distances of 63 m for profile curvature, 135 m for relative elevation, and 9 m for slope. Segregating observation points by three terrain types reduced the number of points in calibration groups. The smaller number of points in terrain subgroups made those results more susceptible to the scale effect of the modifiable area unit problem, thereby increasing agreement in the direction of scale that minimized variability. This effect sometimes caused a shift in the optimal scale for agreement between digital and field assessment. The clarity of calibration signal also declined with smaller sample sizes. Despite the reduced number of samples, different terrain types generally had similar calibrated analysis scales. These results suggest that the most effective analysis scale for capturing hillslope processes is different for each DTA metric, while the calibrated analysis scales may be

transferable to a wide range of terrain. Given the field experience of soil scientists, these calibrations of DTA metrics are likely to have stronger correlations with hillslope properties and could be used together to classify hillslope position consistently across large extents.

Keywords: digital terrain analysis, analysis scale, semantic calibration

1. Introduction

Digital terrain analysis (DTA) metrics are typically scale dependent (Wood, 1996a; Albani et al., 2004; Hupy et al., 2004; Roecker and Thompson, 2010). Therefore, when used as parameters in models, attention needs to be given to using the optimal analysis scale for the process being represented. Otherwise, the use of the incorrect analysis scale could result in erroneous model outcomes or mistakenly disregarding important parameters (Claessens et al., 2005). This study calibrates the analysis scale of three DTA metrics to the expert knowledge of hillslope position classification.

Processes occur at certain phenomenon scales. Analysis scale, on the other hand, is the generalization that is best able to detect that phenomenon (Montello, 2001). In DTA terms, analysis scale is the combination of cell resolution and the number of cells incorporated in an analysis neighborhood (Thompson et al., 2001; Albani et al., 2004). Experience has calibrated field scientists' sense of analysis scale for measuring landscape characteristics. Similar calibration of analysis scale needs to be derived for digital terrain metrics. This is especially true for expert knowledge based models and models that seek to predict or be validated by human-made classifications in the field (i.e. digital soil mapping). Until more field studies are conducted to quantitatively determine the scale at which the processes influencing the variation of

landscape properties operate, utilizing the scale learned by field scientists provides the best supported method for predicting metric-process relationships. Through semantic calibration, DTA can be parameterized to the tacit knowledge of field scientists (Dehn et al., 2001).

Despite the importance of analysis scale, analysis neighborhoods are often set to a 3 by 3 cell area for all DTA metrics, leaving the analysis scale dependent on cell resolution (e.g. Zevenbergen and Thorne, 1987; Gallant and Wilson, 1996; Lapen and Martz, 1996; MacMillan et al., 2000; Shi et al., 2009). In some cases, neighborhood size is considered to be such a fundamental assumption that it is not specified in research methods (e.g. Mitášova and Hofierka, 1993; Joel et al., 1994; Florinsky et al., 2002). By focusing on cell resolution alone, the analysis scale can be inadvertently determined by the best available resolution and computational efficiency (Moore et al., 1993; Sharma et al., 2011).

Although the effect of DEM resolution on geomorphic models has been frequently studied (e.g. Chang and Tsai, 1991; Chaplot et al., 2000; Schoorl et al., 2000; Thompson et al., 2001; Kienzle, 2004; Wu et al., 2008), the effect of analysis scale has been assessed less widely. Nonetheless, the impact of analysis scale has been observed in DTA studies. For example, while testing a circular neighborhood method for calculating slope gradient, Shi et al. (2007) found that reducing analysis scale decreased error more than the difference between any of the calculation methods.

Studies in the context of digital soil mapping have also determined that analysis scale affects results. However, the complex interactions between different DTA metrics, combinations of soil properties, and value systems inherent within soil classification systems,

have clouded interpretation of those results. Smith et al. (2006) varied the analysis scale of slope gradient, plan curvature, and profile curvature as inputs to the SoLIM soil mapping model. Because analysis scale for the parameters was not allowed to vary independently, it is unclear if the determination of different optimal analysis scales for different terrain types (i.e. 24-36 m for high relief, 33-48 m for gently rolling) reflects different phenomenon scales for different landscapes, or a shift in the dominant predictive metric. Behrens et al. (2010) tested analysis scale for terrain metrics independently and found that the optimal analysis scale varied by soil class. The variability of optimal analysis scale between soil classes may be produced by the complexity and values built into the classification system, rather than processes acting at different scales. Therefore, point observations for single attributes need to be examined for determining optimal analysis scale. Roecker and Thompson (2010) did this and concluded analysis scales between 117-189 m to be optimal for correlating point observations of soil carbon, rock fragment content, and clay content at different depths with profile curvature.

Recognizing the value of accumulated field experience, expert knowledge models seek to capture tacit knowledge to improve model performance. Hillslope position is a useful, tacit knowledge based, metric for many geomorphic studies; soil scientists have long used this field metric extensively across the United States in their efforts to inventory soil resources. For this reason, I argue that data collected by the U.S. Soil Survey has the large quantity of observation points needed to calibrate DTA with field terrain analysis and to reduce the noise that is inherent in human observations of continuous variables. Therefore, the purpose of this study is to semantically calibrate the DTA metrics of slope gradient, profile curvature, and relative elevation to the analysis scale used by soil scientists in determining hillslope position. Because

of the categorical nature of hillslope position and high variability of human interpretation, a method of percent agreement is introduced for identifying the analysis scale with the strongest signal. The resulting calibrated metrics can be used as parameters to a variety of models, including fuzzy and discrete classifications.

2. Methods

2.1. Relating Field Assessment of Hillslope Position to Digital Terrain Analysis

Terrain characteristics for describing hillslope process zones and predicting soil properties has been an important area of study in soil geography (e.g. Milne, 1935; Ruhe, 1960; Burras and Scholtes, 1987; Carter and Ciolkosz, 1991; Donald et al., 1993; Stolt et al., 1993; Cerdá, 1998; Yoo et al., 2005). Although largely qualitative, the use of hillslope position has been tuned through decades of scientific study and field experience. Hillslope position is a contextual metric that divides a landscape into areas where the interaction between hydrology and relief affect the properties of the soil in different ways (Wysocki et al., 2000). Summit positions are often flat and higher in elevation than its surrounding areas, which tends to result in more infiltration than runoff, and less influence from the water table. Shoulder positions are also relatively high in elevation, but their convex shape and steep slope shifts the balance to a greater likelihood of runoff over infiltration. Backslopes are generally considered to be transition zones, and although the slope shape is generally linear, the slope gradient is generally the highest of the hillslope positions, and steeper slope gradients promote runoff. Footslope positions are concave in profile curvature and lower on the slope, causing these sites to be wetter and sediment accumulating positions. The toeslope is flatter and lies at the lowest

relative elevation along the slope. Its juxtaposition makes it the zone with the most accumulation of materials transported from upslope and the most affected by the water table.

In the field, soil scientists synthesize the terrain characteristics of slope gradient, profile curvature, and relative elevation to identify the functional zones as defined by hillslope position (Figure 3.1). Although hillslope position is one of the most basic and widely used terrain descriptions for soil geomorphology, it is primarily based on tacit knowledge without quantitative definitions. Soil scientists have calibrated a mental model for identifying soil-landscape patterns. This study focuses on identifying the analysis scales of DTA metrics equivalent to the analysis scales used in the soil scientists' mental model. Chapter 4 uses the calibrated analysis scales determined in this chapter to quantitatively define hillslope position in terms of DTA metrics.

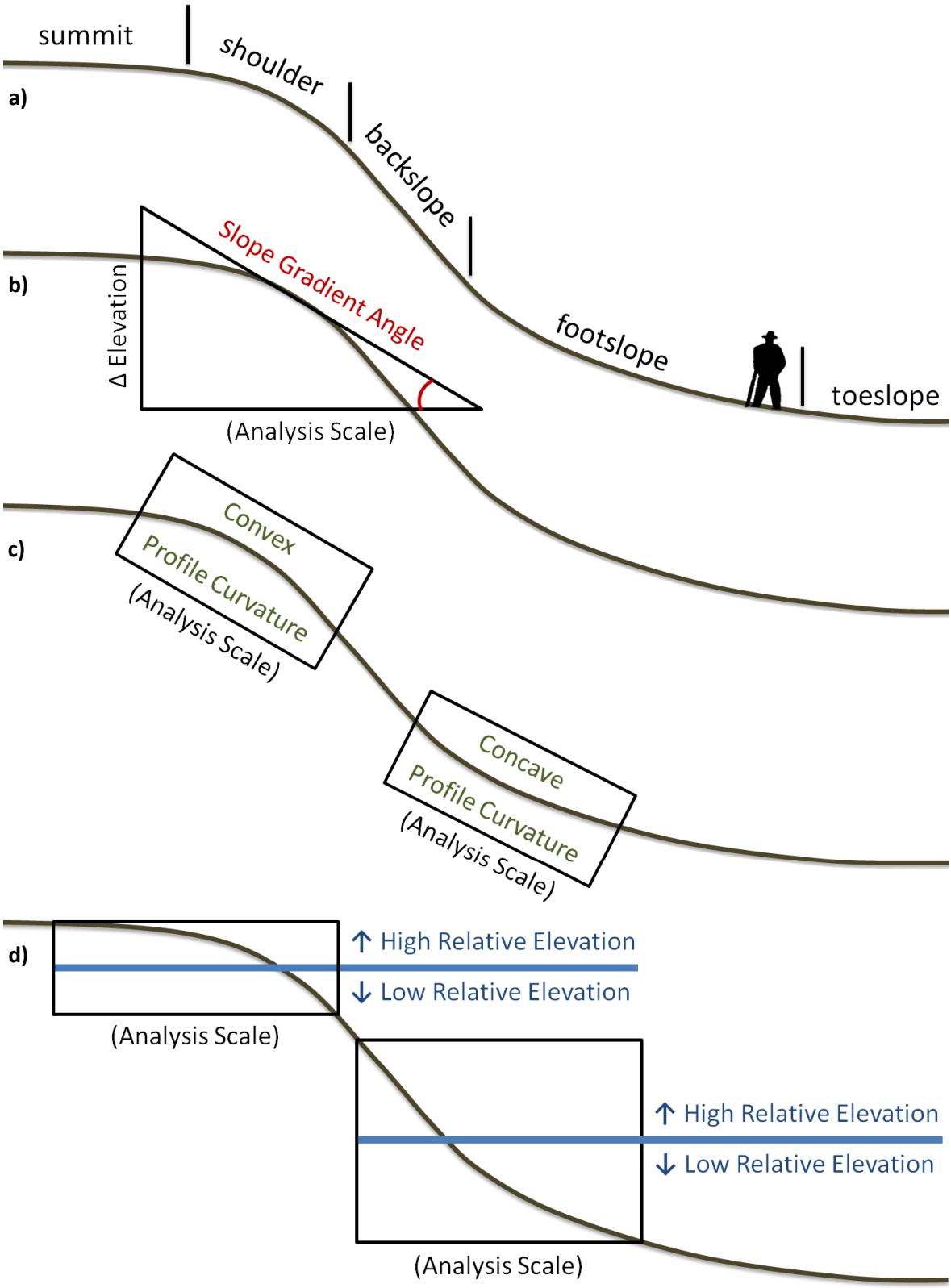


Figure 3.1. In order to classify the functional zones of hillslope position (a), soil scientists in the field synthesize their assessment of b) slope gradient, c) profile curvature, and d) relative elevation to determine the hillslope position of a location.

2.2. Semantic Calibration of Analysis Scale

DTA was performed at multiple analysis scales for comparison with soil scientists' field assessments. Slope gradient and profile curvature were calculated with varying neighborhood sizes using the r.param.scale function in GRASS 6.4.2 (GRASS Development Team, 2012). The r.param.scale function calculates both slope and profile curvature by fitting a quadratic trend surface using least squares (Evans, 1979). The analysis scale can be expanded by including more grid cells in the parameters for the polynomial and solving the least squares via a matrix (Wood, 1996b).

In order to have a user controlled analysis scale for relative elevation, I developed a procedure in ArcGIS 10.1 (ESRI, 2012). This method for calculating relative elevation subtracted an inverse elevation grid from the original elevation grid by analysis neighborhoods. The inverse elevation was the elevation subtracted from the sum of the minimum and maximum elevation values in the analysis neighborhood. The neighborhood size was controlled via the focal statistics used to determine the minimum and maximum elevation. The resulting relative elevation grid had increasing positive values above and decreasing negative values below the analysis neighborhood's middle elevation (Figure 3.2).

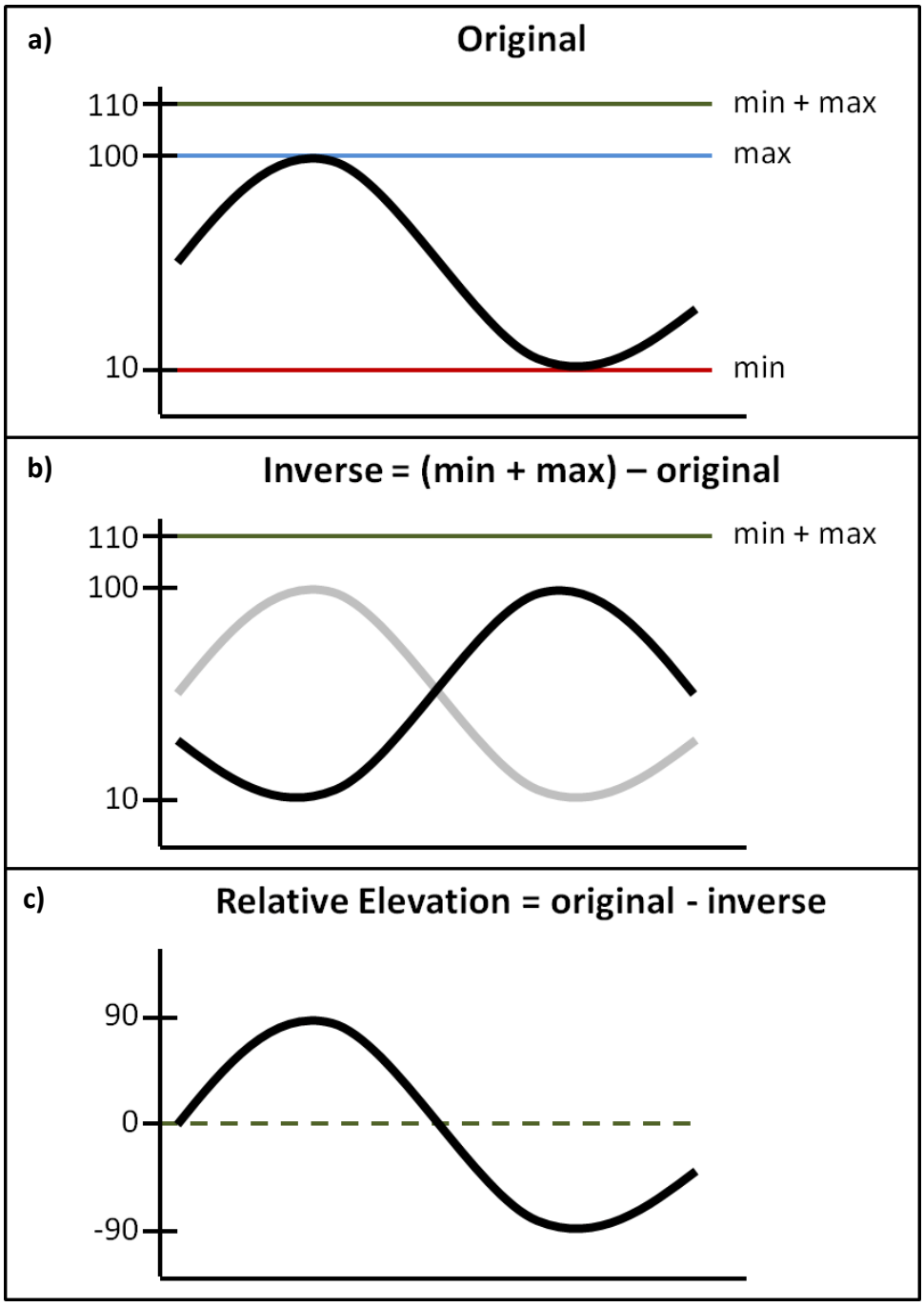


Figure 3.2. In this research, relative elevation is calculated on a neighborhood by neighborhood basis for each cell. a) First, a reference elevation ceiling is calculated by summing the neighborhood minimum and maximum elevations. b) Then, the central cell elevation is subtracted from the elevation ceiling to create an inverse elevation grid. c) By subtracting the inverse from the original elevation grid, a relative elevation grid is created with the mid-point between the neighborhood minimum and maximum having a value of zero. Elevation values above the mid-point are increasingly positive. Below the elevation mid-point, values are negative and decrease with vertical distance.

A LiDAR-derived, 3 m resolution, elevation grid was aggregated to resolutions of 9 m and 27 m to reflect the resolutions of 1/3 arc second and 1 arc second that other elevation grid products are commonly available in, while still preserving cell alignment. Then, all three grids were processed for the three DTA metrics using varied neighborhood sizes by the experimental matrix in Table 3.1. The experimental matrix was designed to cover the full range of reasonable analysis scales and to use combinations of cell resolution and neighborhood size where analysis scale would align across cell resolutions.

Table 3.1. Experimental matrix for varying combinations of DEM cell size and neighborhood size for varying analysis scale.

	Neighborhood Size							
Distance	**9 m**	**15 m**	**27 m**	**45 m**	**63 m**	**81 m**	**135 m**	**189 m**
LiDAR (3 m)	3x3	5x5	9x9	15x15	21x21	27x27	45x45†	63x63†
(9 m resample)			3x3	5x5	7x7	9x9	15x15	21x21
(27 m resample)						3x3	5x5	7x7

†only used for relative elevation

Field observation points, collected by U.S. Natural Resource Conservation Service (NRCS) soil scientists, were then intersected with each of the DTA grids. The resulting match-up allowed for the comparison of DTA calculations with soil scientists' assessment in the field by location. The soil scientists recorded slope gradient as an integer, allowing for a quantitative comparison. Agreement for slope gradient was evaluated by the mean absolute difference between the field observed and the DTA calculated slope gradient in degrees. Because profile curvature and relative elevation are included in hillslope position as categorical attributes, not quantitative measures, comparison between field observation and DTA were compared on a basis of percent agreement by categorical definition (Table 3.2).

Due to the fuzzy nature of landscape elements and the subjectivity of human assessment, agreement was only tested for the definitional extremes. For profile curvature, agreement was evaluated for negative values corresponding to concave slope shape and positive values corresponding to convex slope shapes. Relative elevation was quantified as distance above (positive) or below (negative) the mid-elevation of the analysis neighborhood. Agreement was evaluated as negative values corresponding with low hillslope positions and positive values corresponding with high hillslope positions.

Table 3.2. Definition table for relating qualitative hillslope position descriptions to the DTA of profile curvature and relative elevation. Attributes highlighted in gray were used for the semantic calibration.

Hillslope Position	**Profile Curvature**	**Relative Elevation**
Summit	Linear	High
Shoulder	Convex	High
Backslope	Linear	Middle
Footslope	Concave	Low
Toeslope	Linear	Low

The level of agreement between digital and field assessment should increase as the digital analysis scale is more closely aligned with the analysis scale used by the soil scientists in the field. Therefore, the optimal semantic calibration was determined to be the analysis scale with the highest percent agreement for the qualitative metrics. Specifically, for profile curvature and relative elevation, percent agreement was calculated for each definitional category separately and then summarized with the mean of those results. Using the mean of the categorical results avoided over emphasizing a category that may have more observations than the other. In other words, the mean percent agreement for a particular analysis scale

equally weights the two categories used for evaluation. For slope gradient, agreement could be measured on a continuous scale. Therefore, the optimal semantic calibration for slope gradient was determined by the lowest mean absolute difference between the DTA calculation and the field estimate.

Consistent analysis scale calibration between grid resolutions provided support for the determination that calibration was due to the matching of analysis scales and not to matching an artifact pattern in the source DEM. Therefore, a consistent peak in percent agreement at equivalent analysis scales was considered to be a strong signal for identifying the best matching analysis scales between the two hillslope characterization models.

2.3. Study Area

This study analyzed data for Ottawa County, Michigan, on the eastern shore of Lake Michigan (Figure 3.3). Large dunes have formed on the western edge of Ottawa County (Figure 3.4a). The central part of the county is lake plain formed beneath Glacial Lake Chicago (Figure 3.4b). This glacial lake plain is flat with interspersed dunes of decreasing size (from west to east) that have encroached from the west. The northeast and southeast portions of the area grade into a hummocky terrain, more characteristic of till plains (Figure 3.4c). Across the entire 1,488 km^2 study area the elevation ranges from 173 to 292 meters above sea level.

Ottawa County was chosen because of the availability of a LiDAR-based elevation grid (2004) and a number of georeferenced observations of hillslope position, by NRCS soil scientists, taken in the field. The LiDAR-based elevation grid has a 3 m resolution, and was

provided by the Ottawa County government. Some patterned striping was visible in the original 3 m elevation grid. However, it is not likely that the striped pattern was an artifact of the LiDAR data collection process, because the pattern orientation varied by agricultural field and the spatial frequency was not consistent. A few locations appeared to have the striped pattern occurring at a regular interval of 10 or 30 m. Although the ratio of relief to distance was only 1 to 2% in the striped pattern, the potential for this pattern to affect the DTA of the 3 m resolution grid exists. However, the resampling of the 3 m elevation grid to larger resolutions reduces this type of 'noise' and provides a secondary check for the influence of this patterned striping on the DTA of the original 3 m resolution grid. Additional information on the analysis of the LiDAR-based elevation grid for potential systematic errors is included in Appendix A.

Georeferenced field observations of hillslope position were provided by the Grand Rapids, Michigan Soil Survey Office. Recorded GPS points at observation sites were joined with a database created from the paper records of field observations. Observations were made by the Grand Rapids Soil Survey Office staff between 2007 and 2009. The GPS recorded observations used in this study were all 8-10 point transects, of typically 40-80 m point spacing, for a total of 1,068 points (Figure 3.3). The hillslope position assessment of the soil scientists was converted into categorical attributes in terms of profile curvature and relative elevation (Table 3.2), as interpreted from the hillslope position diagram presented in Schoeneberger et al. (2012). Not all recorded observations were interpretable for these two digital terrain metrics. For example, observation points that were recorded simply as "flat," could not have a relative elevation interpreted from it. From the transect observation points, 966 were interpretable for profile curvature and 572 were interpretable for relative elevation. Field observed values of

slope gradient were available for all 1,068 points. Using only points in the categories that were least likely to overlap reduced the number of field observations that could be used in the calibration. Therefore, 216 points were used for the evaluation of profile curvature and 366 points were used for the evaluation of relative elevation.

In order to test for the analysis scale used by field scientists' dependence on landscape characteristics, three terrain sub-regions were delineated within the study area. Each sub-region was relatively homogenous in epitomizing high relief shoreline dunes, moderate relief hummocky hills, and a low relief glacial lake plain. It should be noted that the terrain sub-regions do not subdivide the entire study area; rather, the sub-regions identify respective areas as consistently similar in relief as possible (Figure 3.3). All three areas are similar in mean elevation, but differ drastically in elevation standard deviation (Table 3.3). The dune landscape contrasts greatly in slope gradient compared to the other two landscapes, but the high slope of a few drainage ditches cut into the lake plain landscape masks the relief contrast between the lake plain and hummocky hills landscapes (Figure 3.5). Using a standard, 3 by 3 neighborhood size on the 3 m resolution elevation grid, the mean slope gradients for the dune, hummocky, and glacial lake plain landscapes were 9.7°, 1.5°, 1.2° respectively (Table 3.3).The same evaluation for semantic calibration was performed on observation points within these sub-regions separately and compared with the calibration for the population of observation points as a whole.

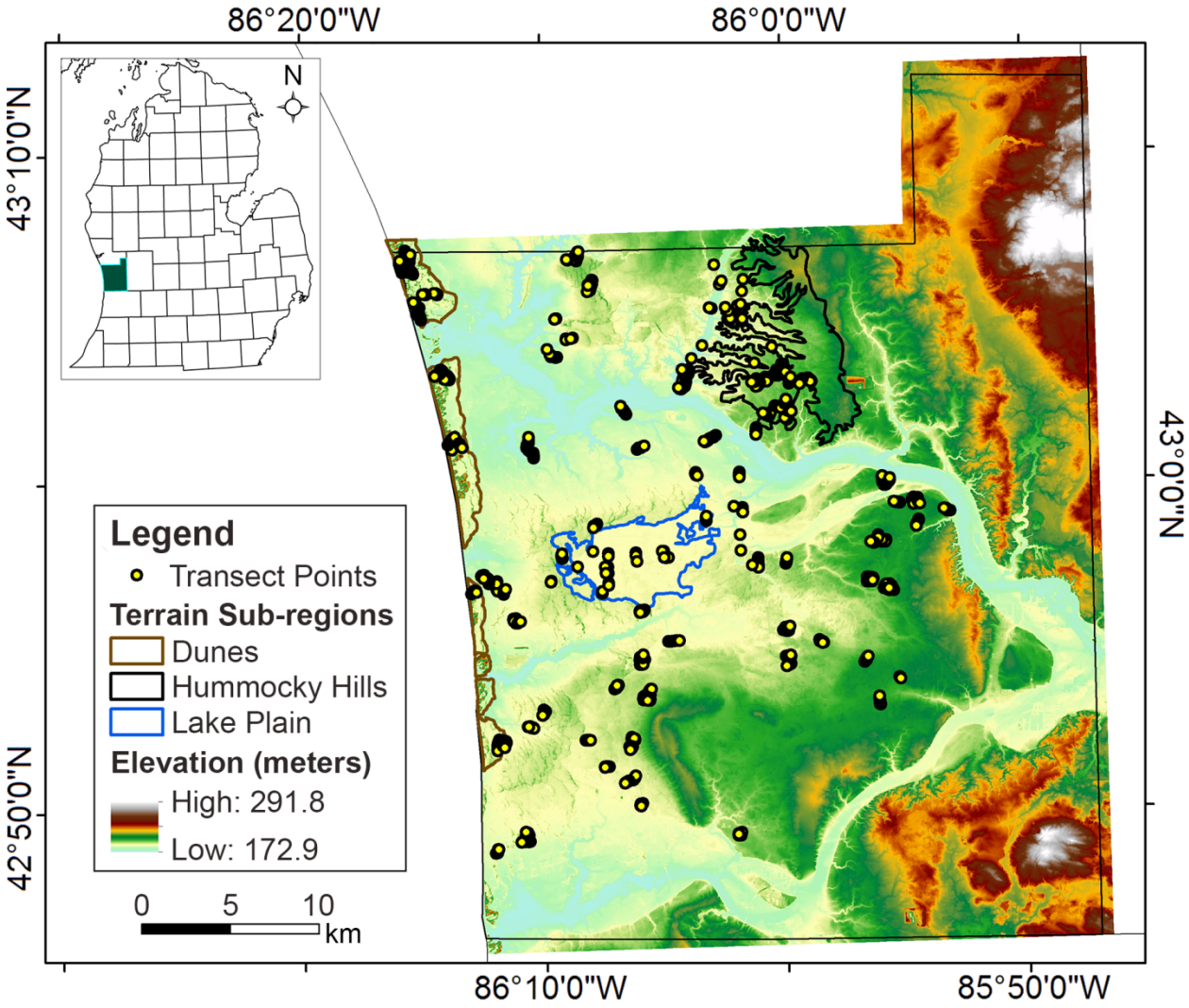


Figure 3.3. Location of study area, Ottawa County, in the lower peninsula of Michigan, U.S. The map also includes locations of field observation transect points and the three study sub-regions delineated for comparing terrain types.

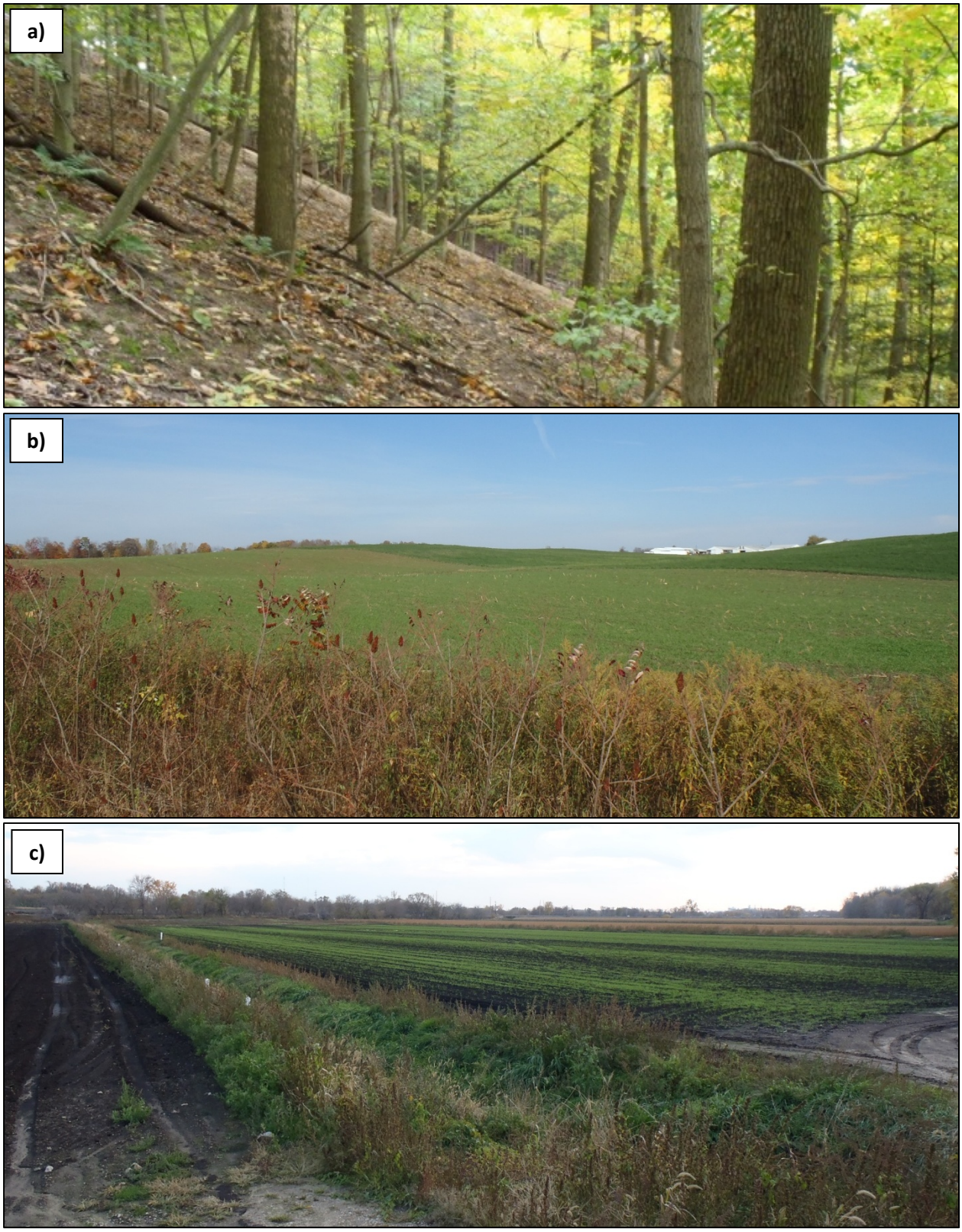


Figure 3.4. Example images from the a) dune landscape, b) hummocky landscape, and c) glacial lake plain landscape. Photos by the author.

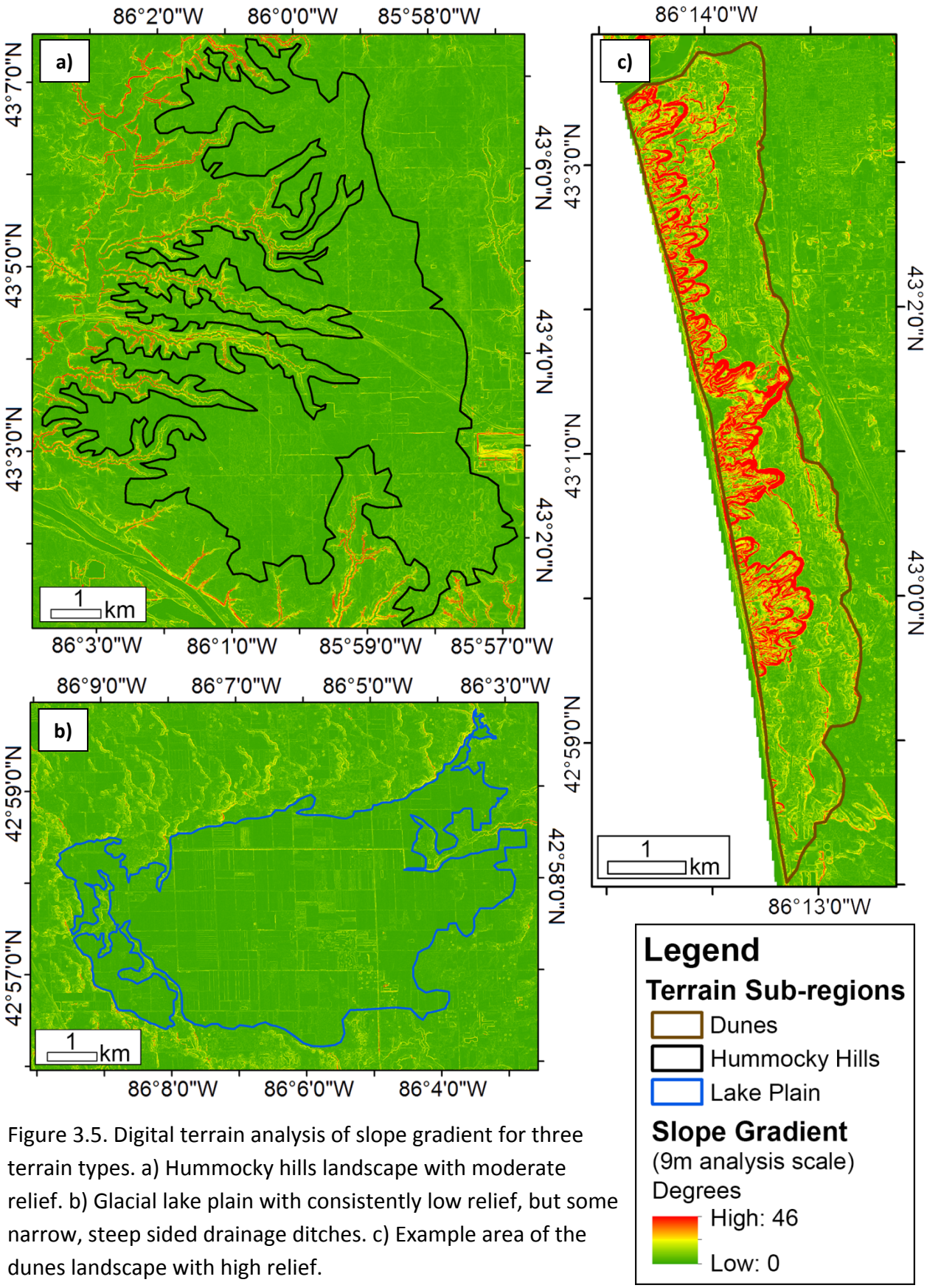


Figure 3.5. Digital terrain analysis of slope gradient for three terrain types. a) Hummocky hills landscape with moderate relief. b) Glacial lake plain with consistently low relief, but some narrow, steep sided drainage ditches. c) Example area of the dunes landscape with high relief.

Table 3.3. Descriptive statistics of elevation and slope gradient for the three landscape sub-regions.

	Dunes	**Hummocky Hills**	**Lake Plain**
Km^2	29.6	42.5	30.5
Elevation (m)			
Min	175.7	186.8	186.7
Max	250.4	216.3	195.2
Range	74.7	29.5	8.5
Mean	192.5	198.8	190.0
Std. Dev.	8.5	5.1	0.6
Slope Gradient (degrees)			
Min	0.0	0.0	0.0
Max	48.3	23.2	35.1
Range	48.3	23.2	35.1
Mean	9.7	1.5	1.2
SD	9.4	1.2	1.2

3. Consideration of the Modifiable Area Unit Problem

As with any scale dependent experiment, the scale effect of the modifiable area unit problem (MAUP) must be considered (Armhein, 1995; Jelinski and Wu, 1996). In the case of slope gradient and profile curvature, increasing analysis scale will reduce the occurrence of extreme values and overall increase the similarity of values (Figures 3.6 and 3.7). Conversely, decreasing analysis scale will reduce variability and occurrence of extreme values for relative elevation (Figure 3.8). Note that this scale effect can have a greater impact on smaller sample populations. Although the authors did not identify it as such, this pattern can also be observed in the data of Roecker and Thompson (2010). As indicated by the reduction in extreme values, there is a potential for inflated agreement at analysis scales with less variability. I attempt to overcome this issue with a large quantity of sample points.

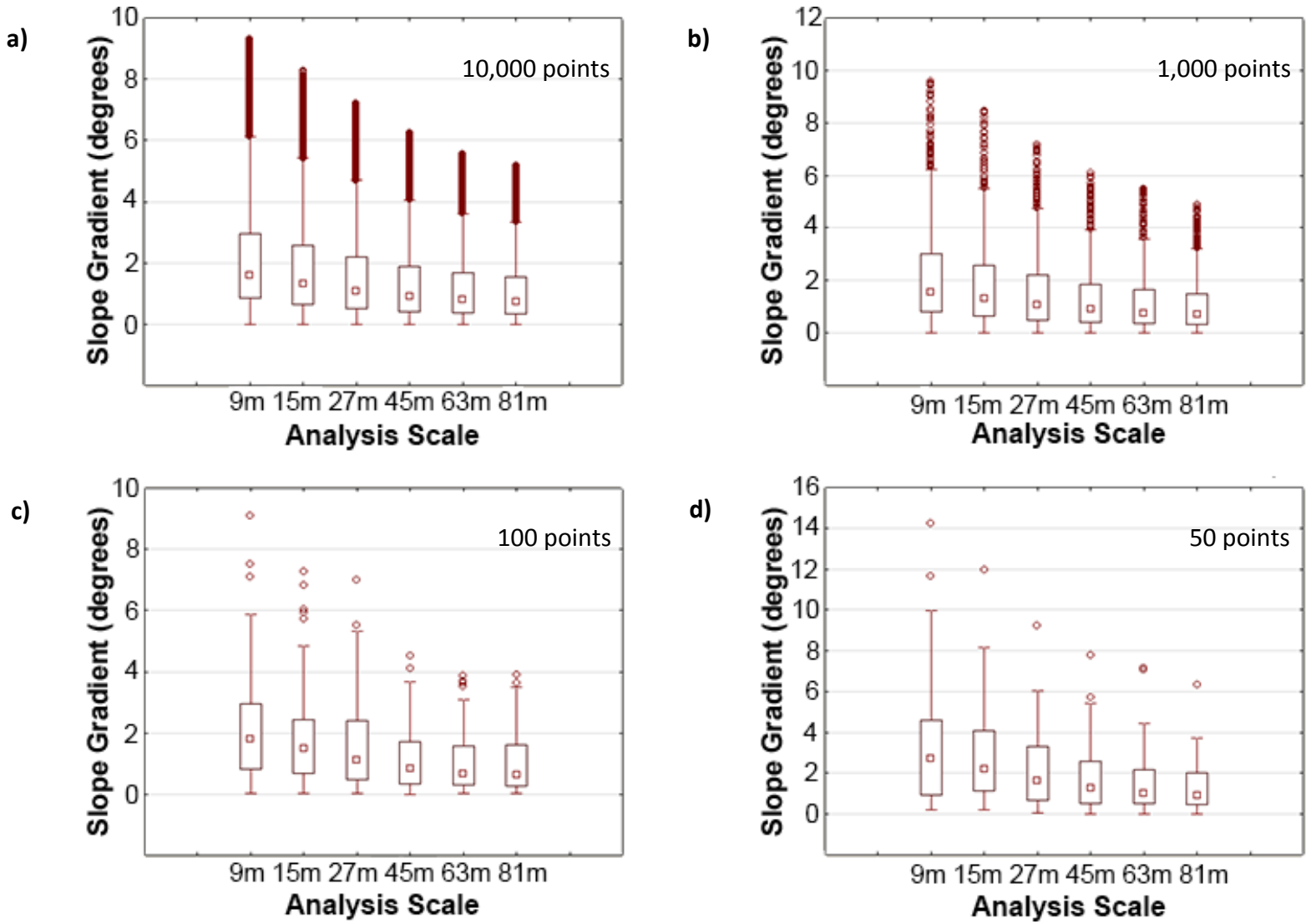


Figure 3.6. Scale effect of the modifiable area unit problem on slope gradient. Fewer extreme values increase the likelihood of agreement/correlation. Sequence of graphs illustrates reduction in extreme values with reduction of random sample size at a) 10,000 points, b) 1,000 points, c) 100 points, and d) 50 points.

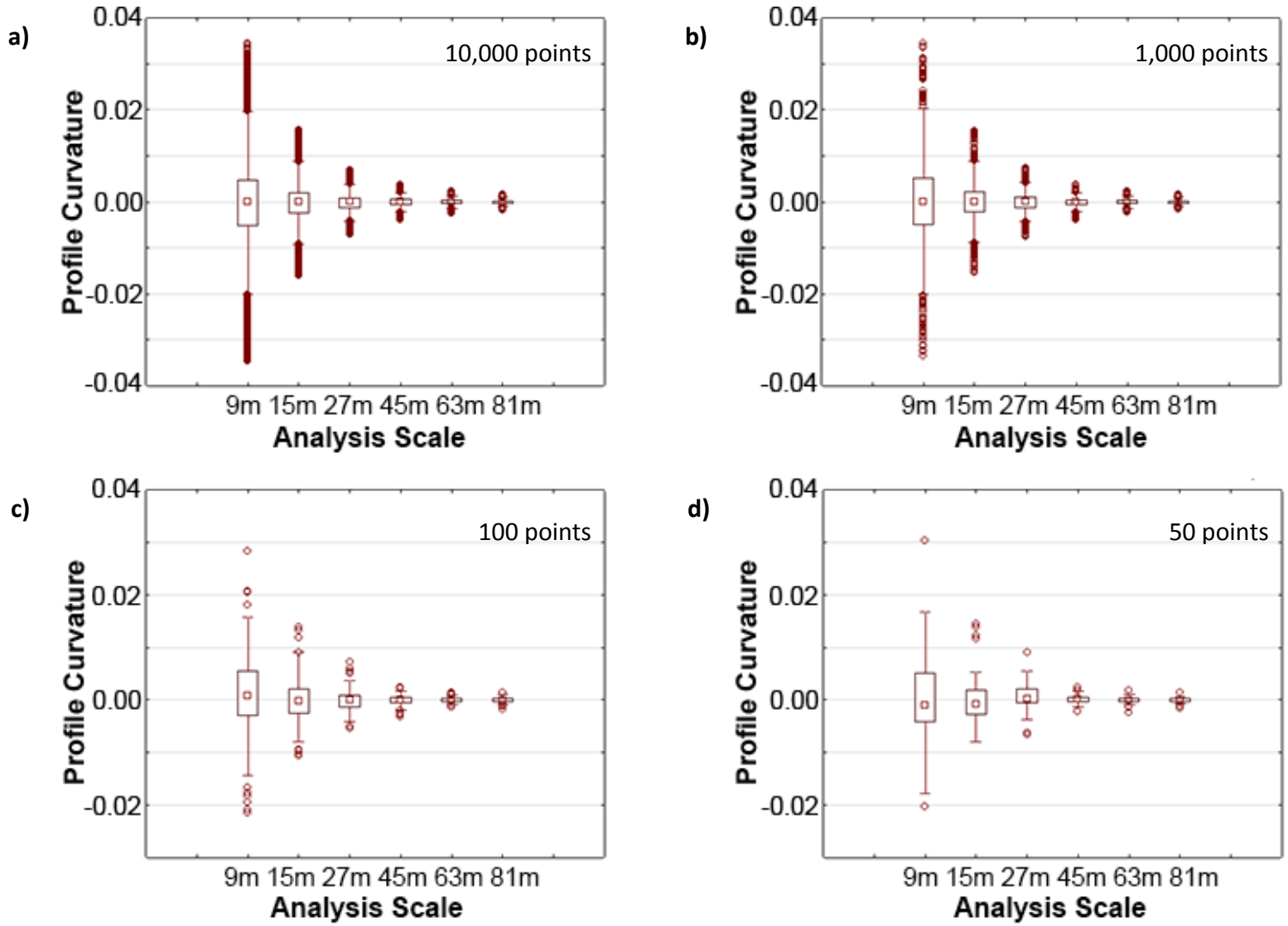


Figure 3.7. Scale effect of the modifiable area unit problem on profile curvature. Fewer extreme values increase the likelihood of agreement/correlation. Sequence of graphs illustrates reduction in extreme values with reduction of random sample size at a) 10,000 points, b) 1,000 points, c) 100 points, and d) 50 points.

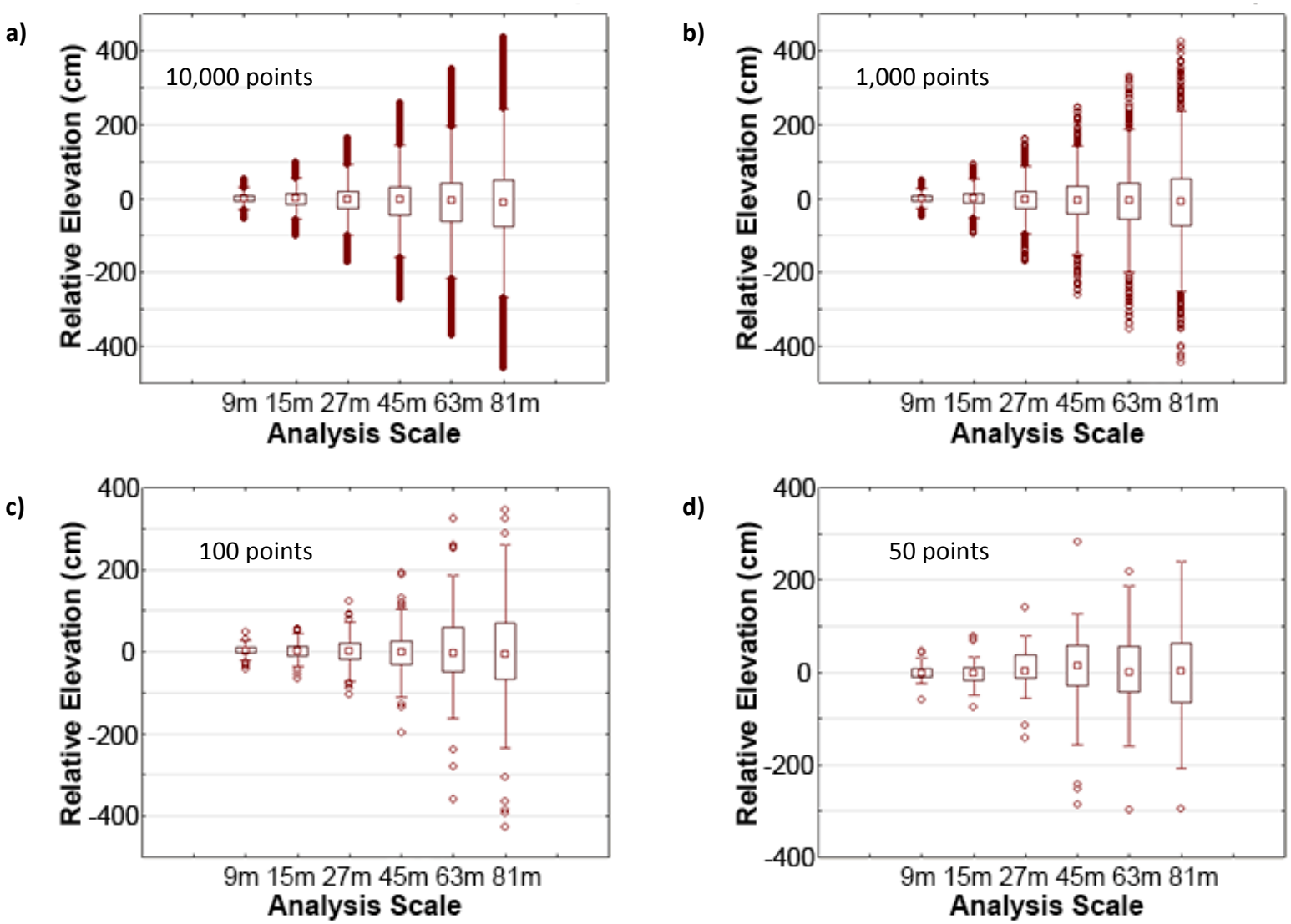


Figure 3.8. Scale effect of the modifiable area unit problem on relative elevation. Fewer extreme values increase the likelihood of agreement/correlation. Sequence of graphs illustrates reduction in extreme values with reduction of random sample size at a) 10,000 points, b) 1,000 points, c) 100 points, and d) 50 points.

4. Results

4.1. Analysis Scale Calibration of all Observation Points

The calibration of all three terrain metrics showed a pattern of increasing agreement up to a certain analysis scale and then decreasing agreement with scales coarser than the optimal matching analysis scale. In describing the result details, the different combinations of grid resolution and neighborhood size will be referred to by the field distance equivalent for the particular analysis scale. Because all analysis scales are based on square neighborhoods of square cells, it is simpler and more relatable to the field environment to use the field equivalent distance for the linear dimension of the analysis scale. However, it should be noted that field observations of hillslope position are likely more linear (aligned with the profile of the hillslope) than the square area used by DTA.

Profile curvature had the highest agreement between digital calculations and field observations at a field equivalent distance of 63 m (Table 3.4). Because the minimum possible analysis scale for a grid resolution of 27 m is 81 m (3 cells * 27 m = 81 m), the same signal could not be observed with the 27 m grid. Instead, the highest percent agreement was at the smallest analysis scale, which is closest to the scale signal observed in the other two resolutions. An exception to this signal was the concave profile curvature agreement for the 9 and 27 m resolution grids, where the highest percent agreement was at a scale of 135 m. However, for the 9 m resolution grid, the percent agreement at 81 m and 63 m was only 3% less than at 135 m. These increases in analysis scale for the highest percent agreement could be caused by the

scale effect of MAUP. The percent agreement peak for the combined concave and convex categories still showed a strong signal at 63 m, or the closest possible analysis scale.

Table 3.4. Percent agreement results for profile curvature of all observation points. Concave and convex agree are the count of points where the digital and field assessments of slope profile shape were in agreement. Percent is the proportion of agreement out of the total number of points.†

Profile Curvature	3 m Grid					
Distance	**9 m**	**15 m**	**27 m**	**45 m**	**63 m**	**81 m**
Concave agree	60	59	72	72	73	70
Convex agree	67	72	75	77	77	76
% concave agree	57.1%	56.2%	68.6%	68.6%	69.5%	66.7%
% convex agree	60.4%	64.9%	67.6%	69.4%	69.4%	68.5%
Mean % agreement	58.8%	60.5%	68.1%	69.0%	69.4%	67.6%

	9 m Grid					
Distance	**27 m**	**45 m**	**63 m**	**81 m**	**135 m**	**189 m**
Concave agree	64	65	71	71	74	65
Convex agree	72	75	76	73	68	74
% concave agree	61.0%	61.9%	67.6%	67.6%	70.5%	61.9%
% convex agree	64.9%	67.6%	68.5%	65.8%	61.3%	66.7%
Mean % agreement	62.9%	64.7%	68.0%	66.7%	65.9%	64.3%

	27 m Grid		
Distance	**81 m**	**135 m**	**189 m**
Concave agree	68	75	68
Convex agree	77	69	75
% concave agree	64.8%	71.4%	64.8%
% convex agree	69.4%	62.2%	67.6%
Mean % agreement	67.1%	66.8%	66.2%

†Analysis scale with strongest signal highlighted in dark gray; other strong agreements shown in lighter gray.

The signal for relative elevation was at 135 m (Table 3.5). To confirm this for the 3 m resolution grid, the experimental matrix needed to be extended beyond a field equivalent distance of 81 m. The signal for a field equivalent distance scale at 135 m was consistent for nearly all measures. The only exception was the percent agreement for relatively high elevation using the 27 m resolution grid. In that case, one more point was in agreement for the 81 m over the 135 m scale, increasing the amount of agreement by 0.5%. The analysis scale for the relative elevation signal indicates relative elevation is considered contextually over a larger area in the field, by mappers, as compared to the other terrain metrics.

The numeric field observations of slope gradient provided a quantitative determination of matching analysis scales. Although it is unrealistic to expect integers recorded by human observation to exactly match the rational numbers calculated by DTA, a minimal difference provides a calibration of the digital method to the analysis scale used in the field. For each grid resolution, the mean difference was lowest at the finest analysis scale possible (Table 3.6). The trend of decreasing mean differences with decreasing neighborhood size suggests the optimal analysis scale for digitally determining slope gradient similar to a soil scientist's characterization in the field is relatively small.

Table 3.5. Percent agreement results for relative elevation of all observation points. Low and high agree are the count of points where the digital and field assessments of relative elevation were in agreement. Percent is the proportion of agreement out of the total number of points.†

Relative Elevation	3 m Grid							
Distance	**9 m**	**15 m**	**27 m**	**45 m**	**63 m**	**81 m**	**135 m**	**189 m**
Low agree	101	115	135	148	158	163	176	173
High agree	109	117	123	136	137	140	144	140
% low agree	49.0%	55.8%	65.5%	71.8%	76.7%	79.1%	85.4%	84.0%
% high agree	54.5%	58.5%	61.5%	68.0%	68.5%	70.0%	72.0%	70.0%
Mean % agreement	51.8%	57.2%	63.5%	69.9%	72.6%	74.6%	78.7%	77.0%

	9 m Grid					
Distance	**27 m**	**45 m**	**63 m**	**81 m**	**135 m**	**189 m**
Low agree	125	152	159	164	177	172
High agree	129	133	139	139	148	132
% low agree	60.7%	73.8%	77.2%	79.6%	85.9%	83.5%
% high agree	64.5%	66.5%	69.5%	69.5%	74.0%	66.0%
Mean % agreement	62.6%	70.1%	73.3%	74.6%	80.0%	74.7%

		27 m Grid		
	Distance	**81 m**	**135 m**	**189 m**
	Low agree	153	167	166
	High agree	145	144	138
	% low agree	74.3%	81.1%	80.6%
	% high agree	72.5%	72.0%	69.0%
	Mean % agreement	73.4%	76.5%	74.8%

†Analysis scale with strongest signal highlighted in dark gray; other strong agreements shown in lighter gray.

Table 3.6. Mean absolute difference results for slope gradient of all observation points.

Slope (degrees)	3 m Grid					
Distance	**9 m**	**15 m**	**27 m**	**45 m**	**63 m**	**81 m**
Mean difference	3.1°	3.2°	3.4°	3.8°	4.0°	4.1°

	9 m Grid					
Distance	**27 m**	**45 m**	**63 m**	**81 m**	**135 m**	**189 m**
Mean difference	3.4°	3.8°	4.0°	4.1°	4.4°	4.5°

	27 m Grid		
Distance	**81 m**	**135 m**	**189 m**
Mean difference	4.1°	4.4°	4.5°

4.2. Analysis Scale Calibration by Terrain Sub-regions

Focusing on smaller sub-groups of observations located in terrain sub-regions had less clear signals due to the smaller quantity of points. However, they provide some insight on terrain's effect on the analysis scale used by the scientists in the field.

The calibrated analysis scale for matching DTA with field observations of profile curvature in all three landscapes remained the field equivalent distance of 63 m for the 3 m resolution grid (Table 3.7). However, the smaller population of observation points showed coarser analysis scales to be optimal for the 9 m and 27 m grids. As relief decreased (dunes to hummocky hills to lake plain) the size of the optimal analysis scale steadily increased for the lower resolution grids.

Relative elevation had the weakest signal when examining the smaller population points within each of the subset terrains (Table 3.8). For the dunes, slightly shorter distances appeared to have the best matching analysis scale. For the 3 m and 27 m grids, the scale with most agreement was 81 m. The 9 m grid differed by having the highest percent agreement at a field

equivalent distance of 27 m. However, all analysis scales greater than 27 m had agreement percentages above 75%. In the hummocky hills terrain, the optimal analysis scale remained the same for the 3 m resolution grid. However, the optimal analysis scale coarsened for both the 9 m and 27 m grids. Most points in the lake plain landscape were recorded as “flat”, leaving only seven points for the calibration evaluation of relative elevation. All three points that were classified as footslopes in the lake plain had negative relative elevation values for field equivalent scales of 15-81 m for the 3 m grid. Because the 15 m analysis scale of the 3 m grid had a positive relative elevation for one of the four summit and shoulder points, it had the highest combined agreement percentage. A similar situation gave the finest possible scale for the 27 m grid the highest percent agreement.

The lowest mean difference for slope gradient still tended to be the finest possible analysis scale for the grid resolution for all landscape types (Table 3.9). The dune landscape had larger mean differences in general, but the differences decreased with decreasing analysis scale. Providing some indication of a signal, a slight dip was evident at the 15 m analysis scale of the 3 m grid for the hummocky hills landscape.

Table 3.7a. Percent agreement results for profile curvature of observation points in the dune landscape. Concave and convex agree are the count of points where the digital and field assessments of slope profile shape were in agreement. Percent is the proportion of agreement out of the total number of points.†‡

Dunes	3 m Grid					
Distance	**9 m**	**15 m**	**27 m**	**45 m**	**63 m**	**81 m**
Concave agree	13	13	15	17	18	17
Convex agree	18	17	17	18	19	20
% concave agree	68.4%	68.4%	78.9%	89.5%	94.7%	89.5%
% convex agree	75.0%	70.8%	70.8%	75.0%	79.2%	83.3%
Mean % agreement	71.7%	69.6%	74.9%	82.2%	87.0%	86.4%

	9 m Grid					
Distance	**27 m**	**45 m**	**63 m**	**81 m**	**135 m**	**189 m**
Concave agree	14	15	18	17	15	15
Convex agree	18	15	19	21	11	10
% concave agree	73.7%	78.9%	94.7%	89.5%	78.9%	78.9%
% convex agree	75.0%	62.5%	79.2%	87.5%	45.8%	41.7%
Mean % agreement	74.3%	70.7%	87.0%	88.5%	62.4%	60.3%

		27 m Grid		
	Distance	**81 m**	**135 m**	**189 m**
	Concave agree	17	14	13
	Convex agree	17	11	11
	% concave agree	89.5%	73.7%	68.4%
	% convex agree	70.8%	45.8%	45.8%
	Mean % agreement	80.2%	59.8%	57.1%

† The number of professionally surveyed points available for evaluation in this sub-region was 19 concave and 24 convex.

‡Analysis scale with strongest signal highlighted in dark gray; other strong agreements shown in lighter gray.

Table 3.7b. Percent agreement results for profile curvature of observation points in the hummocky landscape. Concave and convex agree are the count of points where the digital and field assessments of slope profile shape were in agreement. Percent is the proportion of agreement out of the total number of points.†‡

Hummocky Hills	3 m Grid					
Distance	**9 m**	**15 m**	**27 m**	**45 m**	**63 m**	**81 m**
Concave agree	4	6	8	7	10	10
Convex agree	10	15	14	16	16	15
% concave agree	25.0%	37.5%	50.0%	43.8%	62.5%	62.5%
% convex agree	43.5%	65.2%	60.9%	69.6%	69.6%	65.2%
Mean % agreement	34.2%	51.4%	55.4%	56.7%	66.0%	63.9%

	9 m Grid					
Distance	**27 m**	**45 m**	**63 m**	**81 m**	**135 m**	**189 m**
Concave agree	8	7	10	11	12	11
Convex agree	15	15	15	13	13	14
% concave agree	50.0%	43.8%	62.5%	68.8%	75.0%	68.8%
% convex agree	65.2%	65.2%	65.2%	56.5%	56.5%	60.9%
Mean % agreement	57.6%	54.5%	63.9%	62.6%	65.8%	64.8%

	27 m Grid		
Distance	**81 m**	**135 m**	**189 m**
Concave agree	9	13	13
Convex agree	18	10	15
% concave agree	56.3%	81.3%	81.3%
% convex agree	78.3%	43.5%	65.2%
Mean % agreement	67.3%	62.4%	73.2%

† The number of professionally surveyed points available for evaluation in this sub-region was 16 concave and 23 convex.

‡Analysis scale with strongest signal highlighted in dark gray; other strong agreements shown in lighter gray.

Table 3.7c. Percent agreement results for profile curvature of observation points in the glacial lake plain landscape. Concave and convex agree are the count of points where the digital and field assessments of slope profile shape were in agreement. Percent is the proportion of agreement out of the total number of points.†‡

Lake Plain	3 m Grid					
Distance	**9 m**	**15 m**	**27 m**	**45 m**	**63 m**	**81 m**
Concave agree	2	3	2	2	3	1
Convex agree	1	0	0	1	1	1
% concave agree	66.7%	100%	66.7%	66.7%	100%	33.3%
% convex agree	50.0%	0.0%	0.0%	50.0%	50.0%	50.0%
Mean % agreement	58.3%	50.0%	33.3%	58.3%	75.0%	41.7%

	9 m Grid					
Distance	**27 m**	**45 m**	**63 m**	**81 m**	**135 m**	**189 m**
Concave agree	1	2	2	1	2	1
Convex agree	0	0	1	1	1	2
% concave agree	33.3%	66.7%	66.7%	33.3%	66.7%	33.3%
% convex agree	0.0%	0.0%	50.0%	50.0%	50.0%	100%
Mean % agreement	16.7%	33.3%	58.3%	41.7%	58.3%	66.7%

		27 m Grid	
Distance	**81 m**	**135 m**	**189 m**
Concave agree	0	2	1
Convex agree	2	1	2
% concave agree	0.0%	66.7%	33.3%
% convex agree	100%	50.0%	100%
Mean % agreement	50.0%	58.3%	66.7%

†The number of professionally surveyed points available for evaluation in this sub-region was 3 concave and 2 convex.

‡Analysis scale with strongest signal highlighted in dark gray; other strong agreements shown in lighter gray.

Table 3.8a. Percent agreement results for relative elevation of observation points in the dune landscape. Low and high agree are the count of points where the digital and field assessments of relative elevation were in agreement. Percent is the proportion of agreement out of the total number of points.†‡

Dunes	3 m Grid								
Distance	**9 m**	**15 m**	**27 m**	**45 m**	**63 m**	**81 m**	**135 m**	**189 m**	**243 m**
Low agree	19	24	28	28	31	31	26	28	29
High agree	24	23	22	23	22	25	22	22	23
% low agree	55.9%	70.6%	82.4%	82.4%	91.2%	91.2%	76.5%	82.4%	85.3%
% high agree	82.8%	79.3%	75.9%	79.3%	75.9%	86.2%	75.9%	75.9%	79.3%
Mean % agreement	69.3%	74.9%	79.1%	80.8%	83.5%	88.7%	76.2%	79.1%	82.3%

	9 m Grid					
Distance	**27 m**	**45 m**	**63 m**	**81 m**	**135 m**	**189 m**
Low agree	31	33	34	28	31	33
High agree	25	20	18	23	23	18
% low agree	91.2%	97.1%	100%	82.4%	91.2%	97.1%
% high agree	86.2%	69.0%	62.1%	79.3%	79.3%	62.1%
Mean % agreement	88.7%	83.0%	81.0%	80.8%	85.2%	79.6%

	27 m Grid		
Distance	**81 m**	**135 m**	**189 m**
Low agree	34	34	34
High agree	22	19	18
% low agree	100%	100%	100%
% high agree	75.9%	65.5%	62.1%
Mean % agreement	87.9%	82.8%	81.0%

† The number of professionally surveyed points available for evaluation in this sub-region was 34 low and 29 high.

‡Analysis scale with strongest signal highlighted in dark gray; other strong agreements shown in lighter gray.

Table 3.8b. Percent agreement results for relative elevation of observation points in the hummocky landscape. Low and high agree are the count of points where the digital and field assessments of relative elevation were in agreement. Percent is the proportion of agreement out of the total number of points.†‡

Hummocky Hills	3 m Grid								
Distance	**9 m**	**15 m**	**27 m**	**45 m**	**63 m**	**81 m**	**135 m**	**189 m**	**243 m**
Low agree	10	9	8	12	11	13	7	12	12
High agree	11	14	21	22	24	23	23	23	23
% low agree	50.0%	45.0%	40.0%	60.0%	55.0%	65.0%	35.0%	60.0%	60.0%
% high agree	31.4%	40.0%	60.0%	62.9%	68.6%	65.7%	65.7%	65.7%	65.7%
Mean % agreement	40.7%	42.5%	50.0%	61.4%	61.8%	65.4%	50.4%	62.9%	62.9%

	9 m Grid					
Distance	**27 m**	**45 m**	**63 m**	**81 m**	**135 m**	**189 m**
Low agree	13	17	17	11	16	17
High agree	23	28	26	26	25	26
% low agree	65.0%	85.0%	85.0%	55.0%	80.0%	85.0%
% high agree	65.7%	80.0%	74.3%	74.3%	71.4%	74.3%
Mean % agreement	65.4%	82.5%	79.6%	64.6%	75.7%	79.6%

	27 m Grid		
Distance	**81 m**	**135 m**	**189 m**
Low agree	14	15	16
High agree	26	28	27
% low agree	70.0%	75.0%	80.0%
% high agree	74.3%	80.0%	77.1%
Mean % agreement	72.1%	77.5%	78.6%

† The number of professionally surveyed points available for evaluation in this sub-region was 20 low and 35 high.

‡Analysis scale with strongest signal highlighted in dark gray; other strong agreements shown in lighter gray.

Table 3.8c. Percent agreement results for relative elevation of observation points in the glacial lake plain landscape. Low and high agree are the count of points where the digital and field assessments of relative elevation were in agreement. Percent is the proportion of agreement out of the total number of points.†‡

Lake Plain	3 m Grid								
Distance	**9 m**	**15 m**	**27 m**	**45 m**	**63 m**	**81 m**	**135 m**	**189 m**	**243 m**
Low agree	2	3	3	3	3	3	0	1	1
High agree	1	1	0	0	0	0	0	0	0
% low agree	66.7%	100%	100%	100%	100%	100%	0.0%	33.3%	33.3%
% high agree	25.0%	25.0%	0.0%	0.0%	0.0%	0.0%	0.0%	0.0%	0.0%
Mean % agreement	45.8%	62.5%	50.0%	50.0%	50.0%	50.0%	0.0%	16.7%	16.7%

	9 m Grid					
Distance	**27 m**	**45 m**	**63 m**	**81 m**	**135 m**	**189 m**
Low agree	1	2	0	0	1	0
High agree	0	1	1	3	3	3
% low agree	33.3%	66.7%	0.0%	0.0%	33.3%	0.0%
% high agree	0.0%	25.0%	25.0%	75.0%	75.0%	75.0%
Mean % agreement	16.7%	45.8%	12.5%	37.5%	54.2%	37.5%

		27 m Grid		
	Distance	**81 m**	**135 m**	**189 m**
	Low agree	3	2	1
	High agree	1	1	2
	% low agree	100%	66.7%	33.3%
	% high agree	25.0%	25.0%	50.0%
	Mean % agreement	62.5%	45.8%	41.7%

† The number of professionally surveyed points available for evaluation in this sub-region was 3 low and 4 high.

‡Analysis scale with strongest signal highlighted in dark gray; other strong agreements shown in lighter gray.

Table 3.9a. Mean absolute difference results for slope gradient of observation points in the dune landscape. †

Dunes	3 m Grid					
Distance	**9 m**	**15 m**	**27 m**	**45 m**	**63 m**	**81 m**
Mean difference	14.2°	14.7°	15.9°	17.3°	18.2°	18.8°

	9 m Grid					
Distance	**27 m**	**45 m**	**63 m**	**81 m**	**135 m**	**189 m**
Mean difference	15.7°	17.1°	18.0°	18.8°	20.1°	20.8°

			27 m Grid		
Distance	**81 m**	**135 m**	**189 m**		
Mean difference	18.7°	20.1°	20.9°		

† The number of professionally surveyed points available for evaluation in this sub-region was 139.

Table 3.9b. Mean absolute difference results for slope gradient of observation points in the hummocky hills landscape. †

Hummocky Hills	3 m Grid					
Distance	**9 m**	**15 m**	**27 m**	**45 m**	**63 m**	**81 m**
Mean difference	0.90°	0.85°	0.86°	0.94°	1.02°	1.08°

	9 m Grid					
Distance	**27 m**	**45 m**	**63 m**	**81 m**	**135 m**	**189 m**
Mean difference	0.84°	0.94°	1.02°	1.09°	1.18°	1.23°

			27 m Grid		
Distance	**81 m**	**135 m**	**189 m**		
Mean difference	1.07°	1.18°	1.22°		

† The number of professionally surveyed points available for evaluation in this sub-region was 149.

Table 3.9c. Mean absolute difference results for slope gradient of observation points in the glacial lake plain landscape. †

Lake Plain	3 m Grid					
Distance	**9 m**	**15 m**	**27 m**	**45 m**	**63 m**	**81 m**
Mean difference	0.52°	0.60°	0.75°	0.87°	0.92°	0.95°

	9 m Grid					
Distance	**27 m**	**45 m**	**63 m**	**81 m**	**135 m**	**189 m**
Mean difference	0.73°	0.89°	0.93°	0.95°	0.97°	0.99°

		27 m Grid		
	Distance	**81 m**	**135 m**	**189 m**
	Mean difference	0.96°	0.97°	0.99°

† The number of professionally surveyed points available for evaluation in this sub-region was 38.

5. Discussion

The observed convergence in agreement as neighborhood size approaches an optimal analysis scale suggests 1) soil surveyors are relatively consistent in their use of analysis scale and 2) the calibration methodology was able to capture the analysis scales used by the soil scientists. By comparing a series of analysis scales for DTA metrics with the soil scientists' mental model assessments, the analysis scales of DTA metrics that best correspond to the soil scientists' field experience were identified. In the context of soil scientists describing hillslopes, the analysis scale used decreases from relative elevation to profile curvature to slope gradient. To many field scientists, this hierarchy of analysis scale for these components may sound intuitive, but DTA parameters are often calculated at identical analysis scales for use in environmental models. The field scientists' use of different analysis scales for these parameters should inform quantitative modelling and thereby improve geomorphic and soil predictions.

Comparisons of DTA scales demonstrated the impact of analysis scale choice for each terrain metric, particularly for capturing expert knowledge. For example, when characterizing relative elevation with a 3 m resolution grid, choosing between a field equivalent distance of 9 m versus 135 m had the impact of agreeing with the field scientists 52% of the time or 79% of the time, respectively. Similarly, when simply characterizing profile curvature as concave or convex, choosing an analysis scale of 63 m over 9 m improved agreement with scientists in the field by 10%.

The results of this study are supported by the observations of other researchers investigating the optimal analysis scale for these DTA metrics in other soil related contexts. The semantic calibration of profile curvature scale in this study corresponds to the optimal scale Drăgut et al. (2009) determined for predicting crop yield from profile curvature on an alluvial plain of the Danube River. The increasing agreement between digital and field measurements of slope gradient with decreasing neighborhood size to at least 9 m is also consistent with the results of Shi et al. (2007). The results of Roecker and Thompson (2010) indicated a coarser analysis scale for profile curvature, but the smaller quantity of samples in their study may have been susceptible to the scale effect of MAUP.

The use of only categories that are better separated definitionally was successful in reducing the noise in the soil scientists' mental model outcomes. The high variability of human assessment greatly reduces the predictability of qualitative field metrics such as hillslope position, but does not negate the ability to capture the logic in the experts' knowledge. At a minimum, the DTA should be expected to produce values definitionally compatible with the

field observations. That is, profile curvature should be positive for convex slope shapes and negative for concave slope shapes (note, some profile curvature algorithms may have those definitions switched). Similarly, it would be expected that summits and shoulders would have positive relative elevations with footslopes and toeslopes expected to have negative relative elevations. The calibrated analysis scale at which the DTA has the highest agreement with these definitional relationships provides insight to how the soil scientists conceptualized the landscape in the field.

An intriguing finding was that optimal analysis scales for profile curvature and relative elevation differed between geomorphic regions. Differences in analysis scale could be due to conscious choices made by soil scientists working in different landscapes. However, an alternative conjecture, one supported by the magnitude and direction in differences, is that small sample sizes and the scale effect of MAUP may explain this variation in optimal analysis scale. Besides the relative elevation calibration for the glacial lake plain, the other sub-region calibrations generally had a trend consistent with the concept of MAUP increasing agreement with decreasing variability.

The range of sensitivity between the glacial lake plain terrain (very sensitive) and the dune terrain (less sensitive) indicates a relationship between relief and impact of changing analysis scale. For example, a high relief terrain may have a wide range of DTA scales classifying relative elevation similarly, while the DTA analysis at different scales for an extremely flat landscape could respond to small variations in elevation. In the case of relative elevation in high relief terrain, the wide range of DTA agreement with field observations would make the

calibration signal diffuse. On the other hand, subtleties detected by DTA that the field scientists either ignore (e.g., 15 cm high ridges occurring at 25 m intervals in an agricultural field) or cannot observe (e.g., slight elevation changes in a flat glacial lake plain) could seemingly 'scramble' the calibration signal. This study cannot rule out the possibility that the optimal analysis scale for each of these terrain metrics varies between landscapes. However, it is more likely that the differing results between landscapes are due to a combination of too few observations, the scale effect of MAUP, and differences in sensitivity to scale.

As high resolution, digital elevation products from technologies such as LiDAR become more available, smaller objects on the ground have the potential to affect DTA results. Although the elevation grid used in this study was processed from the LiDAR point cloud to be bare earth, the influence of either non-soil or at least man-made features are present in the elevation. This noise in the DEM could affect DTA metrics. Therefore the semantic calibration in this study may be influenced by not only the scale used by soil scientists, but also the DTA scale that sufficiently smoothes the digital representation of terrain to minimize the influence of features that would naturally be ignored by scientists in the field.

6. Conclusions

Based on data from U.S. soil scientists, this research suggests that there exists an optimal analysis scale for relating DTA to observations made in the field. However, the optimal analysis scale is likely to be different for each DTA metric. The method of semantic calibration presented was able to identify analysis scales that optimized the agreement between DTA and field observations. Results from this study suggest that the optimal analysis scales for slope

gradient, profile curvature, and relative elevation are the field equivalent distances of 9 m, 63 m, and 135 m, respectively. As analysis scales tested were limited to multiples of the grid cell size, these calibrated analysis scales are approximate.

Consideration of the scale effect of MAUP, particularly evident with smaller quantities of observation points, indicates the calibrated analysis scales may not vary widely between terrain types. Results also suggest that for the range of terrain types used in this study, sensitivity to analysis scale decreases with increasing relief. This information should guide the use of these DTA metrics at other locations in two ways. First, a large quantity of sample points is needed to avoid the influence of MAUP when comparing analysis scales. Based on observations in this study, I suggest at least more than 100 points. Second, the results of this study should be transferable to other terrain types, but the choice in analysis scale will be more critical for low relief terrains.

These semantically calibrated analysis scales for DTA provide documentation of the soil scientists' field perspective and experience in the assessment of hillslope processes. Models attempting to predict landscape features traditionally identified by field scientists will likely benefit from using the same analysis scales utilized by those scientists. Similarly, other models using DTA as parameters will likely benefit from the lessons of analysis scale accumulated by scientists in the field over centuries.

The calibration of DTA metric analysis scales to the soil scientists' assessments in the field synchronizes DTA to the accumulated experience of field work. This calibration is only the first step in capturing the expert knowledge inherent in the use of the hillslope position metric.

The next step is to capture the expert knowledge in the classification of hillslope positions. Once a quantitative, DTA definition for hillslope position is established, additional field work will be needed to validate the relationships of this newly quantitative metric to hillslope processes.

APPENDIX

EVALUATION OF THE OTTAWA COUNTY LIDAR ELEVATION GRID

The digital elevation model used for many of the analyses in this dissertation was created from a 2004 LiDAR flight of Ottawa County, Michigan. For the county government's use, the LiDAR point cloud was processed for bare earth and interpolated to a 3 m grid (Figure 3.9). Some striped patterns were observed in the final digital elevation model, particularly in the derived hillshade grid. This appendix explores the characteristics of those patterns to determine if they could be artifacts from the LiDAR data collection and if the patterns could potentially affect the results of this dissertation.

Viewing the hillshade model of an elevation grid can be a useful method to detect potential artifacts in the grid created by systematic errors. However, exaggeration of the relief in creating the hillshade model can lead to unneeded concern over the nature and magnitude of the potential error (Figures 3.10 and 3.11). Further investigation is required to understand the likely sources for the patterns observed. One such investigation is to evaluate the extent over which the pattern is consistent. A second investigation is to evaluate cross section profiles, cutting perpendicular to the observed pattern, to determine the regularity of the spatial frequency. The spatial frequency also informs which analysis scales could be influenced by the observed pattern.

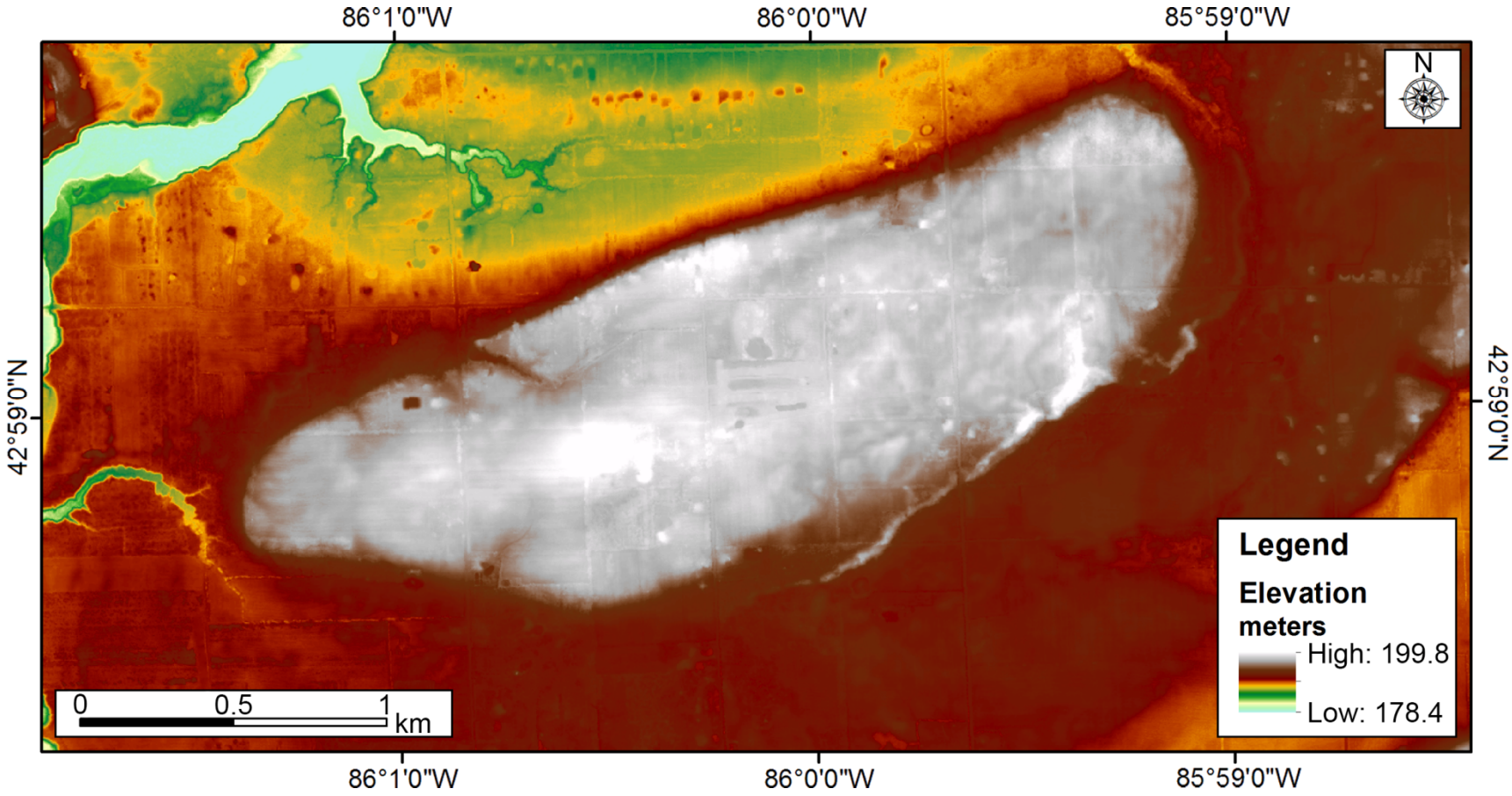


Figure 3.9. Example area from LiDAR elevation grid. Note the striped elevation patterns that can be seen in some portions of the example area.

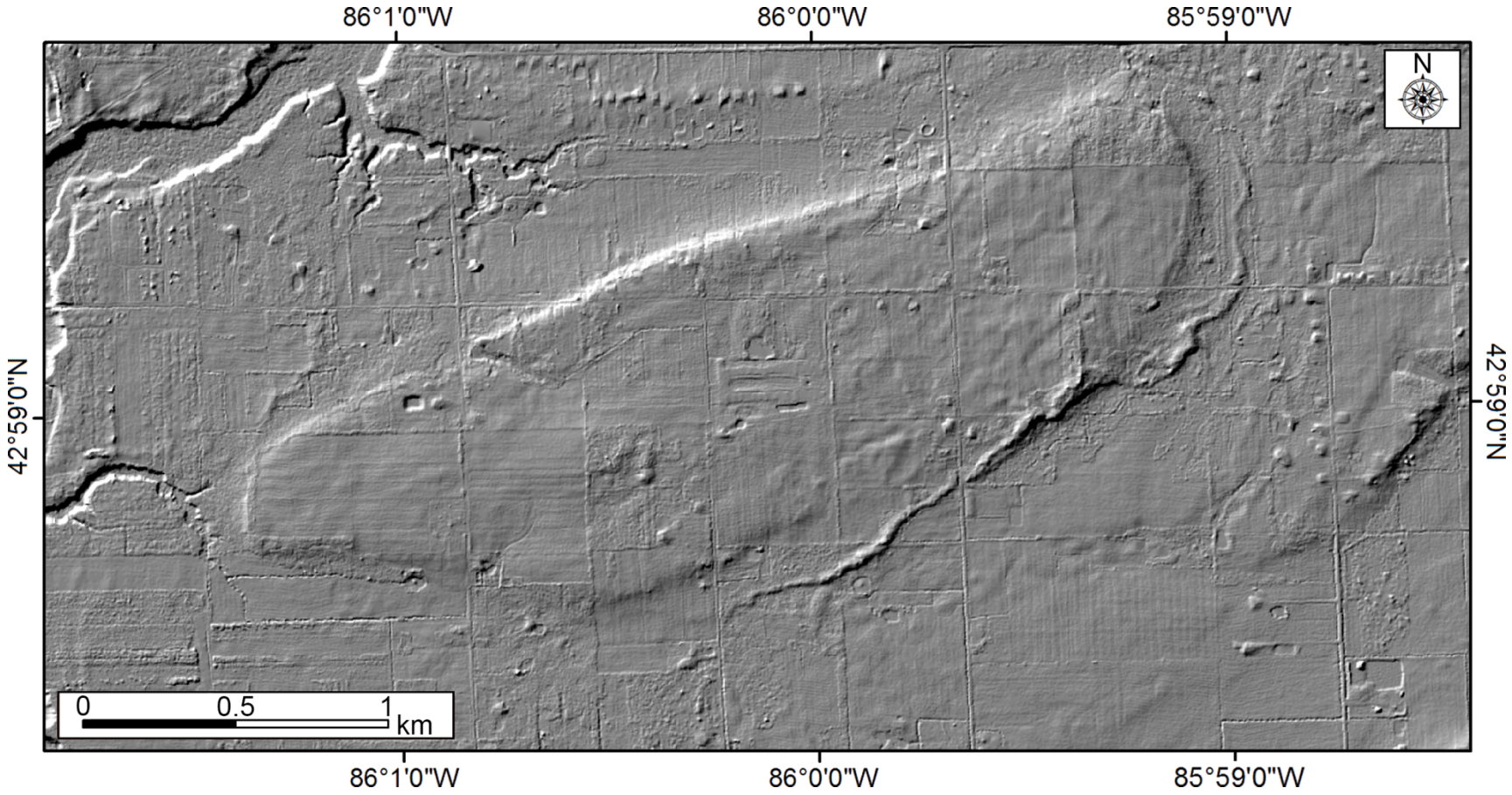


Figure 3.10. Same example area processed as a hillshade from the LiDAR elevation grid, with no vertical exaggeration. Note the additional striped patterns that were not as apparent in the display of elevation in Figure 3.9.

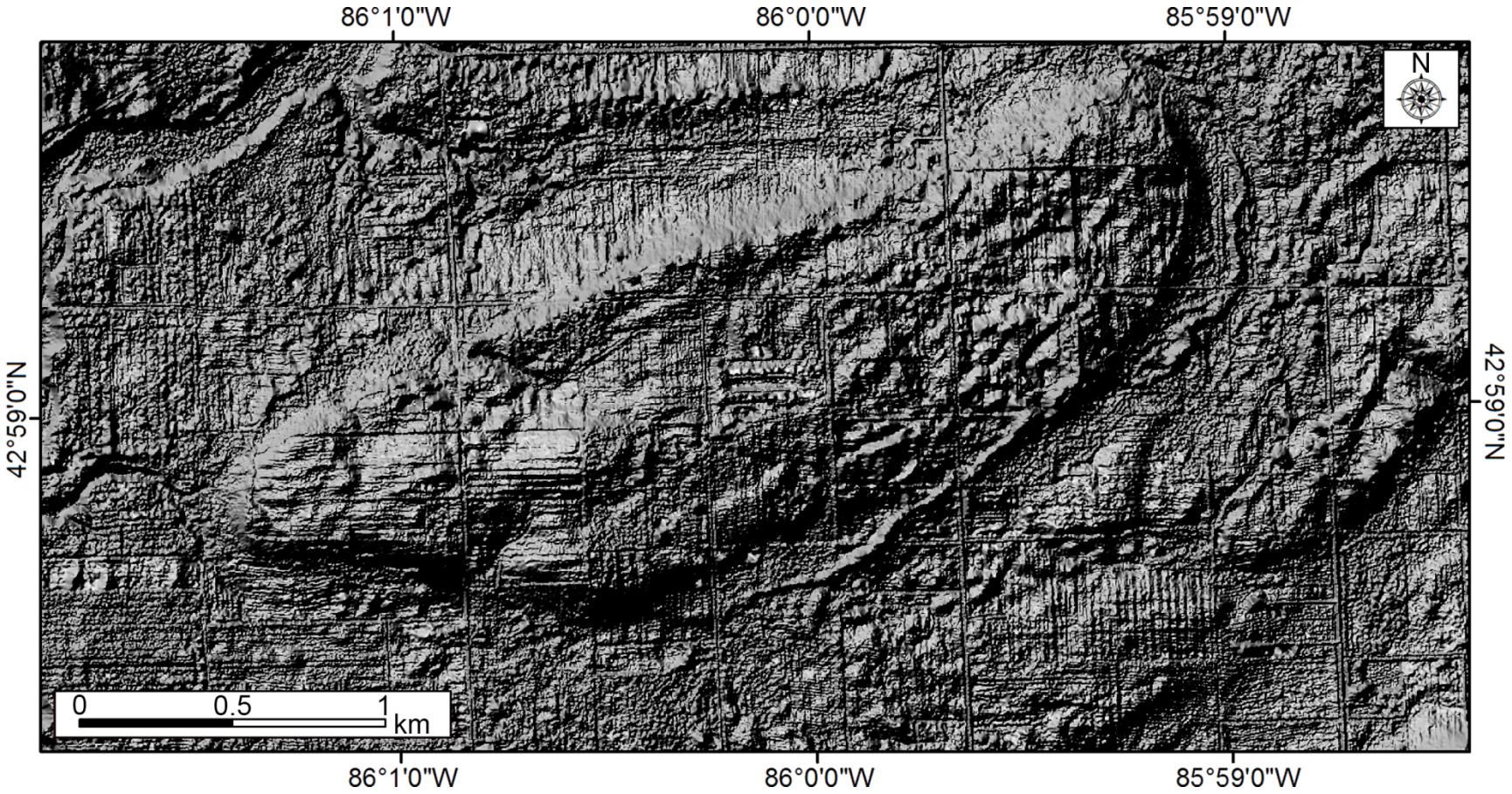


Figure 3.11. Same example area processed as a hillshade from the LiDAR elevation grid, with elevation exaggerated by a factor of 3. Note the increased prominence of striped patterns, as compared to the hillshade without vertical exaggeration (Figure 3.10).

The striped pattern observed in the LiDAR grid used for this dissertation varied in orientation across the study area. As it is unlikely that the flight pattern used to collect the LiDAR points changed orientation, the changes in orientation indicate the pattern is not due to systematic error from the LiDAR measurement method. Instead, the changes in pattern orientation generally coincide with crop field boundaries, indicating an anthropogenic source for the patterns.

In order to determine the spatial characteristics of the striped patterns and understand potential impacts on subsequent digital terrain analyses, six cross section profiles were examined. The cross section sites were chosen to be representative of the different types of striped patterns found in this LiDAR DEM and roughly distributed across the study area (Figure 3.12). The cross section profiles were also oriented to be perpendicular to the observed striping at each site.

Based on the cross sectional profiles, it is apparent that some striped patterns are more strongly expressed than others. Most have a spatial frequency of 10 m and a vertical relief of 5 to 20 cm (Figures 3.13 - 3.20). At this spatial frequency there could be some influence on the smallest analysis neighborhoods possible. With a 3 m resolution, a 3 by 3 analysis neighborhood would have a scale equivalent to 9 m. Despite similar lengths, the low amount of relief makes the potential impact on neighborhood analysis calculations minimal. The vertical relief is 0.5 to 2% of the 10 m distance. Sites with larger vertical relief in the striped pattern also had longer spatial frequencies, maintaining similarly small ratios of about 1%. Any impact from the striped pattern would decrease with larger analysis neighborhoods.

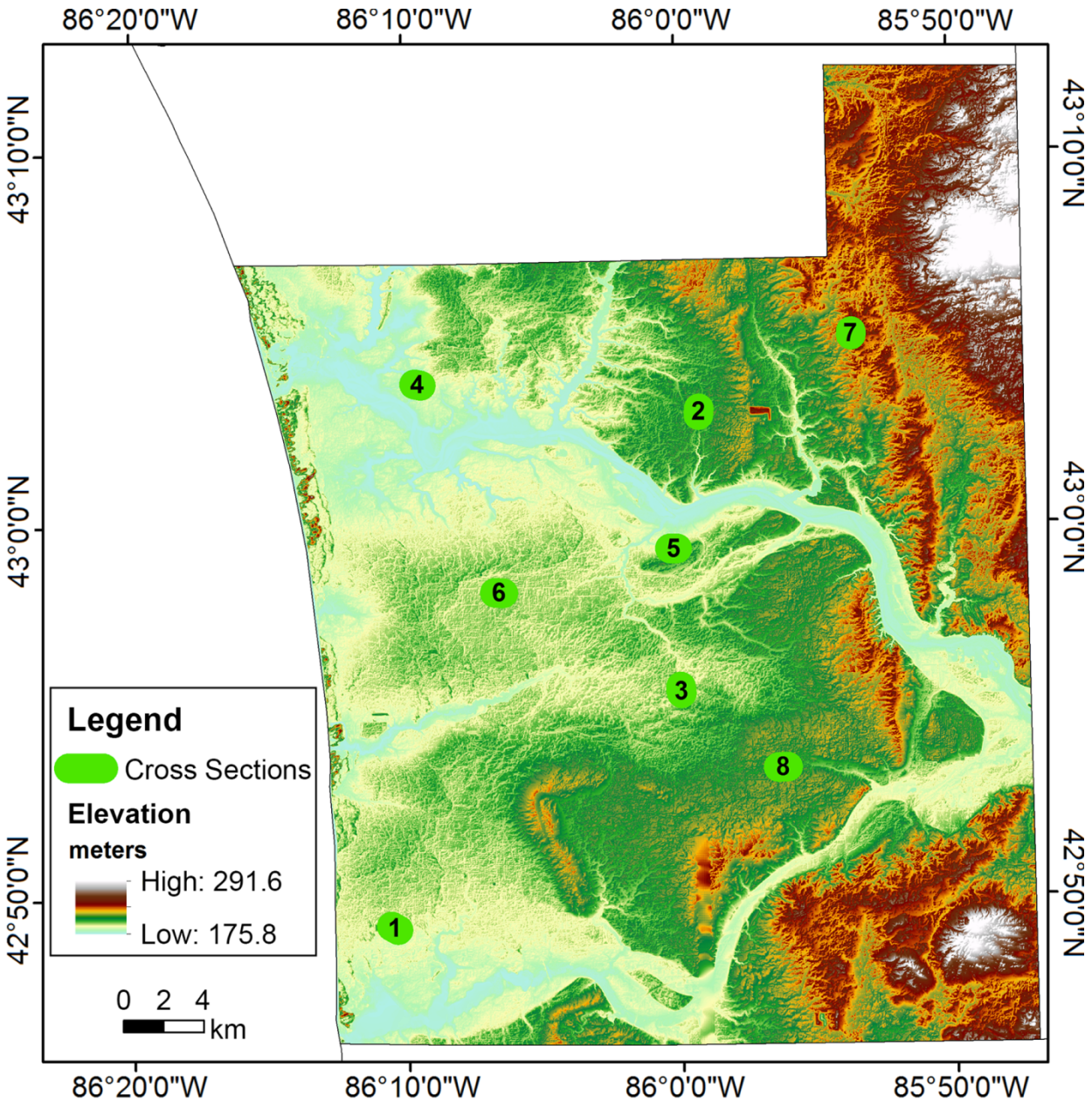


Figure 3.12. Location of cross sections examined in LiDAR elevation grid from Ottawa County, Michigan, USA. The longitudinal orientation of the cross section symbols indicates each profile line's orientation.

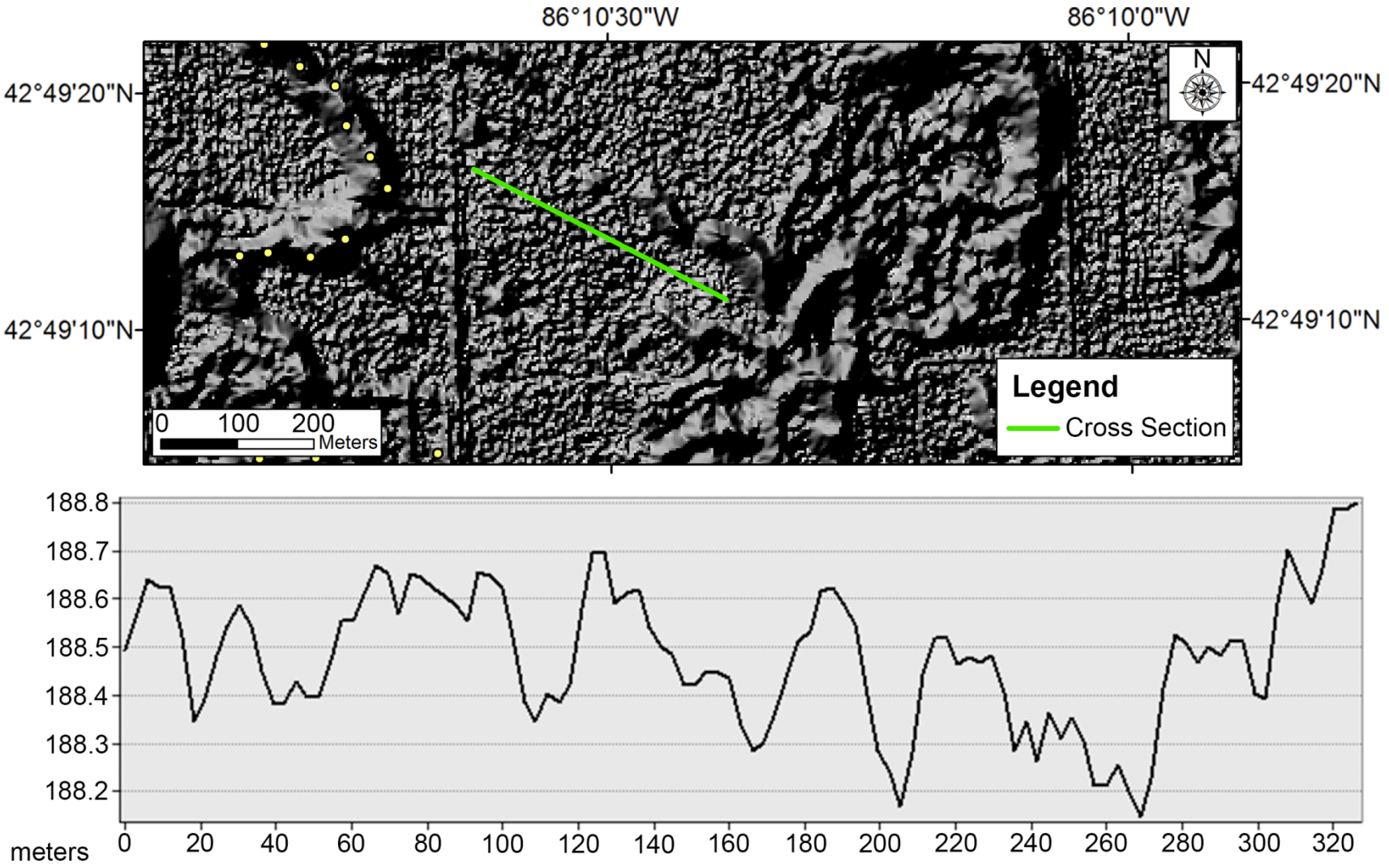


Figure 3.13. Evaluation of site 1. The spatial frequency of the striped pattern does not appear to be regular, but a few peaks occur at an interval of 30 m. The relief between the peaks appears to be approximately 30 cm.

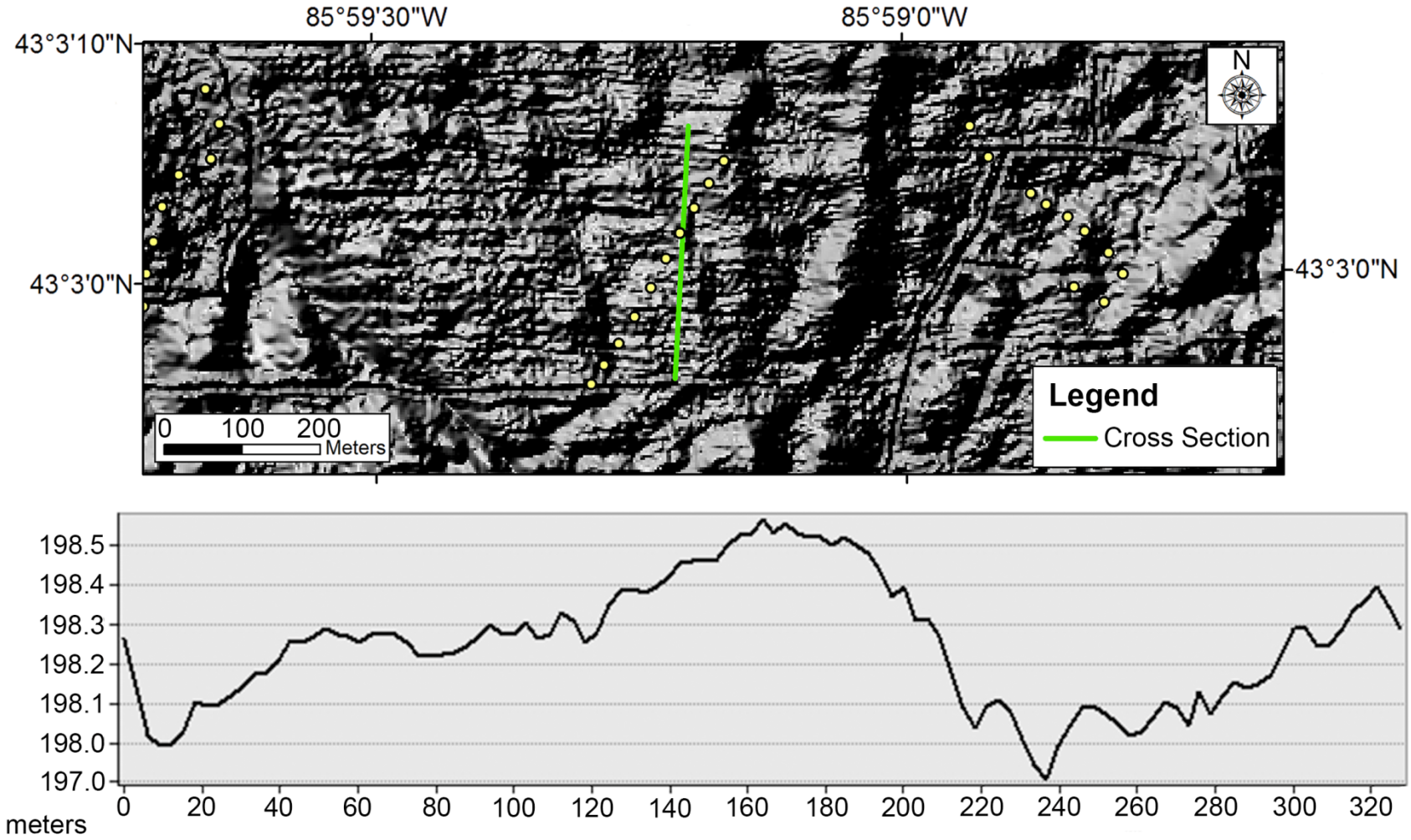


Figure 3.14. Evaluation of site 2. The spatial frequency of the striped pattern does not appear to be regular, but a few peaks occur at an interval of 10 m. The relief between the peaks appears to be approximately 5 cm.

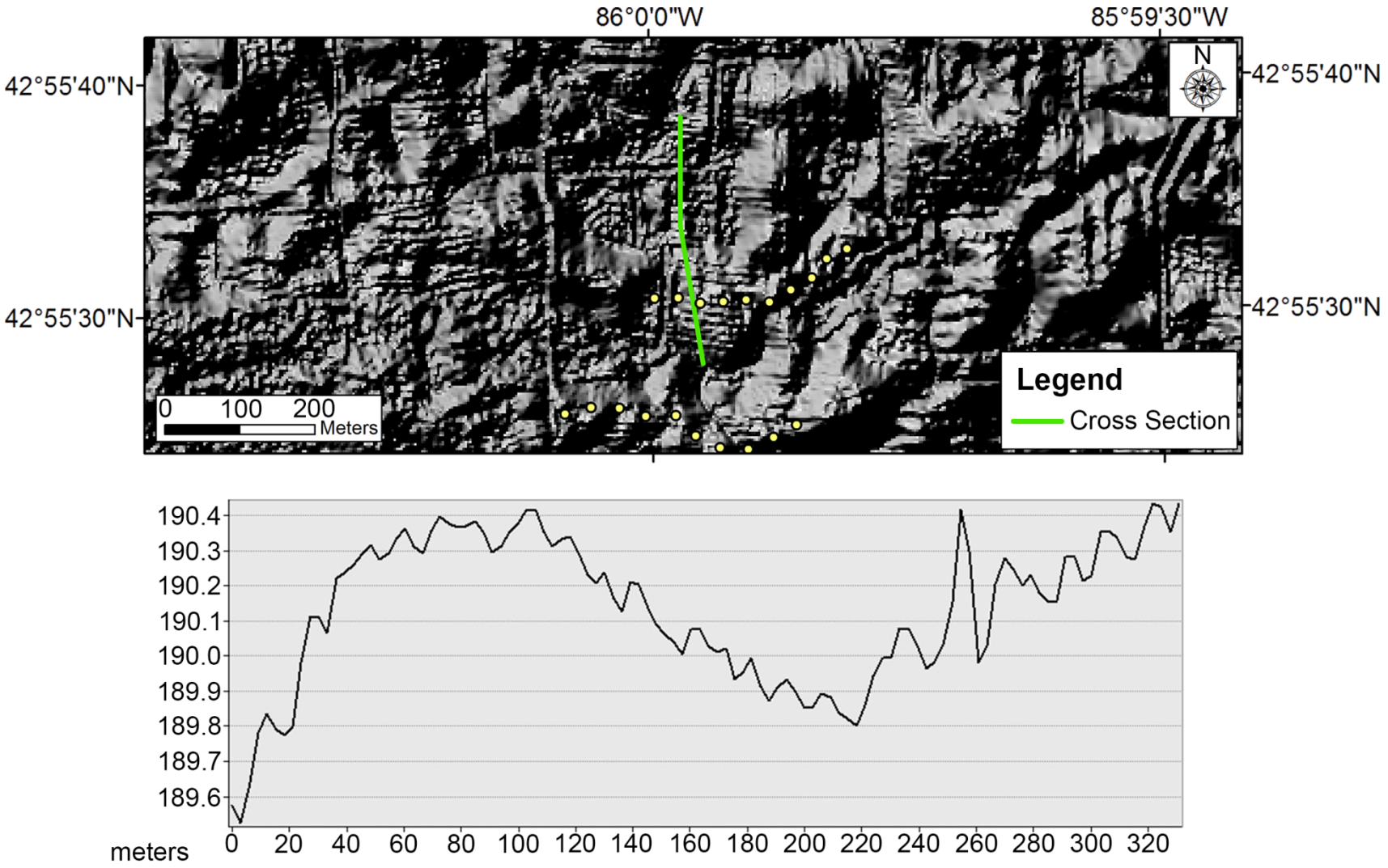


Figure 3.15. Evaluation of site 3. The spatial frequency of the striped pattern does have some regularity, with peaks occurring at an interval of 10 m. The relief between the peaks appears to be approximately 10 cm.

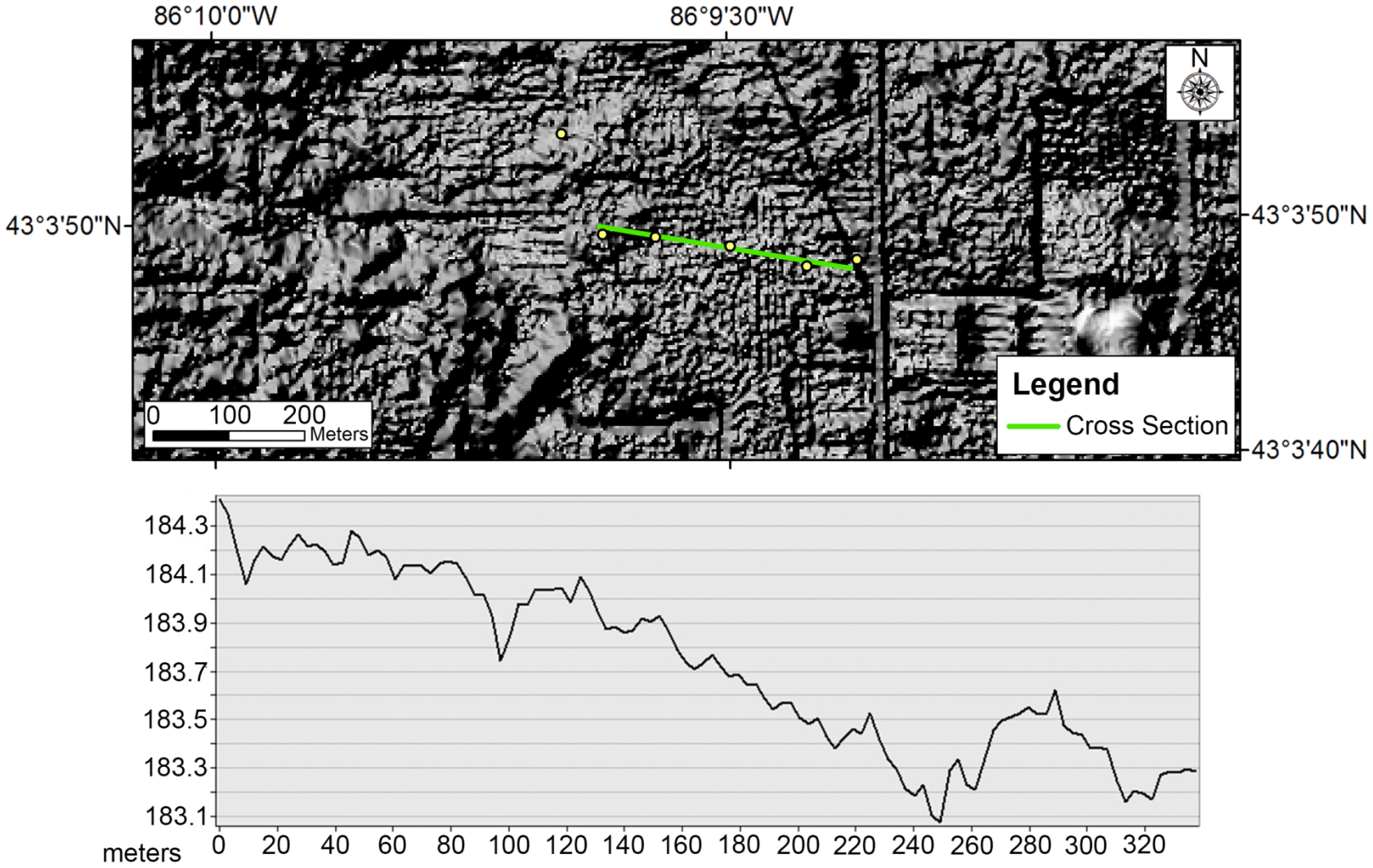


Figure 3.16. Evaluation of site 4. The spatial frequency of the striped pattern does not appear to be regular, but a few peaks occur at an interval of 10 m. The relief between the peaks appears to be approximately 10 cm or less.

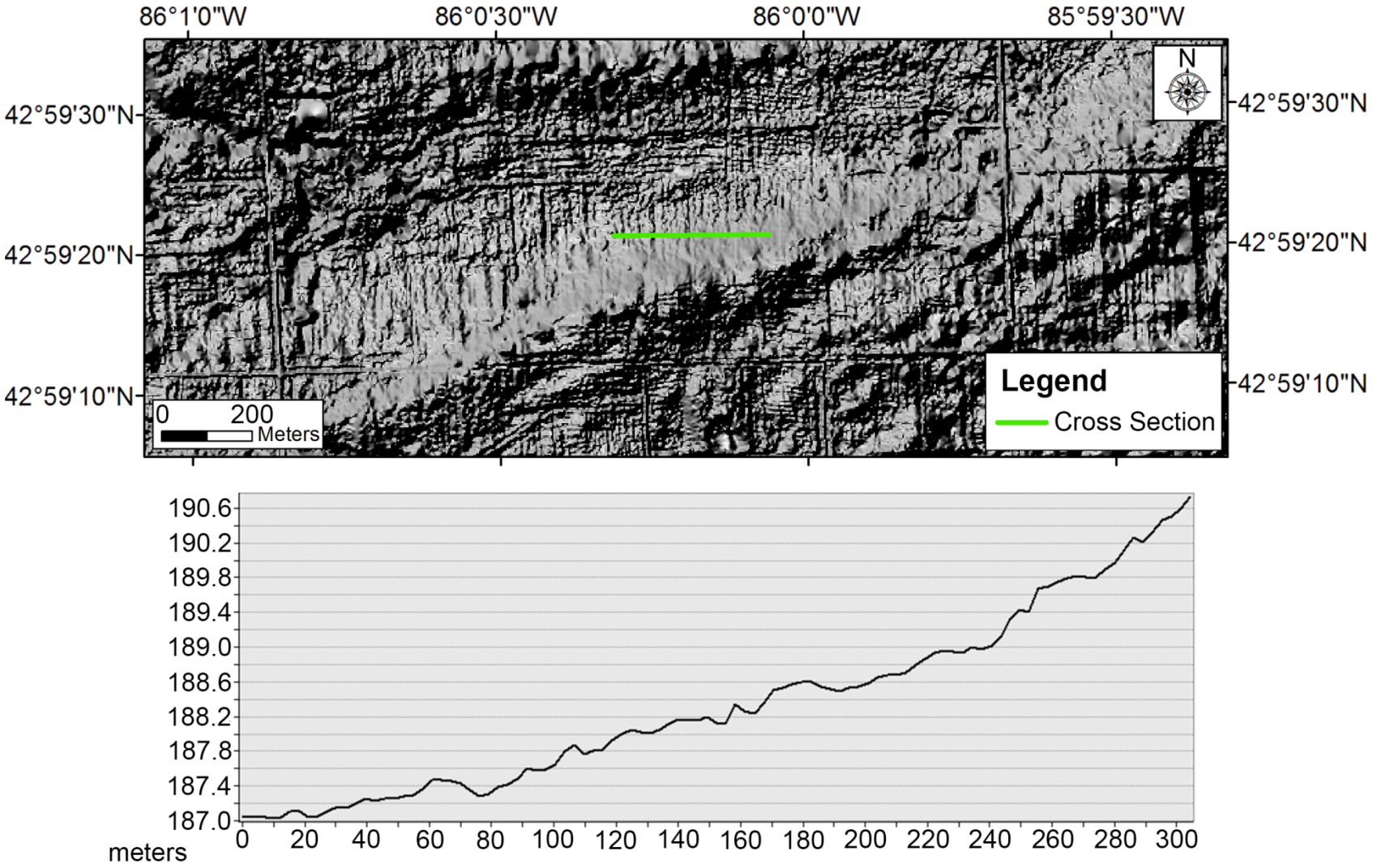


Figure 3.17. Evaluation of site 5. The spatial frequency of the striped pattern is not strongly expressed in the cross section, but a few peaks occur at an interval of 10 m. The relief between the peaks appears to be approximately 20 cm or less.

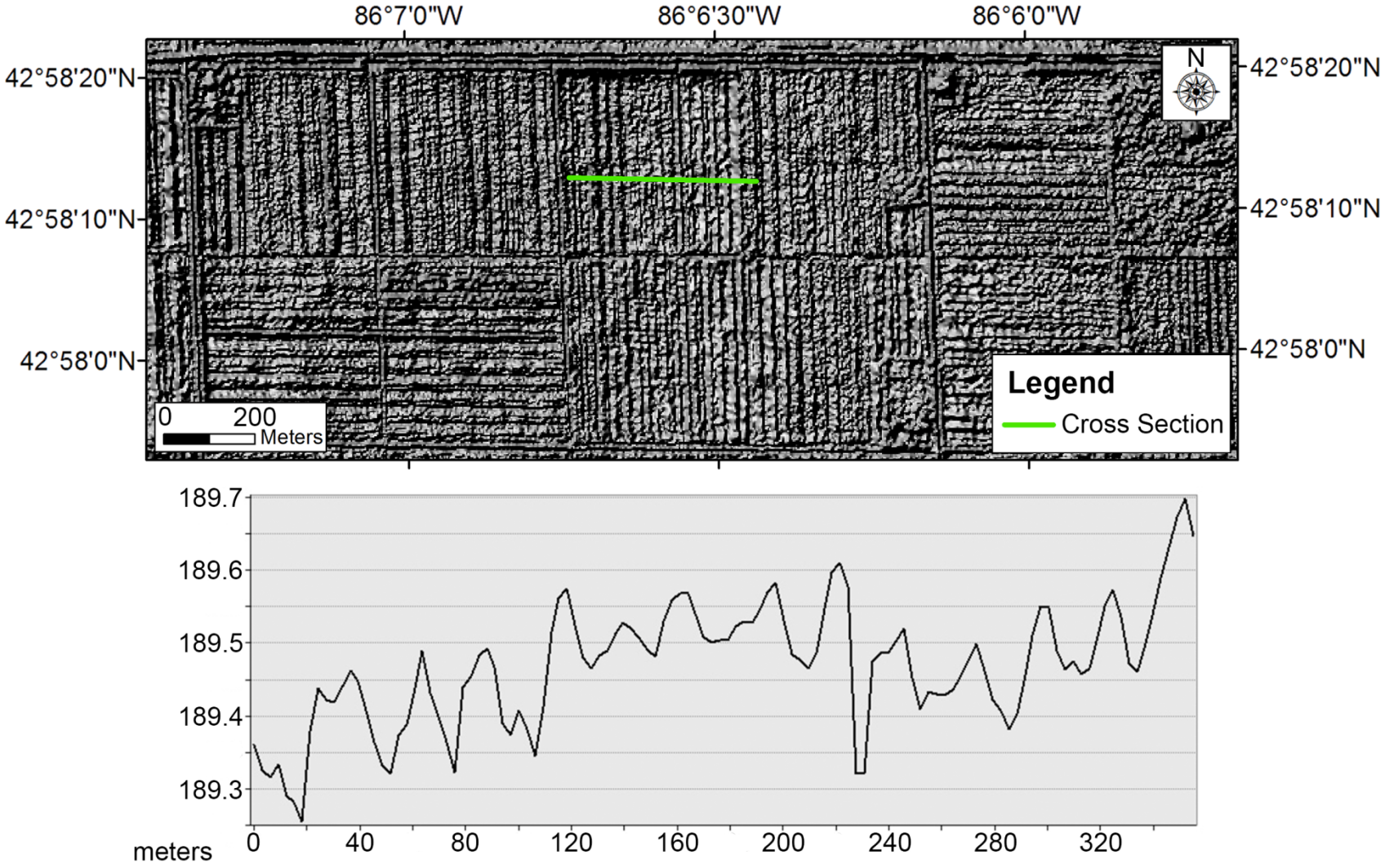


Figure 3.18. Evaluation of site 6. The spatial frequency of the striped pattern does have some regularity, with peaks occurring at an interval of 25 m. The relief between the peaks appears to be approximately 10 to 15 cm.

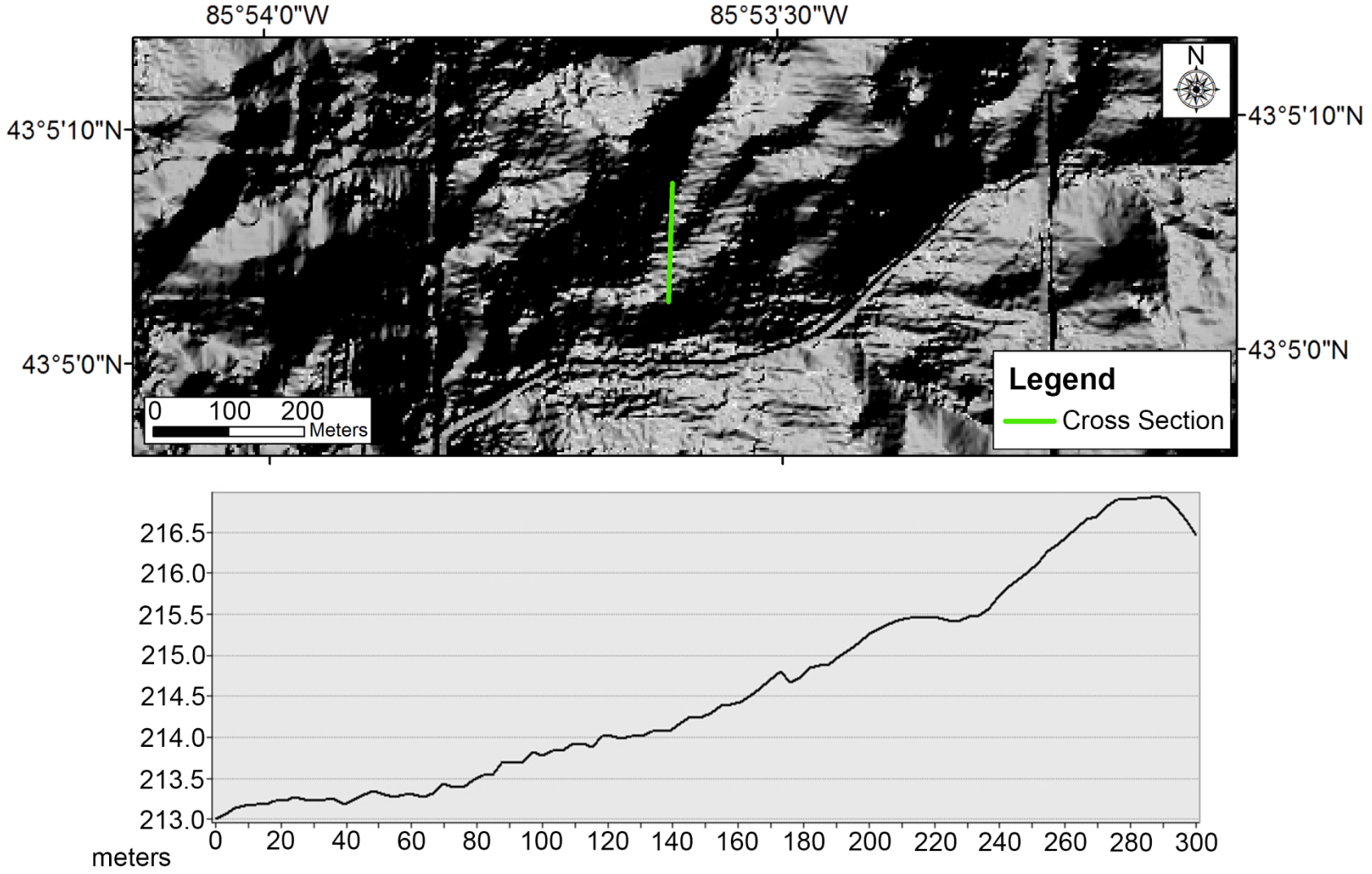


Figure 3.19. Evaluation of site 7. The spatial frequency of the striped pattern is not strongly expressed in the cross section, but a few peaks occur at an interval of 5 m. The relief between the peaks appears to be approximately 10 cm.

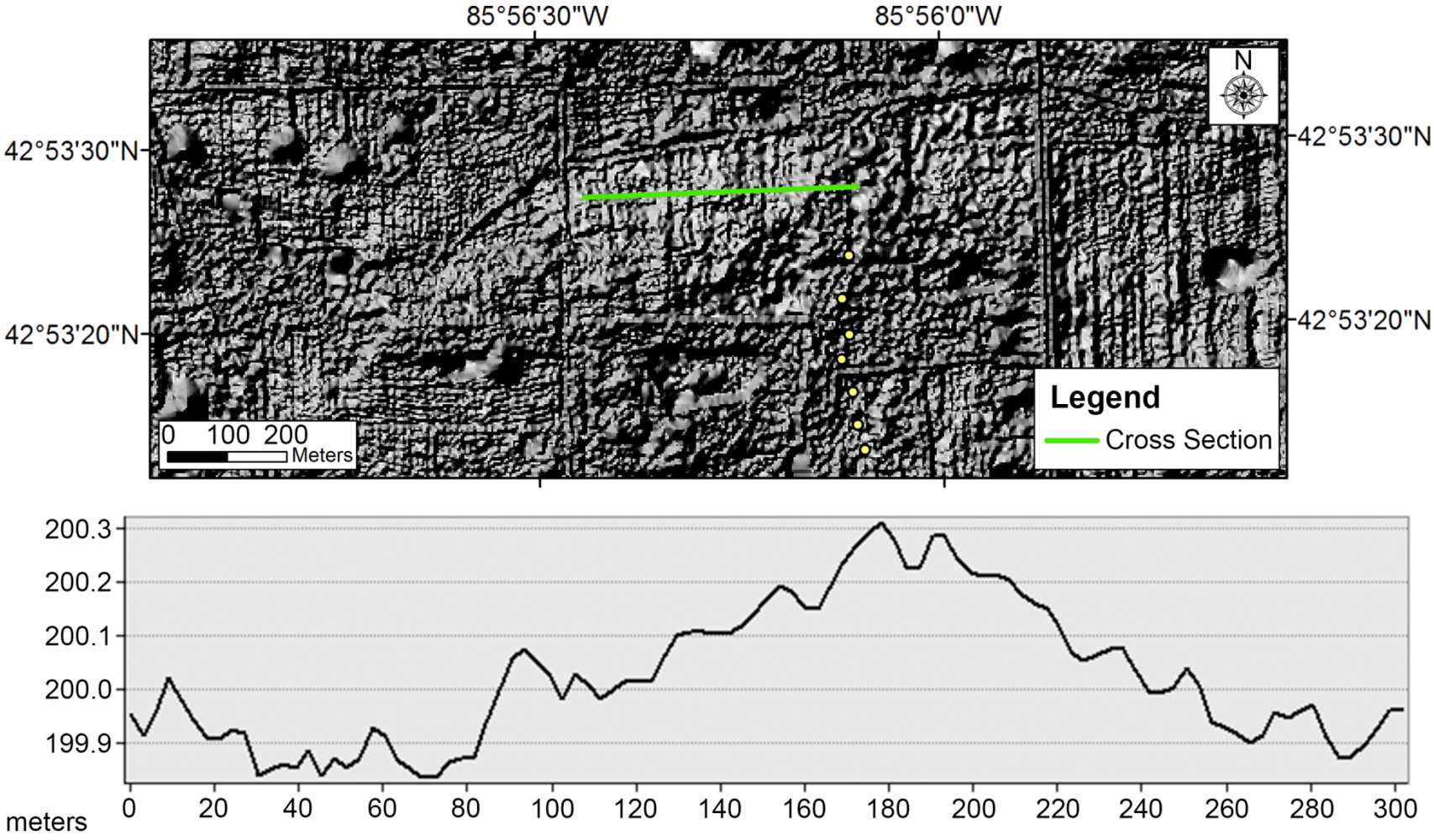


Figure 3.20. Evaluation of site 8. The spatial frequency of the striped pattern does not appear to be regular, but a few peaks occur at an interval of 10 m. The relief between the peaks appears to be approximately 5 cm.

By comparing aerial photographs of the cross section areas, the striped patterns appear to be best explained by agricultural practices. Although aerial photography was not available for the same year the LiDAR data was collected, the orientation of striped patterns observed in the LiDAR often matched striped patterns observed in aerial photos (Figures 3.21 and 3.22). Forested locations had similar patterns, but were expressed in the LiDAR DEM more as aligned bumps than solid stripes. Site 1 examined one of these areas and determined the spatial frequency and relief in DEM pattern was larger than in the crop fields. The 'bumps' at site 1 had a height of 30 cm, which could be an artifact from the processing of the LiDAR points for bare earth or possibly root mounds.



Figure 3.21. Image of area surrounding cross section site 6. The area demonstrates the striped patterns commonly observed on row crop fields. Satellite image courtesy of USGS.

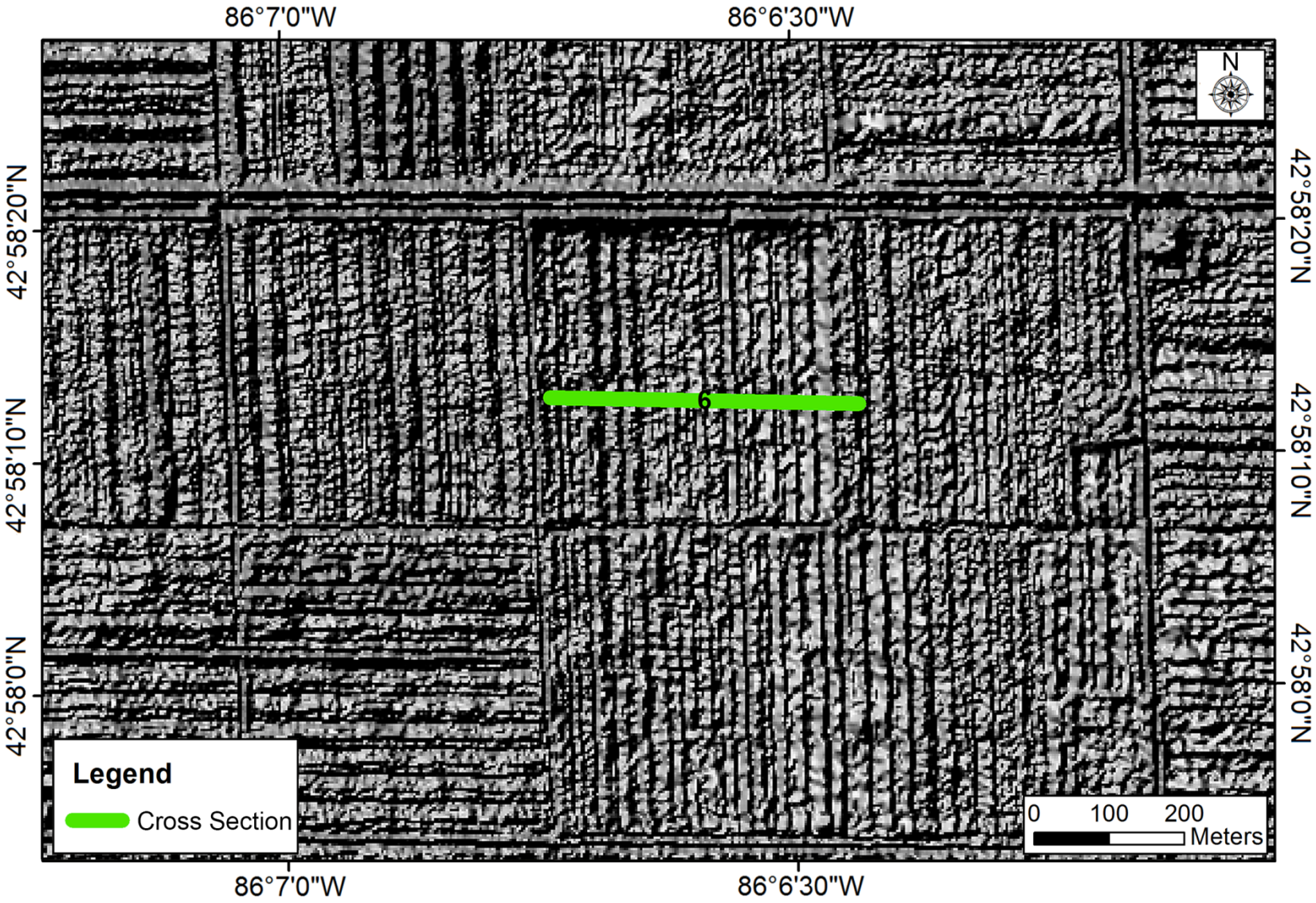


Figure 3.22. LiDAR based hillshade with 3x vertical exaggeration of the same area shown in figure A.13. Note the matching orientations of the striped pattern in both the tone of the aerial image and the hillshading from the elevation grid.

REFERENCES

REFERENCES

Albani, M., B. Klinkenberg, D.W. Andison, and J.P. Kimmins. 2004. The choice of window size in approximating topographic surfaces from digital elevation models. International Journal of Geographical Information Science. 18(6): 577-593.

Armhein, C.G. 1995. Searching for the elusive aggregation effect: Evidence from statistical simulations. Environment and Planning A. 27(1):105-119.

Behrens, T., A. Zhu, K. Schmidt, and T. Scholten. 2010. Multi-scale digital terrain analysis and feature selection for digital soil mapping. Geoderma. 155:175-185.

Burras, C.L. and W.H. Scholtes. 1987. Basin properties and postglacial erosion rates of minor moraines in Iowa. Soil Science Society of America Journal. 51:1541-1547.

Carter, B.J. and E.J. Ciolkosz. 1991. Slope gradient and aspect effects on soils developed from sandstone in Pennsylvania. Geoderma. 49:199-213.

Cerdá, A. 1998. The influence of geomorphic position and vegetation cover on the Erosional and hydrological processes on a Mediterranean hillslope. Hydrological Processes. 12:661-671.

Chang, K., Tsai, B., 1991. The effect of DEM resolution on slope and aspect mapping. Cartography and Geographic Information Systems 18, 69-77.

Chaplot, V., Walter, C., Curmi, P., 2000. Improving soil hydromorphy prediction according to DEM resolution and available pedological data. Geoderma. 97:405-422.

Claessens, L., G.B.M. Heuvelink, J.M. Schoorl, and A. Veldkamp. 2005. DEM resolution effects on shallow landslide hazard and soil redistribution modelling. Earth Surface Processes and Landforms. 30(4):461-477. doi: 10.1002/esp.1115.

Dehn, M. H. Gärtner, and R. Dikau. 2001. Principles of semantic modeling of landform structures. Computers & Geosciences. 27:1005-1010.

Donald, R.G., D.W. Anderson, and J.W.B. Stewart. 1993. The distribution of selected soil properties in relation to landscape morphology in forested Gray Luvisol soils. Canadian Journal of Soil Science. 73:165-172.

Drăgut, L., T. Schauppenlehner, A. Muhar, J. Strobl, and T. Blaschke. 2009. Optimization of scale and parameterization for terrain segmentation: an application to soil-landscape modeling. Computers & Geosciences. 35:1875-1883.

ESRI. 2012. Environmental Systems Research Institute ArcGIS Software, Version 10.1. http://www.esri.com

Evans, I.S. 1979. An integrated system of terrain analysis and slope mapping. Final report on grant DA-ERO-591-73-G0040. University of Durham. England.

Florinsky, I.V., R.G. Eilers, G.R. Manning, and L.G. Fuller. 2002. Prediction of soil properties by digital terrain modelling. Environmental Modelling & Software. 17:295-311.

Gallant, J.G. and J.P. Wilson. 1996. Tapes-G: a grid-based terrain analysis program for the environmental sciences. Computers & Geosciences. 22(7):713-722.

GRASS Development Team, 2012. Geographic Resources Analysis Support System (GRASS) Software, Version 6.4.2. Open Source Geospatial Foundation. http://grass.osgeo.org

Hupy, C.M., R.J. Schaetzl, J.P. Messina, J.P. Hupy, P. Delamater, H. Enander, B.D. Hughey, R. Boehm, M.J. Mitrok, and M.T. Fashoway. 2004. Modeling the complexity of different, recently glaciated soil landscapes as a function of map scale. Geoderma. 123:115-130.

Jelinski, D.E. and J. Wu. 1996. The modifiable areal unit problem and implications for landscape ecology. Landscape Ecology. 11(3):129-140.

Joel, M., D.S. Schimel, M.A. Friedl, F.W. Davis, and R.C. Dubayah. 1994. Regression tree analysis of satellite and terrain data to guide vegetation sampling and surveys. Journal of Vegetation Science. 5:673-686.

Kienzle, S. 2004. The effect of DEM raster resolution on first order, second order and compound terrain derivatives. Transactions in GIS. 8:83–111.

Lapen, D.R. and L.W. Martz. 1996. An investigation of the spatial association between snow depth and topography in a Prairie agricultural landscape using digital terrain analysis. Journal of Hydrology. 184:277-298.

MacMillan, R.A., W.W. Pettapiece, S.C. Nolan, T.W. Goddard. 2000. A generic procedure for automatically segmenting landforms into landform elements using DEMs, heuristic rules and fuzzy logic. Fuzzy Sets and Systems. 113:81-109.

Milne, G. 1935. Some suggested units of classification and mapping particularly for East African soils. Soil Research. 4(3).

Mitášova, H. and J. Hofierka. 1993. Interpolation by regularized spline with tension: II. Application to terrain modeling and surface geometry analysis. Mathematical Geology. 25(6):657-669.

Montello, D.R. 2001. Scale in geography. *In* N.J. Smelser & P.B. Baltes (eds.). International Encyclopedia of the Social & Behavioral Sciences. Pergamon Press. Oxford.

Moore, I.D., P.E. Gessler, G.A. Nielsen, and G.A. Peterson. 1993. Soil attribute prediction using terrain analysis. Soil Science Society of America Journal. 57:443-452.

Roecker, S.M. and J.A. Thompson. 2010. Scale effects on terrain attribute calculation and their use as environmental covariates for digital soil mapping. *In* J.L. Boettinger, D.W. Howell, A.C. Moore, A.E. Hartemink, and S. Kienast-Brown (eds). Digital Soil Mapping: Bridging Research, Environmental Application, and Operation. pp. 55-66.

Ruhe, R.V. 1960. Elements of the soil landscape. Trans. 7th Intl. Cong. Soil Sci., Madison, WI. 4:165-170.

Schoeneberger, P.J., D.A. Wysocki, E.C. Benham, and Soil Survey Staff. 2012. Field Book for Describing and Sampling Soils, Version 3.0. U.S. Department of Agriculture, Natural Resource Conservation Service. Lincoln, Nebraska.

Schoorl, J.M., Sonneveld, M.P.W., Veldkamp, A., 2000. Three-dimensional landscape process modeling: the effect of DEM resolution. Earth Surface Processes and Landforms 25, 1025-1034.

Sharma, A., K.N. Tiwari, and P.B.S. Bhadoria. 2011. Determining the optimum cell size of digital elevation model for hydrologic application. Journal of Earth System Science. 120(4): 573-582.

Shi, X., R. Long, R. Dekett, J. Philippe. 2009. Integrating different types of knowledge for digital soil mapping. Soil Sci. Soc. Am. J. 73:1682-1692. doi:10.2136/sssaj2007.0158.

Shi, X., A. Zhu, J. Burt, W. Choi, R. Wang, T. Pei, B. Li, and C. Qin. 2007. An experiment using circular neighborhood to calculate slope gradient from a DEM. Photogrammetric Engineering & Remote Sensing. 73(2):143-154.

Smith, M.P., A. Zhu, J.E. Burt, and C. Stiles. 2006. The effects of DEM resolution and neighborhood size on digital soil survey. Geoderma. 137:58-69. doi:10.1016/j.geoderma.2006.07.002

Stolt, M.H., J.C. Baker, and T.W. Simpson. 1993. Soil-landscape relationships in Virginia: II. reconstruction analysis and soil genesis. Soil Science Society of America Journal. 57:422-428.

Thompson, J.A., J.C. Bell, and C.A. Butler. 2001. Digital elevation model resolution: effects on terrain attribute calculation and quantitative soil-landscape modeling. Geoderma. 100:67-89.

Wood, J.D. 1996a. Scale-based characterisation of digital elevation models. In: D. Parker, editor, Innovations in GIS 3: Selected Papers from the Third National Conference on GIS Research. Taylor & Francis, London, UK.

Wood, J. 1996b. The Geomorphological characterisation of Digital Elevation Models. Diss., Department of Geography, University of Leicester, U.K. http://www.soi.city.ac.uk/~jwo/phd/. Accessed [4/15/2013].

Wu, W., Y. Fan, Z. Wang, H. Liu. 2008. Assessing effects of digital elevation model resolutions on soil-landscape correlations in a hilly area. Agriculture, Ecosystems & Environment. 126(3-4):209-216.

Wysocki, D.A., P.J. Schoeneberger, and H.E. Garry. 2000. Geomorphology of Soil Landscapes. *In* M.E. Sumner (ed.). Handbook of Soil Science. CRC Press LLC. Boca Raton, Florida.

Yoo, K., R. Amundson, A.M. Heimsath, and W.E. Dietrich. 2005. Erosion of upland hillslope soil organic carbon: coupling field measurements with a sediment transport model. Global Biogeochemical Cycles. 19(3):GB3003. doi: 10.1029/2004GB002271.

Zevenbergen, L.W. and C.R. Thorne. 1987. Quantitative analysis of land surface topography. Earth Surface Processes and Landforms. 12:47-56.

CHAPTER 4. DIGITAL CLASSIFICATION OF HILLSLOPE POSITION: DEVELOPING A BETTER BASE MAP FOR IMPROVING AND DISAGGREGATING EXISTING SOIL MAPS

Abstract

Classification of hillslope position has long been used in soil geomorphology. Many soil landscapes are readily predictable and mappable by using this landscape attribute alone. However, insufficiently detailed base maps - due to lack of detailed data or the proper technology to develop them - have restricted the use of hillslope elements as landscape guides in traditional soil mapping endeavors. In this research, I develop and present a landscape classification model that provides quantitatively defined hillslope positions that are repeatable across landscapes. These types of maps are excellent base maps, which can be used to facilitate the disaggregation of soils currently mapped as complexes, and the identification of inclusions that are mainly due to subtle topographic variation. I test a series of approaches for calibrating the classification of LiDAR elevation data for hillslope position. The classification models use parameters that have already been calibrated to the respective analysis scales used by the soil scientists in the field. Evaluated classification methods include a variety of decision tree structures, with breaks based on calibration groups' mean mid-points, median mid-points, and fuzzy membership, as well as classification by linear discriminant analysis. Model prediction of field scientists' classification of hillslope position ranged from 11% to 59% agreement. The successful prediction rate of 59% is acceptable, given that the model parameters only had

agreement rates with field assessments of 69-79%. The best performing model was a decision tree differentiating the landscape first by slope gradient, then by profile curvature and relative elevation. The best performing classification breaks were those determined by the midpoints of calibration groups' medians. Soil maps, generated from these base maps, resulted in a definitionally consistent characterization of the landscape that reflects the experience of field soil scientists and can be efficiently applied to large extents. Areas of potential mismapping are easily identified by comparing hillslope position classifications with current Soil Survey delineations.

Keywords: hillslope position, digital soil mapping, disaggregation, LiDAR

1. Introduction

1.1 Utility of Hillslope Position

Ruhe and Walker (1968) defined and identified five hillslope profile positions for geomorphically describing landscapes. The transferability (uniformitarianism) of this model for fully developed slopes, regardless of climate or material, has been clearly demonstrated (Wood, 1942; King, 1957; Frye, 1959; Ruhe, 1975). Since that time, the five hillslope positions have become the standard for studying soil toposequences, under the pedogenic model proposed by Jenny (1941), as well as for landscape description and segmentation in general (Conacher and Dalrymple, 1977; Pennock et al., 1987; Giles, 1998; Park and van de Giesen, 2004). Numerous studies - some of them being landmark papers - have leaned on or otherwise built upon this framework to examine the variability of soil properties across hillslopes (Kleiss, 1970; Furley, 1971; Malo et al., 1974; Butler, 1982; Burras and Scholtes, 1987; West et al., 1988; Donald et

al., 1993; Stolt et al., 1993; Korobova and Romanov, 2011; Kagabo et al., 2013; Tsatskin et al., 2013). Also, because of the interrelationship between soil and vegetation, hillslope position has been a useful framework in ecological studies (Arnold et al., 2009; Jien et al., 2010; Khalili-Rad et al., 2011; Koné et al., 2013).

The information gained from intensive studies has since been extended across landscapes using a soil-landscape model (Hudson, 1990; Hudson, 1992). Through spatial association, observations can be related to similar map units, thereby extending the utility of intensive, small extent studies (Milne, 1935; Bushnell, 1943; Hole and Campbell, 1985). For these reasons, this principle has been a successful paradigm for the U.S. Soil Survey in regions where hillslope processes are a major factor in explaining the spatial variability of soils (e.g. Pregitzer, 1972; Dermody, 2009; Pulido, 2011). However, soil map units would be improved by better definition and integration of landscape components, such as hillslope position (Hall and Olson, 1991).

In addition to being a research tool, classification facilitates communication and understanding by providing an orderly arrangement to a complex world (Grealish et al., 2013). It provides unique geographic tools for analyzing spatial patterns (Bunge, 1962). For example, classified soil bodies can be analyzed for density, orientation, and shape complexity (Hole and Campbell, 1985). Indeed, soil bodies reflect geomorphic processes more directly than do individual pedons (Wysocki et al., 2000). For example, soil classification is more amenable to expressing unique combinations of soil properties than are continuous fields (Arnold, 2006).

Classification also provides a means for comparing different soils on a common attribute scale, such as drainage or productivity indexes (Schaetzl et al., 2009; Schaetzl et al., 2012).

As demonstrated in Chapter 2, soil mapping efforts throughout history have been able to delineate smaller map units, with more accuracy, as better base maps have become available. Despite these advances, current U.S. Soil Survey maps contain many soil complexes, rather than consociations, due to limitations in available base maps and resources to delineate that level of detail. Currently, the U.S. Soil Survey primarily relies on stereo aerial photographs, which are limited in resolution and topographic information. Even map units delineated as consociations contain inclusions that were too small to identify in the available base map, or at the scale of the soil map. Many of these areas could have been delineated, had better base maps and more resources (i.e. manpower) been available. Disaggregation of these soil delineations would be a major step for improving soil maps. Better base maps have the ability to facilitate the delineation of soil map units to the resolution of topographic relationships. However, to do so, the five hillslope positions in a mature landscape need to be defined and identified in a manner that is accurate and repeatable across the landscape.

High resolution, digital elevation grids, made optimally from LiDAR data, are necessary to quantitatively define hillslope position. Digital terrain analyses apply characterization algorithms and classification rules to the detailed elevation data, as a means to consistently describe and classify terrain. Hillslope position is a classic terrain characterization that has not been translated to digital methods. Hillslope position is a composite of terrain characteristics that are mentally synthesized by soil scientists in the field, namely profile curvature, slope

gradient, and relative elevation (Figure 4.1). Chapter 3 of this dissertation calibrated the digital analysis scale for each of these terrain parameters to the analysis scale used by soil scientists assessing hillslope position. Optimizing the analysis scale of the parameters provides the setup for testing which model structure best predicts the field classification of hillslope position.

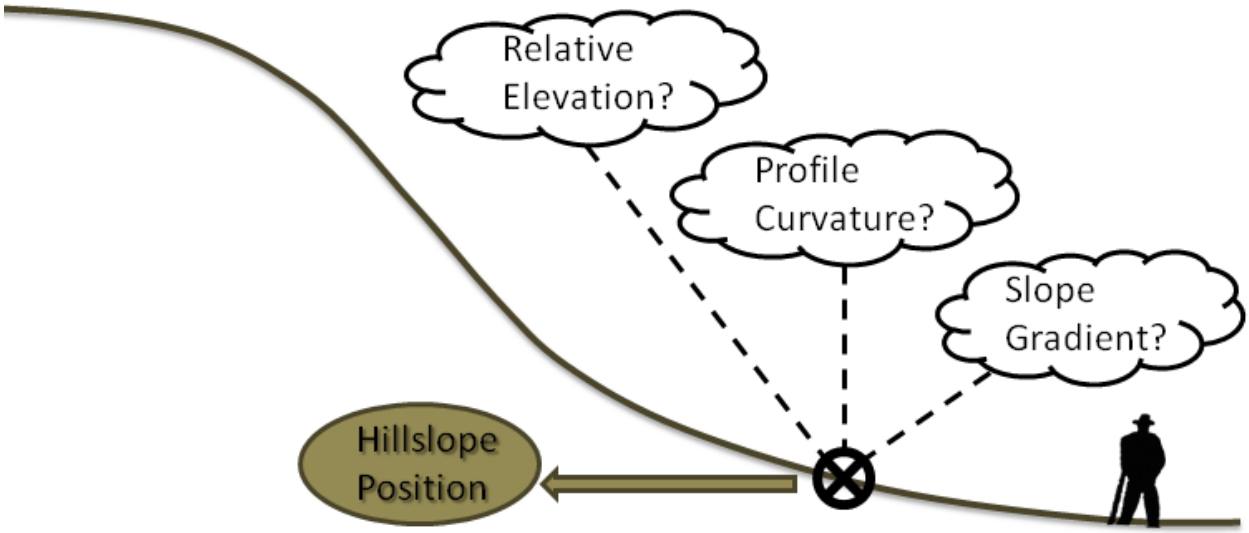


Figure 4.1. Illustration of the mental construct that soil scientists use to assess hillslope position in the field.

As a first step to establishing a quantitative definition of hillslope positions, this study evaluates a series of digital classification approaches for their ability to predict hillslope positions, as initially identified by soil scientists in the field, for a study area in Michigan. The transferability of the hillslope position models is then tested by applying and validating the respective models in two additional study areas in Iowa. Although this study uses the classification of hillslope position to calibrate and validate terrain analysis to the soil scientists' assessments, the result is not limited to discrete classification. One of the hillslope position models utilizes a fuzzy classification approach, which could be used as a parameter in soil

models without hardening the membership classification. Whether discrete or fuzzy membership is desired, the quantitative, repeatable, and transferable classification of hillslope position has the potential to improve soil maps by providing the differentiating criteria for disaggregating map units in a consistent and documented manner.

1.2 Application to Digital Soil Mapping

A popular approach to digital soil mapping has been expert knowledge models that require the user to determine parameter breaks in a digital format (Zhu et al., 2001; Shi et al., 2004; Shi et al., 2009). This method stands in contrast to traditional soil mapping methods where soil scientists relate observations in the field to locations identified on an aerial photograph, viewed stereoscopically. Unlike histograms of digital data, aerial photographs include more of the field context in which soil scientists' have calibrated their mental model of the soil landscape. The special ability of humans to synthesize multiple parameters, contextually, is one of the reasons that human assessment in the field and of aerial photography is a powerful method for soil mapping (Hudson, 1992; Hengl and MacMillan, 2007; MacMillan et al., 2007), and one that is usually lacking in digital soil mapping. Therefore, calibrating soil classification parameters to soil scientists' field interpretations will be more intimately connected to the soil scientists' mental model, and thus potentially result in better landscape classifications. The conceptual model built by individual soil scientists in the field utilizes both implicit and explicit parameters to discern geographic soil patterns. In order to fully utilize the experience of field soil scientists, their expert knowledge needs to be captured in the context that is what calibrated.

Expert knowledge models have also required unique calibrations per mapping area. The unique calibration of digital terrain parameter breaks per mapping area implies that geomorphic processes respond to terrain shape differently by location. Although the balance between surface runoff and infiltration is affected by a number of soil and meteorological conditions (Schaetzl, 2013), if all other variables are held constant, similar slope shapes should have similar soil properties (Milne, 1935; Ellis, 1938; Bushnell, 1943; Hole and Campbell, 1985). The lack of transferability of soil mapping models may be more a product of mapper subjectivity in the complex interpretation of which soil boundaries are important in a soil map. For example, cultivated fields are often mapped in greater detail than adjacent forests (Figure 4.2).

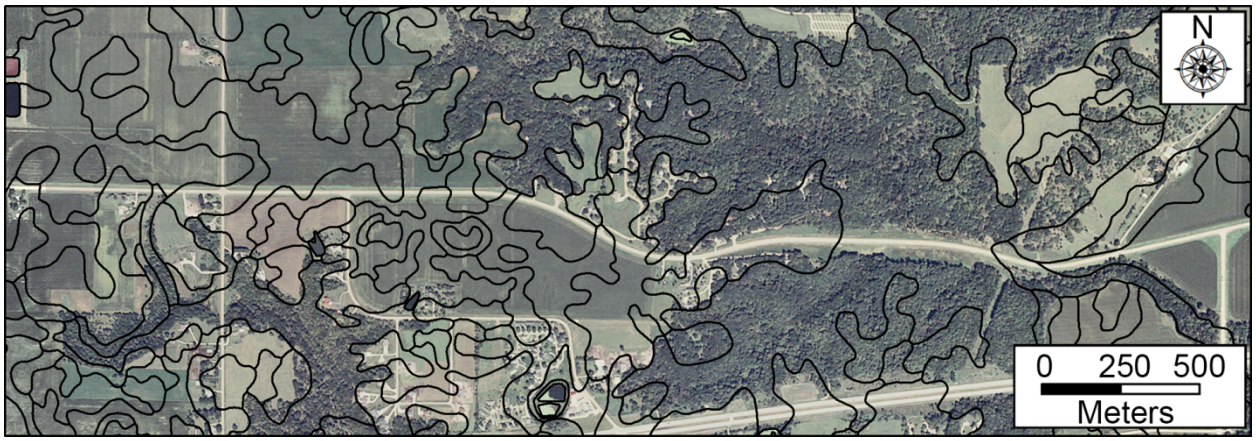


Figure 4.2. Example of subjective shift in soil map detail between cultivated fields (left) and adjacent forest land (right) in the 1:15,840 Soil Survey map of Boone County, Iowa (Andrews and Dideriksen, 1981).

Soil mapping efforts can use the hillslope position base map to combine the strengths of field knowledge with the precision and efficiency of digital terrain analysis. Utilizing the philosophy of expert knowledge models, by translating tacit knowledge to quantified definitions, soil landscapes can be classified in a consistent and documented manner. However,

the expert knowledge models can be better calibrated to the actual expert knowledge by allowing experts to interpret the landscape in the context in which they were trained (i.e. the field) and by examining the individual components of the soil mapper's decision process.

The hillslope position classification model validated in this study provides digital base maps of hillslope position, for the purpose of delineating soil map units by the soil-landscape approach, but at a level of detail unattainable by previous manual methods. Additionally, the delineation of hillslope position boundaries is done in a repeatable manner. The result is a higher resolution criteria for differentiating soil map units, which can be used to identify smaller, more homogenous soil areas and improve line placement.

2. Methods

2.1. General Setup

Using the analysis scales calibrated for each of the terrain parameters (i.e. profile curvature at 63 m, relative elevation at 135 m, and slope at 9 m)(Chapter 3), four approaches to classifying hillslope position were tested. These approaches included a series of decision tree arrangements with breaks based on mid-points between central concept values (assumption of similar variability within groups), a series of decision tree arrangements based on fuzzy membership (allowance for different within group variability), and linear discriminant analysis (LDA). Terrain analysis of slope gradient and profile curvature was conducted on LiDAR-derived, 3 m resolution, elevation grids using the r.param.scale function in GRASS 6.4.2 (GRASS Development Team, 2012). Relative elevation was calculated in ArcGIS 10.1 (ESRI, 2012), using the analysis scale dependent method presented in Chapter 3.

Ottawa County, Michigan was used as the base study area for calibration and validation of the hillslope position models. The elevation grid was obtained from the Ottawa County government based on LiDAR data, flown in 2004. Ottawa County covers 1,488 km^2 and includes a wide variety of terrain, mostly derived from Late Wisconsin glaciation (Pregitzer, 1972). The majority of the county's topography ranges from flat, lake and outwash plains to hummocky, till plains of Wisconsin age. However, there are also large areas of high relief due to more recent sand dune development. Elevation ranges from 173 to 292 meters above sea level with slope gradients ranging from 0° to 46°. The mean slope gradient is 3°.

All field observations of hillslope position in Ottawa County were collected by NRCS soil scientists working out of the Grand Rapids, Michigan Soil Survey (MLRA) Office. The observations were collected as part of regular office operations to better understand boundaries between map units that were difficult to delineate. A pool of 1,039 GPS-located, field observations, taken as 8-10 point transects with 40-80 m spacing, were used for calibration (Figure 4.3). At each point, the mapper made notes as to their interpretation of hillslope position along with additional soil properties. These points were intersected with the digital terrain analysis grids of the model parameters and grouped by the field observers' assessment of hillslope position. Due to field observers' uncertainty in classifying some locations, not all observation points included a description applicable to all components of hillslope position determination. For example, 411 points were described as "flat". Although these points could not be used to calibrate breaks for relative elevation, they could still be used to populate definitional groups for slope gradient and profile curvature. For the decision tree

classifications, 966, 970, and 546 points were used to calibrate breaks for slope gradient, profile curvature, and relative elevation, respectively. The multivariate process of LDA limited the use of points to only those in which the hillslope position was clearly identified by the field observer. This requirement for fully categorized points limited the quantity of calibration points available to 546 for that particular classification method. For validation, 262 field observations taken by the staff of the same Soil Survey office, but not in transects, were used. Of those points, the field observer was unable to decide between two hillslope positions for only 73 of the observation locations. In these cases, model prediction of either hillslope position identified by the field scientists was accepted as valid.

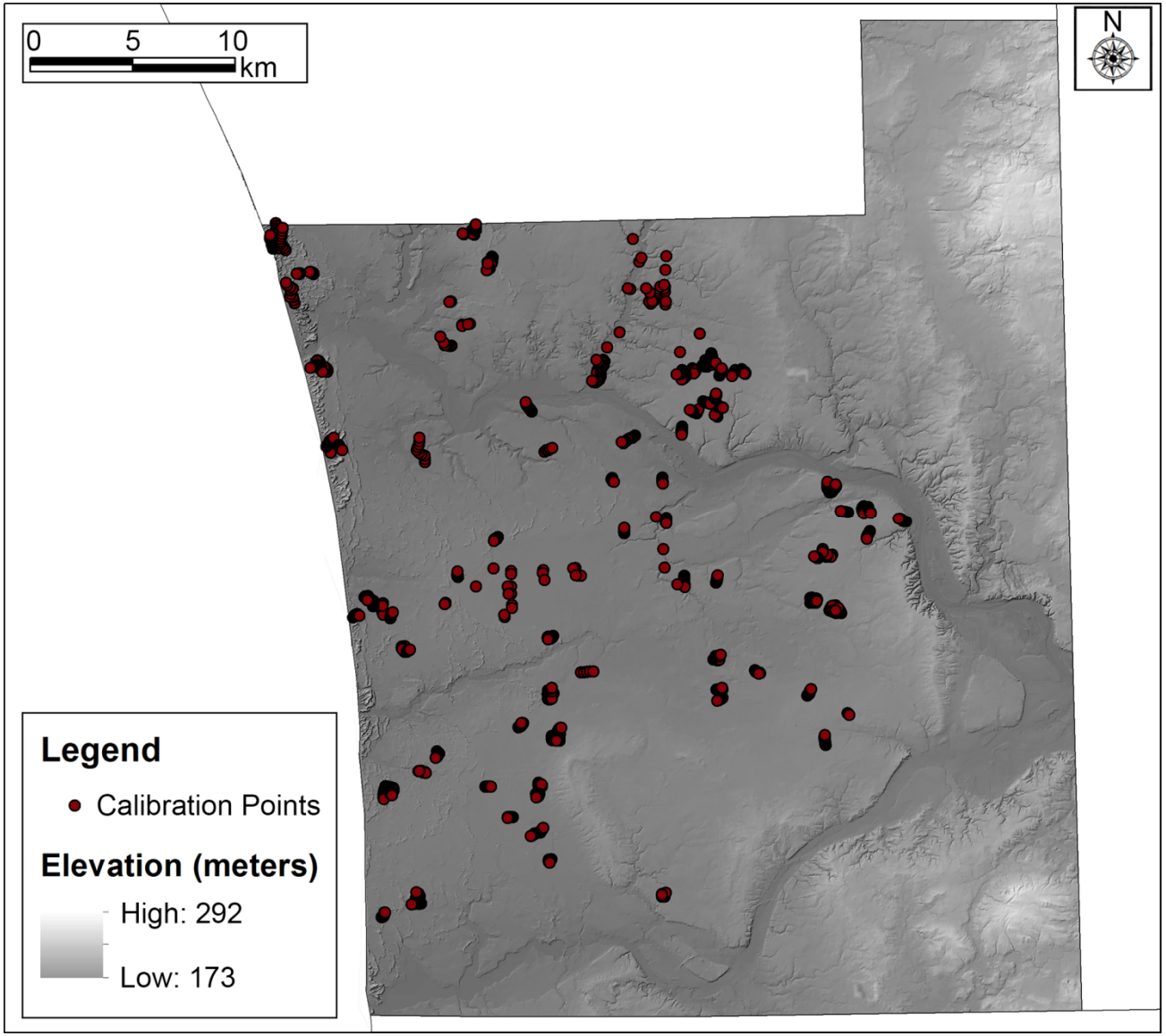


Figure 4.3. Distribution of calibration points in Ottawa County, Michigan. Each set of calibration points represent mapping transects, walked by NRCS field soil scientists, and each contains 8-10 observations.

2.2 Decision Tree Models

Three possible decision trees were identified by the logic of hillslope position definitions after the use of each of the three parameters, respectively, at the top level of the hierarchy. The initial decision tree hierarchy differentiates hillslope positions first by profile curvature, then by slope gradient, and finally by relative elevation. Because this decision tree hierarchy emphasizes profile curvature at the top level, it will be referred to as the *profile curvature priority* decision tree (PrcP) (Figure 4.4a). The second decision tree hierarchy differentiates hillslope positions first by slope gradient, then by profile curvature and relative elevation (Figure 4.4b), and is referred to as the *slope gradient priority* decision tree (SlgP). The third decision tree hierarchy differentiates hillslope positions first by relative elevation, then slope gradient, and is referred to as the *relative elevation priority* decision tree (ReeP) (Figure 4.4c). In this last decision tree hierarchy, the five hillslope positions are differentiated without the use of profile curvature. In all decision trees, the first level of criteria was calibrated for two classification breaks to create three categories. The remaining levels of the decision trees then only required a single break to make two categories within the respective branches of the tree.

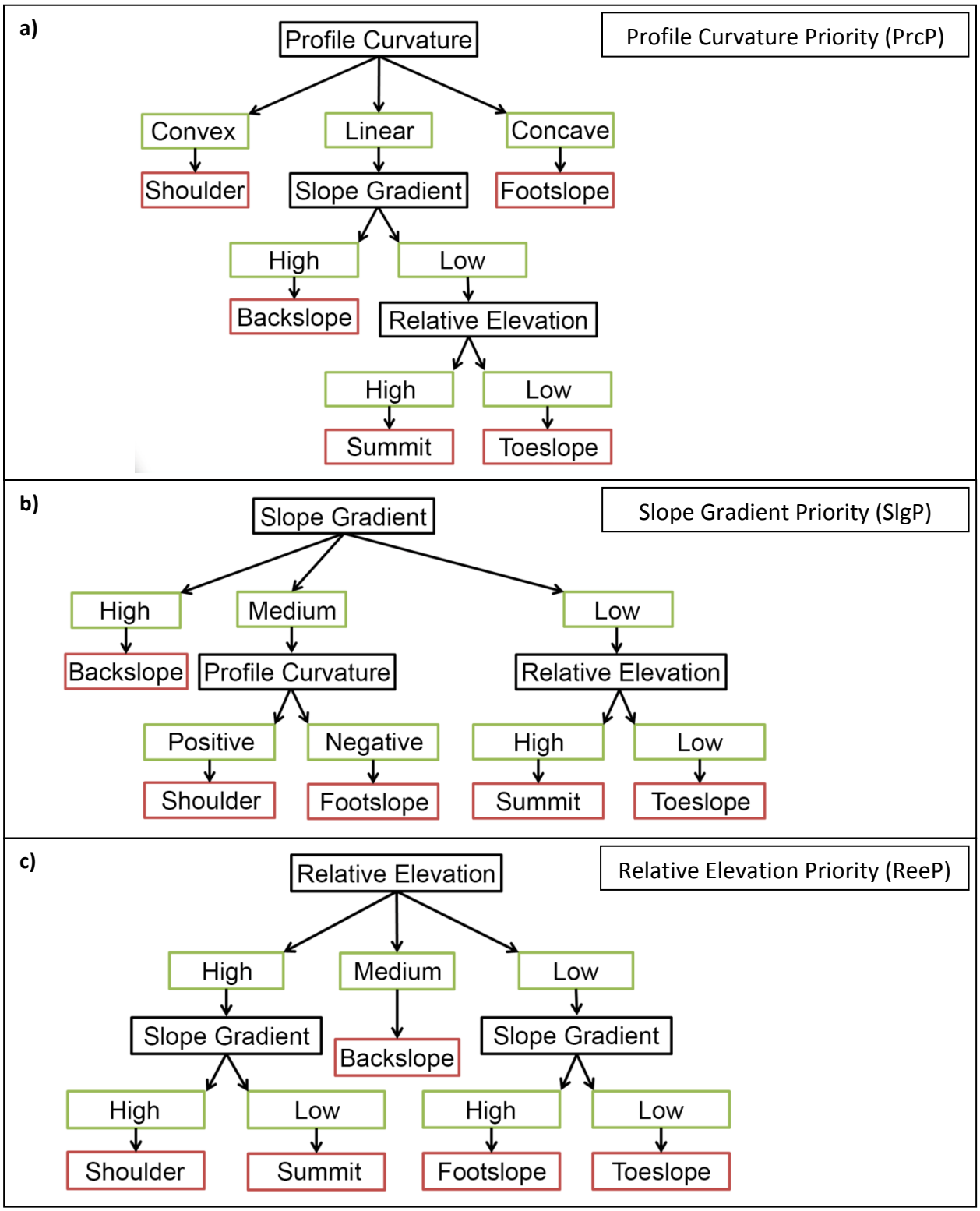


Figure 4.4. Diagrams for the three classification tree hierarchies. Each tree will be referred to by the parameter emphasized in the top level of the hierarchy, specifically: a) the profile curvature priority decision tree (PrcP), b) the slope gradient priority decision tree (SlgP), and c) the relative elevation priority decision tree (ReeP).

2.2.1. Calibration of Classification Breaks

Three methods of classification break calibration were tested on each of the three decision tree structures, leading to nine experimental iterations. The respective calibration methods were used consistently for all levels of a decision tree. For each model parameter, the calibration points were sorted into assessment groups, as per the definitional category of the observed hillslope position (Table 4.1). Statistics for the digital terrain values within the assessment groups were calculated and used as a basis for quantitative calibration of breaks between assessment groups.

Table 4.1. Definitional categories of terrain parameters by hillslope position.

Hillslope Position	**Slope**	**Profile Curvature**	**Relative Elevation**
Summit	Low	Linear	High
Shoulder	Medium	Convex	High
Backslope	High	Linear	Middle
Footslope	Medium	Concave	Low
Toeslope	Low	Linear	Low

The first classification break calibration used the mean as the central concept for the respective assessment groups. Assuming similar, normal distributions around that central concept, the mean of two adjacent central concept values (mid-point), was then used as the break between the two groups. A few extreme values in parameter assessment groups, particularly slope gradient, created the possibility of the mean not being the optimal central concept criterion for the group. To address this potential issue, the second break calibration method used the median instead of the mean to represent the central concept. The classification breaks for this calibration method were determined in the same manner as the

group-mean calibration approach. For example, when profile curvature needed to be classified as convex, linear, or concave, calibration points were categorized into the three assessment groups. The median of each assessment group was used as the respective groups' central concept. The mean between the medians of the convex and linear groups and the mean between the medians of linear and concave groups were used as classification rules to separate the groups respectively in the model.

To allow for the possibility that the value distributions between assessment groups were not similar, a fuzzy membership method was also tested. The statistical characteristics of the grouped calibration points were used to construct a confidence index (CI) of membership. The CI was calculated using a normal probability density function (PDF) based on the group's mean and standard deviation, which was then standardized to set the group mean with a CI value of one. CI values, therefore, grade decreasingly towards and can overlap with an adjacent category. Parameter values on the opposite side of the mean from all other assessment groups were assigned a CI of one plus the inverse result of the PDF. The resulting theoretical CI distribution is illustrated in Figure 4.5. For classification, locations were categorized into the group for which the location had the highest CI of membership.

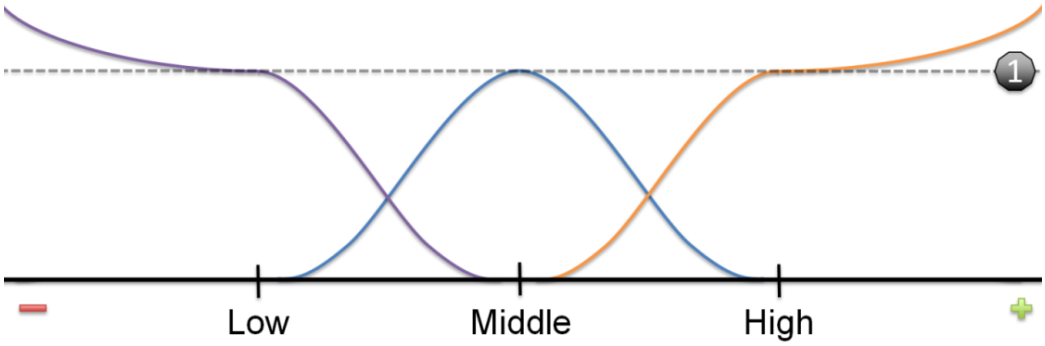


Figure 4.5. Conceptual illustration of the confidence index (CI) used for determining fuzzy membership. The shape of the CI curve for the middle class is calculated by a normal probability density function (PDF) based on the calibration group's mean and standard deviation. CI values for the low and high classes are calculated in the same manner, except that values on the opposite side of the mean from other classes are calculated as one plus the inverse of the PDF result.

2.3. Linear Discriminant Analysis

For the LDA approach, all three terrain parameters were standardized to a mean of zero and a standard deviation of one to remove the possibility of large differences in magnitude affecting results. The standardized grids of the three terrain parameters were then intersected with the calibration points. The values from those intersected points were processed for LDA using the MASS library in the R software package (Venables and Ripley, 2002). The resulting linear combination function and classification rules were then applied to the standardized, terrain parameter grids for determining hillslope position.

2.4. Validation and Transferability

Validation points were intersected with each of the classified hillslope position grids produced by the ten different classification approaches in Ottawa County. Each classification

approach was evaluated by overall percent agreement between soil scientists' field observations and model prediction, as well as with confusion matrixes. The validation results of the hillslope position models in the calibration area of Ottawa County were used to determine if the decision tree or LDA classification approach would be tested for transferability to other landscapes.

Two counties in Iowa with different terrain types were selected to test the transferability of hillslope position models validated in Ottawa County, Michigan. Like the Michigan study site, Dickinson County, Iowa is a landscape dominated by Late Wisconsin-age glacial landforms, but with a much larger proportion of closed basins (Pulido, 2011). The area consists primarily of till, glaciolacustrine, and outwash plains. Elevations range from 387 to 485 m above sea level. The steepest slope gradient in the area is 61°, but the mean is 2°. The second study area for testing transferability was Cedar County, Iowa. This county's physiography has been classified as Southern Iowa Drift plain except for some Iowan Erosion Surface in the northern quarter (Ruhe, 1969; Dermody, 2009). Across the county, Pre-Illinoian glacial deposits have been dissected through several episodes of landscape development (Bettis, 1989). Elevations in Cedar County range from 191 to 295 m above sea level. Slope gradients in the area reach 77°, with a mean of 3°.

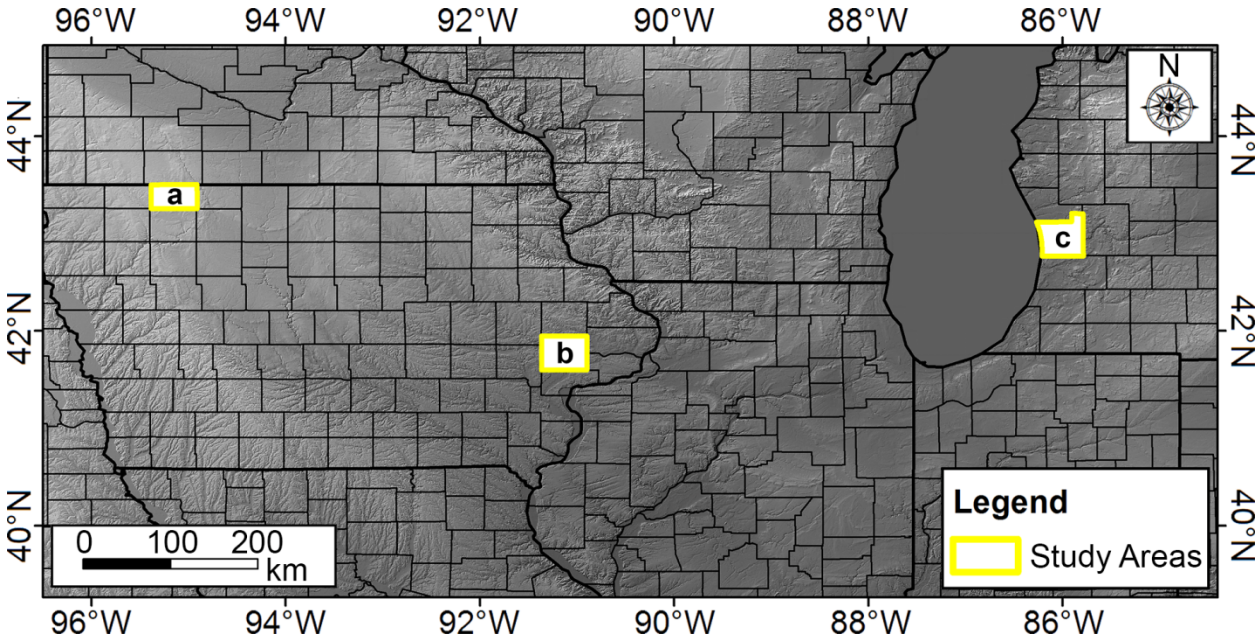


Figure 4.6. Dickinson County, Iowa (a) and Cedar County, Iowa (b) were used to test the transferability of the models calibrated and validated in Ottawa County, Michigan (c).

The same hillslope position models, including classification breaks calibrated in Ottawa County, were used to classify hillslope position in the two Iowa study areas. The models were applied to 3 m resolution elevation grids obtained from the Iowa Department of Natural Resources, which were based on LiDAR data collected between 2007 and 2009 (IDNR, 2009). Hillslope position validation points for Dickinson and Cedar Counties were field observations with locations recorded by GPS, obtained from the Waverly, Iowa Soil Survey Office. Dickinson County had 75 and Cedar County had 35 field observations available, respectively. Agreement between the hillslope position classification model and the NRCS field observations was assessed in the same manner as in the validation procedure for Ottawa County.

The hillslope position model determined to have the most consistently high rate of agreement with validation points in all three study areas was subsequently compared with the

current Soil Survey map delineations. The zonal statistics of the hillslope position classifications based on map units in the Soil Survey Geographic dataset (SSURGO) (Soil Survey Staff, 2013a) were used to quantitatively compare and contrast the two maps.

3. Results and Discussion

3.1. Calibration

The statistics of the assessment groups based on the calibration points are presented in Table 4.2. These statistics were used to calculate the classification breaks tested in this study. For comparison, the determined classification breaks for the mean mid-point, median mid-point, and the equivalent break values (after hardening the fuzzy classification) are presented in Table 4.3. All parameters are calculated at the optimal analysis scale, as determined in Chapter 3. The occurrence of extreme values in the assessment groups caused all the group medians to be different from the group mean. The impact of these differences can be observed in the resulting classification breaks. The smaller influence of extreme values on group medians resulted in classification breaks closer to definitionally expected values for the median mid-point calibration method. The calibrated breaks for concave-convex profile curvature and low-high relative elevation should definitionally be zero. Compared to the other two calibration methods, the median mid-point based breaks are the closest to meeting that definition. The hardened CI breaks are generally similar to the mean mid-point calibration method, but are tempered by the larger standard deviations for steeper slope groups and the middle relative elevation group.

Table 4.2. Statistics of calibration points categorized into the assessment groups of each model parameter.

Slope (9 m)	*Mean*	*Median*	*s.d.*	*Count*
Low	1.26°	0.92°	1.49°	577
Medium	3.67°	1.81°	4.74°	218
High	8.12°	4.02°	9.04°	171
Profile Curvature (63 m)	*Mean*	*Median*	*s.d.*	*Count*
Concave	-0.00538 m^{-1}	-0.00120 m^{-1}	0.02193 m^{-1}	105
Linear	-0.00021 m^{-1}	-0.00004 m^{-1}	0.01938 m^{-1}	751
Convex	0.00388 m^{-1}	0.00136 m^{-1}	0.01500 m^{-1}	111
Relative Elevation (135 m)	*Mean*	*Median*	*s.d.*	*Count*
Low	-2.16 m	-0.74 m	4.41 m	206
Middle	-1.18 m	-0.03 m	8.53 m	166
High	1.35 m	0.55 m	6.33 m	200

Table 4.3. Classification breaks calibrated from the assessment group statistics of each model parameter.

Slope (9 m)	*Mean Mid-point*	*Median Mid-point*	*Hardened CI*
low-medium	2.46°	1.36°	1.83°
medium-high	5.89°	2.91°	5.20°
low-high	4.69°	2.47°	2.23°
Profile Curvature (63 m)	*Mean Mid-point*	*Median Mid-point*	*Hardened CI*
Concave-Linear	-0.00279 m^{-1}	-0.00062 m^{-1}	-0.00263 m^{-1}
Linear-Convex	0.00184 m^{-1}	0.00066 m^{-1}	0.00210 m^{-1}
Concave-Convex	-0.00075 m^{-1}	0.00008 m^{-1}	0.00012 m^{-1}
Relative Elevation (135 m)	*Mean Mid-point*	*Median Mid-point*	*Hardened CI*
Low-Middle	-1.67 m	-0.38 m	-1.83 m
Middle-High	0.09 m	0.26 m	0.28 m
Low-High	-0.40 m	-0.10 m	-0.71 m

3.2. Ottawa County Validation

3.2.1. Decision Tree Models

For Ottawa County, the decision tree models correctly predicted 36% to 59% of field scientists' assessment of hillslope position (Table 4.4). Disagreement between digital and field assessment occurs because of errors in the elevation values of the grid, positional uncertainty, and the subjectivity associated with human judgment. Given these potential sources of prediction error, with as much as 30% disagreement for the field assessment of the model parameters, a successful prediction rate of 59% is considered very acceptable.

Table 4.4. Percent agreement between soil scientists' field assessments and each hillslope position models' prediction by classification break method for Ottawa County, Michigan.

Model	Mean	Median	Confidence Index
PrcP	58%	46%	57%
SlgP	59%	53%	58%
ReeP	38%	42%	36%

The SlgP decision tree, using the classification breaks based on mean mid-points, had the highest level of agreement with field assessments. However, the agreement rates for the CI based SlgP were nearly as high. The agreement rates were also nearly as high for the mean mid-points and CI calibration methods for PrcP. Although the influence of different standard deviations between assessment groups shifted the CI based breaks, the shift did not have a large impact on general agreement results for any of the decision tree structures. Greater differences in model results are observed in the confusion matrixes (Tables 4.5-4.7). For simplicity in comparing models, the classification break calibration method will be abbreviated in conjunction with the decision tree structure abbreviation (e.g. PrcP based on mean mid-

points (PrcP-mean), PrcP based on median mid-points (PrcP-med), PrcP based on confidence index (PrcP-ci)).

Table 4.5. Confusion matrixes for classification breaks based on the mid-point between assessment groups' means for a) PrcP decision tree (Kappa = 0.44), b) SlgP decision tree (Kappa = 0.49), and c) ReeP decision tree (Kappa = 0.27).

a)

		Field Observation					
Model	**PrcP-mean**	summit	shoulder	backslope	footslope	toeslope	*User**
	summit	74	16	20	8	6	*59.7%*
	shoulder	4	4	7	0	0	*26.7%*
	backslope	1	4	25	1	1	*78.1%*
	footslope	0	0	4	0	4	*0.0%*
	toeslope	1	3	11	16	48	*60.8%*
	*Producer**	*92.5%*	*14.8%*	*37.3%*	*0.0%*	*81.4%*	

b)

		Field Observation					
Model	**SlgP-mean**	summit	shoulder	backslope	footslope	toeslope	*User**
	summit	71	5	1	0	0	*92.2%*
	shoulder	12	9	3	1	2	*33.3%*
	backslope	16	14	28	0	9	*41.8%*
	footslope	6	6	0	2	11	*8.0%*
	toeslope	4	3	1	2	44	*81.5%*
	*Producer**	*65.1%*	*24.3%*	*84.8%*	*40.0%*	*66.7%*	

c)

		Field Observation					
Model	**ReeP-mean**	summit	shoulder	backslope	footslope	toeslope	*User**
	summit	52	14	18	5	1	*57.8%*
	shoulder	1	4	21	0	1	*14.8%*
	backslope	8	7	19	16	15	*29.2%*
	footslope	0	0	6	0	1	*0.0%*
	toeslope	0	1	2	4	24	*77.4%*
	*Producer**	*85.2%*	*15.4%*	*28.8%*	*0.0%*	*57.1%*	

*User's and Producer's accuracy calculated by correct classification divided by all classifications in category.

Table 4.6. Confusion matrixes for classification breaks based on the mid-point between assessment groups' medians for a) PrcP decision tree (Kappa = 0.35), b) SlgP decision tree (Kappa = 0.46), and c) ReeP decision tree (Kappa = 0.36).

a)

		Field Observation					
Model	**PrcP-med**	summit	shoulder	backslope	footslope	toeslope	*User**
	summit	49	7	13	4	1	*66.2%*
	shoulder	10	14	20	1	1	*30.4%*
	backslope	3	2	12	4	3	*50.0%*
	footslope	0	3	14	7	17	*17.1%*
	toeslope	4	2	8	9	38	*62.3%*
	*Producer**	*74.2%*	*50.0%*	*17.9%*	*28.0%*	*63.3%*	

b)

		Field Observation					
Model	**SlgP-med**	summit	shoulder	backslope	footslope	toeslope	*User**
	summit	43	7	6	4	0	*71.7%*
	shoulder	8	8	8	3	1	*28.6%*
	backslope	6	8	41	7	4	*62.1%*
	footslope	0	1	6	6	12	*24.0%*
	toeslope	2	3	7	5	40	*70.2%*
	*Producer**	*72.9%*	*29.6%*	*60.3%*	*24.0%*	*70.2%*	

c)

		Field Observation					
Model	**ReeP-med**	summit	shoulder	backslope	footslope	toeslope	*User**
	summit	37	7	10	2	1	*64.9%*
	shoulder	3	10	26	1	1	*24.4%*
	backslope	8	6	11	5	5	*31.4%*
	footslope	1	2	10	7	3	*30.4%*
	toeslope	0	2	9	11	44	*66.7%*
	*Producer**	*75.5%*	*37.0%*	*16.7%*	*26.9%*	*81.5%*	

*User's and Producer's accuracy calculated by correct classification divided by all classifications in category.

Table 4.7. Confusion matrixes for classification breaks based on the confidence index to differentiate parameters for a) PrcP decision tree (Kappa = 0.45), b) SlgP decision tree (Kappa = 0.49), and c) ReeP decision tree (Kappa = 0.28).

a)

		Field Observation					
Model	**PrcP-ci**	summit	shoulder	backslope	footslope	toeslope	*User**
	summit	74	12	13	7	4	*67.3%*
	shoulder	3	3	6	0	0	*25.0%*
	backslope	5	10	40	8	6	*58.0%*
	footslope	0	0	4	0	4	*0.0%*
	toeslope	0	1	7	10	33	*64.7%*
	*Producer**	*90.2%*	*11.5%*	*57.1%*	*0.0%*	*70.2%*	

b)

		Field Observation					
Model	**SlgP-ci**	summit	shoulder	backslope	footslope	toeslope	*User**
	summit	73	13	12	6	4	*67.6%*
	shoulder	4	9	14	2	1	*30.0%*
	backslope	2	4	30	1	2	*76.9%*
	footslope	1	1	6	6	7	*28.6%*
	toeslope	0	1	5	10	33	*67.3%*
	*Producer**	*91.3%*	*32.1%*	*44.8%*	*24.0%*	*70.2%*	

c)

		Field Observation					
Model	**ReeP-ci**	summit	shoulder	backslope	footslope	toeslope	*User**
	summit	37	7	6	2	1	*69.8%*
	shoulder	3	11	30	1	1	*23.9%*
	backslope	9	9	23	18	15	*31.1%*
	footslope	0	1	5	3	4	*23.1%*
	toeslope	0	0	2	2	20	*83.3%*
	*Producer**	*75.5%*	*39.3%*	*34.8%*	*11.5%*	*48.8%*	

*User's and Producer's accuracy calculated by correct classification divided by all classifications in category.

The PrcP-mean and PrcP-ci models tended to over classify points as summits and toeslopes, particularly those points identified as backslopes by the soil scientists. This issue suggests that the break between low and high slope gradients was set too high in those models. A similar pattern can be seen in the confusion matrixes for the SlgP-mean and SlgP-ci models,

but these models had more misclassifications for shoulder and backslope positions. This issue for the SlgP-mean and SlgP-ci models suggests a similar problem: the break between low and medium slope gradients was set too high.

The overall performance levels of the PrcP-med and SlgP-med models were lower than the PrcP-mean, SlgP-mean, PrcP-ci, and SlgP-ci models. However, the PrcP-med and SlgP-med confusion matrixes show closer agreement between field observations and model predictions when they do not agree exactly. In all cases, for both of these models, the highest number of misclassifications is in a neighboring category (adjacent to the correct classification category). The SlgP-med performed better than the PrcP-med model due to a higher rate of correctly classifying backslope positions. The SlgP-med model separates all areas classified as having high slope gradients as backslopes, suggesting that slope gradient is the most important parameter for identifying backslopes.

The ReeP models all suffered from difficulty in classifying backslope positions. Although the CI calibration method improved model performance, the ReeP-ci model still had successful prediction rates substantially lower than the PrcP and SlgP models. The classification errors for the ReeP models suggest that the range for middle relative elevation was too wide and the break between middle and high relative elevations was too low. The ReeP-ci model's performance was slightly improved by a higher middle-high classification break, but not enough to improve its correct prediction rate. The ReeP-med model had the highest performance of the ReeP calibration methods, because it was unaffected by a few extremely low relative elevation values in the calibration data set.

3.2.2. Linear Discriminant Analysis Model

Classification by LDA had the lowest rate of correct predictions (33%). The LDA method had difficulty classifying locations as summits (Table 4.8). However, in contrast to most of the decision tree approaches, LDA was much more successful in classifying backslopes. Potential issues with LDA of this data set were the correlation between profile curvature and relative elevation (R^2 = 0.42) and low separation values. The calculated separation values for calibration groups of slope gradient, relative elevation, and profile curvature were 25.2, 7.8, and 5.8 respectively. Although LDA has proven to be a powerful tool when little is known about the relationship of variables, a weakness may be its inability to consider the contextual relationships between variables to make classifications more distinguishable. However, the LDA function did agree with the SlgP decision tree model's emphasis on slope gradient. The computed LDA function was:

$$LD1 = -0.600\mathrm{S} + -0.014\mathrm{E} + 0.002\mathrm{C}$$

where S is standardized slope gradient, E is standardized relative elevation, and C is standardized profile curvature.

Table 4.8. Confusion matrix for the LDA classification (Kappa = 0.26).

		Field Observation					
Model	**LDA**	summit	shoulder	backslope	footslope	toeslope	*User**
	summit	0	0	0	0	0	*0.0%*
	shoulder	5	8	16	8	8	*17.8%*
	backslope	2	5	35	1	2	*77.8%*
	footslope	19	10	13	14	16	*19.4%*
	toeslope	10	4	4	3	31	*59.6%*
	*Producer**	*0.0%*	*29.6%*	*51.5%*	*53.8%*	*54.4%*	

*User's and Producer's accuracy calculated by correct classification divided by all classifications in category.

3.3 Validation in Different Landscapes (Transferability)

Using the same classification breaks calibrated in Ottawa County, the decision tree models were applied to two different counties in Iowa. Because of the relatively low performance of LDA in Ottawa County, I discontinued its use in additional testing.

The performance of most of the models was reduced when applied outside of the calibration area (Table 4.9). Although very different landscapes, both Cedar County, Iowa and Ottawa County, Michigan have a mean slope gradient of 3°. This similarity in relief between Cedar and Ottawa Counties may account for the better performance of several transferred models in Cedar County compared to Dickinson County, Iowa. However, unlike the other models, the SlgP-med model performed consistently well in all three landscapes. Despite not being calibrated for the respective counties, the SlgP-med model was still able to predict field assessment of hillslope position at a rate comparable to the best performing models in the calibration area (Table 4.10).

Table 4.9. Percent agreement between soil scientists' field assessments and each hillslope position models' prediction by classification break method for a) Dickinson County and b) Cedar County, Iowa.

a)

Model	Mean	Median	Confidence Index
PrcP	19%	21%	25%
SlgP	29%	52%	36%
ReeP	12%	12%	11%

b)

Model	Mean	Median	Confidence Index
PrcP	49%	34%	51%
SlgP	46%	54%	49%
ReeP	34%	37%	31%

Table 4.10. Confusion matrix for SlgP-med model prediction of field assessments of hillslope position in a) Dickinson County (Kappa = 0.35) and b) Cedar County, Iowa (Kappa = 0.37).

a)

		Field Observation					
	SlgP-med	summit	shoulder	backslope	footslope	toeslope	*User**
Model	summit	5	1	1	1	2	*50.0%*
	shoulder	3	0	1	3	1	*0.0%*
	backslope	1	1	23	2	6	*69.7%*
	footslope	0	0	1	11	3	*73.3%*
	toeslope	1	0	0	8	0	*0.0%*
	*Producer**	*50.0%*	*0.0%*	*88.5%*	*44.0%*	*0.0%*	

b)

		Field Observation					
	SlgP-med	summit	shoulder	backslope	footslope	toeslope	*User**
Model	summit	6	1	1	2	1	*54.5%*
	shoulder	2	2	1	0	1	*33.3%*
	backslope	0	1	6	0	0	*85.7%*
	footslope	1	0	1	0	0	*0.0%*
	toeslope	2	0	1	1	4	*50.0%*
	*Producer**	*54.5%*	*50.0%*	*60.0%*	*0.0%*	*66.7%*	

*User's and Producer's accuracy calculated by correct classification divided by all classifications in category.

Interestingly, in Dickinson County, model performance was adversely affected by a series of validation points along a drainage ditch (Figure 4.7). All twelve points in this series were identified in the field as being located on a toeslope. The hillslope position models recognized the area of these validation points as flat, but the low elevation values inside the adjacent ditch caused the zone surrounding the ditch to be classified by the models as a high relative elevation. If the validation points adjacent to the drainage ditch are excluded, the successful prediction rate of the SlgP-med model is increased to 62%. Other than the set of points adjacent to a drainage ditch, the variation of field to model agreement did not exhibit a spatial pattern in any of the three counties (Figures 4.8 - 4.10).

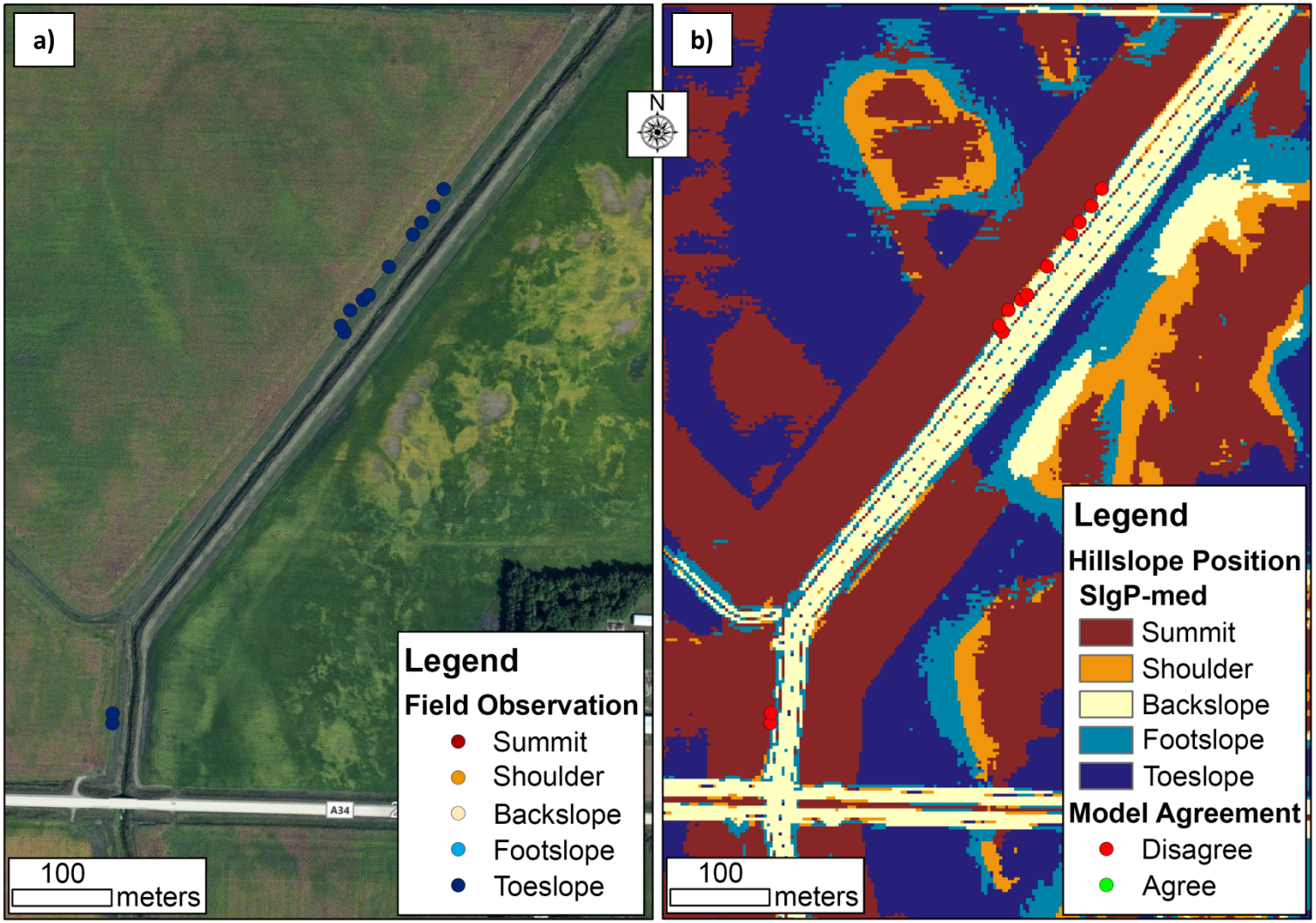


Figure 4.7. Example of disagreement between field observations and a digital hillslope position classification. Clearly, the soil scientist would have ignored the drainage ditch in deciding if the flat area containing the observation points was a toeslope or summit (a). However, the digital model considered the low elevation values within the drainage ditch for the adjacent area equivalent to the relative elevation analysis scale (b). Satellite image courtesy of USGS.

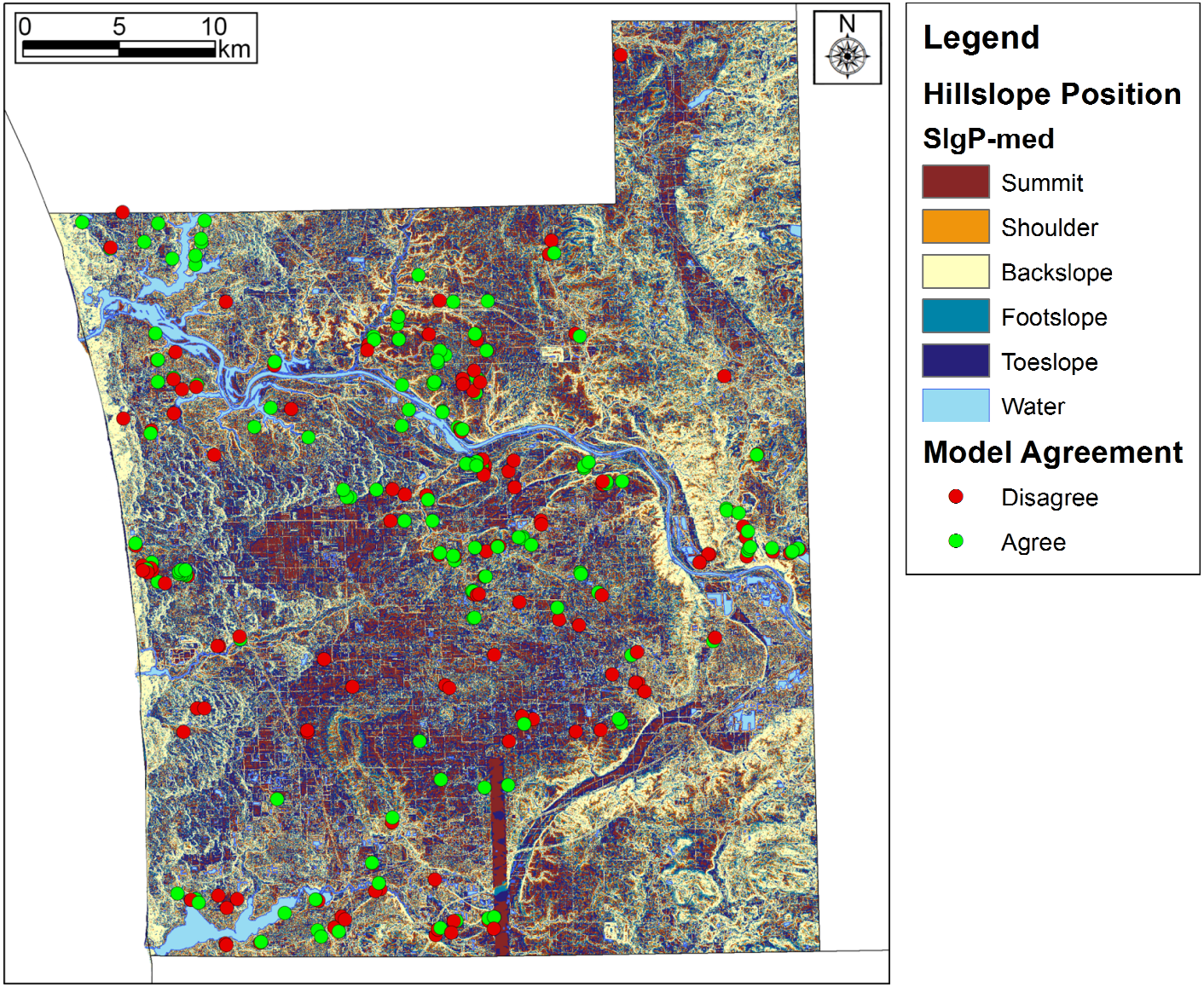


Figure 4.8. Digital hillslope position map of Ottawa County, Michigan with validation points showing agreement or disagreement with the predicted classification.

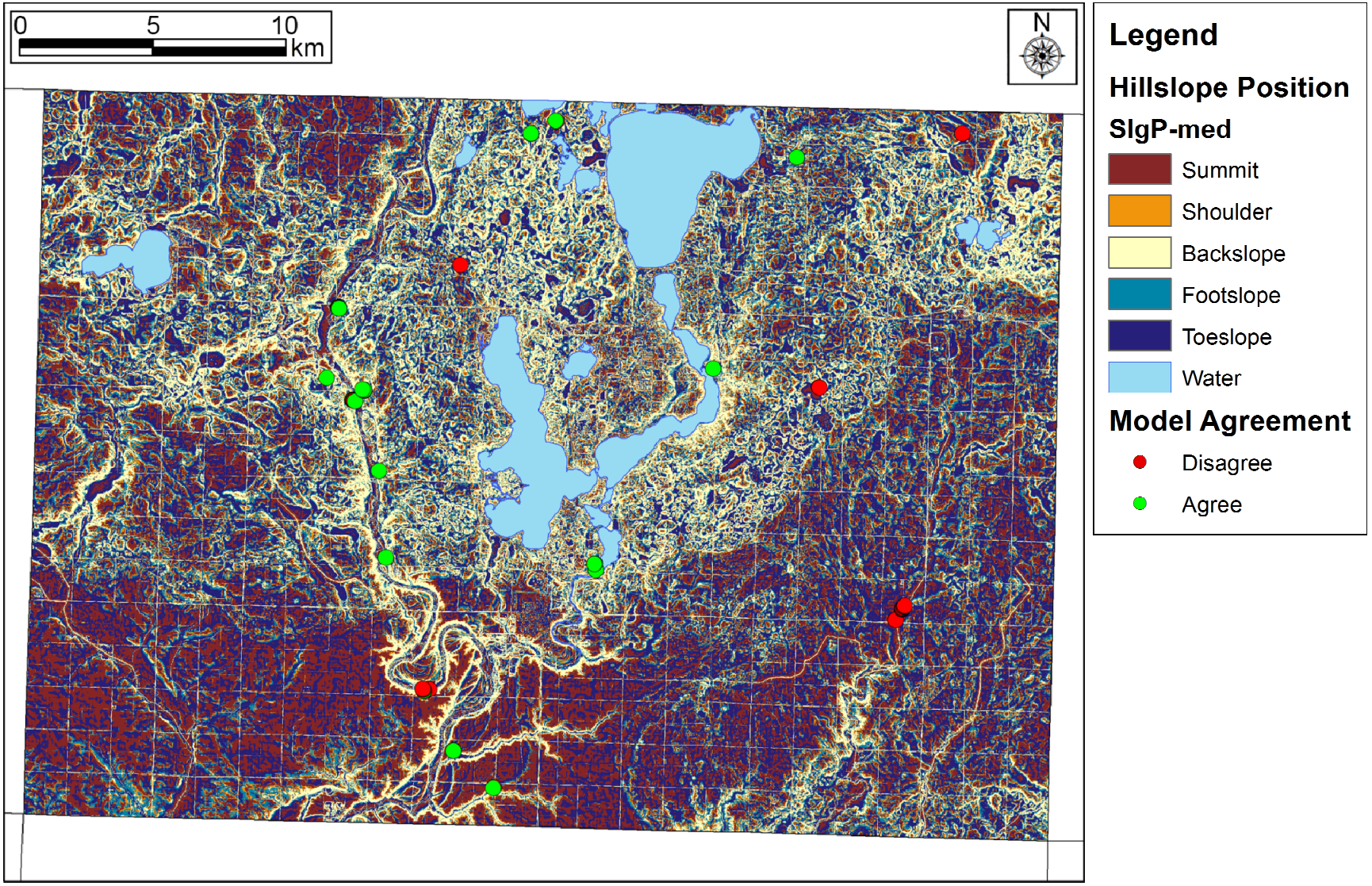


Figure 4.9. Digital hillslope position map of Dickinson County, Iowa with validation points showing agreement or disagreement with the predicted classification.

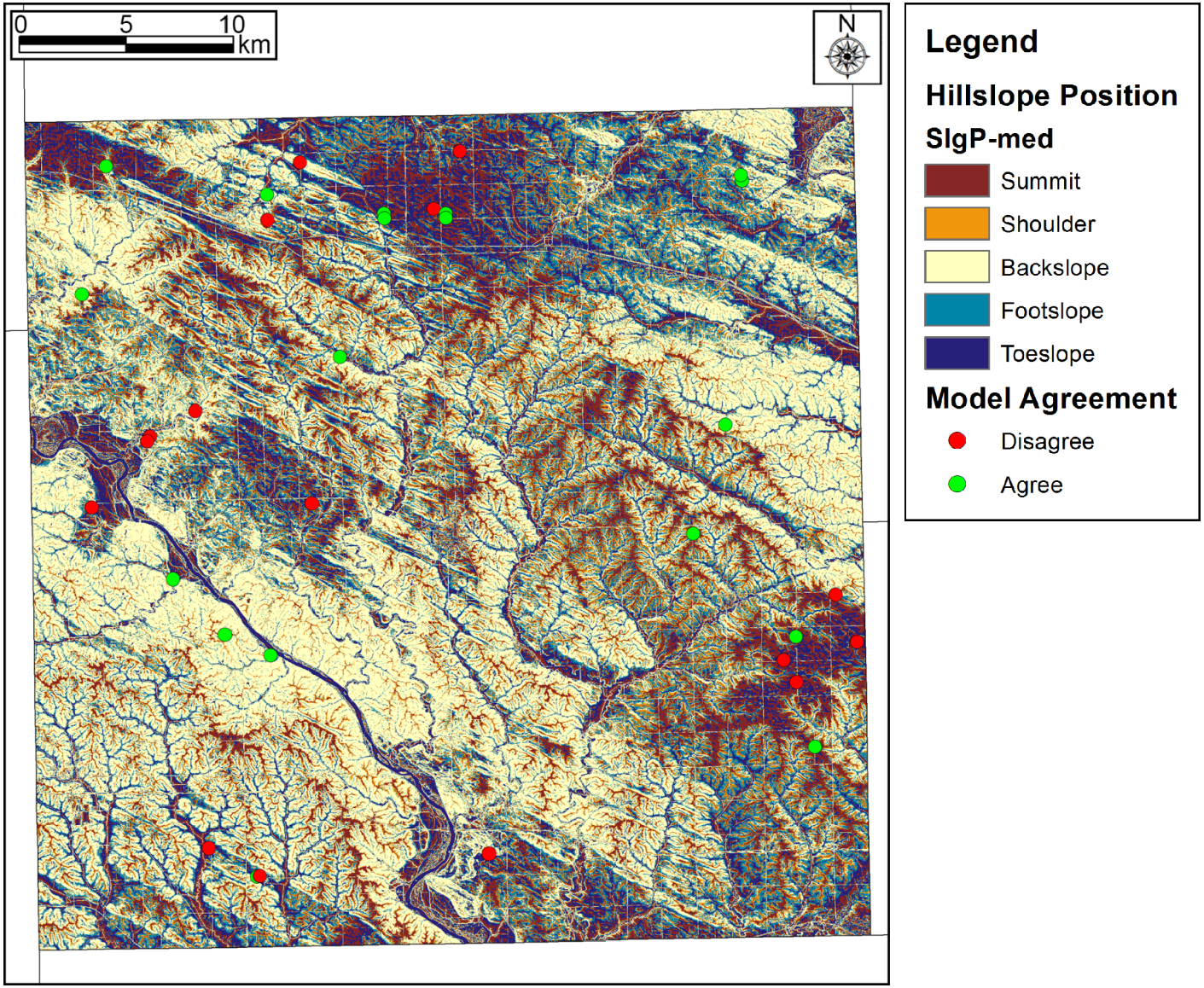


Figure 4.10. Digital hillslope position map of Cedar County, Iowa with validation points showing agreement or disagreement with the predicted classification.

The SlgP decision tree consistently had the highest prediction success rates, indicating that its logic best matches field scientists' mental model. This decision tree model first determines if a location has a low, medium, or high slope gradient. Medium slope gradients are then differentiated by slope shape as either convex or concave. Finally, flat areas are determined to have a high or low relative elevation. This is not necessarily every field scientists' thought process; many may determine hillslope position more by intuition than a stepwise decision process. Nonetheless, the SlgP decision tree, using classification breaks determined by the median mid-point method, was able to predict the field scientists' classification 52-54% of the time in three different landscapes, based on model parameters that only agreed with the field scientists' assessment of the landscape 69-79% of the time. This suggests that the largest issue in digitally replicating expert knowledge is not in the classification process, rather in the characterization of terrain properties.

3.4. Map Comparisons

Using the digital hillslope position classification with the most consistently high agreement with field assessment (SlgP-med) as values, zonal statistics were performed on the SSURGO polygons (Soil Survey Staff, 2013a) for each of the three study areas. Zones were defined by map unit symbol and the digitally classified hillslope positions were summarized by the percent of the Soil Survey map unit classified as the respective hillslope positions. Complete tables of the zonal statistics for all three counties are presented in Appendix B.

Before analyzing the quantitative, zonal statistics of soil map units, I visually compared the current Soil Survey map and the digital hillslope position map, for insight into the

relationships between them. Landscapes often do not match the idealized illustrations of hillslope position presented in textbooks and guidebooks. For this reason, the consistent application of quantitative hillslope classification rules results in a map that does not always have sequence patterns of hillslope position in their theoretical order. This pattern of non-sequential hillslope positions is observed in both the digital hillslope position classification and the Soil Survey map (Figure 4.11). Landscape mapping of hillslope positions focuses on classifying areas that meet functional definitions, in contrast to dividing hillslopes into all five components. For example, there may be no true summit positions on hilltops that do not include areas that are low enough in slope gradient or linear enough in profile curvature to function like a summit. Similarly, a slope that does not include an area that is sufficiently steep or linear in curvature to be a backslope will have shoulders directly adjacent to footslopes. Nonetheless, the SlgP-med hillslope position does produce a map with many similarities to current Soil Survey delineations (Figure 4.11). These two maps would not have been expected to agree exactly, because of the generalization and lower resolution elevation data used to create the 1:15,840 Soil Survey maps. The digital hillslope position model should produce a more accurate classification of the landscape by applying the soil scientists' logic consistently (without the need to generalize inclusions) and by utilizing higher resolution elevation data. Also, LiDAR-based, bare earth, digital elevation data includes subtleties in the landscape often obscured on aerial photographs by vegetative cover (i.e. forests) or undetectable by basic field observation. The LiDAR-based hillslope classification model includes all detected landscape subtleties that meet classification definitions for shifts in terrain character.

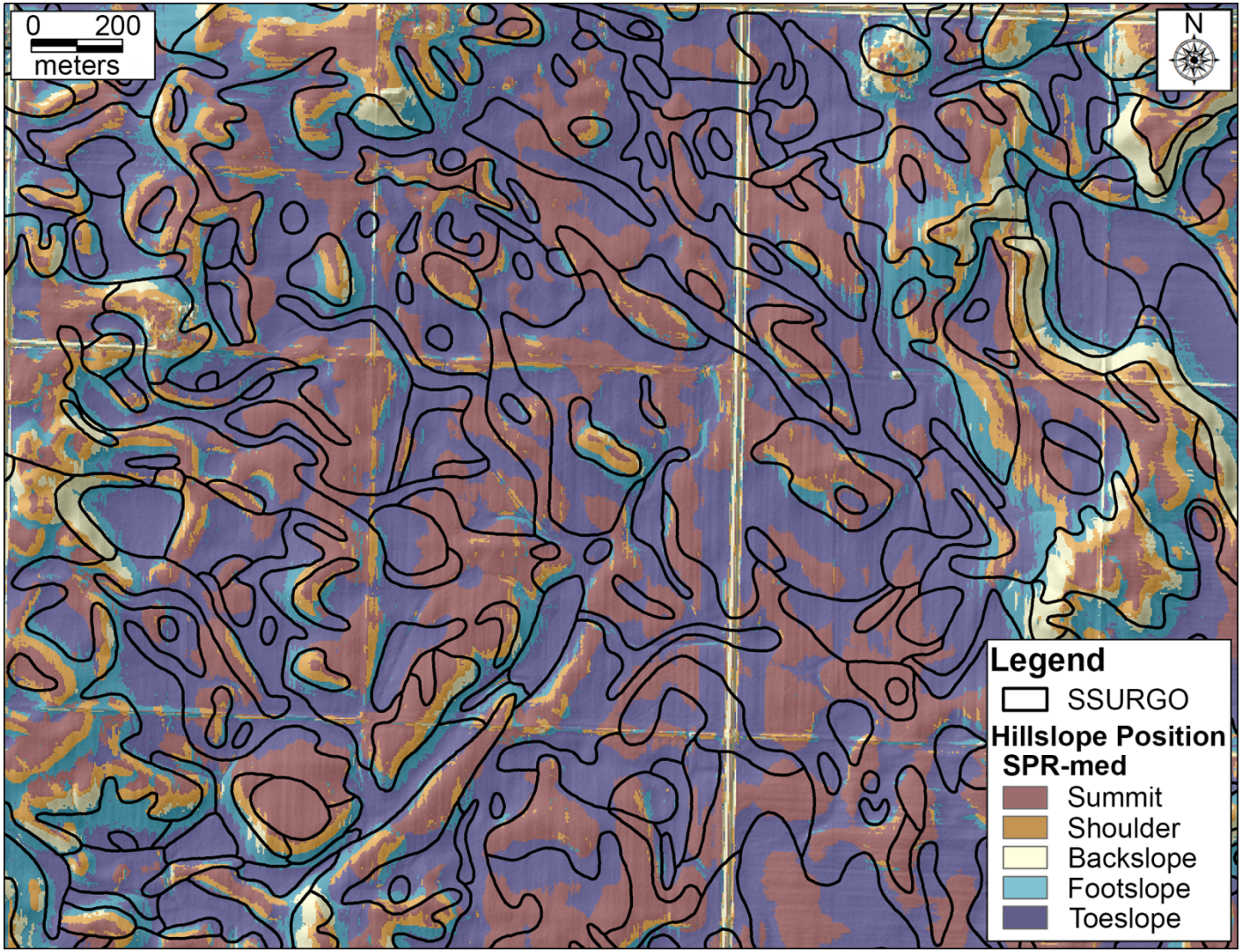


Figure 4.11. Example of SlgP-med hillslope position classification compared with current SSURGO delineations in Dickinson County, Iowa (overlain on a hillshade of the LiDAR elevation grid). Note the many areas that transition directly from summit to toeslope. These areas are also sensitive to sharp rises in elevation. For example, the raised road running north-south in the center of the map causes the adjacent flat areas to be digitally classified as toeslopes.

For the majority of Soil Survey map units, areas within delineations were classified with a hillslope position consistent with the slope shape described in the official soil series description (OSSD) (Soil Survey Staff, 2013b). For example, on the loess parent material in Cedar County, the summit-flat Muscatine soil series (Fine-silty, mixed, superactive, mesic Aquic Hapludolls) is predominantly mapped on digitally classified summit positions (Figure 4.12). The pattern of agreement continues through the summit-shoulder Downs (Fine-silty, mixed, superactive, mesic Mollic Hapludalfs) and Tama (Fine-silty, mixed, superactive, mesic Typic Argiudolls) soils. The Soil Survey's block diagram suggests that both Downs and Tama soils are mapped across summit, shoulder, and backslope positions. As the slope class increases for the respective soil map unit of these two soil series, the percentage of their area mapped as backslopes increases. The upland, depressional, Garwin soil series (Fine-silty, mixed, superactive, mesic Typic Endoaquolls) has the majority of its area mapped on toeslopes. The floodplain complex of Colo-Ely soil series (Fine-silty, mixed, superactive, mesic Cumulic Endoaquolls and Aquic Cumulic Hapludolls, respectively) is predominantly mapped on footslopes and toeslopes.

On the hummocky till plain of Dickinson County (Figure 4.13), where hillslope position units tend to be small in areal extent, a transition in hillslope position can be observed through a sequence of slope classes. The upland convex Clarion soil series (Fine-loamy, mixed, superactive, mesic Typic Hapludolls) progresses from being mostly mapped on summits to more so on shoulders to predominately on backslopes on the sequence of B, C, and D slope classes. In this landscape of numerous closed basins, the swales between convex hills have been filled in with local alluvium, resulting in only small areas meeting the digital definition of footslopes.

Concave and depressional soil series, such as Canisteo (Fine-loamy, mixed, superactive, calcareous, mesic Typic Endoaquolls), Harps (Fine-loamy, mixed, superactive, mesic Typic Calciaquolls) and Okoboji (Fine, smectitic, mesic Cumulic Vertic Endoaquolls), have some areas mapped on footslopes, but are predominately delineated on toeslope areas.

Where the soil description did not specify slope shape, such as for many of the soils in Ottawa County (Figure 4.14), a correspondence between hillslope position and drainage class (DC) can be used. The majority of the B slope class map unit for the somewhat poorly drained Kawkawlin soil (Fine, mixed, semiactive, frigid Aquic Glossudalfs) is mapped on footslopes, while the A slope class of the same soil is mostly mapped on toeslopes. The poorly drained Sims soil series (Fine, mixed, semiactive, nonacid, frigid Mollic Epiaquepts) is also predominately mapped on toeslopes. The Nester soil series (Fine, mixed, semiactive, frigid Oxyaquic Glossudalfs) is illustrated in the Soil Survey's block diagram as topographically diverse, which is also reflected in the distribution of hillslope positions within Nester map units. Nester soils are an example of a consociation that could benefit from disaggregation, based on hillslope position. Soils within the Nester delineations could be differentiated by three or more hillslope positions. A similar situation exists on the sandy parent materials of Ottawa County, where the Au Gres (Sandy, mixed, frigid Typic Endoaquods) and Deer Park (Mixed, frigid Spodic Udipsamments) soil series are also topographically diverse (Figure 4.15). The Au Gres soil series is differentiated by lower slope gradients and lower elevations. This distinction is also recognized in the hillslope position classification, with Au Gres soil map units primarily on toeslopes and Deer Park soil map units primarily on backslopes.

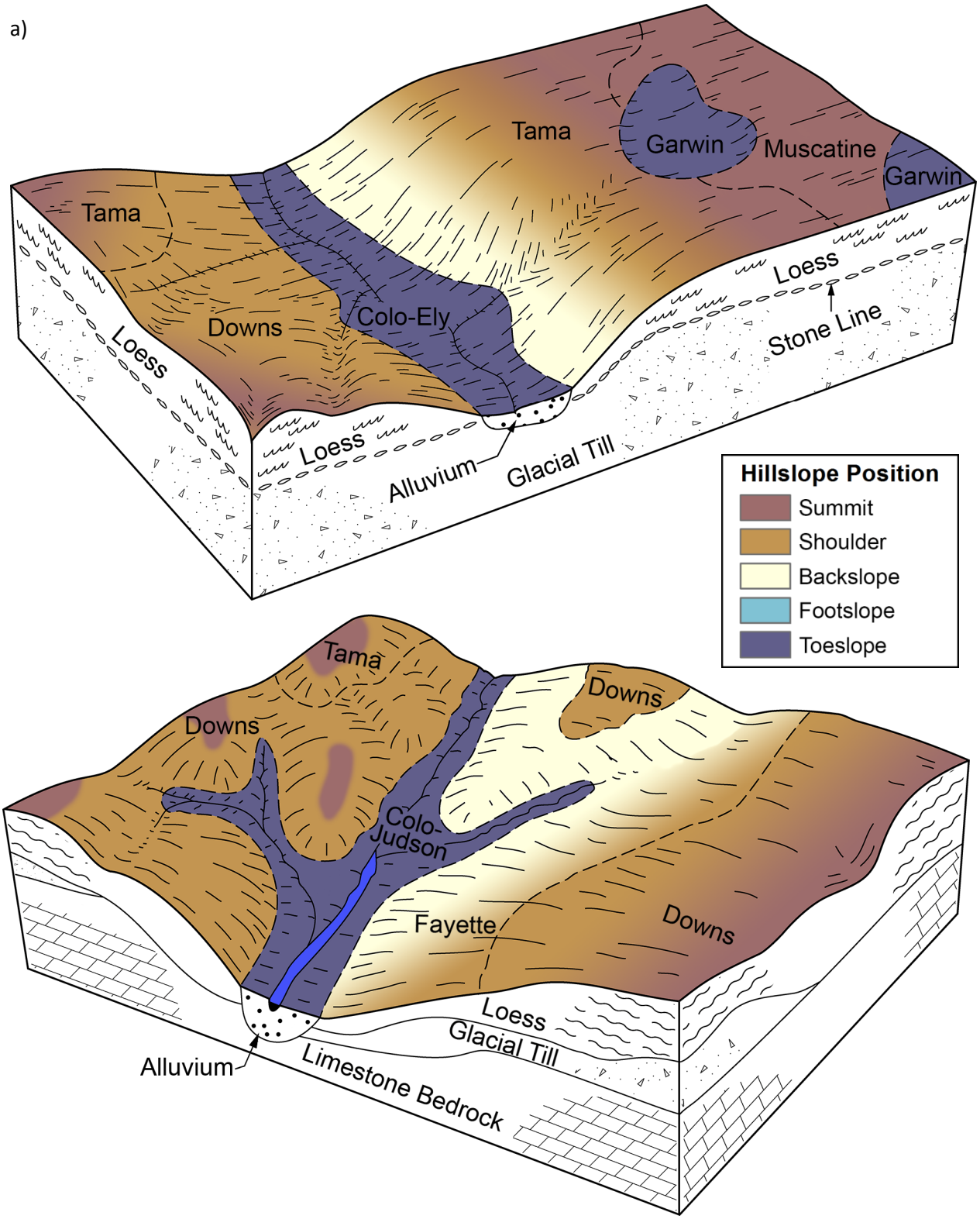


Figure 4.12. a) Block diagram of the Tama-Downs-Muscatine soil association from the NRCS Soil Survey Staff (2009). b) Zonal statistics of the SlgP-med hillslope position model by the SSURGO map units in Cedar County, Iowa.

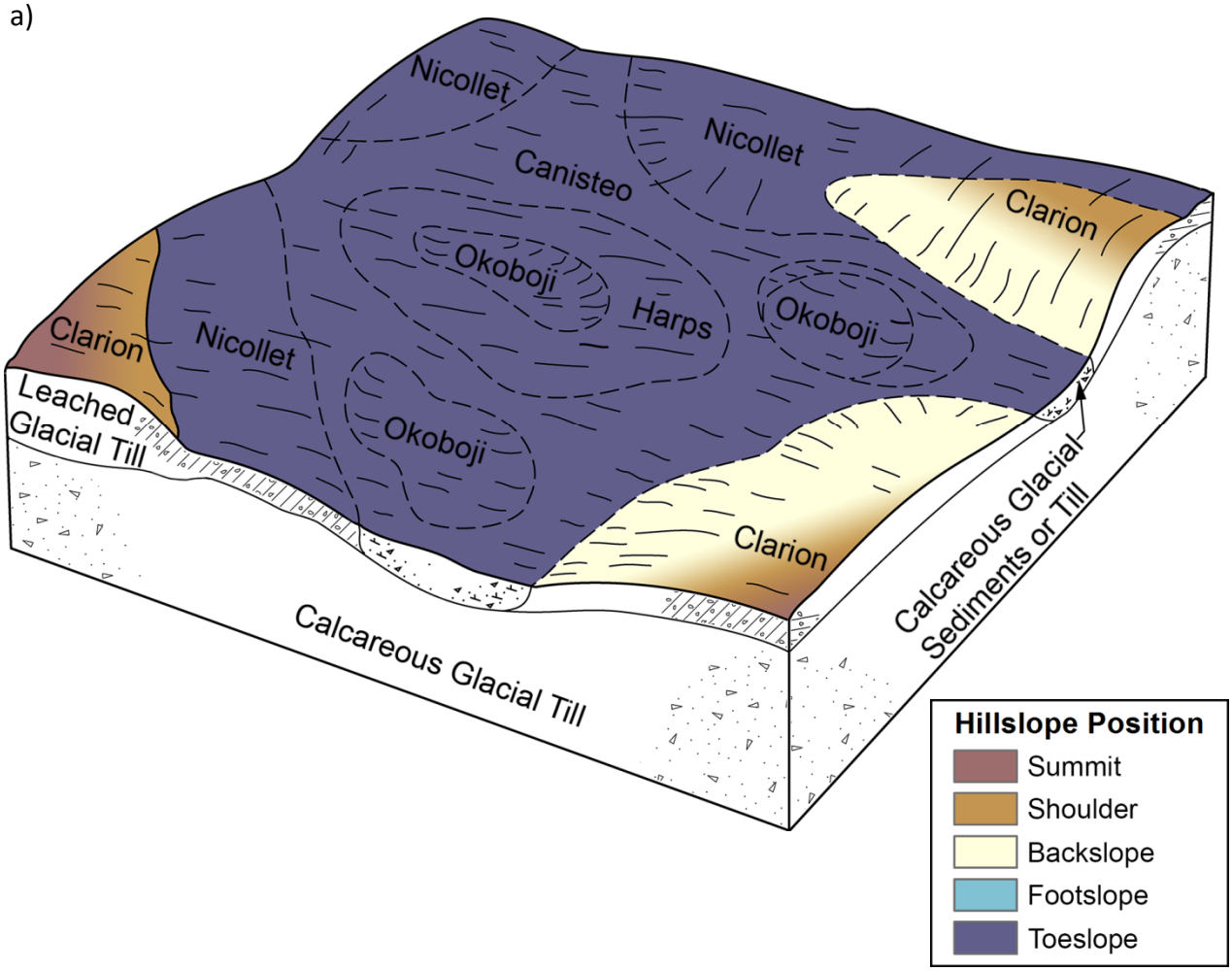
Figure 4.12. (cont'd)

b)

SSURGO				Hillslope Position Model					
Name	**Parent Material**	**Geographic Setting**	**DC***	**Max**	**su**	**sh**	**bs**	**fs**	**ts**
Colo-Ely	Alluvium	Floodplain	PD-SPD	fs	4%	3%	9%	44%	39%
Colo-Ely {B}	Alluvium	Floodplain	PD	ts	26%	3%	13%	19%	39%
Downs {B}	Loess	Summit-Shoulder	WD	sh	36%	41%	7%	14%	3%
Downs {C}	Loess	Summit-Shoulder	WD	sh	6%	36%	21%	33%	4%
Downs {D}	Loess	Summit-Shoulder	WD	bs	1%	14%	45%	36%	3%
Ely	Loess	Transitional Swale	SPD	fs	6%	4%	4%	53%	33%
Fayette {B}	Loess	Interfluves-Sideslopes	WD	sh	35%	42%	12%	10%	2%
Fayette {C}	Loess	Interfluves-Sideslopes	WD	bs	7%	41%	39%	12%	1%
Fayette {D-G}	Loess	Interfluves-Sideslopes	WD	bs	1%	10%	71%	16%	2%
Garwin	Loess	Summit-Flat	PD	ts	35%	2%	2%	10%	51%
Muscatine	Loess	Summit-Flat	SPD	su	72%	6%	2%	7%	14%
Muscatine {B}	Loess	Summit-Flat	SPD	su	37%	10%	2%	30%	21%
Tama	Loess	Summit-Shoulder	WD	su	67%	13%	1%	10%	10%
Tama {B}	Loess	Summit-Shoulder	WD	su	42%	30%	3%	20%	5%
Tama {C}	Loess	Summit-Shoulder	WD	fs	5%	30%	10%	48%	6%
Tama {D}	Loess	Summit-Shoulder	WD	fs	1%	15%	34%	46%	4%
Judson {B}	Colluvium	Transitional Swale	WD	fs	6%	5%	9%	57%	23%

*DC = drainage class

a)



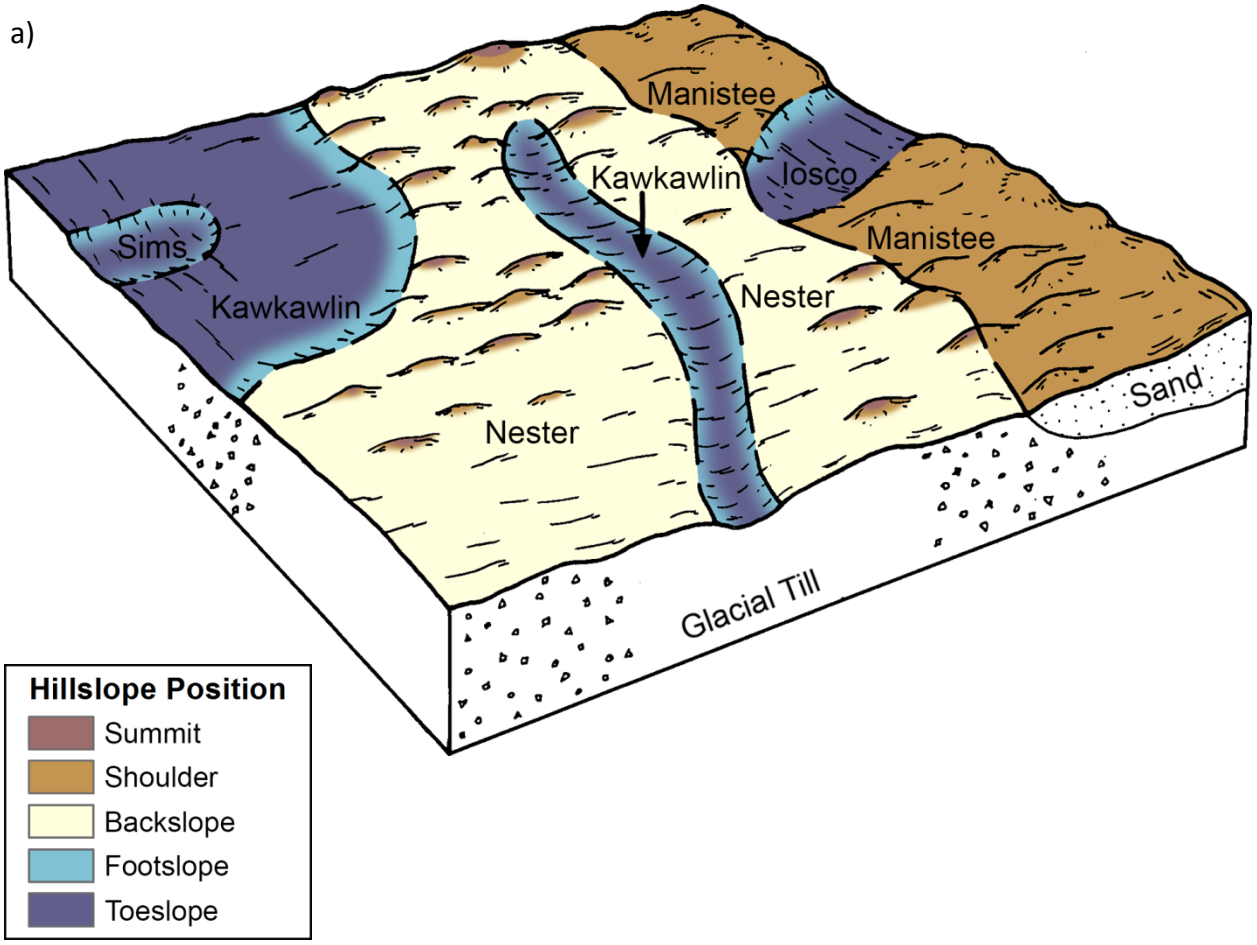
b)

SSURGO				Hillslope Position Model					
Name	**Parent Material**	**Geographic Setting**	**DC***	**Max**	**su**	**sh**	**bs**	**fs**	**ts**
Canisteo	Dows Till Alluvium	Upland Concave	PD-VPD	ts	13%	3%	7%	16%	60%
Clarion {B}	Dows Till	Upland Convex	MWD	su	27%	25%	19%	21%	9%
Clarion {C}	Dows Till	Upland Convex	MWD	bs	8%	19%	55%	15%	3%
Clarion {D}	Dows Till	Upland Convex	MWD	bs	3%	8%	82%	6%	1%
Harps	Dows Till Alluvium	Upland Depression	PD	ts	22%	6%	3%	13%	56%
Nicollet	Dows Till	Upland Flat	SPD	ts	25%	10%	10%	24%	30%
Okoboji	Dows Till Alluvium	Upland Depression	VPD	ts	5%	2%	5%	13%	76%

*DC = drainage class

Figure 4.13. a) Block diagram of the Canisteo-Clarion-Nicollet soil association from the NRCS Soil Survey Staff (2000). b) Zonal statistics of the SlgP-med hillslope position model by SSURGO map units of this soil association in Dickinson County, Iowa.

a)



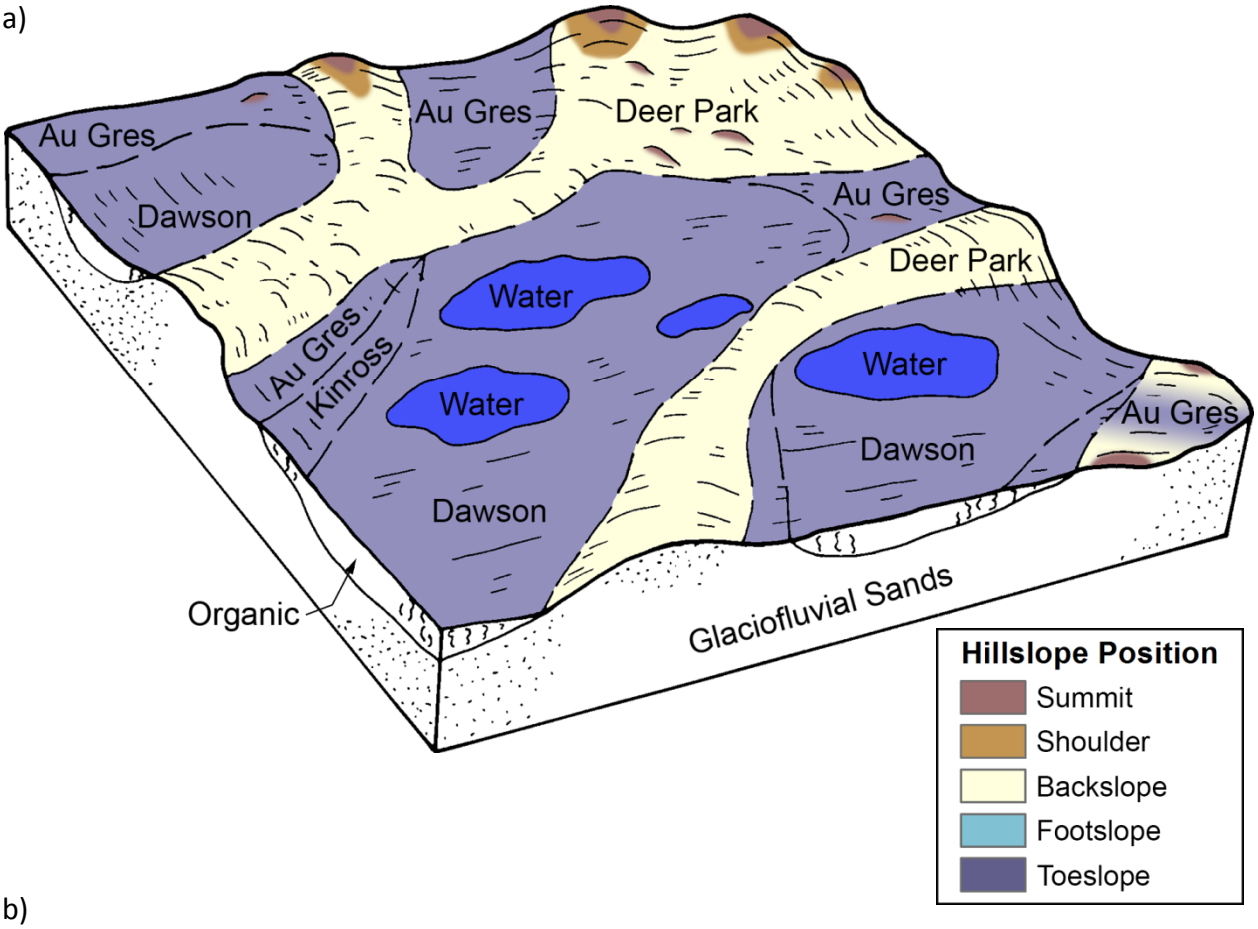
b)

SSURGO				Hillslope Position Model					
Name	**Parent Material**	**Geographic Setting**	**DC***	**Max**	**su**	**sh**	**bs**	**fs**	**ts**
Iosco {A}	Outwash	Plain	SPD	su	29%	15%	15%	18%	24%
Kawkawlin {A}	Till	Plain	SPD	ts	24%	12%	13%	20%	30%
Kawkawlin {B}	Till	Plain	SPD	fs	22%	15%	17%	23%	23%
Nester {B}	Till	Plain	WD-MWD	bs	18%	23%	31%	20%	8%
Nester {C}	Till	Plain	WD-MWD	bs	6%	14%	61%	15%	4%
Nester {D-F}	Till	Plain	WD-MWD	bs	3%	7%	81%	6%	3%
Sims	Till	Plain	PD	ts	13%	8%	18%	24%	36%

*DC = drainage class

Figure 4.14. a) Block diagram of the Nester-Kawkawlin-Manistee soil association from the NRCS Soil Survey Staff (1985). b) Zonal statistics of the SlgP-med hillslope position model by SSURGO map units of this soil association in Ottawa County, Michigan. The sandy Manistee soil series is not currently mapped in Ottawa County. For a soil association on sand parent materials, see Figure 4.15.

a)



b)

SSURGO				Hillslope Position Model					
Name	**Parent Material**	**Geographic Setting**	**DC***	**Max**	**su**	**sh**	**bs**	**fs**	**ts**
Adrian muck	Organic	Depression	PD	ts	8%	8%	23%	24%	36%
Adrian-Houghton mucks	Organic	Depression	VPD	ts	11%	9%	23%	24%	34%
Au Gres {B}	Outwash	Complexes	SPD	ts	26%	12%	14%	17%	31%
Au Gres-Saugatuck {B}	Outwash	Complexes	SPD	ts	15%	10%	16%	21%	38%
Deer Park {B}	Sand	Dunes	WD	bs	11%	15%	44%	17%	13%
Deer Park {D}	Sand	Dunes	WD	bs	7%	12%	54%	15%	12%
Edwards	Organic	Depression	VPD	ts	13%	9%	22%	20%	36%
Linwood	Organic	Depression	VPD	ts	6%	7%	22%	24%	41%

*DC = drainage class

Figure 4.15. a) Block diagram of the Deer Park-Dawson-Au Gres soil association from the Soil Survey Staff (1992). b) Zonal statistics of the SlgP-med hillslope position model by SSURGO map units of this soil association in Ottawa County, Michigan. The organic Dawson and Kinross soils are not currently mapped in Ottawa County. Instead, organic soils are classified as Adrian, Houghton, Edwards, or Linwood soil series (Sandy or sandy-skeletal, mixed, euic, mesic Terric Haplosaprists; Euic, mesic Typic Haplosaprists; Marly, euic, mesic Limnic Haplosaprist; Loamy, mixed, euic, mesic Terric Haplosaprists; respectively).

Map units with large proportions of their area split between digital hillslope positions are likely to contain many inclusions of other soil series. The model can determine that these areas are different, but if they are not mapped differently on the soil map it is because the geographer (1) was unable to observe the differences in the field or on the aerial photograph, (2) was unable to map these areas out because of minimum mapping area issues, or (3) thought that the differences were so small as to not affect classification, use or management.

The most common situation for soil map units to be split between areas of hillslope position occurs on flat landscapes such as glaciolacustrine plains and floodplains. As described above, the digital hillslope position classification recognizes most flat areas as either summits or toeslopes. A slight rise in elevation in an area like a floodplain will be classified by the model as a summit. If the digitally generated hillslope position classification is being used as a base map, the soil geographer can decide if the differences in soil properties for these slight changes in relative elevation are significant in the context of the soil map's purpose (3 above). Areas of slightly higher elevation on a floodplain may have slightly deeper water tables. Also, those small rises will be slightly less likely to flood and be the first to dry out after a flood. In the context of agricultural production, the differences between these areas may not be important. However, for estimating the amount of carbon stored in the soil landscape or determining the spatial distribution of wetland types (Miller et al., 2009), these slight changes in elevation could add useful detail. Use of the hillslope position classification model to identify such topographically small areas has great potential to improve existing soil maps, especially as regards disaggregation. Specific examples for where hillslope position provides differentiating criteria for disaggregating soil delineations are provided below.

3.4.1. Opportunity for Disaggregation of Existing Soil Map Units

Soil series mapped in consociations, but described as occurring on a mixture of hillslope positions, are excellent examples of map units that could be easily disaggregated by digital hillslope position classification. For example, the Fayette (Fine-silty, mixed, superactive, mesic Typic Hapludalfs), Basset (Fine-loamy, mixed, superactive, mesic Mollic Hapludalfs), and Kenyon (Fine-loamy, mixed, superactive, mesic Typic Hapludolls) soil series in Cedar County are all described by the OSSD (Soil Survey Staff, 2013b) as occurring on interfluves and side-slopes. Figure 4.16 demonstrates how the digital hillslope position classification is able to identify summits and shoulders within Fayette delineations. These summits and shoulders meet the geographic setting definition for the Downs soil series. In fact, for part of an interfluve shown in Figure 4.16 an area of Downs soil is delineated on the summit-shoulder within a Fayette delineation, while similar locations in the vicinity are not.

In Dickinson County, probably because of map scale limitations, obvious map unit inclusions have been identified by the Soil Survey as point locations. The identified inclusions for depressional areas often exist in close proximity to areas classified as isolated toeslopes (Figure 4.17). The offset between the inclusion points and the digitally identified areas of isolated toeslopes is likely due to the resolution limitation of the base map on which the original inclusion points were drawn and the orthorectification process required to digitize the paper soil map. This positional difference illustrates the advantage of utilizing the more spatially accurate LiDAR data.

Soil series like Nester, which is illustrated in Figure 4.14 as varying in relief, are likely to contain variations in soil properties due to the effect of topography on soil formation. Areas like these are often not mapped in great detail due to the combination of mapping difficulty and low value of the extra mapping effort. Modern interests in environmental and ecological services of soils increase the importance of mapping these areas, but do not make them easier to map. Figure 4.18 demonstrates the classification model's ability to disaggregate a delineation of the Nester soil series by hillslope position.

a)

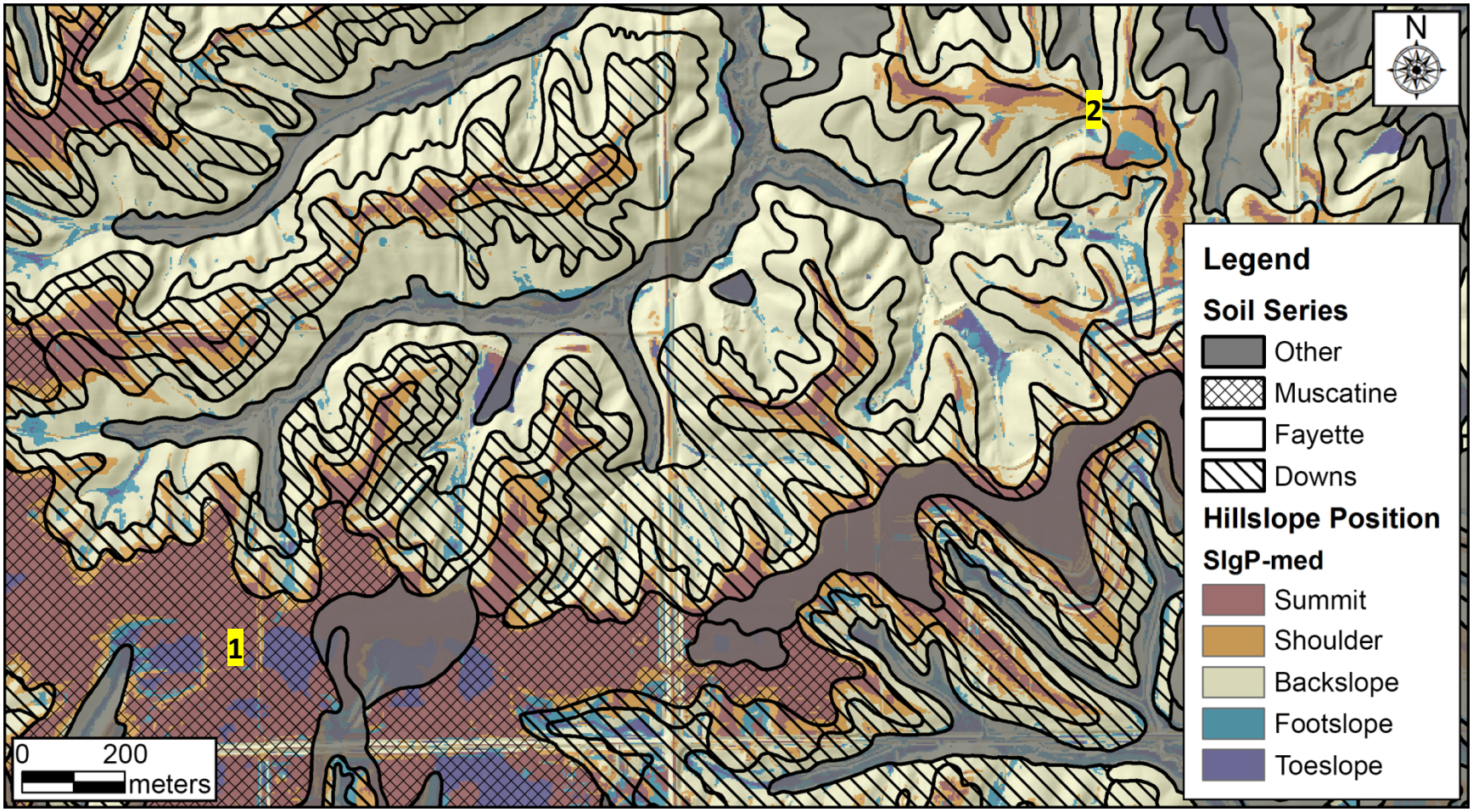
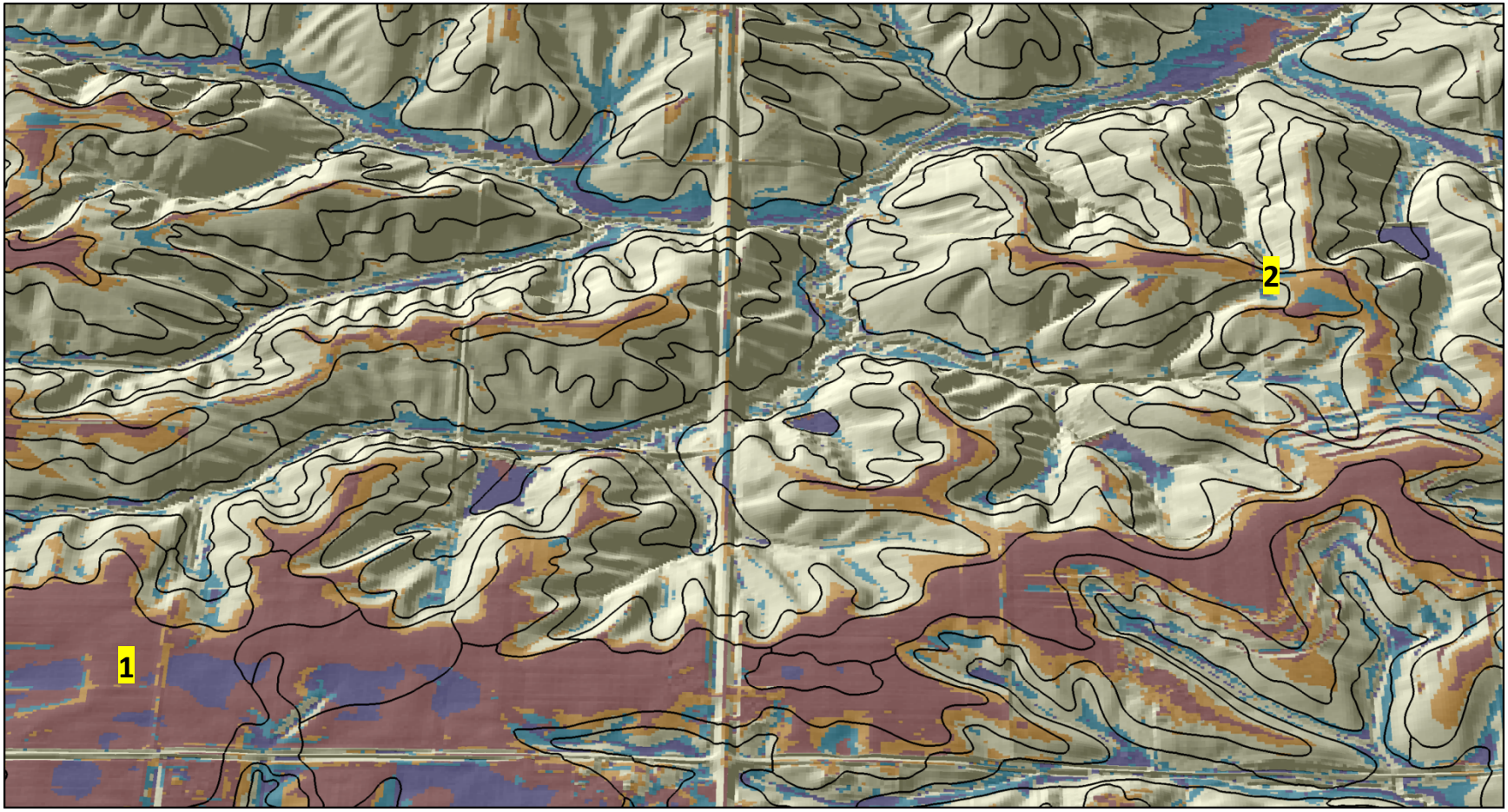


Figure 4.16. Examples of disaggregation opportunities in Cedar County, shown in a) plan view, and b) perspective view (relief exaggerated 3x). Numbers indicate matching points of reference. 1) Depressions identified by the model, potentially Garwin soil series, within Muscatine soil series delineations. 2) The Fayette soil series is described as occurring on interfluves and side-slopes. However, summits on the interfluves match the geographic setting for the Downs soil series.

Figure 4.16. (cont'd)

b)



a)

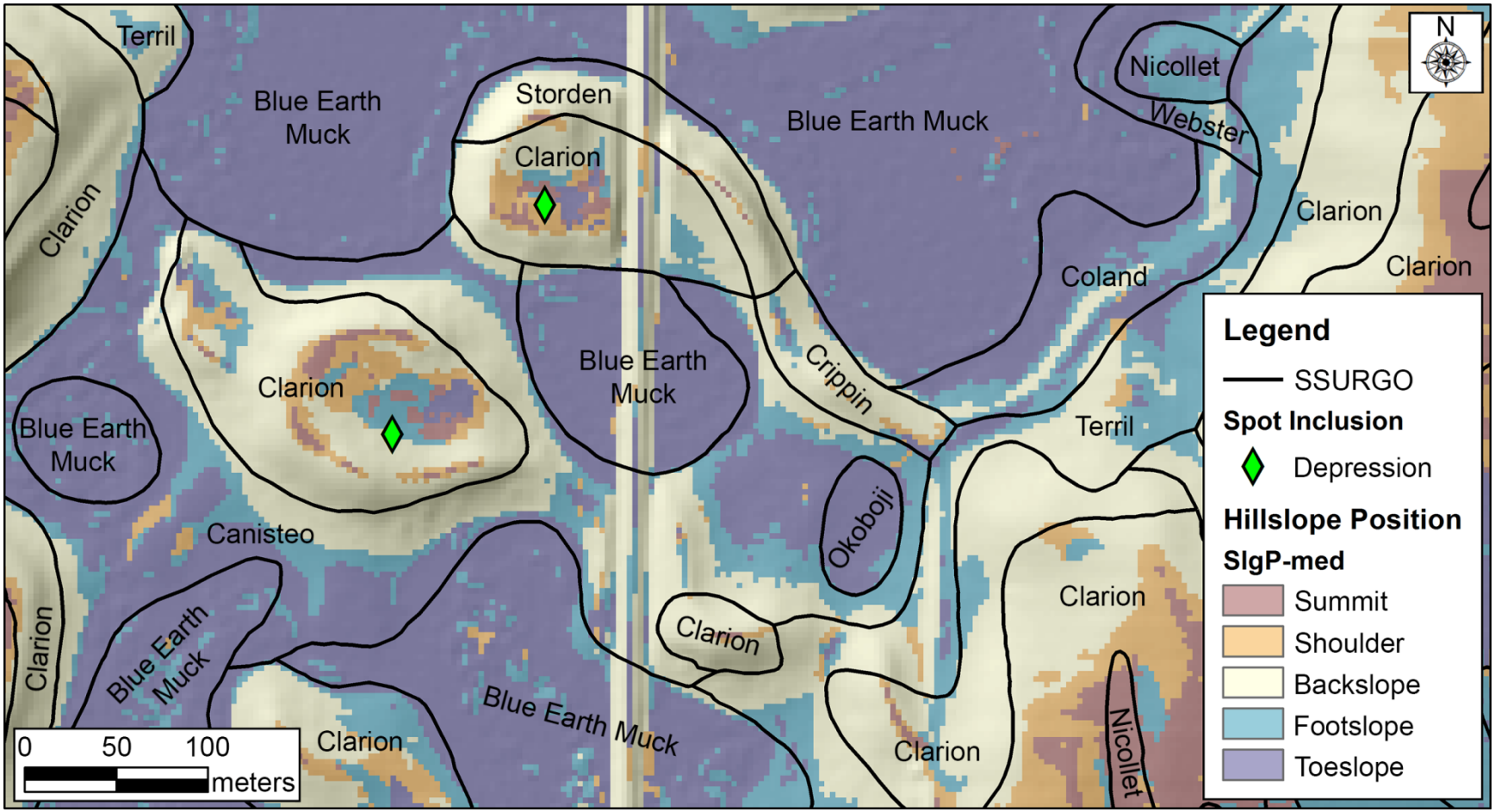
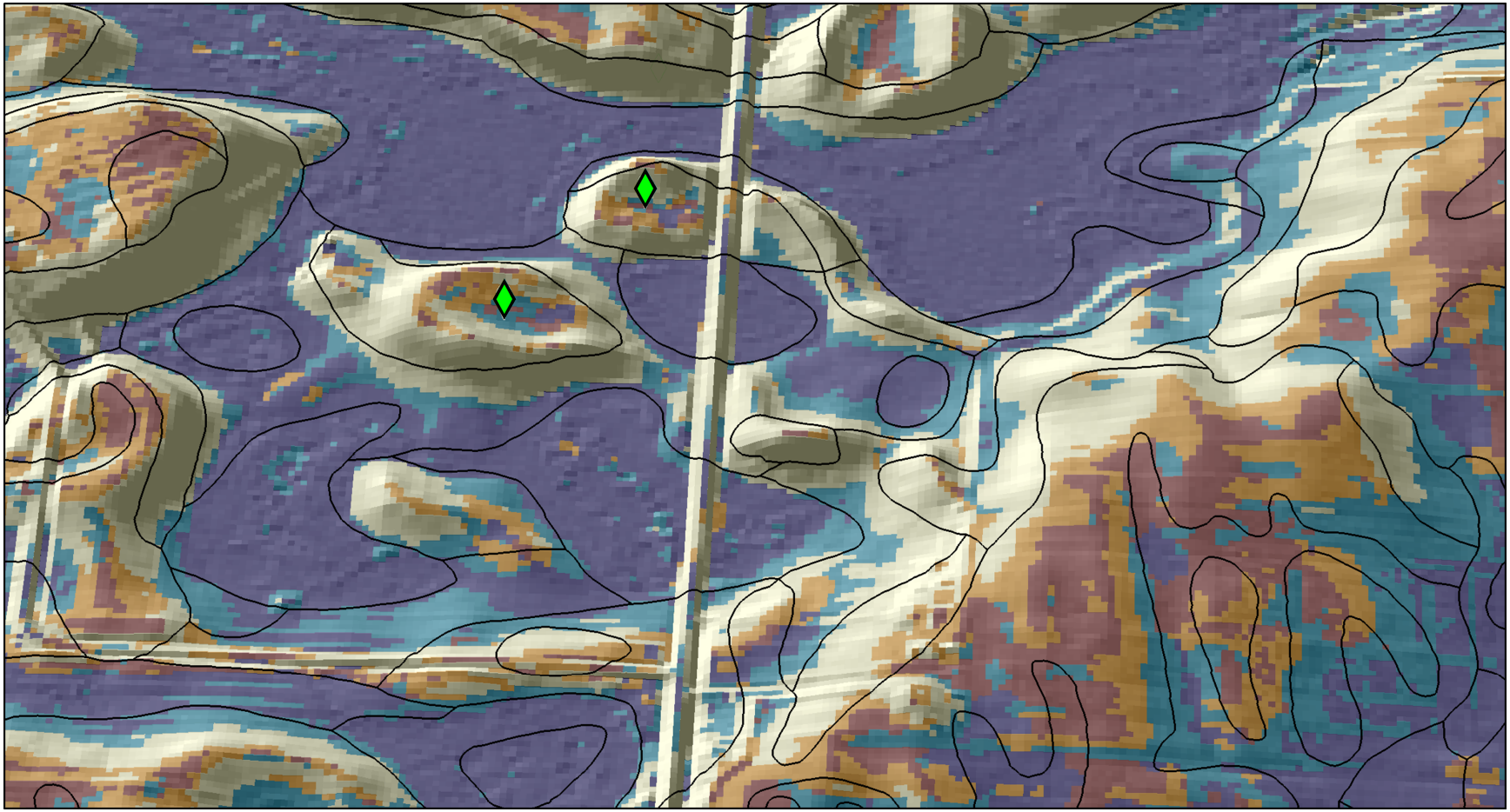


Figure 4.17. Two depression inclusions identified by Soil Survey Staff located within delineations of the convex Clarion map unit in Dickinson County. Note the proximity of the inclusion points to isolated areas of toeslopes. In a) plan view, and b) perspective view (relief exaggerated 3x).

Figure 4.17. (cont'd)

b)



a)

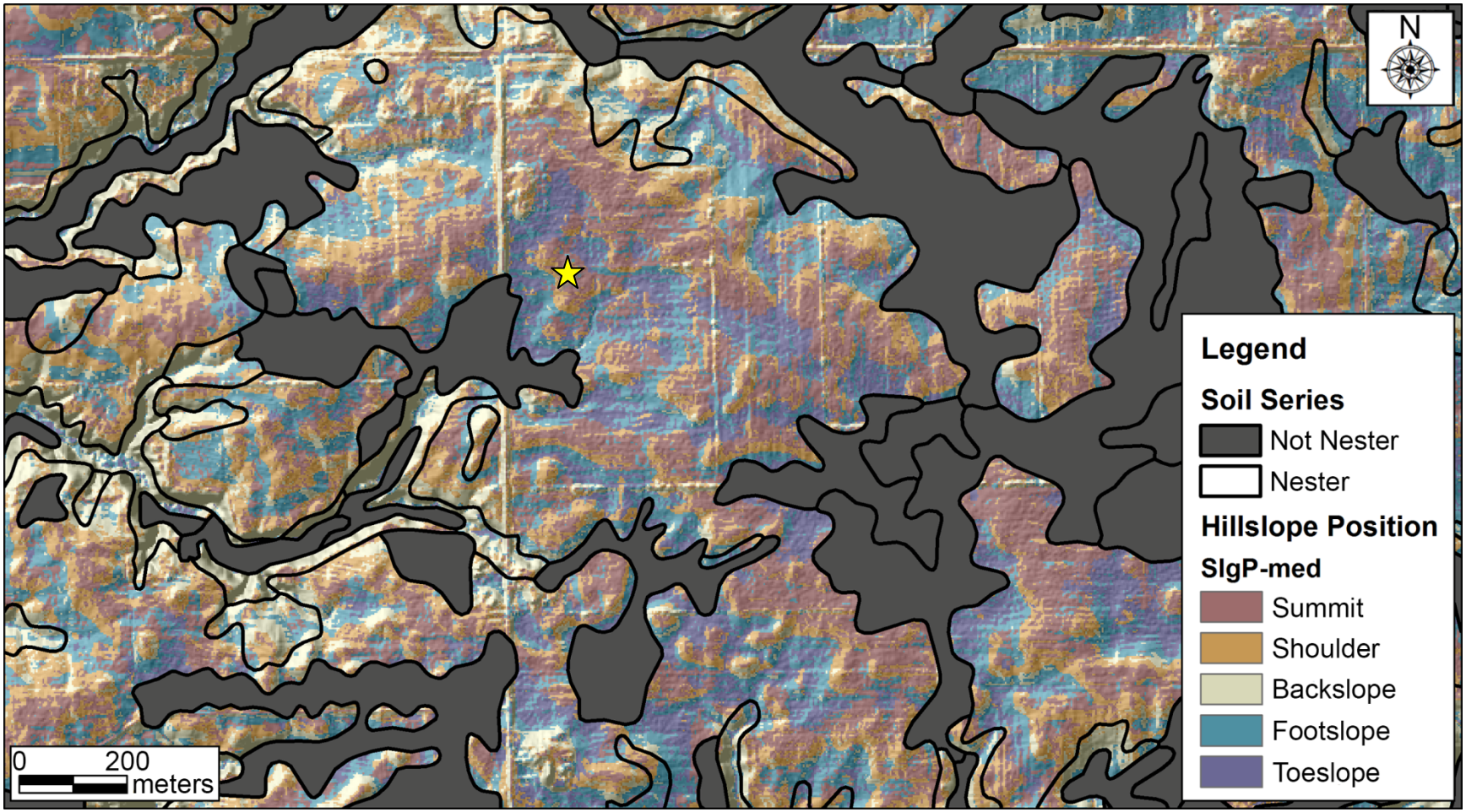
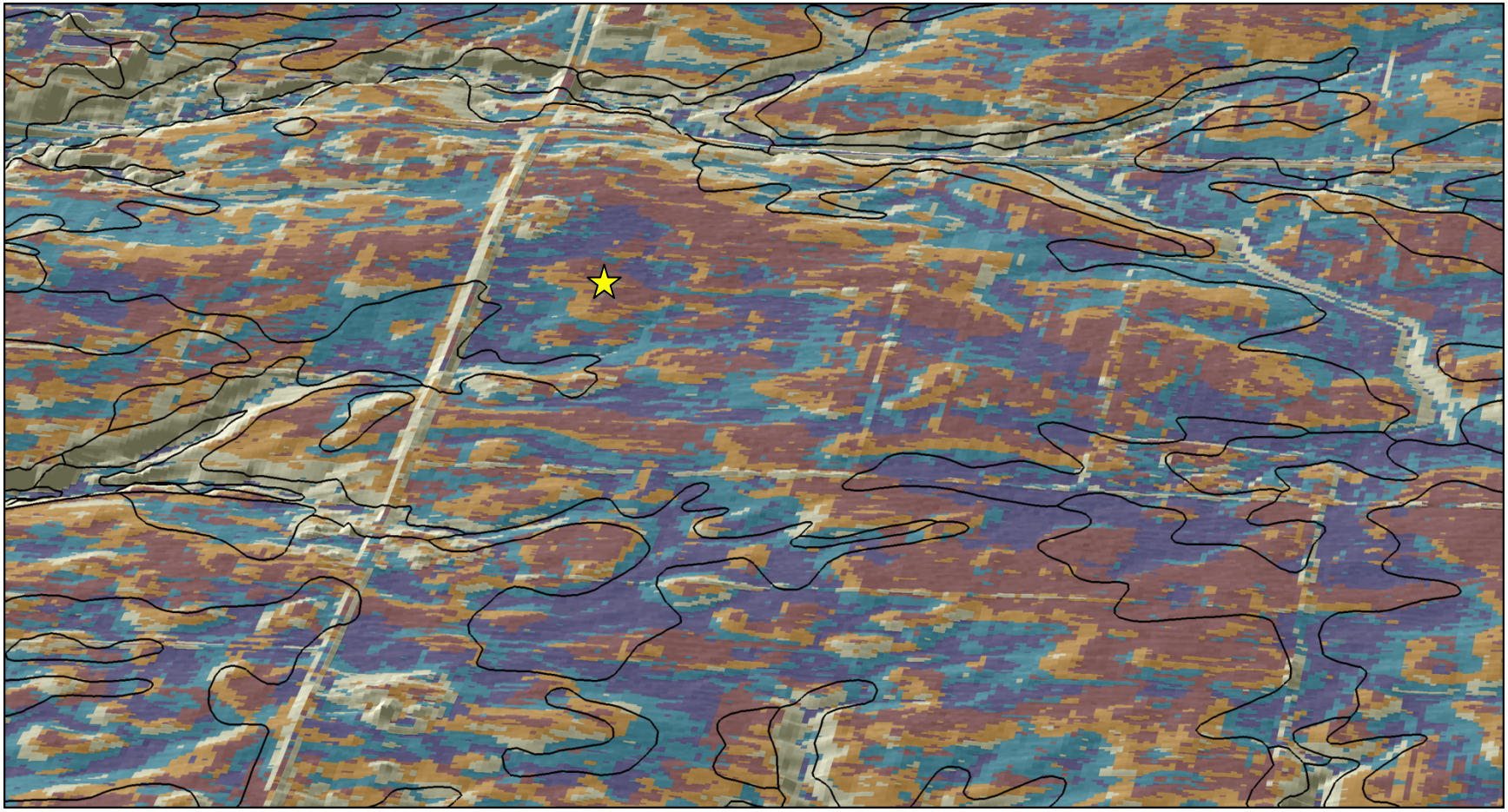


Figure 4.18. Nester soil series in Ottawa County, which is illustrated in the Soil Survey block diagram as varying in topography (Figure 4.14). Digital classification of hillslope position efficiently differentiates slope elements within this Nester soil delineation. In a) plan view, and b) perspective view (relief exaggerated 3x). Star indicates a matching point of reference.

Figure 4.18. (cont'd)

b)



3.5. A Quantified Definition for Hillslope Position

Based on the consistent performance of the SlgP-med model for predicting field assessment of hillslope position, an expert-based definition for digital classification was next established. The median mid-point calibrated breaks for profile curvature (convex-concave = 0.00008 m^{-1}) and relative elevation (low-high = 0.1 m) were practically zero. Simply setting these breaks as zero would be both consistent with model tests and more definitionally satisfactory. Therefore, I recommend the following classification structure for digitally determining hillslope position:

1) Slope gradient: < 1.4° is low, 1.4° to 2.9° is medium, > 2.9° is high
    a. If slope gradient is high, then position is backslope
    b. If slope gradient is medium, then:
        i. Profile curvature: > 0 m^{-1} is convex (as defined by Wood, 1996)
            1. If profile curvature is convex, then position is shoulder
            2. If profile curvature is not convex, then position is footslope
    c. If slope gradient is low, then:
        i. Relative elevation: > 0 m is high (as defined in Chapter 3)
            1. If relative elevation is high, then position is summit
            2. If relative elevation is not high, then position is toeslope

The calibrated breaks for slope gradient are low, as compared to slope gradients typically observed in the field. In Chapter 3, I identified the smallest possible digital analysis scale as the closest match to field observations of slope gradient. Therefore, the optimal digital

analysis scale for slope gradient may be smaller than 9 m. Because slope gradient values become smaller with greater generalization, these calibration breaks may be a compensation for that effect. If finer resolution elevation grids become practical for digital terrain analysis, the slope gradient breaks may need to be adjusted accordingly. However, the classification break at 3° corresponds with a well established threshold for slope processes (Pennock et al., 1987). For example, Govers (1985) observed slope gradients below 3° did not have sufficient erosive energy to form rills.

3.5.1. Applicability beyond Discrete Boundaries

Even though this study has focused on the discrete classification of hillslope position, the calibrated characterization of hillslope position could also be easily applied as a fuzzy membership classification. The consistent ability of the SlgP-med model to correctly classify hillslope position suggests that the group median for terrain parameters is a better choice to represent the central concept (particularly for fuzzy classification applications) than the mean. The comparable results of mean mid-point (assumed identical distribution spread) and CI (distribution spread based on standard deviation) calibration methods suggest that assuming similar variability for terrain parameter groups is an acceptable assumption. Utilizing a fuzzy classification of hillslope position or its component variables can be used as parameters in other digital soil models. The parameterization of hillslope position presented in this dissertation has the potential to better integrate expert knowledge into digital soil models, including representations of a continuous soil landscape.

4. Conclusions

The purpose of this study was to calibrate a landscape classification model that could predict hillslope positions identified by soil scientists in the field. Parameters to the hillslope position classification model agreed with field assessment 69% and 79% of the time for profile curvature and relative elevation, respectively. Therefore, model predictions of hillslope position are likely to agree with field assessment at lower rates. Despite the limitation of field to digital assessment agreement for parameters, model prediction of hillslope position ranged from 11% to 59% agreement. The hillslope position model, utilizing a slope gradient, then profile curvature and relative elevation decision tree hierarchy, consistently provided the best agreement with soil scientists' field assessment. Given the subjectivity of human assessment, the level of agreement between the best performing model and field assessment suggests that digital classification of hillslope position can be similar to field determination of hillslope position.

The classification breaks calibrated by the median mid-points of the assessment groups in Ottawa County, Michigan continued to perform equally well in two different Iowa landscapes suggesting that the SlgP-med hillslope position model can be used in a variety of landscapes, without recalibration. The consistently strong performance of the calibration group median also suggests that it is the more representative value for defining the central concept for fuzzy membership approaches.

Many current digital soil mapping models attempt to capture the complex, contextual nature of expert knowledge summarily by zonal statistics or require field experts to interpret

digital parameters. In contrast, the hillslope position classification model focuses on a single delineation criteria and is calibrated to the field experts' interpretations. The resulting classification model provides a consistent delineation of common soil map unit boundaries that is not limited to small study areas.

The digital classification of hillslope position improves upon human assessment by applying rules of classification consistently across the landscape. This trait reduces the variability of classification due to human error and judgment. Consistent application of classification rules also identifies areas that meet the criteria for different hillslope elements, but were previously unmapped due to cartographic, base map or resource limitations. Consistent classification of all landscape locations, regardless of map unit extent, presents the opportunity to disaggregate map units. This type of disaggregation would be best applied to topographically complex landscapes where two or three soil series vary predictably as a function of hillslope position and/or drainage class; the model would be much more able to delineate small map units amidst what may have been originally mapped as a complex or a consociation with inclusions. The map produced by the hillslope position classification model provides the appropriate base data for increasing the resolution of soil maps in a documented, repeatable and cost-effective manner.

APPENDIX

FULL ANALYSIS TABLES OF HILLSLOPE POSITION CLASSIFICATION BY SOIL MAP UNITS

Table 4.11. Zonal statistics of the SlgP-med hillslope position model by SSURGO map units in Ottawa County, Michigan.

SSURGO			Hillslope Position Model					
Map Unit	**Geographic Setting**	**DC**	**Max**	**su**	**sh**	**bs**	**fs**	**ts**
Washtenaw	Depression	PD	bs	4%	7%	35%	30%	25%
Algansee	Floodplain	SPD	bs	8%	13%	47%	18%	15%
Ceresco	Floodplain	SPD	bs	9%	7%	41%	23%	21%
Cohoctah	Floodplain	VPD	bs	5%	7%	43%	24%	21%
Glendora	Floodplain	PD-VPD	bs	7%	8%	32%	25%	27%
Shoals	Floodplain	SPD	bs	10%	9%	38%	21%	23%
Sloan	Floodplain	PD	bs	7%	8%	37%	22%	25%
Wallkill	Floodplain	PD	ts	19%	6%	18%	18%	40%
Warners	Floodplain	VPD	ts	12%	10%	26%	19%	32%
Allendale {A}	Plain	SPD	su	27%	15%	16%	19%	23%
Bowers {A}	Plain	SPD	ts	27%	10%	15%	16%	31%
Bowers {B}	Plain	SPD	su	40%	17%	16%	13%	14%
Hettinger	Plain	PD	ts	15%	9%	20%	22%	34%
Pinconning	Plain	PD	ts	18%	10%	17%	21%	34%
Pinconning-Breckenridge	Plain	PD	ts	28%	7%	8%	14%	43%
Toledo	Plain	PD	ts	21%	10%	18%	19%	32%
Tuscola {B}	Plain	MWD	bs	17%	20%	32%	19%	12%
Adrian muck	Depression	PD	ts	8%	8%	23%	24%	36%
Adrian-Houghton mucks	Depression	VPD	ts	11%	9%	23%	24%	34%
Edwards	Depression	VPD	ts	13%	9%	22%	20%	36%
Linwood	Depression	VPD	ts	6%	7%	22%	24%	41%
Au Gres {B}	Complexes	SPD	ts	26%	12%	14%	17%	31%
Au Gres-Saugatuck {B}	Complexes	SPD	ts	15%	10%	16%	21%	38%
Croswell {B}	Complexes	MWD	ts	22%	16%	19%	19%	23%
Croswell-Au Gres {B}	Complexes	SPD	ts	18%	13%	20%	20%	28%
Gilford	Depression	PD-VPD	ts	18%	11%	24%	19%	28%
Boyer {B}	Plain	WD	bs	16%	17%	37%	19%	11%
Boyer {C}	Plain	WD	bs	6%	12%	63%	14%	5%
Breckenridge	Plain	PD	ts	17%	8%	18%	21%	36%
Brevort	Plain	PD	ts	16%	9%	20%	21%	34%
Bruce	Plain	PD	ts	17%	10%	16%	24%	33%
Fox {B}	Plain	WD	bs	21%	16%	27%	18%	19%
Gladwin {A}	Plain	SPD	ts	25%	13%	17%	18%	27%
Gladwin {B}	Plain	SPD	su	25%	15%	23%	19%	18%

Table 4.11. (cont'd)

SSURGO			Hillslope Position Model					
Map Unit	**Geographic Setting**	**DC**	**Max**	**su**	**sh**	**bs**	**fs**	**ts**
Granby	Plain	PD-VPD	ts	23%	8%	13%	18%	38%
Iosco {A}	Plain	SPD	su	29%	15%	15%	18%	24%
Iosco-Belding {B}	Plain	SPD	su	29%	18%	13%	21%	20%
Kalkaska {C}	Plain	WD	bs	18%	19%	36%	14%	14%
Kibbie {A}	Plain	SPD	ts	25%	9%	15%	18%	34%
Kibbie {B}	Plain	SPD	fs	18%	13%	22%	25%	22%
Lacota	Plain	PD	ts	20%	9%	19%	18%	33%
Mancelona {A}	Plain	WD-MWD	su	27%	16%	20%	17%	21%
Mancelona {B}	Plain	WD-MWD	bs	23%	19%	27%	18%	13%
Mancelona {C}	Plain	WD-MWD	bs	9%	16%	57%	12%	6%
Matherton {A}	Plain	SPD	ts	27%	11%	18%	16%	29%
Menominee {B}	Plain	WD-MWD	su	26%	20%	22%	19%	13%
Menominee {C}	Plain	WD-MWD	bs	10%	15%	50%	18%	7%
Metamora {A}	Plain	SPD	ts	23%	12%	20%	19%	26%
Metamora {B}	Plain	SPD	ts	20%	14%	22%	21%	22%
Newaygo {B}	Plain	WD	su	25%	16%	22%	16%	20%
Oshtemo {A}	Plain	WD	su	30%	16%	17%	17%	20%
Oshtemo {B}	Plain	WD	bs	17%	20%	33%	20%	10%
Oshtemo {C}	Plain	WD	bs	6%	14%	61%	14%	5%
Oshtemo {D}	Plain	WD	bs	4%	10%	70%	12%	4%
Owosso {B}	Plain	WD-MWD	bs	19%	19%	35%	17%	9%
Plainfield {B}	Plain	ED	bs	21%	17%	24%	20%	19%
Plainfield {D-F}	Plain	ED	bs	4%	9%	68%	11%	8%
Richter {A}	Plain	SPD	ts	27%	11%	15%	18%	29%
Richter {B}	Plain	SPD	fs	20%	15%	19%	23%	23%
Spinks {A}	Plain	WD	bs	17%	16%	27%	21%	18%
Spinks {B}	Plain	WD	bs	12%	17%	41%	20%	10%
Spinks {C}	Plain	WD	bs	8%	13%	60%	13%	7%
Tonkey	Plain	PD	ts	20%	10%	15%	20%	35%
Wasepi {A}	Plain	SPD	bs	17%	15%	29%	19%	21%
Braceville {A}	Terrace	MWD	bs	22%	18%	24%	19%	17%
Spinks-Montcalm {D-F}	Plain	WD	bs	4%	8%	77%	8%	3%
Chelsea {B}	Dunes	WD	su	26%	18%	20%	17%	18%
Chelsea {C}	Dunes	WD	bs	10%	15%	46%	17%	11%
Deer Park {B}	Dunes	WD	bs	11%	15%	44%	17%	13%
Deer Park {D}	Dunes	WD	bs	7%	12%	54%	15%	12%
Dune land	Dunes		bs	2%	5%	79%	9%	6%

Table 4.11. (cont'd)

SSURGO			Hillslope Position Model					
Map Unit	**Geographic Setting**	**DC**	**Max**	**su**	**sh**	**bs**	**fs**	**ts**
Hillsdale {B}	Moraines	WD	bs	14%	22%	32%	24%	8%
Hillsdale {C}	Moraines	WD	bs	7%	16%	57%	17%	3%
Belding {A}	Plain	SPD	ts	23%	11%	14%	21%	31%
Belding {B}	Plain	SPD	su	25%	14%	15%	23%	22%
Blount {A}	Plain	SPD	su	30%	14%	14%	17%	25%
Blount {B}	Plain	SPD	su	24%	17%	19%	22%	18%
Conover {B}	Plain	SPD	fs	13%	15%	27%	28%	17%
Kawkawlin {A}	Plain	SPD	ts	24%	12%	13%	20%	30%
Kawkawlin {B}	Plain	SPD	fs	22%	15%	17%	23%	23%
Miami {B}	Plain	WD	bs	14%	21%	40%	20%	5%
Miami {C}	Plain	WD	bs	7%	15%	58%	16%	4%
Miami {D-F}	Plain	WD	bs	2%	8%	81%	7%	2%
Montcalm {A}	Plain	WD-MWD	su	32%	16%	17%	16%	20%
Montcalm {B}	Plain	WD-MWD	bs	22%	20%	28%	19%	11%
Montcalm {C}	Plain	WD-MWD	bs	6%	14%	58%	16%	6%
Morley {B}	Plain	WD-MWD	bs	18%	23%	36%	16%	6%
Morley {C}	Plain	WD-MWD	bs	6%	14%	61%	14%	4%
Morley {D-F}	Plain	WD-MWD	bs	3%	7%	82%	6%	3%
Nester {B}	Plain	WD-MWD	bs	18%	23%	31%	20%	8%
Nester {C}	Plain	WD-MWD	bs	6%	14%	61%	15%	4%
Nester {D-F}	Plain	WD-MWD	bs	3%	7%	81%	6%	3%
Selkirk {A}	Plain	SPD	ts	17%	9%	11%	23%	40%
Selkirk {B}	Plain	SPD	ts	19%	13%	18%	23%	27%
Sims	Plain	PD	ts	13%	8%	18%	24%	36%
Ubly {A}	Plain	WD	su	31%	18%	18%	17%	16%
Ubly {B}	Plain	WD	bs	19%	23%	27%	22%	9%
Ubly {C}	Plain	WD	bs	6%	15%	57%	17%	5%

Table 4.12. Zonal statistics of the SlgP-med hillslope position model by SSURGO map units in Dickinson County, Iowa.

SSURGO			Hillslope Position Model					
Map Unit	**Geographic Setting**	**DC**	**Max**	**su**	**sh**	**bs**	**fs**	**ts**
Calco	Floodplain	VPD-PD	ts	23%	5%	18%	12%	42%
Millington	Floodplain	PD	bs	5%	7%	38%	17%	33%
Spillville	Floodplain	SPD-MWD	ts	19%	7%	20%	13%	41%
Spillville {B}	Floodplain	SPD-MWD	bs	2%	5%	41%	32%	20%
Coland	Side Slope	PD	ts	12%	4%	21%	19%	45%
Coland-Spillville	Side Slope	PD-MWD	bs	1%	3%	36%	32%	28%
Orthents	Not Defined		bs	19%	13%	35%	14%	19%
Bolan {B}	Not Defined	WD	su	32%	19%	12%	22%	16%
Bolan {C}	Not Defined	WD	bs	9%	19%	50%	17%	5%
Blue Earth Muck	Depression	VPD	ts	8%	2%	7%	9%	74%
Collinwood	Flat	SPD	su	33%	13%	9%	20%	25%
Collinwood {B}	Flat	SPD	su	33%	25%	14%	20%	8%
Collinwood {C}	Flat	SPD	bs	7%	19%	53%	17%	3%
Kingston	Flat	SPD	su	48%	5%	3%	7%	37%
Madelia	Flat	PD	ts	20%	2%	4%	9%	65%
Spicer	Flat	VPD-PD	ts	23%	2%	3%	7%	64%
Waldorf	Flat	PD	ts	22%	4%	6%	15%	53%
Everly	Convex	MWD	su	78%	6%	3%	3%	10%
Everly {B}	Convex	MWD	su	44%	19%	11%	16%	10%
Everly {C}	Convex	MWD	bs	3%	15%	67%	13%	2%
Letri	Undefined	PD	ts	20%	3%	5%	9%	64%
Pits	Disturbed		bs	6%	9%	56%	12%	16%
Cylinder	Flat	SPD	ts	39%	4%	4%	8%	44%
Biscay	Plain	VPD-PD	ts	22%	3%	8%	9%	58%
Dickman	Plain	SED	su	34%	22%	16%	18%	10%
Estherville	Plain	SED	su	47%	10%	11%	8%	25%
Estherville {B}	Plain	SED	su	29%	22%	20%	18%	12%
Estherville {C}	Plain	SED	bs	7%	15%	61%	13%	4%
Salida {D-G}	Plain	ED	bs	4%	7%	83%	4%	2%
Talcot	Plain	VPD-PD	ts	35%	2%	6%	6%	51%
Wadena	Plain	WD	su	48%	6%	5%	7%	34%
Wadena {B}	Plain	WD	su	28%	16%	20%	18%	18%
Wadena {C}	Plain	WD	bs	6%	16%	58%	15%	5%
Sac	Convex	MWD	su	56%	12%	5%	14%	13%
Ransom	Flat	SPD	su	54%	3%	3%	6%	35%
Wilmonton	Flat	SPD	su	41%	4%	3%	10%	41%
Clarion {B}	Convex	MWD	su	27%	25%	19%	21%	9%
Clarion {C}	Convex	MWD	bs	8%	19%	55%	15%	3%

Table 4.12. (cont'd)

SSURGO			Hillslope Position Model					
Map Unit	**Geographic Setting**	**DC**	**Max**	**su**	**sh**	**bs**	**fs**	**ts**
Clarion {D}	Convex	MWD	bs	3%	8%	82%	6%	1%
Storden {C}	Convex	WD	bs	7%	16%	62%	12%	3%
Storden {D-G}	Convex	WD	bs	2%	5%	88%	4%	1%
Harps	Depression	PD	ts	22%	6%	3%	13%	56%
Crippin	Flat	SPD	ts	32%	9%	5%	13%	41%
Fostoria	Flat	SPD	ts	35%	3%	3%	12%	47%
Nicollet	Flat	SPD	ts	25%	10%	10%	24%	30%
Ocheyedan	Flat	MWD	su	63%	8%	4%	8%	17%
Ocheyedan {B}	Flat	MWD	su	41%	18%	12%	18%	10%
Canisteo	Concave	VPD-PD	ts	13%	3%	7%	16%	60%
Webster	Concave	PD	ts	10%	4%	10%	23%	53%
Okoboji	Depression	VPD	ts	5%	2%	5%	13%	76%
Rolfe	Depression	VPD	ts	18%	3%	6%	10%	63%
Terril {C}	Swale	MWD	bs	1%	2%	75%	16%	6%
Terril {B}	Swale	MWD	bs	3%	6%	44%	31%	15%

Table 4.13. Zonal statistics of the SlgP-med hillslope position model by SSURGO map units in Cedar County, Iowa.

SSURGO			Hillslope Position Model					
Map Unit	**Geographic Setting**	**DC**	**Max**	**su**	**sh**	**bs**	**fs**	**ts**
Alluvial-Spillville	Floodplain	SPD-MWD	ts	27%	10%	14%	17%	33%
Arenzville	Floodplain	MWD	ts	18%	3%	13%	25%	41%
Colo-Ely	Floodplain	PD-SPD	fs	4%	3%	9%	44%	39%
Colo-Ely {B}	Floodplain	PD	ts	26%	3%	13%	19%	39%
Hanlon	Floodplain	MWD	su	60%	5%	4%	6%	25%
Kennebec	Floodplain	MWD	su	40%	4%	16%	12%	27%
Nodaway	Floodplain	MWD	ts	11%	4%	30%	22%	33%
Nodaway-Arenzville	Floodplain	MWD	fs	2%	3%	35%	37%	23%
Radford	Floodplain	SPD	ts	19%	3%	12%	23%	43%
Sawmill	Floodplain	PD	ts	39%	2%	6%	12%	41%
Spillville	Floodplain	SPD-MWD	ts	22%	5%	21%	17%	35%
Nevin	Lowland Flat	SPD	su	50%	2%	3%	9%	36%
Rockton {D}	Lowland Flat	WD	fs	6%	27%	26%	36%	5%
Lamont {C}	Not Defined	WD	fs	12%	28%	18%	35%	8%
Lamont {E}	Not Defined	WD	bs	3%	17%	51%	25%	4%
Bassett {B}	Interfluves-Sideslopes	MWD	sh	16%	51%	6%	25%	2%
Bassett {C}	Interfluves-Sideslopes	MWD	fs	4%	33%	12%	48%	3%
Bassett {D}	Interfluves-Sideslopes	MWD	bs	1%	15%	44%	39%	2%
Kenyon {B}	Interfluves-Sideslopes	MWD	sh	25%	38%	2%	30%	5%
Kenyon {C}	Interfluves-Sideslopes	MWD	fs	5%	31%	5%	56%	3%
Fayette {B}	Interfluves-Sideslopes	WD	sh	35%	42%	12%	10%	2%
Fayette {C}	Interfluves-Sideslopes	WD	bs	7%	41%	39%	12%	1%
Fayette {D-G}	Interfluves-Sideslopes	WD	bs	1%	10%	71%	16%	2%
Waukegan {B}	Outwash Plain	WD	su	36%	23%	3%	25%	12%
Waukegan {C}	Outwash Plain	WD	fs	7%	29%	12%	46%	6%
Atterberry	Summit-Flat	SPD	su	64%	5%	2%	7%	22%
Atterberry {B}	Summit-Flat	SPD	su	35%	11%	2%	28%	23%
Franklin	Summit-Flat	SPD	su	42%	5%	2%	23%	29%
Garwin	Summit-Flat	PD	ts	35%	2%	2%	10%	51%
Maxfield	Summit-Flat	PD	ts	30%	2%	2%	13%	53%

Table 4.13. (cont'd)

SSURGO			Hillslope Position Model					
Map Unit	**Geographic Setting**	**DC**	**Max**	**su**	**sh**	**bs**	**fs**	**ts**
Muscatine	Summit-Flat	SPD	su	72%	6%	2%	7%	14%
Muscatine {B}	Summit-Flat	SPD	su	37%	10%	2%	30%	21%
Dinsdale {B}	Summit-Shoulder	MWD	su	39%	25%	2%	26%	8%
Dinsdale {C}	Summit-Shoulder	MWD	fs	5%	26%	5%	59%	5%
Downs {B}	Summit-Shoulder	WD	sh	36%	41%	7%	14%	3%
Downs {C}	Summit-Shoulder	WD	sh	6%	36%	21%	33%	4%
Downs {D}	Summit-Shoulder	WD	bs	1%	14%	45%	36%	3%
Klinger	Summit-Shoulder	SPD	su	34%	6%	2%	28%	30%
Tama	Summit-Shoulder	WD	su	67%	13%	1%	10%	10%
Tama {B}	Summit-Shoulder	WD	su	42%	30%	3%	20%	5%
Tama {C}	Summit-Shoulder	WD	fs	5%	30%	10%	48%	6%
Tama {D}	Summit-Shoulder	WD	fs	1%	15%	34%	46%	4%
Walford	Summit-Shoulder	VPD-PD	ts	37%	3%	2%	12%	46%
Waubeek {B}	Summit-Shoulder	MWD	sh	17%	37%	9%	33%	4%
Whittier {B}	Terrace	WD	fs	26%	23%	12%	27%	12%
Whittier {C}	Terrace	WD	fs	8%	29%	17%	38%	8%
Ansgar	Transitional Swale	PD	ts	42%	3%	1%	12%	42%
Ely	Transitional Swale	SPD	fs	6%	4%	4%	53%	33%
Sperry	Upland Depression	VPD-PD	ts	28%	2%	1%	7%	61%
Judson {B}	Transitional Swale	WD	fs	6%	5%	9%	57%	23%
Palms	Upland Depression	VPD	ts	28%	2%	6%	19%	44%
Marsh	Wetland		ts	14%	4%	12%	17%	54%
Brady	Outwash Plain	SPD	ts	21%	6%	6%	25%	41%
Richwood	Outwash Plain	WD	su	50%	4%	5%	15%	26%
Saude	Outwash Plain	WD	su	46%	9%	7%	14%	24%
Sparta {B}	Outwash Plain	ED	su	38%	17%	8%	19%	18%
Sparta {C}	Outwash Plain	ED	fs	9%	31%	17%	38%	6%
Sparta {E}	Outwash Plain	ED	bs	4%	22%	40%	31%	3%
Rock {G}	Not Defined		bs	0%	3%	88%	5%	3%
Sogn {E}	Not Defined	SED	bs	1%	11%	69%	15%	4%
Chelsea {B}	Sideslopes	ED	su	39%	19%	11%	17%	13%
Chelsea {C}	Sideslopes	ED	bs	9%	28%	34%	23%	5%
Chelsea {E}	Sideslopes	ED	bs	2%	12%	61%	19%	5%
Chelsea-Lamont-Fayette {C}	Sideslopes	ED	bs	8%	29%	32%	26%	4%
Chelsea-Lamont-Fayette {E-F}	Sideslopes	ED	bs	2%	10%	70%	16%	2%
Dickinson {B}	Not Defined	WD	su	37%	25%	3%	22%	13%
Dickinson {C}	Not Defined	WD	fs	6%	29%	10%	51%	5%
Dickinson-Tama {C}	Not Defined	WD	fs	12%	32%	18%	37%	2%
Lindley {D-F}	Side Slope	WD	bs	1%	6%	72%	18%	3%

REFERENCES

REFERENCES

Andrews, W.F. and R.O. Dideriksen. 1981. Soil Survey of Boone County, Iowa. Soil Conservation Service, U.S. Department of Agriculture. Washington, D.C.

Arnold, J., M.D. Corre, and E. Veldkamp. 2009. Soil N cycling in old-growth forests across an Andosol toposequence in Ecuador. Forest Ecology and Management. 257(10):2079-2987. doi:10.1016/j.foreco.2009.02.014

Arnold, R.W. 2006. Soil survey and soil classification. *In* S. Grunwald (ed.). Environmental Soil-Landscape Modeling: Geographic Information Technologies and Pedometrics. Taylor & Francis Group. Boca Raton.

Bettis, E.A. 1989. Late Quaternary history of the Iowa River valley in the Coralville Lake area. *In* O.W. Plocher (ed.). Geologic Reconnaissance of the Coralville Lake Area. Geological Society of Iowa Guidebook 51.

Bunge, W. 1962. Theoretical Geography. Gleerup. Lund, Sweden.

Burras, C.L. and W.H. Scholtes. 1987. Basin properties and postglacial erosion rates of minor moraines in Iowa. Soil Science Society of America Journal. 51(6):1541-1547.

Bushnell, T.M. 1943. Some aspects of the soil catena concept. Soil Science Society Proceedings. 7(C):466-476.

Butler, B.E. 1982. A new system for soil studies. Journal of Soil Science. 33(4):581-595.

Conacher, A.J. and J.B. Dalrymple. 1977. Landsurface mapping. Geoderma. 18(1-2):111-115.

Dermody, R.P. 2009. Soil Survey of Cedar County, Iowa. Natural Resource Conservation Service, U.S. Department of Agriculture. Washington, D.C.

Donald, R.G., D.W. Anderson, J.W.B. Stewart. 1993. The distribution of selected soil properties in relation to landscape morphology in forested Gray Luvisol soils. Canadian Journal of Soil Science. 73:165-172.

Ellis, J.H. 1938. The soils of Manitoba. Manitoba Economic Survey Board. Winnipeg, Manitoba.

ESRI. 2012. Environmental Systems Research Institute ArcGIS Software, Version 10.1. http://www.esri.com

Frye, J.C. 1959. Climate and Lester King's "Uniformitarian nature of hillslopes." Journal of Geology. 67:111-113.

Furley, P.A. 1971. Relationships between slope form and soil properties developed over chalk parent materials. Institute of British Geographers Special Publication. 3:141-163.

Giles, P.T. 1998. Geomorphological signatures: classification of aggregated slope unit objects from digital elevation and remote sensing data. Earth Surface Processes and Landforms. 23(7):581-594.

Govers, G. 1985. Selectivity and transport capacity of thin flows in relation to rill erosion. Catena. 12:35-49.

GRASS Development Team, 2012. Geographic Resources Analysis Support System (GRASS) Software, Version 6.4.2. Open Source Geospatial Foundation. Available online at: http://grass.osgeo.org. Accessed [11/12/2012].

Grealish, G., R.W. Fitzpatrick, P. King, S.A. Shahid. 2013. Conceptual soil-regolith toposequences models to support soil survey and land evaluation. *In* S.A. Shahid, F.K. Taha, and M.A. Abdelfattah (eds.). Developments in Soil Classification, Land Use Planning and Policy Implications: Innovative Thinking of Soil Inventory for Land Use Planning and Management of Land Resources. Springer. Dordrecht.

Hall, G.F. and C.G. Olson. 1991. Predicting variability of soils from landscape models. *In* M.J. Mausbach and L.P. Wilding (eds.). Spatial Variabilities of Soils and Landforms. SSSA Special Publication Number 28. Soil Science Society of America. Madison, Wisconsin.

Hengl, T. and R.A. MacMillan. 2007. Geomorphology as a key tool to map and model natural landscapes. *In* T. Hengl and H.I. Reuter (eds.). Geomorphometry: Concepts, Software, Applications. Office for Official Publications of the European Communities. Luxembourg.

Hole, F.D. and J.B. Campbell. 1985. Soil Landscape Analysis. Rowman & Allanheld. Totowa, New Jersey.

Hudson, B.D. 1990. Concepts of soil mapping and interpretation. Soil Survey Horizons. 31(3):63-72.

Hudson, B.D. 1992. The soil survey as a paradigm-based science. Soil Science Society of America. 56:836-841.

IDNR. 2009. The Iowa LiDAR Project. Iowa Department of Natural Resources. Available online at: http://geotree2.geog.uni.edu/lidar. Accessed [3/23/2013].

Jenny, H. 1941. Factors of Soil Formation: A System of Quantitative Pedology. Dover Publications. New York.

Jien, S., S. Wu, Z. Chen, T. Chen, and C. Chiu. 2010. Characteristics and pedogenesis of podzolic forest soils along a toposequence near a subalpine lake in northern Taiwan. Botanical Studies. 51:223-236.

Kagabo, D.M., L. Stroosnijder, S.M. Visser, and D. Moore. 2013. Soil erosion, soil fertility and crop yield on slow-forming terraces in the highlands of Buberuka, Rwanda. Soil and Tillage Research. 128:23-29.

Khalili-Rad, M. F. Nourbakhsh, A. Jalalian, and M.K. Eghbal. 2011. The effects of slope position on soil biological properties in an eroded toposequence. Arid Land Research and Management. 25(3):308-312.

King, L.C. 1957. The uniformitarian nature of hillslopes. Transactions of the Edinburgh Geological Society. 17:81-102.

Kleiss, H.J. 1970. Hillslope sedimentation and soil formation in northeastern Iowa. Soil Science Society of America Proceedings. 34:287-290.

Koné, B., A. Touré, G.L. Amadji, A. Yao-Kouamé, P.T. Angui, and J. Huat. 2013. Soil characteristics and Cyperus spp. Occurrence along a toposequence. African Journal of Ecology. doi: 10.1111/aje.12050

Korobova, E. and S. Romanov. 2011. Experience of mapping spatial structure of Cs-137 in natural landscape and patterns of its distribution in soil toposequence. Journal of Geochemical Exploration. 109(1-3):139-145.

MacMillan, R.A., D.E. Moon, and R.A. Coupé. 2007. Automated predictive ecological mapping in a forest region of B.C. Canada: 2001-2005. Geoderma. 140(4):353-373.

Malo, D.D., B.K. Worchester, D.K. Cassel, and K.D. Matzdorf. 1974. Soil-landscape relationships in a closed drainage system. Soil Science Society of America Proceedings. 38:813-818.

Miller, B.A., W.G. Crumpton, A.G. van der Valk. 2009. Spatial distribution of historical wetland classes on the Des Moines Lobe, Iowa. Wetlands. 29(4):1146-1152.

Milne, G. 1935. Some suggested units of classification and mapping particularly for East African soils. Soil Research. 4(3).

Park, S.J. and N. van de Giesen. 2004. Soil-landscape delineation to define spatial sampling domains for hillslope hydrology. Journal of Hydrology. 295(1-4):28-46.

Pennock, D.J., B.J. Zebarth, and E. De Jong. 1987. Landform classification and soil distribution in hummocky terrain, Saskatchewan, Canada. Geoderma. 40:297-315.

Pregitzer, K.E. 1972. Soil Survey of Ottawa County, Michigan. Soil Conservation Service, U.S. Department of Agriculture. Washington, D.C.

Pulido, D. 2011. Soil Survey of Dickinson County, Iowa. Natural Resource Conservation Service, U.S. Department of Agriculture. Washington, D.C.

Ruhe, R.V. 1969. Quaternary Landscapes in Iowa. Iowa State University Press. Ames, Iowa.

Ruhe, R.V. 1975. Climatic geomorphology and fully developed slopes. Catena. 2:309-320.

Ruhe, R.V. and P.H. Walker. 1968. Hillslope models and soil formation: I. Open systems. Transactions of the 9th International Congress of Soil Science. 4:551-560. Adelaide, Australia.

Schaetzl, R.J., F.J. Krist Jr., K.E. Stanley, and C.M. Hupy. 2009. The natural soil drainage index: an ordinal estimate of long-term, soil wetness. Physical Geography. 30:383-409.

Schaetzl, R.J., F.J. Krist Jr., and B.A. Miller. 2012. A taxonomically based, ordinal estimate of soil productivity for landscape-scale analyses. Soil Science. 177(4): 288-299. doi:10.1097/SS.0b013e3182446c88.

Schaetzl, R.J. 2013. Catenas and Soils. *In* J.F. Shroder (ed.). Treatise on Geomorphology, Vol. 4. Academic Press. San Diego, California. pp. 145-158.

Shi, X., R. Long, R. Dekett, J. Philippe. 2009. Integrating different types of knowledge for digital soil mapping. Soil Science Society of America. 73(5):1682-1692.

Shi, X., A.X. Zhu, J.E. Burt, F. Qi, and D. Simonson. 2004. A case-based reasoning approach to fuzzy soil mapping. Soil Science Society of America Journal. 68:885-894.

Soil Survey Staff. 1985. Pattern of soils and underlying material in the Nester-Kawkawlin-Manistee association. Natural Resource Conservation Service, U.S. Department of Agriculture. Available online at: http://soils.usda.gov/education/training/job_aids.html. Accessed [4/4/2013].

Soil Survey Staff. 1992. Typical pattern of soils and parent material in the Deer Park-Dawson-Au Gres association. Natural Resource Conservation Service, U.S. Department of Agriculture. Available online at: http://soils.usda.gov/education/training/job_aids.html. Accessed [4/4/2013].

Soil Survey Staff. 2000. Typical pattern of soils and parent material in the Canisteo-Clarion-Nicollet association. Natural Resource Conservation Service, U.S. Department of Agriculture. Available online at: http://soils.usda.gov/education/training/job_aids.html. Accessed [4/4/2013].

Soil Survey Staff. 2009. Typical pattern of soils and parent material in the Tama-Downs-Muscatine association. Natural Resource Conservation Service, U.S. Department of Agriculture. Available online at: http://soils.usda.gov/education/training/job_aids.html. Accessed [4/4/2013].

Soil Survey Staff. 2013a. Soil Survey Geographic (SSURGO) Database. Natural Resource Conservation Service, U.S. Department of Agriculture. Available online at: http://soildatamart.nrcs.usda.gov. Accessed [3/23/2013].

Soil Survey Staff. 2013b. Official Soil Series Descriptions (OSSD). Natural Resource Conservation Service, U.S. Department of Agriculture. Available online at: http://soils.usda.gov/technical/classification/osd/. Accessed [3/23/2013].

Stolt, M.H., J.C. Baker, and T.W. Simpson. 1993. Soil-landscape relationships in Virginia: II. reconstruction analysis and soil genesis. Soil Science Society of America Journal. 57:422-428.

Tsatskin, A., A. Sandler, and N. Porat. 2013. Toposequence of sandy soils in the northern coastal plain of Israel: Polygenesis and complexity of pedogeomorphic development. Geoderma. 197-198:87-97.

Venables, W.N. and B.D. Ripley. 2002. Modern Applied Statistics with S. Fourth Edition. Springer. New York.

West, L.T., L.P. Wilding, and C.T. Hallmark. 1988. Calciustolls in central Texas: I. Parent material uniformity and hillslope effects on carbonate-enriched horizons. Soil Science Society of America Journal. 52:1722-1731.

Wood, A. 1942. The development of hillside slopes. Proceedings of the Geologists' Association. 53:128-138.

Wood, J. 1996. The Geomorphological characterisation of Digital Elevation Models. Diss., Department of Geography, University of Leicester, U.K. http://www.soi.city.ac.uk/~jwo/phd/. Accessed [10/1/2012].

Wysocki, D.A., P.J. Schoeneberger, H.E. LaGarry. 2000. Geomorphology of Soil Landscapes. *In* M.E. Sumner (ed.). Handbook of Soil Science. CRC Press. Boca Raton, Florida.

Zhu, A.X., B. Hudson, J. Burt, K. Lubich, and D. Simonson. 2001. Soil mapping using GIS, expert knowledge, and fuzzy logic. Soil Science Society of America Journal. 65:1463-1472.

CHAPTER 5. THE IMPACT OF PARAMETER ACCURACY VERSUS RESOLUTION ON A SIMPLE HILLSLOPE POSITION CLASSIFICATION MODEL

Abstract

Many soil geomorphology models are dependent upon both the accuracy and resolution of terrain parameters. Therefore, to understand the uncertainty of model outcomes, it is important to know the sensitivity of the model to differences in the quality of input data. This study examines the sensitivity of a landscape classification model to differences in elevation data resolution and accuracy. The landscape classification model is a two-tier decision tree for classifying hillslope position as calibrated to the analysis scales and classification breaks used by soil scientists in the field. LiDAR-derived, 3 m resolution, elevation grids were used as the reference landscape surfaces for three different study areas. The results of the hillslope classification model using these grids were compared to the results of using NED (9 m) and SRTM (27 m) elevation grids as inputs. In order to identify which part of the changes in model outcomes are due to inaccurate elevation data and grid resolution, respectively, the LiDAR-derived elevation grid was aggregated to 9 m and 27 m resolutions. In general, reducing grid resolution changed approximately 20% of classifications between 3 m and 9 m resolutions, while changing approximately 35% of classifications between 3 m and 27 m resolutions. Inaccuracy in the SRTM elevation data added approximately 30% more changes to the modeled hillslope classifications. Generalizations cannot be made about the impact of inaccuracies in the NED, because they vary greatly depending on the production method of the area. However, in

the areas analyzed in this study, inaccuracies in the NED contributed to between 5% and 35% change in hillslope position classification.

Keywords: hillslope position, LiDAR, NED, SRTM, classification error, grid resolution

1. Introduction

Topographic parameters are among the most valuable landscapes metrics for geomorphology and soil geography applications (Ruhe, 1975; Hudson, 1990; McBratney et al., 2003). For this reason, digital terrain analysis has become a popular type of research approach for the study of physical landscapes. The widespread availability of digital elevation data has facilitated the development and application of digital terrain metrics and models (Moore et al., 1991; Wilson and Gallant, 2000). However, questions exist about the repeatable nature of the analysis results because each analysis has a unique sensitivity to errors in the elevation data (Lee et al., 1992; Holmes et al., 2000; Fisher and Tate, 2006; Lindsay, 2006). Classification is a strategy for dealing with uncertainty by setting category ranges that balance the resolution of information needed with the sensitivity of the categories to errors (Pilkey and Pilkey-Jarvis, 2007).

Soil classification is a classic example of an application that utilizes landscape classification categories to account for attribute variability and uncertainty. Soil mapping and classification balances the need to express variation of important soil characteristics, with the practical ability to spatially represent the heterogeneous soil landscape (Soil Survey Staff, 1993). Through geographic association, observations of soil properties in a few locations are extended across a landscape by predicting locations with similar conditions; i.e., similar

topographic characteristics, will have similar soils (Milne, 1935; Bushnell, 1943). This form of environmental correlation has been undergoing refinement since the introduction of the soil forming factors in 1883 (Dokuchaev, 1967). More recent developments have focused on environmental conditions controlled by topography to predict soil variability for increasingly detailed maps (Pennock et al., 1987; Lark, 1999; Young and Hammer, 2000). At fine analysis scales, soil scientists have traditionally used topographic classifications of hillslope position - formal or otherwise - to differentiate areas of contrasting geomorphic processes and to map the resulting spatial variability in soil properties (Chapter 2). However, despite the ability of hillslope position (HP) classification to represent the spatial structure of soil variability at the resolution of current understanding of pedogeomorphic processes, the classification of landscapes into hillslope positions is still susceptible to uncertainty in the elevation data on which the classification is based.

Chapters 3 and 4 introduced a digital method for classifying hillslope position (HP) that was calibrated to soil scientists' field experience and validated in three different landscapes. In order to maximize accuracy and utility, the calibration and validation of the digital HP classification was conducted on high resolution, LiDAR-derived elevation data. However, this type of high quality elevation data is not available in all landscapes. Before applying digital HP classification to elevation data from different sources, the sensitivity of the model to parameters of differing quality (i.e. spatial resolution and attribute certainty), needs to be tested.

The purpose of this study is to test the sensitivity of the HP classification model to the quality of the elevation data. I define the quality of elevation data as a function of resolution and accuracy. Differences between the HP classification of LiDAR and other elevation data sources are considered to be the result of a combination of both aspects of elevation data quality. In order to differentiate the effects of these two aspects of elevation data quality, I modelled the effect of resolution alone. To accomplish this, I aggregated LiDAR-based elevation data to the same resolution of alternative elevation data sources, in a manner similar to the methods used by Barber and Shortridge (2005). The difference in HP classifications, caused by an alternative elevation data source and the modelled changes due to coarser resolutions, is used as a surrogate for the sensitivity of the HP classification model to uncertainty in elevation values.

2. Methods

2.1. Comparison of Different Elevation Data Sources

Using the HP classification model validated in Chapter 4, the sensitivity of that classification to elevation data of differing quality was tested on three counties of differing terrain (Figure 5.1). Ottawa County, Michigan and Dickinson County, Iowa were both glaciated during the late Wisconsin. However, the Dickinson County landscape consists of predominantly closed basins, while Ottawa County has major areas of glaciolacustrine plains and sand dunes. Cedar County, Iowa is a landscape glaciated during the Pre-Illinoisan, with a cover of loess.

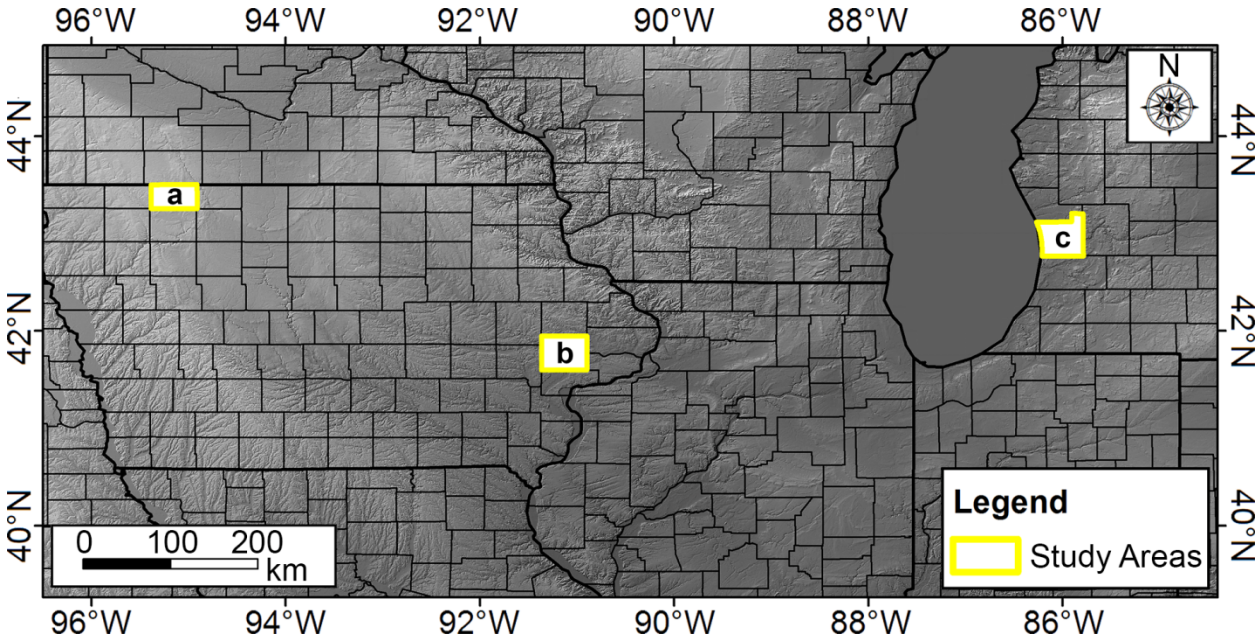


Figure 5.1. Areas used for this study were a) Dickinson County, Iowa, b) Cedar County, Iowa, and c) Ottawa County, Michigan.

For the purpose of this study, I define the quality of an elevation data set as the combination of its resolution and uncertainty in elevation attributes. The estimated uncertainty is often expressed as a spatial root mean square error (RMSE) associated with the data collection method (Li, 1988; Desmet, 1997; Hunter and Goodchild, 1997). LiDAR is considered to be the highest quality elevation data because of its fine spatial resolution and typically having a $RMSE_Z$ of 0.15-0.43 m (Krabill et al., 1995; Krabill et al., 2000; Bowen and Waltermire, 2002; Schumann et al., 2008). However, the error in digital elevation datasets is not only dependent upon the production method, but also characteristics of the landscape. The $RMSE_Z$ for digital elevation data tends to increase with terrain relief and ruggedness (Aguilar et al., 2005; USGS, 2006). In addition to increasing with relief, $RMSE_Z$ for LiDAR has also been observed to vary as a

function of the vegetation cover. Hodgson et al. (2003) reported the $RMSE_Z$ of LiDAR elevation data on the North Carolina Piedmont to be 0.33-0.37 m for grasslands, 0.46 m for pine forests, 1.22 m for deciduous forests, and 1.53 m for shrubland.

The first test of sensitivity applied the HP classification model to the United States Geological Survey (USGS) 1/3 arc second national elevation dataset (NED). The NED is a mixture of the best available elevation data sources, merged together to create a continuous grid (USGS, 2013a; USGS, 2013b). The 1/3 arc second resolution, generally equivalent to a 9 m cell size in the study areas, is the finest resolution available that covers the entire United States in 2013. As a composite of multiple data collection methods, the uncertainty in elevation attributes of this data set varies. In Ottawa County, Michigan and Cedar County, Iowa, the NED was compiled using the LT4X method. This method interpolates contour lines to grids (Gesch et al., 2002). The metadata for the NED in these two areas reports a $RMSE_Z$ of 1 m for Ottawa County and 2 m for Cedar County (USGS, 2013a). In Dickinson County, Iowa, the NED has incorporated LiDAR data. Therefore, the Dickinson County area is a test of the lower resolution in the 1/3 arc second NED, but has a $RMSE_Z$ comparable to the LiDAR (actual $RMSE_Z$ not yet reported).

The second test of sensitivity used elevation data from the Shuttle Radar Topography Mission (SRTM) (USGS, 2002). This dataset covers 80% of the Earth's land surface from 60° N to 60° S (Farr et al., 2007) at a spatial resolution of one arc second, which in the study region is a cell size of approximately 27 m. The $RMSE_Z$ of this elevation dataset has been reported to be

between 1.5 and 6 m (Rodriguez et al, 2005; Schumann et al., 2008). SRTM data tends to have a positive bias with increasing slope gradient and percent forest cover (Shortridge and Messina, 2011).

The HP classification model was calibrated to both the analysis scale (Chapter 3) and classification breaks (Chapter 4) of soil scientists in the field. The classification of the LiDAR-derived, 3 m resolution, elevation grids for each of the three study areas were treated as the reference classification. The HP classification model was then applied to the two lower quality, but more widely available digital elevation data sets. Although the classification breaks were held constant, the coarser grid resolutions of the alternative elevation data sources limited the ability to match analysis scales. The most severely affected was slope gradient, which had been calibrated to an analysis scale of 9 m. The closest analysis scale possible was instead used for the respective elevation grids. The 9 m NED was analyzed at a scale of 27 m and the 27 m SRTM was analyzed at a scale of 81 m for slope gradient. The calibrated scale of profile curvature at 63 m was able to be matched for the NED, but the smallest possible analysis scale for the SRTM (81 m) had to again be used for profile curvature. The larger calibrated analysis scale for relative elevation was able to be matched for all elevation datasets.

After generating grids classified for HP from each of the elevation data sources for each of the three counties, the areas were divided by township, resulting in 45 test zones. Areas identified as water by the U.S. Soil Survey (Soil Survey Staff, 2013) were excluded from the test zones. Exactly 1,000 random points were generated in ArcGIS 10.1 (ESRI, 2012), for each of the test zones and intersected with the HP grids. Agreement of HP classification was then evaluated

at those points and compared between test zones. Because the HP classification model is dependent upon three parameters (i.e. slope gradient, profile curvature, and relative elevation), summary statistics of these digital terrain analyses were compared with rates of classification agreement per test zone. Slope gradient was summarized by the mean statistic. Because profile curvature and relative elevation are centered on zero, they were summarized using range instead of mean.

2.2. Isolating Effect of Grid Resolution

In order to distinguish the change in model results due to differences in elevation values versus the decrease in spatial resolution, the same evaluation was carried out on aggregated versions of the reference 3 m elevation grid. The LiDAR-based, 3 m resolution grid was aggregated by calculating the unweighted mean elevation at resolutions of 9 m and 27 m for simulating the spatial resolutions of the NED and SRTM-based elevation grids, respectively. These aggregations were accomplished with the Spatial Analyst Block Mean function in ArcGIS 10.1 using 3x3 and 9x9 neighborhoods, respectively. The aggregated grids were then intersected with the same test points used for the NED and SRTM evaluations for comparison.

3. Results and Discussion

3.1 Sensitivity to LiDAR, NED, and SRTM as Data Sources

Overall, agreement in HP classification between the LiDAR and alternative data sources declined with lower quality elevation data. In Ottawa County, Michigan, 33% of the sample locations agreed in classification between the 3 m LiDAR and 9 m NED, which declined to an

agreement rate of 26% between the 3 m LiDAR and 27 m SRTM-derived elevation grids. Agreement was higher in the Iowa counties, but had the same pattern. The 9 m NED in Cedar County agreed with the LiDAR classification 49% of the time and declined to 38% for the 27 m SRTM. The NED agreement with the 3 m LiDAR was much higher in Dickinson County due to the NED being based on the same LiDAR data as the reference grid, but the decrease in resolution from 3 m to 9 m resulted in an agreement rate of only 74%. The agreement rate between the 3 m LiDAR and 27 m SRTM declined to 30% in Dickinson County.

Examination of the confusion matrix of NED versus LiDAR HP classification for the combined areas indicates a tendency for the NED classification to over classify summits and toeslopes (Table 5.1b). In other words, errors of commission are most common for summit and toeslope classifications of the NED. This pattern implies that the NED contains areas of lower slope gradient, which is expected with the required coarser analysis scale for slope gradient. However, the same pattern was not observed in the SRTM classification, despite the coarser resolution of the SRTM requiring an even coarser analysis scale than the NED. Instead, the SRTM classification had a greater tendency to misclassify points to categories adjacent to the correct category (Table 5.1c).

Table 5.1. a) LiDAR-based, 3 m resolution, HP classification of all test points for context in evaluating confusion matrices comparing LiDAR-based classification of hillslope position with b) NED-based classification of hillslope position (Kappa = 0.36) and b) SRTM-based classification of hillslope position (Kappa = 0.14).

a)

LiDAR				
summit	shoulder	backslope	footslope	toeslope
17.7%	12.8%	30.7%	18.2%	20.6%

b)

		LiDAR					
		summit	shoulder	backslope	footslope	toeslope	*User**
NED	summit	10.4%	4.0%	3.4%	3.7%	4.3%	*40.5%*
	shoulder	1.6%	3.8%	3.4%	2.1%	0.7%	*32.9%*
	backslope	0.5%	1.8%	17.1%	2.4%	0.7%	*75.9%*
	footslope	0.9%	1.0%	3.1%	4.9%	1.7%	*42.5%*
	toeslope	4.2%	2.1%	3.8%	5.2%	13.1%	*46.2%*
	*Producer**	*58.9%*	*30.0%*	*55.8%*	*26.8%*	*63.9%*	

c)

		LiDAR					
		summit	shoulder	backslope	footslope	toeslope	*User**
SRTM	summit	4.9%	2.6%	2.9%	2.8%	4.2%	*28.1%*
	shoulder	4.3%	3.3%	5.6%	3.9%	4.0%	*15.7%*
	backslope	2.4%	3.0%	14.6%	4.3%	3.3%	*52.9%*
	footslope	3.7%	2.6%	5.6%	4.7%	5.1%	*21.6%*
	toeslope	2.4%	1.2%	2.1%	2.5%	4.0%	*32.6%*
	*Producer**	*27.5%*	*26.0%*	*47.4%*	*25.6%*	*19.5%*	

*User's and Producer's accuracy calculated by correct classification divided by all classifications in category.

3.1.1. Analysis of LiDAR, NED, and SRTM Agreement by Test Zones

Comparisons of classification agreement with terrain characteristics in the test zones demonstrated an increase in classification agreement with increased relief (Figure 5.2). Mean slope gradient and relative elevation range showed the strongest correlation with classification agreement. Profile curvature range showed similar trends with a weaker correlation. All three

HP classification model parameters are closely correlated to relief. However, slope gradient and relative elevation are more closely correlated, because larger ranges in relative elevation necessitate larger slope gradients. Therefore, it is expected that relative elevation and slope gradient would exhibit similar patterns. Profile curvature, on the other hand, is less dependent on elevation change, because both flat and steep slopes can have equal amounts and types of linear profile curvature.

Mean gradient compared to the NED classification agreement had a positive correlation in both Ottawa County ($R^2 = 0.39$) and Cedar County ($R^2 = 0.86$). This trend was not true for the NED classifications in Dickinson County. Because the NED in Dickinson County had been derived from more accurate LiDAR data, actually the same LiDAR data as the reference elevation grid, HP classification of the LiDAR and NED resulted in high agreement rates. The coarser resolution NED of Dickinson County showed only a small trend of decreasing agreement with an increase of mean slope ($R^2 = 0.51$). The contradictory trends in Dickinson County suggest that the relationship between classification agreement and terrain characteristics is connected more to production method than resolution of the elevation grids.

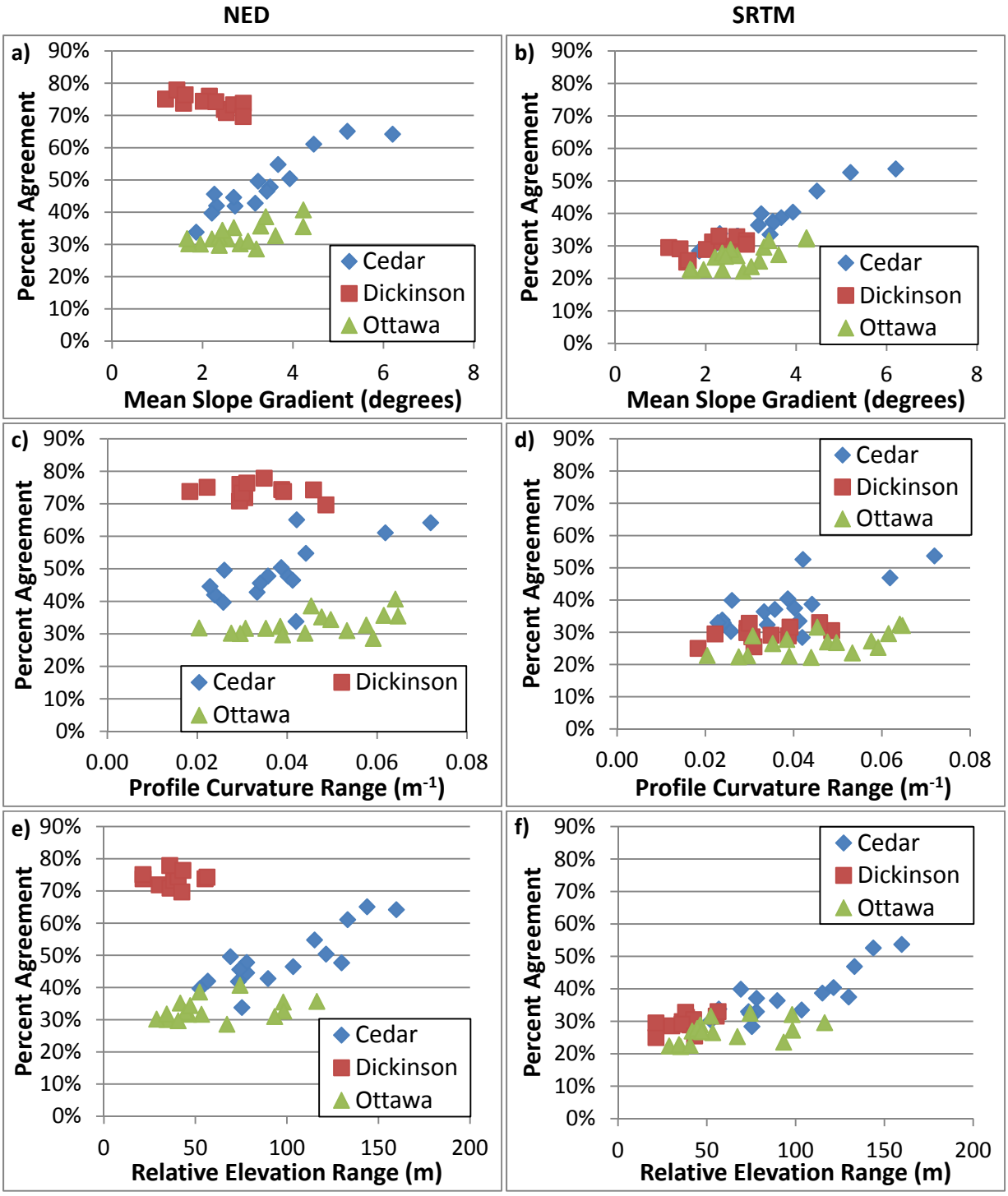


Figure 5.2. Terrain characteristics of test zones compared to HP classification agreement: LiDAR-based classification agreement with a) NED-based classification versus mean slope gradient, b) SRTM-based classification versus mean slope gradient, c) NED-based classification versus profile curvature range, d) SRTM-based classification versus profile curvature range, e) NED-based classification versus relative elevation range, f) SRTM-based classification versus relative elevation range.

Comparisons of relative elevation range versus NED classification agreement generally exhibited similar trends as did the analysis of mean slope gradient versus NED classification agreement. The correlation in Cedar County remained strong (R^2 = 0.70), but the correlation declined in the other two counties. In Dickinson County, where differences in classification were primarily a product of the generalization to a coarser grid resolution, there was no correlation between classification agreement and relative elevation (R^2 = 0.00). In Ottawa County, the correlation with relative elevation was much less than the correlation with mean slope gradient (R^2 = 0.12). Although relative elevation and slope gradient are intimately linked, the higher correlations of percent agreement with slope gradient than with relative elevation reflect the classification tree structure. The HP classification model applied in this study divides the landscape first by three categories of slope gradient. Then, high slope gradients are classified as backslopes, medium slope gradients are differentiated by profile curvature as shoulders or footslopes, and low slope gradients are differentiated by relative elevation as summits or toeslopes (Figure 5.3). Therefore, agreement in slope gradient classification between elevation datasets has the largest impact on HP classification agreement.

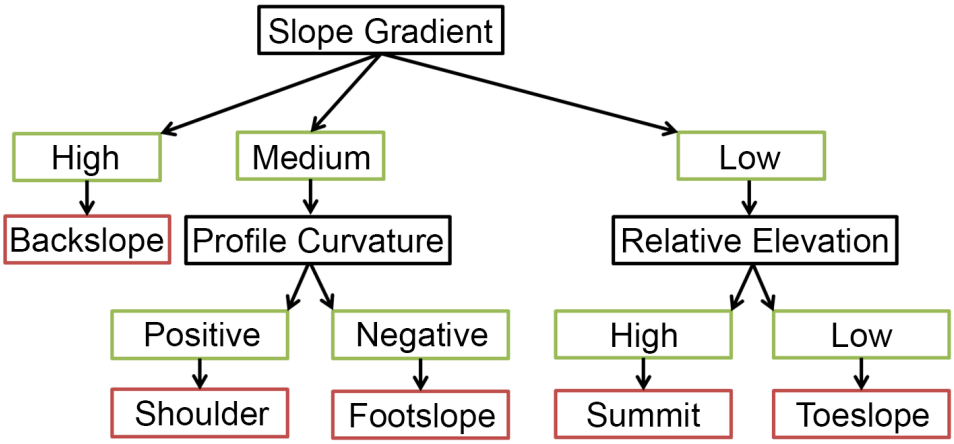


Figure 5.3. Diagram for the classification tree tested in this study, which was validated in Chapter 4.

Similar trends were also observed in the comparison of the SRTM classification agreements, but the maximum percent agreement was less (Figure 5.2). Agreement in HP classification between the LiDAR and SRTM data sources increased with increases in mean slope gradient and relative elevation range. Being based on exactly the same data source, Dickinson County was no longer an exception to the trends of the other two counties. Correlations for these trends of increasing agreement with greater relief were even stronger for SRTM classification than those observed for the NED classification. The positive correlation for mean slope gradient was strongest for Cedar County (R^2 = 0.92), followed by Ottawa County (R^2 = 0.56) and Dickinson County (R^2 = 0.35). The relative strengths of these correlations are most likely due to the greater diversity of slope gradients for the test zones within Cedar County. Although the correlation strengths for relative elevation range versus percent agreement of the SRTM classification were stronger, they were more comparable with the correlation strengths of the NED classification with relative elevation range. The positive correlation for relative

elevation range remained strongest for Cedar County (R^2 = 0.70), but Dickinson County (R^2 = 0.30) had a slightly stronger correlation than Ottawa County (R^2 = 0.27).

3.2. Sensitivity to Grid Resolution Alone

In order to test the sensitivity of the HP classification model to only changes in resolution, the LiDAR-based 3 m elevation grid was aggregated to resolutions of 9 m and 27 m and evaluated in the same manner as the NED and SRTM grid classifications. In Ottawa County, 61% of the classifications were consistent between the aggregated 9 m elevation grid and the original 3 m elevation grid classification. That agreement rate declined to 45% with the aggregated 27 m elevation grid. The amount of disagreement between grids of different resolutions was not as large in the Iowa counties. In Cedar County, 83% of the classifications were in agreement for the 9 m elevation grid and 67% of classifications were in agreement for the 27 m grid. Dickinson County was similar with 81% and 63% agreement for the 9 m and 27 m grids, respectively.

The rates of agreement for the resolution tests were all higher than the corresponding rates of agreement for tests of alternative grid sources, regardless of study area or data source. With the exception of the LiDAR-based NED in Dickinson County, the agreement rates for the alternative data sources were 48-59% of the agreements rates for the change in grid resolution alone. This relatively consistent relationship between the impact of the overall elevation grid quality and the spatial resolution alone suggests differences in HP classification are equally due to spatial resolution and accuracy.

The impact of increasing the minimum possible analysis scale was primarily observed in the decrease of locations classified as backslopes, as well as shoulders and footslopes (Table 5.2). The HP classification model classifies all areas with a slope gradient greater than 3° as backslopes. Therefore, the decline in agreement for classifying backslopes is purely due to fewer locations with those slope gradients. Similarly, the decrease in slope gradient values shifted many shoulder and footslope classifications to summit and toeslope classifications. However, these dominant trends were not universal. A few test points did shift to steeper slope gradient classifications.

Table 5.2. a) LiDAR-based, 3 m resolution, HP classification of all test points for context in evaluating confusion matrices comparing 3 m resolution classification with b) 9 m resolution classification (Kappa = 0.67) and c) 27 m resolution classification (Kappa = 0.47).

a)

summit	shoulder	backslope	footslope	toeslope
17.7%	12.8%	30.7%	18.2%	20.6%

b)

		3 m					
		summit	shoulder	backslope	footslope	toeslope	*User**
9 m	summit	14.5%	2.9%	1.0%	1.4%	0.4%	*71.8%*
	shoulder	1.0%	7.8%	2.8%	1.3%	0.3%	*59.3%*
	backslope	0.2%	0.9%	23.0%	1.1%	0.2%	*90.7%*
	footslope	0.3%	0.2%	2.6%	9.9%	1.2%	*69.5%*
	toeslope	1.7%	1.0%	1.3%	4.6%	18.4%	*68.1%*
	*Producer**	*81.8%*	*61.2%*	*75.0%*	*54.3%*	*89.4%*	

c)

		3 m					
		summit	shoulder	backslope	footslope	toeslope	*User**
27 m	summit	13.2%	4.8%	3.0%	2.5%	1.7%	*52.4%*
	shoulder	1.2%	5.1%	4.4%	1.4%	0.2%	*41.2%*
	backslope	0.2%	0.9%	15.9%	1.0%	0.3%	*87.2%*
	footslope	0.2%	0.6%	4.2%	6.8%	1.7%	*50.5%*
	toeslope	2.8%	1.4%	3.3%	6.5%	16.7%	*54.3%*
	*Producer**	*74.6%*	*39.7%*	*51.8%*	*37.6%*	*81.1%*	

*User's and Producer's accuracy calculated by correct classification divided by all classifications in category.

Although the decrease in resolution did not impact classifications based on profile curvature or relative elevation as much as slope gradient, there were some shifts due to changes in these parameters as well. Approximately 2% of the test points changed their classification between summit and toeslope due to a shift from low to high relative elevation and vice versa for the 9 m aggregation. The proportion of locations making the same type of classification shift increased to 4.5% for the 27 m aggregation. Although not as severe, a similar

trend was observed for shifts between convex and concave profile curvatures (shoulder versus footslope). Due to differences between convex and concave profile curvature, 1.5% of test points changed classification for the 9 m aggregation, which increased to 2.0% for the 27 m aggregation.

3.2.1. Analysis of Sensitivity to Grid Resolution by Test Zones

The sensitivity of HP classification to grid resolution did not show the same relationship to terrain characteristics as did the sensitivity tests based on different elevation grid production methods (Figure 5.4). Rates of agreement remained relatively constant between test zones within each of the counties. Cedar County was somewhat of an exception, with a slight trend of increasing agreement with increasing mean slope gradient, profile curvature range, and relative elevation range. However, Dickinson County had an inverse relationship between classification agreement and mean slope gradient for the 27 m resolution elevation grid.

Agreement rates were consistently higher in Cedar and Dickinson County, regardless of grid resolution or terrain characteristics. Within these two counties, agreement rates were above 80% for most test zones for the 9 m grid. Similarly, the mean of agreement rates for test zones excluding Ottawa County was 66% for the 27 m grid. Interestingly, the combined trends for Cedar and Dickinson Counties have a dip in test zone agreement rates near a mean slope gradient of 3°, which may reflect calculated slope gradients crossing the threshold for backslope classification.

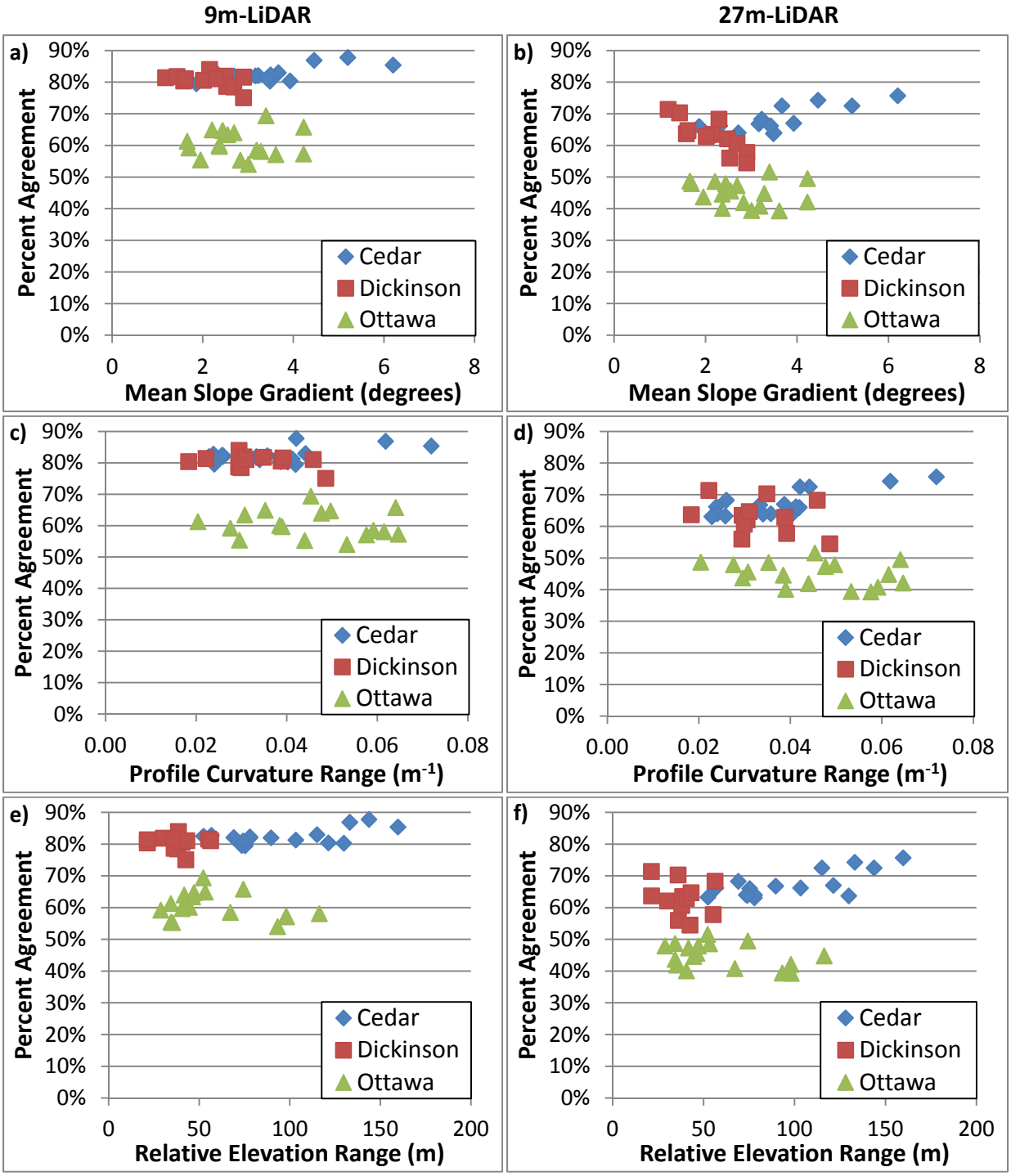


Figure 5.4. Terrain characteristics of test zones compared to HP classification agreement: original 3 m resolution grid and the same grid aggregated to a) 9 m resolution versus mean slope gradient, b) 27 m resolution classification versus mean slope gradient, c) 9 m resolution versus profile curvature range, d) 27 m resolution versus profile curvature range, e) 9 m resolution classification versus relative elevation range, f) 27 m resolution classification versus relative elevation range.

The contrast of HP classification sensitivity to grid resolution between Ottawa County and the Iowa counties is substantial. This difference could be due to the unique arrangement of terrain in Ottawa County that was not reflected by comparing test zones. For example, Ottawa County has very flat areas on glaciolacustrine plains, where slight changes in elevation could change classification between summits and toeslopes. The flatness of these areas could have been masked in the test zone statistics by a few interspersed dunes and steep drainage ditches. Another potential cause for the difference is the quality of the original LiDAR data. Although the LiDAR data for the Iowa counties were collected and processed as part of the same statewide project, the Ottawa County LiDAR was collected and processed by a different company, approximately seven years prior to the data collection in Iowa.

3.3. Comparison of Classification Agreements between Differing Data Sources and Grid Resolution

Disagreement in HP classification between elevation data sources is caused by differences in elevation values and generalization to coarser grid resolutions. Modelling the rate of disagreement due to grid resolution allows for the estimation of the rate of disagreement due to differences in elevation values by subtracting the amount of disagreement due to resolution from the overall disagreement.

For the Iowa counties, the cause of the SRTM classification's disagreement with the LiDAR classification was equally split between the effect of coarser resolution and the SRTM's lack of vertical accuracy (Table 5.3). Although the impact of grid resolution was consistent between Cedar and Dickinson Counties, the different production methods of the NED in the

two areas greatly affected the rate of disagreement due to NED accuracy. In Dickinson County, where the NED is derived from LiDAR data, the rate of disagreement due to elevation inaccuracy was only 6.6%. The method the USGS used to incorporate the LiDAR data into the NED is unknown. Therefore, it cannot be determined if the 6.6% disagreement was due to inaccuracies in the elevation data, grid processing methods, or my method of estimation. In contrast to the LiDAR-based, Dickinson County NED, the LT4X-derived, Cedar County NED has a much higher proportion of its disagreement in HP classification due to differences in elevation values than due to the coarser resolution.

Table 5.3. Rates of disagreement and estimated causes of disagreement for a) Ottawa County, Michigan, b) Cedar County, Iowa, and c) Dickinson County, Iowa.

a)

Ottawa County	Total Disagreement	Due to Resolution	Due to Lack of Accuracy
NED	67.1%	39.5%	27.5%
SRTM	73.4%	55.1%	18.4%

b)

Cedar County	Total Disagreement	Due to Resolution	Due to Lack of Accuracy
NED	51.4%	17.6%	33.8%
SRTM	62.0%	32.7%	29.4%

c)

Dickinson County	Total Disagreement	Due to Resolution	Due to Lack of Accuracy
NED	26.0%	19.5%	6.6%
SRTM	70.4%	37.0%	33.4%

In general, Ottawa County had higher rates of classification disagreement. It is unclear if the larger impact of aggregating the Ottawa County elevation data on HP classification was due to peculiarities of the area's topography or in the original LiDAR data collection. The larger impact of aggregating the original LiDAR grid on HP classification somewhat diminished the impact of differences in elevation values for the NED and especially the SRTM elevation grids.

The similar rates of disagreement due to coarsening of grid resolution in Cedar and Dickinson Counties suggest that some generalizations about the impact of grid resolution on the HP classification model can be made. Regardless of topography, the HP classification model outcomes can generally be expected to change approximately 20% between 3 m and 9 m resolutions, and approximately 35% between 3 m and 27 m resolutions. The lower accuracy of the SRTM data appears to be responsible for a change in approximately 30% of the LiDAR-based HP classifications. The classification errors attributed to the accuracy of the SRTM grid could also be connected to measurement resolution. The effective resolution of the one arc second SRTM has been observed to be more comparable to the two arc second NED grid (Guth, 2006). Similar generalizations regarding the impact of NED accuracy on HP classification cannot be made as the NED accuracy varies by the production method of particular areas.

4. Conclusions

The HP classification model is sensitive to differences in the calculation of slope gradient, which is highly dependent upon analysis scale. Coarser elevation grid resolutions increase the minimum analysis scale possible. For example, a 3 m resolution grid can be analyzed for slope gradient by areas of 9x9 m, compared to a 27 m resolution grid that cannot

be analyzed for slope gradient of areas smaller than 81x81 m. The HP classification model was calibrated to soil scientists' field training for assessing slope gradient, which was the smallest analysis scale possible for a 3 m grid (Chapter 3). Therefore, coarsening the grid resolution will increase differences from soil scientists' field assessment of slope gradient, resulting in more misclassifications by the HP classification model.

The HP classification model is less sensitive to elevation data uncertainty with increasing relief. However, the classification model is consistent in sensitivity to grid resolution, independent of terrain characteristics. This suggests that the HP classification model is more robust in high relief terrain, but it should be recognized that the hillslope position framework was designed for describing mature slopes.

The quality of elevation data has a large impact on the outcomes of landscape models, even simple models such as the HP classification model tested in this study. For analysis scale dependent parameters, the grid resolution can have as high of an impact as elevation uncertainty. Given the predictably high impact of not calculating parameters at their optimal analysis scale, upsampling - increasing resolution by interpolation - may be a justified approach to mitigating limitations in grid resolution.

REFERENCES

REFERENCES

Aguilar, F.J., F. Agüera, M.A. Aguilar, and F. Carvajal. 2005. Effects of terrain morphology, sampling density, and interpolation methods on grid DEM accuracy. Photogrammetric Engineering & Remote Sensing. 71(7):805-816.

Barber, C.P. and A. Shortridge. 2005. Lidar elevation data for surface hydrologic modeling: resolution and representation issues. Cartography and Geographic Information Science. 32(4):401-410.

Bowen, Z.H. and R.G. Waltermire. 2002. Evaluation of light detection and ranging (LIDAR) for measuring river corridor topography. Journal of American Water Resources Association. 38(1):33-41.

Bushnell, T.M. 1943. Some aspects of the soil catena concept. Soil Science Society Proceedings. 7(C):466-476.

Desmet, P.J.J. 1997. Effects of interpolation errors on the analysis of DEMs. Earth Surface Processes and Landforms. 22:563-580.

Dokuchaev, V.V. 1967. The Russian Chernozem (N. Kaner, Trans.).Israel Program for Scientific Translations. Jerusalem.

ESRI. 2012. Environmental Systems Research Institute ArcGIS Software, Version 10.1. http://www.esri.com

Farr, T.G., P.A. Rosen, E. Caro, R. Crippen, R. Duren, S. Hensley, M. Kobrick, M. Paller, E. Rodriguez, L. Roth, D. Seal, S. Shaffer, J. Shimada, J. Umland, M. Werner, M. Oskin, D. Burbank, and D. Alsdorf. 2007. The shuttle radar topography mission. Reviews of Geophysics. 45:RG2004. doi: 10.1029/2005RG000183.

Fisher, P.F. and N.J. Tate. 2006. Causes and consequences of error in digital elevation models. Progress in Physical Geography. 30(4):467-489. doi:10.1191/0309133306pp492ra

Gesch, D.B., M. Oimoen, S. Greenlee, C. Nelson, M. Steuck, and D. Tyler. 2002. The national elevation dataset. Photogrammetric Engineering & Remote Sensing. 68(1):5-11.

Guth, P.L. 2006. Geomorphometry from SRTM: comparison to NED. Photogrammetric Engineering & Remote Sensing. 72(3):269-277.

Hodgson, M.E., J.R. Jensen, L. Schmidt, S. Schill, B. Davis. 2003. An evaluation of lidar- and IFSAR- derived digital elevation models in leaf-on conditions with USGS Level 1 and Level 2 DEMs. Remote Sensing of Environment. 84:295-308.

Holmes, K.W., O.A. Chadwick, and P.C. Kyriakidis. 2000. Error in a USGS 30-meter digital elevation model and its impact on terrain modeling. Journal of Hydrology. 233(1):154-173.

Hudson, B.D. 1990. Concepts of soil mapping and interpretation. Soil Survey Horizons. 31(3):63-72.

Hunter, G.J. and M.F. Goodchild. 1997. Modeling the uncertainty of slope and aspect estimates derived from spatial databases. Geographical Analysis. 29(1):35-49.

Krabill, W.B., R.H. Thomas, C.F. Martin, R.N. Swift, and E.B. Frederick. 1995. Accuracy of airborne laser altimetry over the Greenland Ice Sheet. International Journal of Remote Sensing. 16: 1211-1222.

Krabill, W.B., C.W. Wright, R.N. Swift, E.B. Frederick, S.S. Manizade, J.K. Yungel, C.F. Martin, J.G. Sonntag, M. Duffy, W. Hulslander, J.C. Brock. 2000. Airborne laser mapping of Assateague National Seashore beach. Photogrammetric Engineering and Remote Sensing. 66:6571.

Lark, R.M. 1999. Soil-landform relationships at within-field scales: an investigation using continuous classification. Geoderma. 92(3-4):141-165.

Lee, J., P.K. Snyder, and P.F. Fisher. 1992. Modeling the effect of data errors on feature extraction from digital elevation models. Photogrammetric Engineering & Remote Sensing. 58(10):1461-1467.

Li, Z. 1988. On the measure of digital terrain model accuracy. Photogrammetric Record. 12:873-877.

Lindsay, J.B. 2006. Sensitivity of channel mapping techniques to uncertainty in digital elevation data. International Journal of Geographical Information Science. 20(6):669-692.

McBratney, A.B., M.L. Mendonça Santos, and B. Minasny. 2003. On digital soil mapping. Geoderma. 117:3-52.

Milne, G. 1935. Some suggested units of classification and mapping particularly for East African soils. Soil Research. 4(3).

Moore, I.D., R.B. Grayson, and A.R. Ladson. 1991. Digital terrain modelling: a review of hydrological, geomorphological, and biological applications. Hydrological Processes. 5(1):3-30.

Pennock, D.J., B.J. Zebarth, E. De Jong. 1987. Landform classification and soil distribution in hummocky terrain, Saskatchewan, Canada. Geoderma. 40(3-4):297-315.

Pilkey, O.H. and L. Pilkey-Jarvis. 2007. Useless Arithmetic: Why Environmental Scientists Can't Predict the Future. Columbia University Press. New York.

Rodriguez, E., C.S. Morris, J.E. Belz, E.C. Chapin, J.M. Martin, W. Daffer, S. Hensley. 2005. An assessment of the SRTM topographic products. Technical Report JPL D-31639, Jet Propulsion Laboratory. Pasadena, California. Available online at: http://www2.jpl.nasa.gov/srtm/srtmBibliography.html. Accessed [3/31/2013].

Ruhe, R.V. 1975. Geomorphology. Houghton Mifflin. Boston.

Schumann, G. P. Matgen, M.E.J. Cutler, A. Black, L. Hoffmann, and L. Pfister. 2008. Comparison of remotely sensed water stages from LiDAR, topographic contours and SRTM. ISPRS Journal of Photogrammetry and Remote Sensing. 63(3):283-296.

Shortridge, A. and J. Messina. 2011. Spatial structure and landscape associations of SRTM error. Remote Sensing of Environment. 115(6):1576-1587.

Soil Survey Staff. 1993. Soil Survey Manual. U.S. Department of Agriculture Handbook No. 18. Washington, D.C.

Soil Survey Staff. 2013. Soil Survey Geographic (SSURGO) Database. Natural Resource Conservation Service, U.S. Department of Agriculture. Available online at: http://soildatamart.nrcs.usda.gov. Accessed [3/23/2013].

USGS. 2002. Shuttle Radar Topography Mission, 1 Arc Second. United States Geological Survey. Available online at: http://earthexplorer.usgs.gov/. Accessed [3/31/2013].

USGS. 2006. Accuracy of the National Elevation Dataset. United States Geological Survey. Available online at: http://ned.usgs.gov/Ned/accuracy.asp. Accessed [5/9/2013].

USGS. 2013a. National Elevation Dataset. United States Geological Survey. Available online at: http://ned.usgs.gov. Accessed [3/31/2013].

USGS. 2013b. National Elevation Dataset Viewer. United States Geological Survey. Available online at: http://ned.usgs.gov/usgs_gn_ned_dsi/viewer.htm. Accessed [4/18/2013].

Wilson, J.P. and J.C. Gallant. 2000. Digital Terrain Analysis. *In* J.P. Wilson and J.C. Gallant (eds.). Terrain Analysis: Principles and Applications. John Wiley & Sons, Inc. New York.

Young, F.J. and R.D. Hammer. 2000. Soil-landform relationships on a loess-mantled upland landscape in Missouri. Soil Science Society of America Journal. 64(4):1443-1454.

CHAPTER 6. CONCLUSIONS

The digital classification model developed, applied and evaluated in this dissertation was successful in contextually classifying hillslope position in three different Midwestern landscapes. The model was able to replicate the majority of hillslope position determinations of field soil scientists. The analysis scales and classification breaks used in the model, individually, are also supported by the results of studies by other researchers. Therefore, the model has shown that it can build on expert knowledge and make use of increasingly accurate digital topographic data to potentially advance digital soil mapping opportunities.

Through a review of the historical literature of soil geography, a hierarchy of phenomenon scales for soil formation factors was observed. That hierarchy consists of climate-vegetation at coarse analysis scales, parent material at moderate analysis scales, and topography at fine analysis scales. This pattern suggests that the resolution of the current 'detailed' (county-wide) soil maps can best be increased by improving topographic base maps, which are, of course, a reflection of the relief factor of soil formation. Although LiDAR provides high resolution elevation data, it alone does not provide the contextual assessment of topography used explicitly by soil scientists in the field. In field studies, soil scientists commonly characterize topographic context with the metric of hillslope position in mind.

This dissertation addressed the issue of applying the proven field metric of hillslope position to digital terrain analysis, for the likely end application of improving existing soil maps. A quantitative model was developed, which was calibrated to the analysis scales, classification breaks, and logic structure of soil scientists' field assessments of hillslope position. To

accomplish this, a new technique for calculating relative elevation with a user controlled analysis scale was introduced. Also, methods for calibrating digital analysis scale and classification breaks to field observations were tested.

The optimal analysis scales for predicting soil cover patterns, as observed by field scientists, vary by terrain metric. The digital analysis scales that best matched soil scientists' assessment in the field were 9 m, 63 m, and 135 m for slope gradient, profile curvature, and relative elevation, respectively. Supported by this tacit knowledge, correlations between these terrain metrics and soil properties are likely to be stronger at these respective analysis scales. However, the maximum agreements between field and digital assessments for the most basic definitions of profile curvature (concave vs. convex) and relative elevation (high vs. low elevation) were only 70% and 80%, respectively. This finding is informative for more complex models (i.e. expert knowledge based digital soil mapping) that seek to replicate assessments of soil scientists in the field. Potential sources of error include uncertainty in location, uncertainty in the elevation attribute, and the always-present variability of human assessment.

The fully calibrated classification model differentiated areas on the landscape using a decision tree hierarchy that divided the landscape first by slope gradient, then by profile curvature and relative elevation. Areas > 2.9° in slope gradient were classified as backslopes. Areas between 1.4° and 2.9° in slope gradient were differentiated by profile curvature as shoulders (convex curvature) or footslopes (concave curvature). Areas < 1.4° in slope gradient were differentiated by relative elevation as summits (high elevation) or toeslopes (low elevation).

The hillslope position classification model was then validated in three different counties with unique terrain. In all three study areas, the model was able to successfully predict the field assessment of hillslope position 52-54% of the time, despite only being calibrated in the first study area. The digital classifications showed an appropriate level of agreement with current Soil Survey delineations while demonstrating clear areas for improvement of soil map unit boundary placement and map unit disaggregation. The model provides a more detailed and reliable base map, which will assist soil mappers in their initial mapping efforts, as well as for post-mapping upgrades, e.g., disaggregation of existing map units, or remapping/relocation of existing soil boundaries.

Finally, the sensitivity of the model to the quality of elevation data source was tested. In the three terrain types analyzed, classification of hillslope position was sensitive to both grid resolution and uncertainty in the elevation attribute. Reducing the resolution from a 3 m grid increased the minimum analysis scale, which changed approximately 20% and 35% of classifications at the 9 m and 27 m resolutions, respectively. The increase in uncertainty by shifting from LiDAR ($RMSE_Z$ = 0.15-0.43 m) to a NED elevation grid ($RMSE_Z$ = 1-2 m) or a SRTM elevation grid ($RMSE_Z$ = 1.5-6 m), changed approximately 35% of classifications. Although uncertainty in the elevation attribute is important, calculating all of the digital terrain metrics at the proper analysis scale had a predictable, increasing impact with decreasing spatial resolution.